

Synthesis and SAR Analysis of a Family of STAT3 Inhibitors

A DISSERTATION SUBMITTED TO THE GRADUATE DIVISION
OF THE UNIVERSITY OF HAWAI'I AT MĀNOA IN PARTIAL
FULFILLMENT OF THE REQUIREMENTS FOR THE DEGREE OF

MASTER OF SCIENCE
IN
CHEMISTRY

AUGUST 2019

By

Airlia Marie Shonkwiler

Thesis Committee:

Marcus A. Tius, Chairperson
Matthew F. Cain
James K. Turkson

ACKNOWLEDGEMENTS

I would like to thank my advisor, Professor Marcus A. Tius, for his guidance and for allowing me to contribute to this project.

I would like to thank Dr. Francisco Lopez-Tapia for his help in analog design and synthesis and for all his valuable contributions to this project.

Many thanks go to Dr. James Turkson and Dr. Peibin Yue at the University of Hawai'i Cancer Center for running biological tests on the STAT3 inhibitors. I would like to thank Duk Kim for his help in obtaining mass spectra. I would also like to thank the members of the Tius research group for their help.

ABSTRACT

Inhibiting STAT3 dimerization and the interaction of STAT3 with the DNA-binding domain is important for preventing the progression of malignant transformations in glioma, breast, prostate, ovarian and other cancers. The Tius group has designed STAT3 inhibitors that disrupt STAT3 dimerization/DNA-binding. However, for these STAT3 inhibitors to be developed into effective anti-cancer drugs, the potency and physicochemical properties of these molecules needs to be improved.

Previous SAR analysis was performed to improve the potency and physicochemical properties of the STAT3 inhibitors and from this analysis a general scaffold was developed (Chapter 1, **Figure 7**). It was determined that pyridine or pyrazine structural motifs in region 2 (R_2) produced the most potent compounds compared to analogs with different heterocycles. To resolve which heteroarene, pyridine or pyrazine, produces the most potent compounds more analogs containing these functional groups were needed for comparison. It was also shown that one compound with difluorocyanobenzenesulfonamide in region 3 (R_3) had improved potency over its pentafluorobenzenesulfonamide analog. To confirm that the difluorocyanobenzenesulfonamide fragment generally improves compound potency, more analogs needed to be examined. Furthermore, it was discovered that compounds containing a carboxyl or hydroxamic acid functional group in region 4 (R_4) have good potency, but poor permeability. Functionalities in R_4 needed to be varied to improve both potency and permeability.

In an attempt to optimize R_2 , R_3 , and R_4 in terms of potency and physicochemical properties 12 small molecule STAT3 inhibitors were prepared. These compounds were designed

and synthesized using convergent routes containing 7-15 synthetic steps. The synthetic route employed had broad functional group tolerance that easily enabled the development of a small molecule library for biological screening. Each molecule prepared was tested for STAT3 DNA-binding inhibitory activity using the EMSA assay. The physicochemical properties of lead inhibitory agents will be tested in the near future.

SAR analysis on R₂ was inconclusive; more analogs comparing pyridine and pyrazine need to be explored to resolve which heterocycle leads to the most potent compounds. Replacing the pentafluorobenzenesulfonamide functional group with difluorocyanobenzenesulfonamide increased potency in three out of the four analog comparisons suggesting that compounds with R₃ = difluorocyanobenzenesulfonamide have better potency compared to analogs with R₃ = pentafluorobenzenesulfonamide. Compounds with R₄ = *N*-methylsalicylamide, *N,N*-dimethylsalicylamide, meta-difluoromethylbenzene, or meta-fluorobenzene had similar or lower STAT3 inhibitory activity than the parent compounds with R₄ = salicylic acid. However, replacing the salicylic acid functionality with benzene enhanced potency. This suggests that functional groups on the benzene ring in R₄ are not necessary for enhancing potency.

Table of Contents

Acknowledgments	ii
Abstract	iii
List of Tables	vii
List of Figures	viii
List of Synthetic Schemes	x
List of Abbreviations	xii
Chapter 1. STAT3, STAT3 Structural Domains and Signaling Pathway, Small Molecule Inhibitors of STAT3, and STAT3 Inhibitor Targets	1
STAT3 Structural Domains and Signaling Pathway	2
First Lead STAT3 Inhibitor, BP-1-102	3
Second and Third Lead STAT3 Inhibitors, SH5-07 and SH4-54	5
SAR Analysis on BP-1-102 , SH5-07 , and SH4-54	7
SAR Variation in Region 1	7
SAR Variation in Region 2	8
SAR Variation in the Linker Region	9
SAR Variation in Region 3	11
SAR Variation in Region 4	13
Targeted STAT3 Inhibitors to be Prepared	15
Chapter 2. Synthesis of the Targeted Small Molecule STAT3 Inhibitors	17
2.1 Proposed Synthetic Routes for the Targeted STAT3 Inhibitors	18
2.2 Synthesis of S3I-H204	21

2.3 Synthesis of S3I-H212	24
2.4 Attempts at Synthesizing Compound 41	26
2.5 Synthesis of S3I-H222	29
2.6 Synthesis of S3I-H224	31
2.7 Synthesis of S3I-H230	32
2.8 Synthesis of S3I-H235	33
2.9 Synthesis of S3I-H233	34
2.91 Synthesis of S3I-H228	35
2.92 Synthesis of S3I-H237	36
2.93 Synthesis of S3I-H239	37
2.94 Synthesis of S3I-H244	38
2.95 Synthesis of S3I-H245	39
Conclusion for Chapter 2	41
Chapter 3. Results and Conclusions	43
Summary of Chapter 1	44
Summary of Chapter 2	46
Targeted STAT3 Compounds - SAR Variation in Region 2	46
Targeted STAT3 Compounds - SAR Variation in Region 3	48
Targeted STAT3 Compounds - SAR Variation in Region 4	49
Concluding Remarks.....	51
Experimental	53
Appendix I. Spectra for Selected Compounds in Chapter 2	118
Appendix II. References	161

List of Tables

1. SAR Variation in Region 1 (R ₁)	8
2. Structure and Metabolic Stability of SH4-54 , SH5-07 , S3I-H048 , and S3I-H089	11
3. SAR variation in Region 3 (R ₃)	12
4. SAR Variation in Region 4 (R ₄)	14
5. Structure, Solubility, and Permeability of SH4-54 , SH5-07 , and S3I-H048	15
6. Targeted STAT3 Compounds - SAR Variation in Region 2 (R ₂)	47
7. Targeted STAT3 Compounds - SAR Variation in Region 3 (R ₃)	49
8. Targeted STAT3 Compounds - SAR Variation in Region 4 (R ₄)	51

List of Figures

1. Diagram of the Structural Domains of the STAT3 Protein	2
2. Diagram of the STAT3 Signaling Pathway	3
3. Structure of BP-1-102 (A) and Computational Model of BP-1-102 Interacting with the STAT3 SH2 Domain (B).....	4
4. Antitumor Effects of Bp-1-102 in Human Breast (A, B) and Lung (C) Tumor Xenografts	5
5. Structure of SH5-07 and SH4-54 (A) and STAT3 DNA-Binding EMSA Analysis of Nuclear Extracts from U251MG Cells Overexpressing STAT3 SH2 or DB Domain That Were Treated with SH4-54	6
6. Antitumor Effects of SH5-07 and SH4-54 in Human Glioma U251MG (A) and Breast MDA-MB-231 Tumor Xenografts	6
7. General Scaffold for STAT3 Inhibitors	7
8. Structures of S3I-H098 , S3I-H127 , S3I-H142 , S3I-H143 , and S3I-H144	9
9. Structures of BP-1-102 , S3I-H011-12 , S3I-H069-70 , and S3I-H098	10
10. Structures of S3I-H142 and S3I-H203	13
11. Structures of the Targeted STAT3 Inhibitory Agents.....	16
12. Mechanism for the Formation of Hydrazine with Magnesium and the Structure of the Byproduct from Reaction (a), Scheme 4.....	23
13. Side-product of Reaction (a), Scheme 5	25

14. Side-product for Reaction (a), Scheme 6.....	26
15. Structure of Byproduct 53 from reaction (j3), Scheme 7.....	29
16. STAT3 Inhibitory Agents Synthesized	45

List of Synthetic Schemes

1. Proposed Synthetic Routes A and B for the Synthesis of <i>N</i> -((5-cyclohexylpyridin-2-yl)methyl)aniline 7 and <i>N</i> -((5-cyclohexylpyrazin-2-yl)methyl)aniline 8	19
2. Proposed Synthetic Routes C and D for the Synthesis of the Difluorocyanobenzenesulfonamide Core Scaffolds (18 and 19) and the Pentafluorobenzenesulfonamide Core Scaffolds (21 and 22)	20
3. Synthetic Routes A and B for the Synthesis of 2-(chloromethyl)-5-cyclohexylpyridine 3	22
4. Synthesis of S3I-H204	24
5. Synthesis of S3I-H212 and the Structure of HATU	25
6. First Attempt at Synthesizing 41	26
7. Second Attempt at Synthesizing 41	28
8. Synthesis of S3I-H222	30
9. Synthesis of S3I-H224	31
10. Synthesis of S3I-H230	32
11. Synthesis of S3I-H235	33
12. Synthesis of S3I-H233	35
13. Synthesis of S3I-H228	36
14. Synthesis of S3I-H237	37

15. Synthesis of S3I-H239	38
16. Synthesis of S3I-H244	39
17. Synthesis of S3I-H245	40

List of Abbreviations

Å	angstrom(s)
ACN	acetonitrile
Ar	argon
Arg	arginine
BnBr	benzyl bromide
Boc	<i>Tert</i> -butoxycarbonyl
δ (ppm)	chemical shift (parts per million)
cat.	catalytic
CCD	coiled-coil domain
CDCl ₃	deuterated chloroform
CHCl ₃	chloroform
cm	centimeter(s)
COCl ₂	oxalyl chloride
Cs ₂ CO ₃	cesium carbonate
°C	degrees celsius
DBD	deoxyribonucleic acid binding domain
DCM	dichloromethane
DIPEA	<i>N,N</i> -diisopropylethylamine
DMAP	4-dimethylaminopyridine
DMF	dimethylformamide

DMSO	dimethyl sulfoxide
DMSO- <i>d</i> ₆	deuterated dimethyl sulfoxide
DNA	deoxyribonucleic acid
EMSA	electrophoretic mobility shift assay
eq	equivalence
ESI	electrospray ionization
EtOAc	ethyl acetate
EtOH	ethanol
Fe	iron
g	gram(s)
Glu	glutamic acid
h	hour(s)
H ₂	hydrogen gas
H ₂ O	water
HATU	1-[bis(dimethylamino)methylene]-1H-1,2,3-triazolo[4,5- b]pyridinium-3-oxide hexafluorophosphate
HCl	hydrochloric acid
HLM	human liver microsomes
HN(CH ₃) ₂	dimethylamine
HPLC	high performance liquid chromatography
HRMS	high resolution mass spectrum
IC ₅₀	half maximal inhibitory concentration
Ile	isoleucine

J	coupling constant
JAKs	janus kinases
K_2CO_3	potassium carbonate
K_3PO_4	potassium phosphate tribasic
kg	kilogram(s)
KHMDS	potassium hexamethyldisilazide
L	liter(s)
LC-MS TOF	liquid chromatography-mass spectrometry time-of-flight
LCMS	liquid chromatography mass spectrometry
Lys	lysine
μg	microgram(s)
μm	micrometer(s)
μM	micromolar
μmol	micromole(s)
M	molar
m/z	mass-to-charge ratio
M^+	molecular ion
MeMgBr	methyl magnesium bromide
MeOH	methanol
mg	milligram(s)
$MgSO_4$	magnesium sulfate
MHz	megahertz

min	minute(s)
mL	milliliter(s)
MLM	mouse liver microsomes
mmol	millimole(s)
MsCl	methanesulfonyl chloride
Na	sodium
Na ₂ SO ₄	sodium sulfate
NaBH ₃ OMe	sodium monomethoxyborohydride
NaBH ₄	sodium borohydride
NaH	sodium hydride
NaHCO ₃	sodium bicarbonate
NaI	sodium iodide
NaOMe	sodium methoxide
ND	N-terminal domain
NH ₄ Cl	ammonium chloride
nm	nanometer(s)
NMR	nuclear magnetic resonance
Papp	apparent permeability coefficient
PBS	phosphate-buffered saline
Pd(OAc) ₂	palladium (II) acetate
Pd(OH) ₂	palladium (II) hydroxide
Pd/C	palladium on carbon
Pd ⁰	palladium (0)

%	percent
pH	power of hydrogen
pKa	acid dissociation constant
PTLC	preparative thin layer chromatography
PtO ₂	platinum (IV) oxide
s	second(s)
SAR	structure-activity relationship
Sat	saturated
SH2	src homology 2
SIF	simulated intestinal fluid
S _N 2	nucleophilic substitution, second order
S _N Ar	nucleophilic aromatic substitution
SOCl ₂	thionyl chloride
SPHos	2-dicyclohexylphosphino-2',6'-dimethoxybiphenyl
Src	sarcoma
STAT3	signal transducer and activator of transcription 3
<i>t</i> - or <i>tert</i> -	tertiary
<i>t</i> _{1/2}	half-life
TAD	transactivation domain
TEA	triethylamine
TFA	trifluoroacetic acid
TFAA	trifluoroacetic anhydride
THF	tetrahydrofuran

TLC	thin layer chromatography
UH	university of Hawai'i
Xantphos	4,5-bis(diphenylphosphino)-9,9-dimethylxanthene

Chapter 1

STAT3, STAT3 Structural Domains and Signaling Pathway, Small Molecule Inhibitors of STAT3, and STAT3 Inhibitor Targets

The signal transducer and activator of transcription (STAT) proteins are a family of proteins that are activated by cytokine and growth factor responses.^{1,2} Activation of STAT proteins by cytokines and growth factors promote cell growth, differentiation, and varying immune responses.^{1,2} There are seven identified STAT family members: STAT1, 2, 3, 4, 5A, 5B, and 6. All of the STAT proteins contain common structural domains: N-terminal (ND), coiled-coil (CCD), DNA binding (DBD), Src homology 2 (SH2), and a transactivation domain (TAD) which contains a critical Tyrosine (Y) residue (**Figure 1**).³

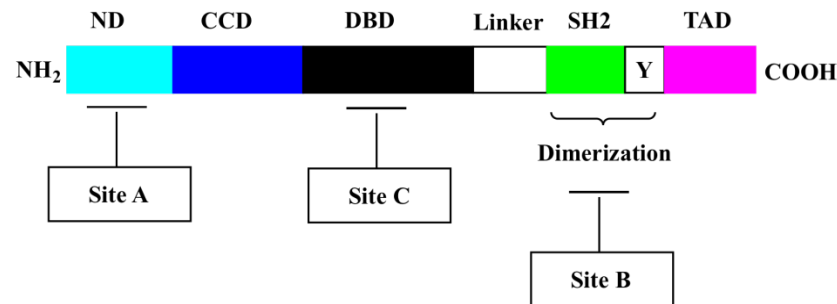


Figure 1: Diagram of the Structural Domains of the STAT3 Protein³

Note: Sites A-B are sites where STAT3 inhibitors can interact with the STAT3 protein.

Each protein contains a tyrosine residue in the TAD domain at the C-terminus which is phosphorylated during activation.³ STAT activation is induced by phosphorylation which is controlled by growth factor tyrosine kinases, cytoplasmic kinases, cytokine receptor-associated Janus kinases (JAKs), and Src family kinases (Site A, **Figure 2**).³ Once STAT proteins are phosphorylated, dimer formation is stimulated between two STAT monomers (Site B, **Figure 2**). The STAT: STAT dimer is formed through a reciprocal phosphorylated tyrosine Y-SH2 domain interaction (**Figure 1**).³ The STAT: STAT dimer is translocated to the nucleus where it binds DNA specific genes which stimulate cell transcription (Site C, **Figure 2**).³

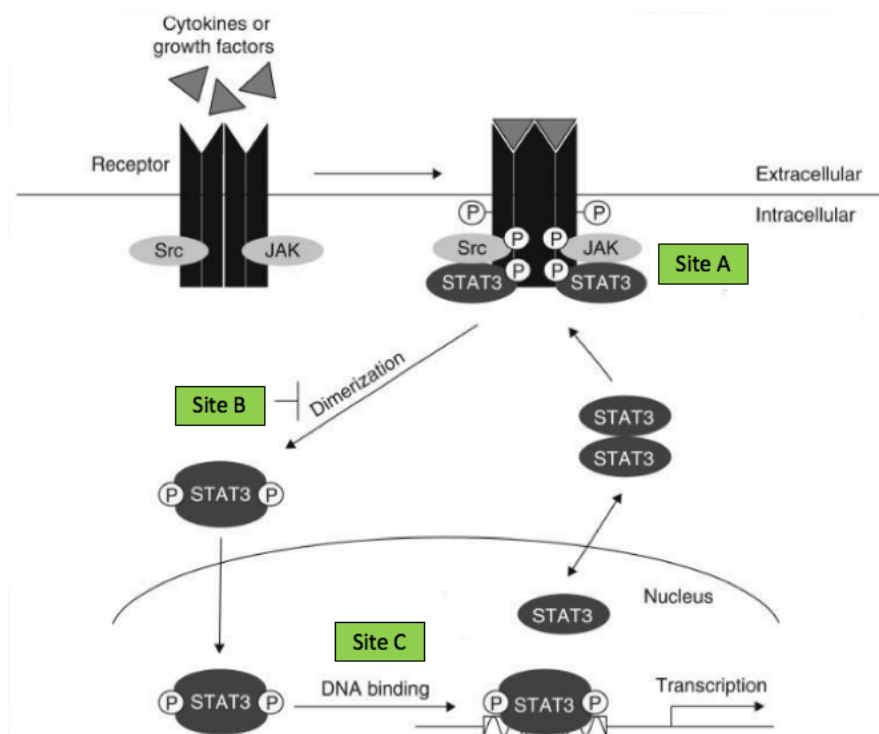


Figure 2: Diagram of the STAT3 Signaling Pathway³

STAT activation in normal cells only persists for a short time period. However, aberrant activation of STAT3 occurs in cancerous transformations and has been shown to be associated with glioma, breast, prostate, and other cancers.³⁻⁶ STAT3 induces tumorigenesis by dysregulating gene expression which leads to uncontrolled tumor growth and represses tumor immune surveillance.^{1,4-10} Thus, STAT3 is an enticing target for the discovery of anticancer drugs.⁶

Currently, the most promising way of disrupting the STAT3 signaling pathway is by inhibiting the dimerization step (Site B, **Figures 1 & 2**) with STAT3 inhibitors.^{5, 11-18} The first promising STAT3 dimerization inhibitor discovered by Turkson and Gunning was **BP-1-102** (A, **Figure 3**).

Computational modeling predicted that **BP-1-102** binds to three sub-pockets of the STAT3-STAT3 dimer interface, with the pentafluorobenzenesulfonamide moiety projecting into the third sub-pocket composed of Lys591, Glu594, Ile634, and Arg595 (B, **Figure 3**).¹³ **BP-1-102** was also shown to inhibit STAT3 DNA-binding activity in vitro with an $IC_{50} = 6.8 \pm 0.8 \mu M$ as measured by the electrophoretic mobility shift assay (EMSA).¹³ Moreover, **BP-1-102** inhibited growth of mouse xenografts of human breast (MDA MB-231) and lung (A549) tumors that contain aberrantly active STAT3 when administered intravenously or by oral gavage (**Figure 4**).¹³

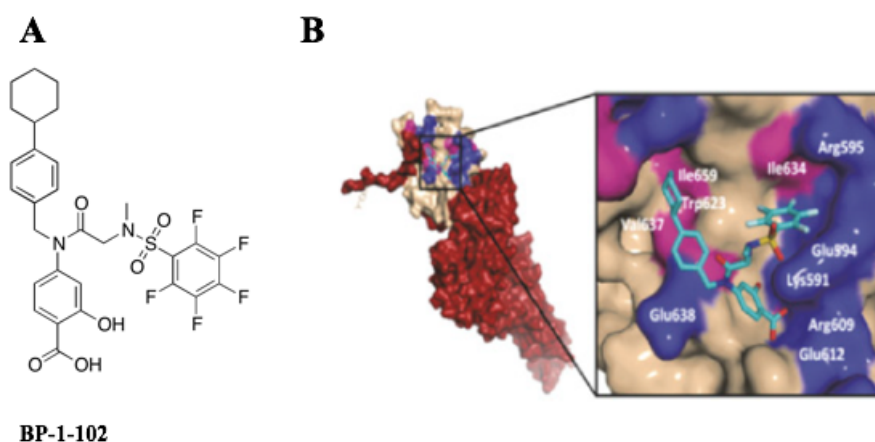


Figure 3. Structure of **BP-1-102** (A) and Computational Model of **BP-1-102** Interacting with the STAT3 SH2 Domain (B)¹³

Note: (B, Left) STAT3 monomer: solvent accessible surface of the SH2 domain (off-white), hydrophobic residues (pink), hydrophilic residues (blue), and **BP-1-102** (cyan). (B, Right) **BP-1-102** accessing the three sub-pockets of the SH2 domain surface.¹³

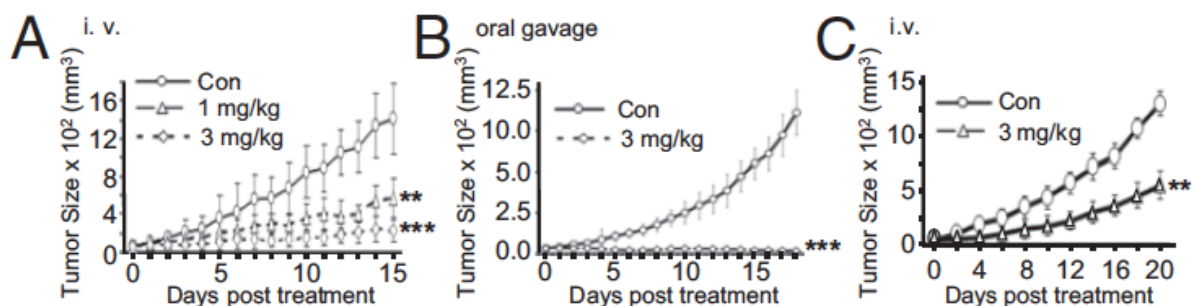


Figure 4. Antitumor Effects of **Bp-1-102** in Human Breast (A, B) and Lung (C) Tumor Xenografts¹³

Note: Mice with MDA-MB-231 (A, B) or A549 (C) tumors were given **BP-1-102** via i.v., 1-3 mg/kg or control (0.05% DMSO in PBS) every 2 or 3 days or oral gavage, 3mg/kg or control (0.05% DMSO) every day.¹³

SH5-07 and **SH4-54** were the second and third lead STAT3 inhibitors that emerged from the collaboration between the Tius and Turkson groups and they are analogs of **BP-1-102** (**Figure 5**). **SH5-07** and **SH4-54** showed improved inhibition of STAT3 DNA-binding with EMSA $IC_{50} = 3.9 \pm 0.6 \mu M$ and $4.7 \pm 0.5 \mu M$, respectively, compared to **BP-1-102** ($IC_{50} = 6.8 \pm 0.8 \mu M$) (A, **Figure 5**).⁶ The improved potency of **SH5-07** and **SH4-54** suggests that the hydroxyl functionality in the salicylic acid moiety of **BP-1-102** may not be necessary. NMR experiments showed that **SH4-54** interacts with the SH2 and DB domains and that **SH4-54** is likely interacting with the DBD by alkylating a cysteine residue.⁶ Furthermore, EMSA analysis showed that transiently expressed STAT3 SH2 domain rescued STAT3 activity from **SH4-54** compared with moderate rescue by the DBD domain (B, **Figure 5**).⁶ This suggests that the small molecule inhibitors **SH4-54** and **SH5-07** interact with both domains. Similar to **BP-1-102**, **SH5-07** and **SH4-54** inhibited the growth of human breast (MDA-MB-231) and glioma (U251MG) tumor xenografts in mice (**Figure 6**).⁶

No significant changes in body weight, blood cell counts, or signs of toxicity were observed in mice.⁶ Altogether these results indicate that **SH5-07** and **SH4-54** have potential as anti-cancer drugs.

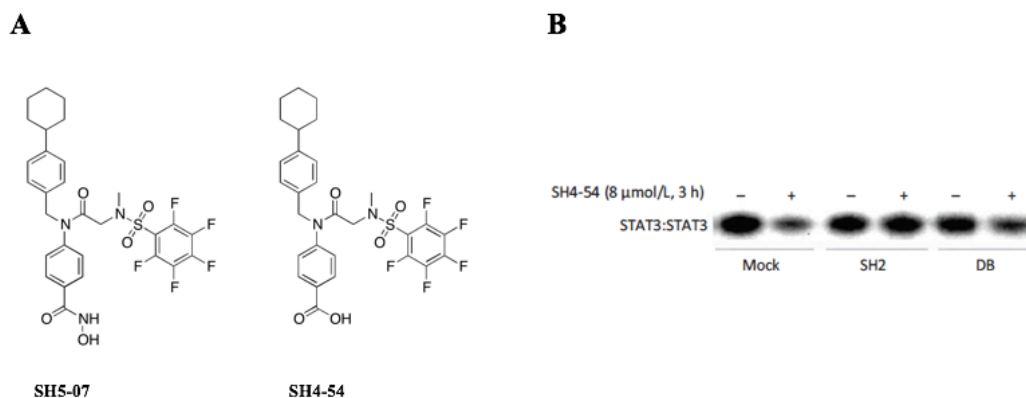


Figure 5. Structures of **SH5-07** and **SH4-54** (A) and STAT3 DNA-Binding EMSA Analysis of Nuclear Extracts from U251MG Cells Overexpressing STAT3 SH2 or DB Domain That Were Treated with **SH4-54**⁶

Note: (B) Control lanes (-) represent nuclear extracts treated with 0.05% DMSO.

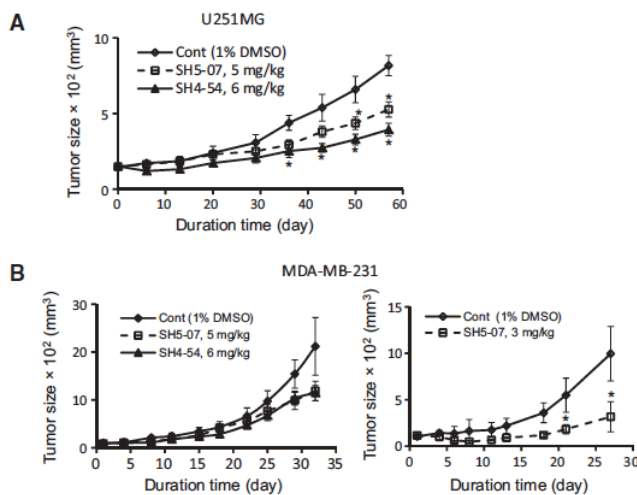


Figure 6. Antitumor Effects of **SH5-07** and **SH4-54** in Human Glioma U251MG (A) and Breast MDA-MB-231 Tumor Xenografts⁶

Note: (A) and (B) left plots are from intravenous administration of **SH5-07** and **SH4-54** (5 or 6 mg/kg every 2 to 3 days), (B) right plot is from oral gavage delivery of **SH5-07** and **SH4-54** (3 mg/kg).

Extensive structure-activity relationship (SAR) analysis on **BP-1-102**, **SH5-07**, and **SH4-54** was performed to improve the potency and physicochemical properties. This analysis led to the formation of a general scaffold for the STAT3 inhibitors (**Figure 7**). In an attempt to increase the potency of the lead compounds (**BP-1-102**, **SH4-57**, and **SH5-07**) the cyclohexane functionality was substituted with heterocycles. Replacing the cyclohexane moiety with tetrahydro-4H-pyran (**S3I-H003**, **S3I-H005**, and **S3I-H006**) or piperidine (**S3I-H020** and **S3I-H039**) decreased the activity compared to the parent analogs, **BP-1-102**, **SH4-54**, and **SH5-07** (**Table 1**).¹⁹ Replacing the cyclohexane group with 4,4-difluorocyclohexane (**S3I-H014**) or cycloheptane (**S3I-H040**) resulted in diminished STAT3 inhibitory activity (**Table 1**).¹⁹ These results show that the most potent compounds are those which contain a cyclohexane functionality in region 1 (**R₁**) (**Figure 7**).

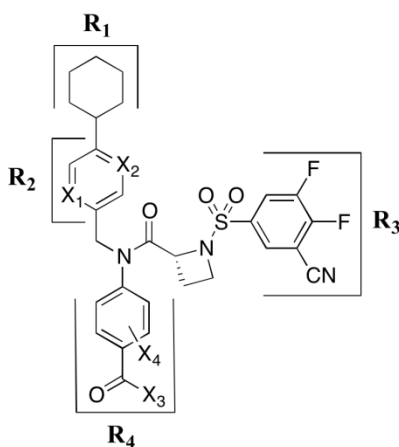
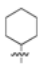
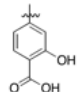
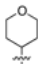
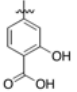

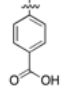
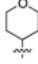
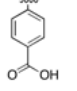

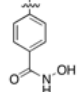
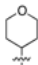
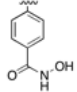
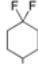
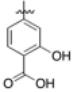
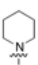
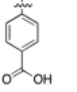

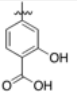

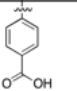
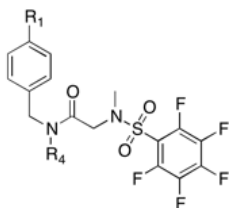


Figure 7. General Scaffold for STAT3 Inhibitors

Note: **R₂** (**X₁/X₂** = N or CH), **R₄** (**X₃** = OH, NHOH, H, etc., **X₄** = H, OH, ONa, CH₂COOH, etc., **X₃** to **X₄** = CONHCH₂, CHN₂H, etc.)

Table 1. SAR Variation in Region 1 (R₁)¹⁹

Compound	R ₁	R ₄	EMSA IC ₅₀ (μM)	Compound	R ₁	R ₄	EMSA IC ₅₀ (μM)
BP-1-102			6.8 ± 0.8	S3I-H003			11.4 ± 4.4
SH4-54			4.7 ± 0.5	S3I-H005			>30
SH5-07			3.9 ± 0.6	S3I-H006			19.0 ± 3.4
				S3I-H014			16.6 ± 6.4
				S3I-H020			36.4 ± 3.4
				S3I-H039			30.1 ± 3.8
				S3I-H040			10.9 ± 3.3



SAR analysis revealed that when the functionality in R₂ is changed from phenyl (**S3I-H098**) to pyridine (**S3I-H127**) the potency is enhanced (IC₅₀ = 0.546 ± 0.014 μM vs. 0.384 ± 0.024 μM) (**Figure 7, Figure 8**). Pyrimidine **S3I-H143** (IC₅₀ = 0.497 μM) and pyridazine **S3I-H144** (IC₅₀ = 0.721 μM) decreased activity compared to the parent pyridine analog **S3I-H127** (IC₅₀ = 0.384 ± 0.024 μM). Recent SAR analysis has shown that when pyridine is replaced with pyrazine the potency remains the same or slightly diminishes.

This is evident when comparing **S3I-H127** with **S3I-H142**, $IC_{50} = 0.384 \pm 0.024 \mu M$ vs. $0.42 \mu M$ (**Figure 8**). These results indicate that more analogs comparing pyridine and pyrazine need to be explored to determine which functionality is optimal for R_2 .

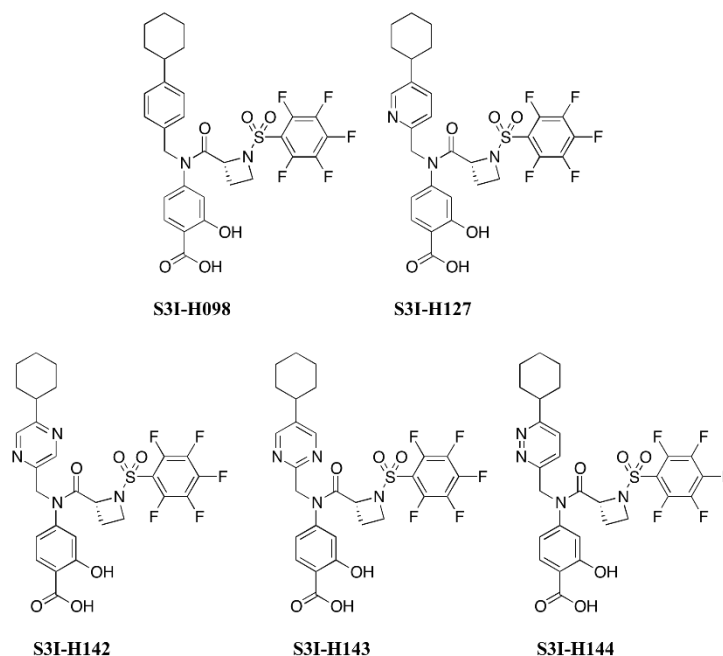


Figure 8. Structures of **S3I-H098**, **S3I-H127**, **S3I-H142**, **S3I-H143**, and **S3I-H144**

Substitution of glycine in **BP-1-102** ($IC_{50} = 6.8 \pm 0.8 \mu M$) with (*R*)-alanine in the linker region to form **S3I-H012** ($IC_{50} = 3.0 \pm 0.9 \mu M$) led to improved activity in disrupting STAT3 DNA-binding in vitro (**Figure 9**).¹⁹ However, the (*S*)-alanine analog **S3I-H011** ($IC_{50} = 5.0 \pm 0.2 \mu M$) had lower activity (**Figure 9**).¹⁹ Unfortunately, it was found that alanine based compounds have lower metabolic stability compared to glycine based compounds. For example, **S3I-H048**, Mouse Liver Microsomes (MLM)/Human Liver Microsomes (HLM) half-life ($t_{1/2}$) ≤ 5 min vs. **SH4-54** and **SH5-07** MLM/HLM $t_{1/2} \geq 17$ min (**Table 2**).¹⁹ This suggests that the alanine compounds may be prone to *N*-demethylation.²⁰

With the hope of improving metabolic stability while maintaining potency, proline linker compounds were designed and prepared. When the linker was changed from (*R*)-alanine to (*R*)-proline to form **S3I-H070** ($IC_{50} = 2.4 \pm 0.2 \mu M$), potency was enhanced.¹⁹ Like the (*S*)-alanine analog the (*S*)-proline analog **S3I-H069** ($IC_{50} = 7.2 \pm 3.4 \mu M$) of **S3I-H070** showed diminished activity (**Figure 9**).¹⁹ Satisfyingly, it was found that proline based analog **S3I-H089** had improved microsomal metabolic stability over **S3I-H048**, MLM/HLM $t_{1/2} = 18$ and 15 min vs. MLM/HLM $t_{1/2} \leq 5$ min (**Table 2**).¹⁹ When the linker was changed from (*R*)-proline to (*R*)-azetidine to form **S3I-H098** ($IC_{50} = 0.546 \pm 0.014 \mu M$) the inhibition activity was enhanced even further (**Figure 9**).¹⁹ The metabolic stability of azetidine containing compounds is currently being tested. These results show that the most potent compounds are currently those which have azetidine in the linker region (**Figure 7**).

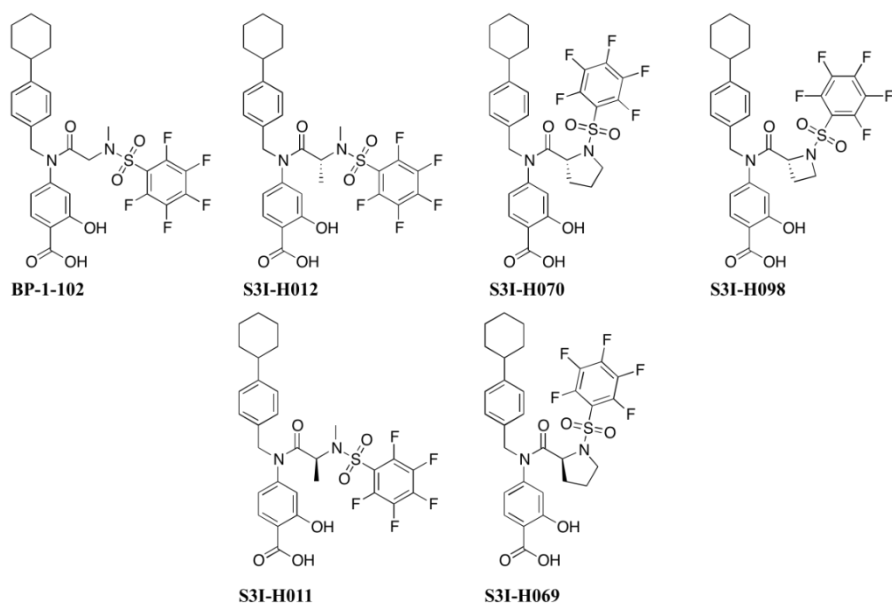
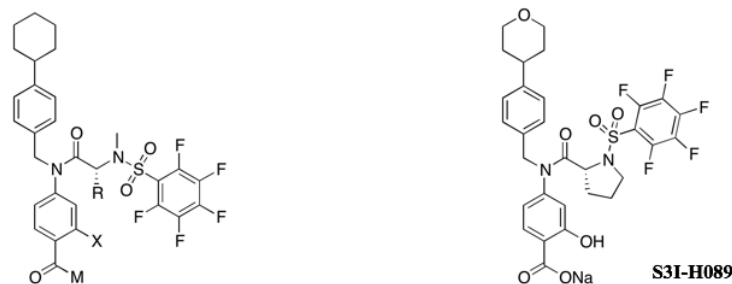


Figure 9. Structures of **BP-1-102**, **S3I-H011-12**, **S3I-H069-70**, and **S3I-H098**

Table 2. Structure and Metabolic Stability of **SH4-54**, **SH5-07**, **S3I-H048**, and **S3I-H089**¹⁹



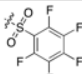
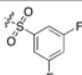
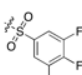
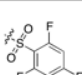
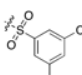
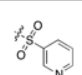
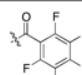
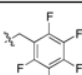
Compound	M	R	X
SH4-54	OH	H	H
SH5-07	NHOH	H	H
S3I-H048	ONa	Me	OH

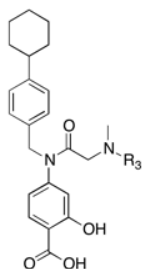
Compound	Metabolic Stability Half-Life (min) - MLM	Metabolic Stability Half-Life (min) - HLM
SH4-54	26	37
SH5-07	17	19
S3I-H048	5	4
S3I-H089	18	15

It was determined that when the number of fluorine atoms is decreased in varying ways on the aromatic ring in **R₃ STAT3 DNA-binding inhibition** is significantly reduced when compared to the parent compound, **BP-1-102** vs. **S3I-H001**, **S3I-H007**, and **S3I-H101** (**Table 3**).¹⁹ Additionally, when the pentafluorophenyl group is replaced with 3,5-bis(trifluoromethyl)phenyl (**S3I-H009**) or pyridyl (**S3I-H002**) activity was reduced substantially (**Table 3**).¹⁹ Replacing the pentafluorobenzenesulfonamide with pentafluorobenzamide (**S3I-H086**) or pentafluorobenzylamine (**S3I-H087**) was not tolerated and reduced inhibitory activity (**Table 3**).¹⁹ Further SAR analysis revealed that when the pentafluorobenzenesulfonamide in

S3I-H142 ($IC_{50} = 0.42 \mu M$) is replaced with difluorocyanobenzenesulfonamide to form **S3I-H203** ($IC_{50} = 0.283 \pm 0.031 \mu M$), a slight increase in STAT3 DNA-binding inhibition is observed (**Figure 10**).¹⁹ These results indicate that more analogs bearing the pentafluorobenzenesulfonamide and difluorocyanobenzenesulfonamide functionalities in R_3 need to be compared to confirm that compounds with difluorocyanobenzenesulfonamide are more potent (**Figure 7**).

Table 3. SAR variation in Region 3 (R_3)¹⁹

Compound	R_3	EMSA IC_{50} (μM)
BP-1-102		6.8 ± 0.8
S3I-H001		>30
S3I-H007		>30
S3I-H101		>30
S3I-H009		36.0 ± 5.4
S3I-H002		>30
S3I-H086		>30
S3I-H087		>30



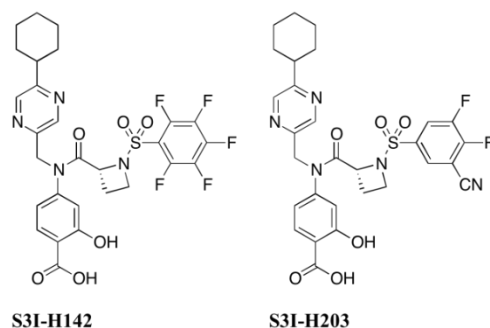


Figure 10. Structures of **S3I-H142** and **S3I-H203**

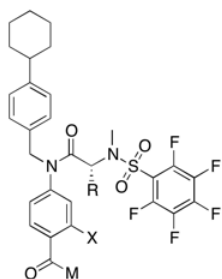
To improve the potency of the lead compounds **SH5-07** and **SH4-54**, region 4 (R_4) was modified with various functional groups (**Figure 7**). Replacing the aromatic system with heterocycles such as pyridine or oxazole (**S3I-H019** or **S3I-H030**) reduced STAT3 DNA-binding inhibitory activity compared to the parent compounds, **SH5-07** and **SH4-54** (**Table 4**).¹⁹ Additionally, it was found that replacing the 4-substituted benzoic acid moiety with 3-substituted phenylacetic acid (**S3I-H008**) significantly reduced the inhibitory activity (**Table 4**).¹⁹ Likewise, isoindolinone and indazole (**S3I-H033** and **S3I-H043**) had weaker inhibitory activity compared to the parent compounds, **S3I-H015** and **S3I-H017** (**Table 4**).¹⁹ Together, this data suggests that the carboxyl group in R_4 can only be replaced by the hydroxamic acid moiety for STAT3 inhibitory activity to be maintained (**Figure 7**).

The sodium benzoate analog (**S3I-H048**) had decreased inhibitory activity compared to the parent compound, **S3I-H012** (**Table 4**).¹⁹ As predicted, **S3I-H048** had better solubility in pH 7.4 phosphate-buffered saline (PBS) and pH 6.8 buffered simulated intestinal fluid (SIF) compared to **SH4-54** and **SH5-07**, which, as acids, have limited solubility (**Table 5**).¹⁹

It was shown that **SH4-54**, **SH5-07**, and the sodium benzoate analog, **S3I-H048**, were impermeable by the Caco-2-cell permeability assay (**Table 5**).¹⁹ The Caco-2 cell line is derived from human colon carcinoma and these cells are used to model the human intestinal absorption of drugs.²⁹ Caco-2-cells are grown on a semi-permeable plastic support which is fitted into a multi-well plate and compounds are added to the apical (cells of the monolayer facing the lumen) or basolateral (cells of the monolayer not facing the lumen) sides of the monolayer and the flux from apical to basolateral or vice versa is measured.²⁹ Compounds with good permeability need to have an apical to basolateral efflux $> 0.9 \times 10^{-6}$ cm/s.²⁴ These results indicate that functional groups that contain a carboxyl or hydroxamic acid moiety in R₄ have good potency but poor permeability (**Figure 7**). Functionalities in this region need to be varied to improve permeability without compromising potency.

Table 4. SAR Variation in Region 4 (R₄)¹⁹

Compound	R ₄	X	EMSA IC ₅₀ (μM)	Compound	R ₄	X	EMSA IC ₅₀ (μM)
SH5-07		CH ₂	3.9 ± 0.6	S3I-H008		CH ₂	33.0 ± 0.7
SH4-54		CH ₂	4.7 ± 0.5	S3I-H019		CH ₂	13.6 ± 3.3
S3I-H012		(R)-CHMe	3.0 ± 0.9	S3I-H030		CH ₂	17.3 ± 4.8
S3I-H048		(R)-CHMe	6.4 ± 2.0	S3I-H033		(R)-CHMe	10.8 ± 3.4
S3I-H015		(R)-CHMe	9.3 ± 5.0	S3I-H043		(R)-CHMe	18.3 ± 6.9
S3I-H017		(R)-CHMe	5.3 ± 1.8				

Table 5. Structure, Solubility, and Permeability of SH4-54, SH5-07, and S3I-H048¹⁹

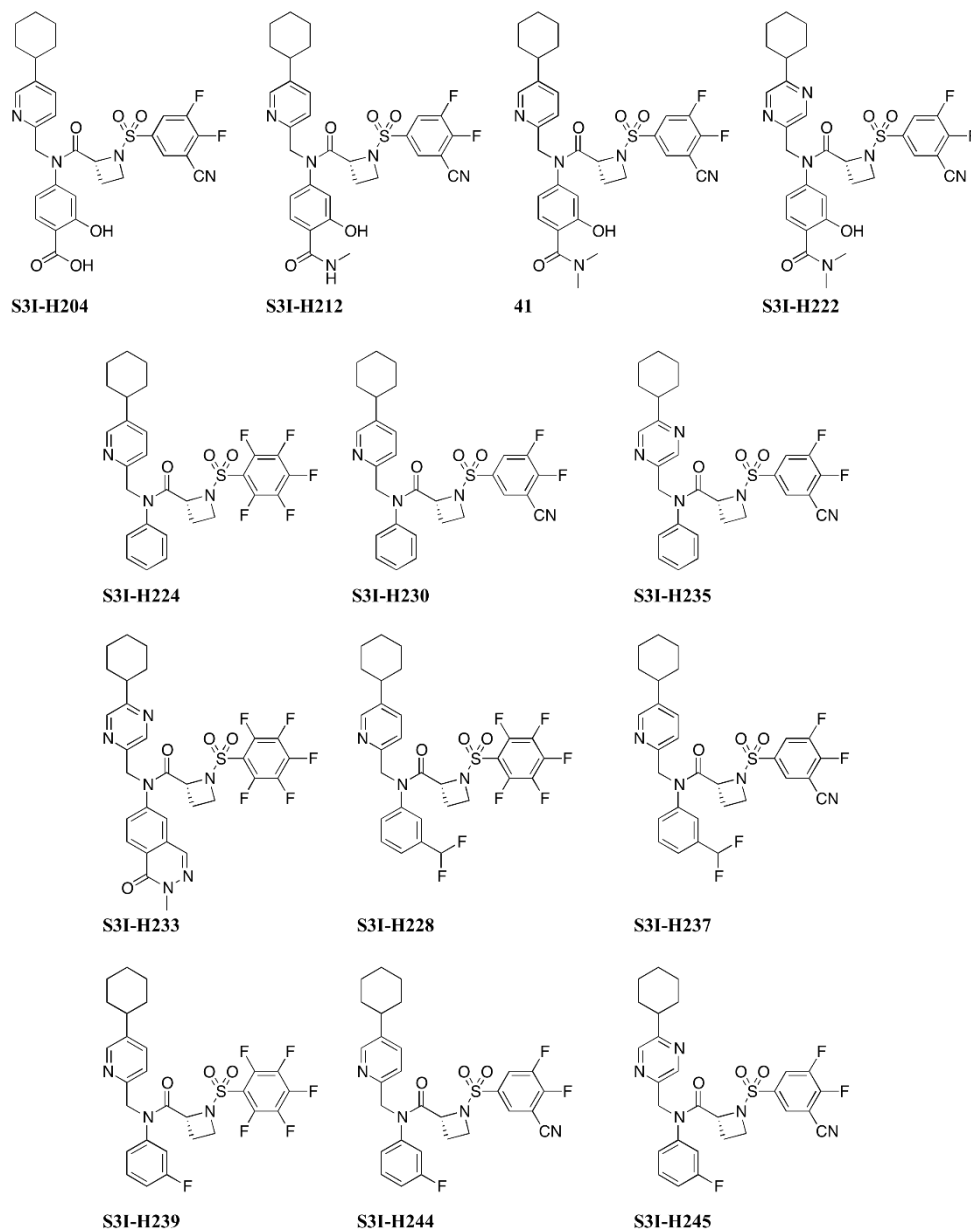
Compound	M	R	X
SH4-54	OH	H	H
SH5-07	NHOH	H	H
S3I-H048	ONa	Me	OH

Compound	Solubility ($\mu\text{g/mL}$)		Caco-2-Cells Permeability ($\text{Papp } 10^{-6} \text{ cm/s}$) / Recovery (%)	
	PBS	SIF	A to B	B to A
SH4-54	7.6	14	0/7	0/29
SH5-07	0.3	74	0/2	0/8
S3I-H048	127	127	0/6	0/2

The research goals of this thesis were to optimize R_2 , R_3 , and R_4 in terms of potency as well as physicochemical properties (**Figure 7**). The design of the targets whose structures are shown in **Figure 11** was based on the SAR analysis of the lead STAT3 inhibitory agents as previously discussed. Each target was designed, synthesized, characterized, and subsequently tested for STAT3 DNA-binding inhibitory activity using the EMSA IC_{50} assay at the UH Cancer Center. The physicochemical properties of lead inhibitory agents will be tested in the near future. The synthesis of each compound in **Figure 11** will be discussed in detail in Chapter 2.

To determine which functionality, pyridine or pyrazine, is the most potent group for R_2 , targets **S3I-H204**, **S3I-H222**, **S3I-H230**, **S3I-H235**, **S3I-H233**, **S3I-H244**, and **S3I-H245** were compared to their pyridine or pyrazine analogs (**Figure 7**, **Figure 11**). Additionally, targets

S3I-212, S3I-H224, S3I-H230, S3I-H228, S3I-H237, S3I-H239, and S3I-H244 were compared to their difluorocyanobenzenesulfonamide or pentafluorobenzenesulfonamide analogs to determine which functionality is optimal in R₃ (**Figure 7, Figure 11**). Various functionalities on the aromatic ring in R₄ were examined in hopes of increasing the potency, metabolic stability, and cellular permeability (**Figure 7, Figure 11**).



Chapter 2

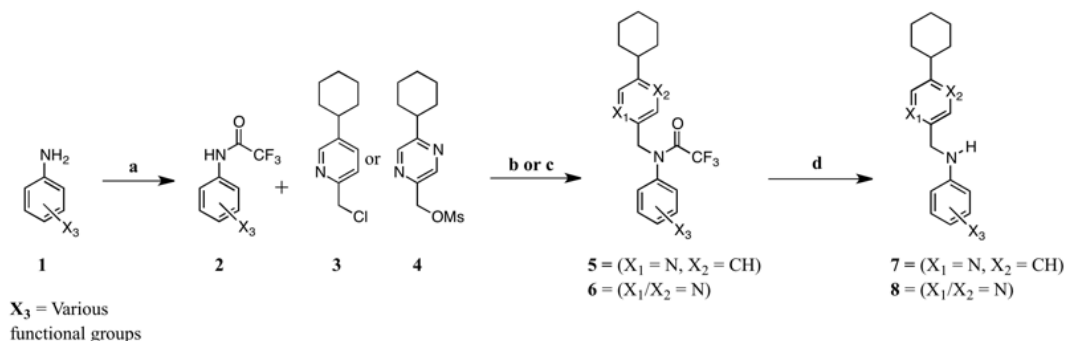
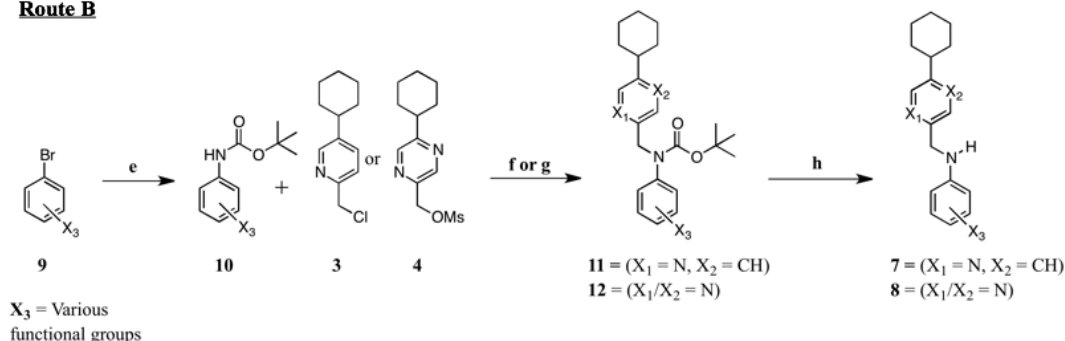
Synthesis of the Targeted Small Molecule STAT3 Inhibitors

2.1 Proposed Synthetic Routes for the Targeted STAT3 Inhibitors

All of the targeted STAT3 inhibitors shown in **Figure 11** are based on the azetidinamide scaffold and have two amine groups condensed with three different functionalities. It was envisioned that each target could be synthesized using common synthetic routes developed by our group, and derivatized further if necessary.^{19, 22} Our group has developed a convergent synthesis of our core scaffolds, in which **3**, **17**, and **20** are made in bulk (**Scheme 1**, **Scheme 2**).

The synthesis of *N*-((5-cyclohexylpyridin-2-yl)methyl)aniline **7** and *N*-((5-cyclohexylpyrazin-2-yl)methyl)aniline **8** precursors could proceed by previously developed synthetic routes A and B (**Scheme 1**).²² Using route A, aniline **1** can easily be converted to its trifluoroacetamide derivative **2** using TFAA and pyridine (route A; reaction a).²³ A S_N2 reaction with catalytic iodide can be used to convert trifluoroacetamide **2** to its *N*-((5-cyclohexylpyridin-2-yl)methyl)trifluoroacetamide **5** and *N*-((5-cyclohexylpyrazin-2-yl)methyl)trifluoroacetamide **6** derivatives (route A; reactions b and c).²² Subsequent deprotection of **5** or **6** with potassium carbonate in MeOH/THF will yield the desired *N*-((5-cyclohexylpyridin-2-yl)methyl)aniline **7** and *N*-((5-cyclohexylpyrazin-2-yl)methyl)aniline **8** precursors (route A; reaction d).²⁵

Alternatively, the synthesis of *N*-((5-cyclohexylpyridin-2-yl)methyl)aniline **7** and *N*-((5-cyclohexylpyrazin-2-yl)methyl)aniline **8** precursors could proceed by synthetic route B (route B; **Scheme 1**). Using Buchwald-Hartwig amidation conditions, bromobenzene **9** can be transformed into its *tert*-butyl carbamate derivative **10** (route B; reaction e).²⁶ Reacting carbamate **10** with 2-(chloromethyl)-5-cyclohexylpyridine **3** or (5-cyclohexylpyrazin-2-yl)methyl methanesulfonate **4** using typical S_N2 reaction conditions should provide carbamates **11** or **12** (route B; reactions f and g).²² Deprotection of **11** and **12** with TFA should yield the desired aniline precursors **7** and **8** respectively (route B; reaction h).²⁷

Route A**Route B**

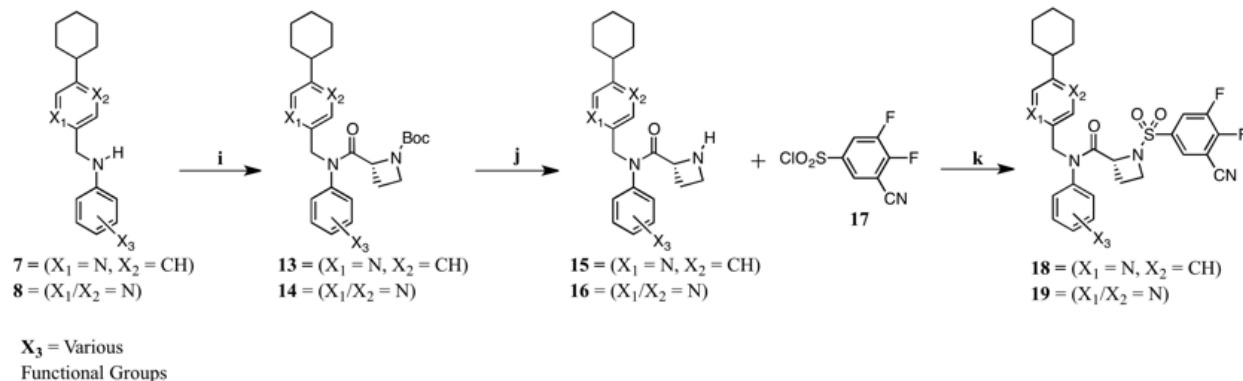
Scheme 1: Proposed Synthetic Routes A and B for the Synthesis of *N*-((5-cyclohexylpyridin-2-yl)methyl)aniline **7** and *N*-((5-cyclohexylpyrazin-2-yl)methyl)aniline **8**^a

^aReagents and Conditions: **Route A** – (a) TFAA, pyridine, DCM, 0 to 25 °C; (b) **3**, NaI (cat.), K₂CO₃, ACN, 65 °C; (c) **4**, NaI, K₂CO₃, ACN, 60 °C; (d) K₂CO₃, THF/MeOH, 25 °C; **Route B** – (e) *t*-butyl carbamate, Pd(OAc)₂, Xantphos, Cs₂CO₃, dioxane, 100 °C; (f) **3**, KHMDS, DMF, 0 to 25 °C; (g) **4**, KHMDS, DMF, 0 to 25 °C; (h) TFA, DCM, 25 °C

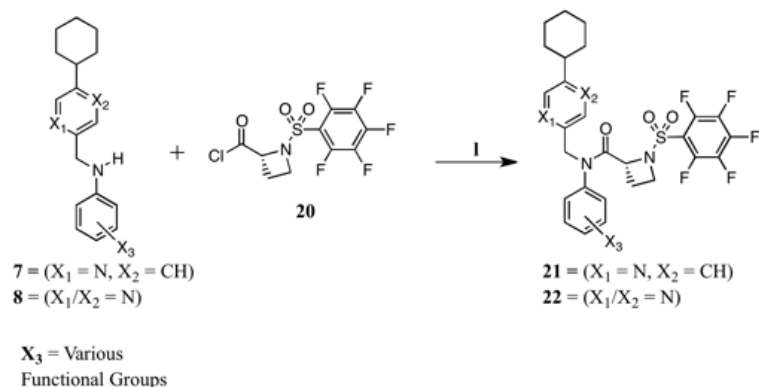
For the synthesis of the targets (**S3I-H204**, **S3I-H212**, **41**, **S3I-H222**, **S3I-H230**, **S3I-H235**, **S3I-H237**, **S3I-H244**, and **S3I-H245**) in which R₃ is difluorocyanobenzenesulfonamide, synthetic route C will be utilized (**Figure 7**, **Figure 11**, **Scheme 2**). Anilines **7** and **8** can be converted to their anilide derivatives **13** and **14** using MeMgBr and (*R*)-tert-butyl-2-(chlorocarbonyl)azetidine-1-carboxylate (route C; reaction i, **Scheme 2**).²² Azetidine deprotection of anilides **13** and **14** with TFA will yield amines **15** and **16** (route C; reaction j).²⁸

Subsequent reaction of amines **15** and **16** with 3-cyano-4,5-difluorobenzene-1-sulfonyl chloride **17** will yield the pyridine and pyrazine core scaffolds **18** and **19** for the synthetic targets (route C; reaction k).²² For the synthesis of targets (**S3I-H224**, **S3I-H233**, **S3I-H228**, and **S3I-H239**) containing the pentafluorobenzenesulfonamide functionality in R₃ it was imagined that synthetic route D could be used (**Figure 7**, **Figure 11**, **Scheme 2**). Reaction of anilines **7** and **8** with **20** using MeMgBr will yield the pyridine and pyrazine scaffolds **21** and **22**, respectively, for the synthetic targets (route D; reaction l, **Scheme 2**).²²

Route C



Route D



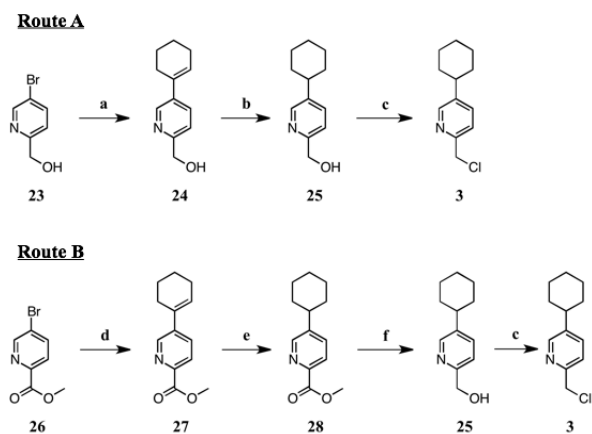
Scheme 2: Proposed Synthetic Routes C and D for the Synthesis of the Difluorocyanobenzenesulfonamide Core Scaffolds (**18** and **19**) and the Pentafluorobenzenesulfonamide Core Scaffolds (**21** and **22**)^a

^aReagents and Conditions: **Route C** – (i) MeMgBr, (*R*)-*tert*-butyl-2-(chlorocarbonyl)azetidine-1-carboxylate, THF, 0 to 25 °C; (j) TFA, DCM, 25 °C; (k) **17**, DIPEA, DCM, 0 to 25 °C; **Route D** – (l) MeMgBr, **20**, THF, 0 to 25 °C

2.2 Synthesis of S3I-H204

For the synthesis of **S3I-H204** synthetic routes A (**Scheme 1**) and C (**Scheme 2**) were utilized. Synthesis of **S3I-H204** commenced with the synthesis of **3** at the gram scale (**Scheme 3**). Synthetic route A, a synthetic route developed by previous group members, was first attempted to synthesize **3**.²² However, the conversion of **23** to **24** using standard Suzuki reaction conditions produced **24** in low yield, 45% (route A; reaction a).²² The poor yield of this reaction may be because **23** is chelating the palladium catalyst thereby inhibiting cross-coupling. Subsequent reduction of **24** to **25** and conversion of **25** to alkyl chloride **3** proceeded efficiently and duplicated previously reported yields by the group (route A; reactions b and c).²²

In an attempt to increase the yield of the Suzuki cross-coupling reaction, synthetic route B was developed (route B, **Scheme 3**). Satisfyingly, **26** was converted to **27** in good yield, 82%, using standard Suzuki cross-coupling conditions (route B; reaction d). A higher yield was obtained in the Suzuki reaction with the pyridyl ester **26** compared to the pyridyl alcohol **23** because chelation of Pd⁰ by the pyridyl ester is less efficient than by the pyridyl alcohol. Reduction of **27** using Adams' catalyst in the presence of hydrogen gas gave **28** in excellent yield, 96% (route B; reaction e).²² Reduction of ester **28** to form (5-cyclohexylpyridin-2-yl) methanol **25** was accomplished using NaBH₄ and NaOMe in 80% yield (route B; reaction f).³⁰ The purpose of NaOMe in this reaction is to stabilize NaBH₄ in methanol and it is postulated that NaBH₃OMe is the active reducing agent.³⁰ Subsequent reaction of **25** with thionyl chloride gave 1 gram of alkyl chloride **3** in quantitative yield (route B; reaction c).²²



Scheme 3: Synthetic Routes A and B for the Synthesis of 2-(chloromethyl)-5-cyclohexylpyridine **3^a**

^aReagents and Conditions: **Route A** - (a) Pd(OAc)₂ (0.5 eq), SPhos (0.1 eq), cyclohex-1-en-1-yl boronic acid (3.0 eq), K₃PO₄ (2.0 eq), HPLC-grade H₂O (2.0 eq), THF, 40 °C, 24 h, 45%; (b) PtO₂ (0.1 eq), H₂ (g), 1:1 EtOAc/MeOH, 25 °C, 4 h, 94%; (c) SOCl₂ (1.5 eq), DCM, 0 to 25 °C, 3 h, quantitative yield; **Route B** - (d) Pd(OAc)₂ (0.5 eq), SPhos (1.0 eq), cyclohex-1-en-1-yl boronic acid (2.0 eq), K₃PO₄ (2.0 eq), HPLC-grade H₂O (2.0 eq), THF, 40 °C, 24 h, 82%; (e) PtO₂ (0.1 eq), H₂ (g), 1:1 EtOAc/MeOH, 25 °C, 4 h, 96%; (f) NaBH₄ (7.0 eq), NaOMe (1.1 eq), MeOH, 50 °C, 3 h, 80%.

The synthetic route to **S3I-H204** is outlined in **Scheme 4**. Reduction of **29** with iron powder and ammonium chloride gave amine **30** in 91% yield (reaction a).^{22, 31} It should be noted that reaction (a) is heterogeneous and requires vigorous stirring. Slow stirring of the reaction mixture leads to the formation of byproduct **39**, which is difficult to separate from **30** using flash chromatography (**Figure 12**). The mechanism for the conversion of **29** to **30** using Fe/NH₄Cl involves reduction of the nitro group by single electron transfer (SET) from iron. It is unclear how byproduct **39** is formed mechanistically due to the lack of literature on the formation of hydrazines from nitrobenzenes using iron. Formation of hydrazines from nitroarenes by SET from magnesium has been reported and the mechanism is shown in **Figure 12**.³⁴ Byproduct **39** may be formed by a similar mechanism when iron is the reducing agent.

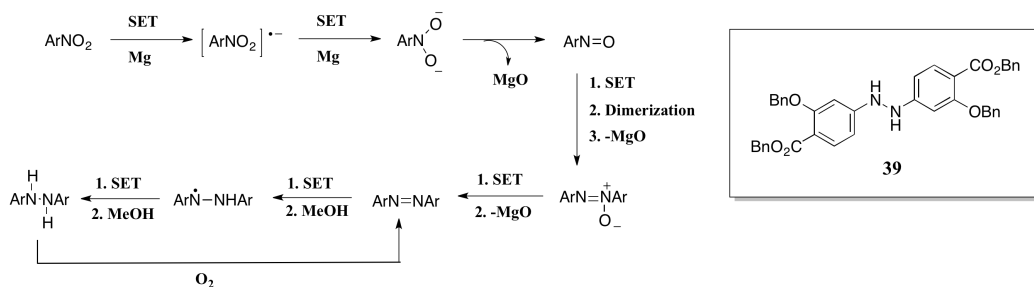
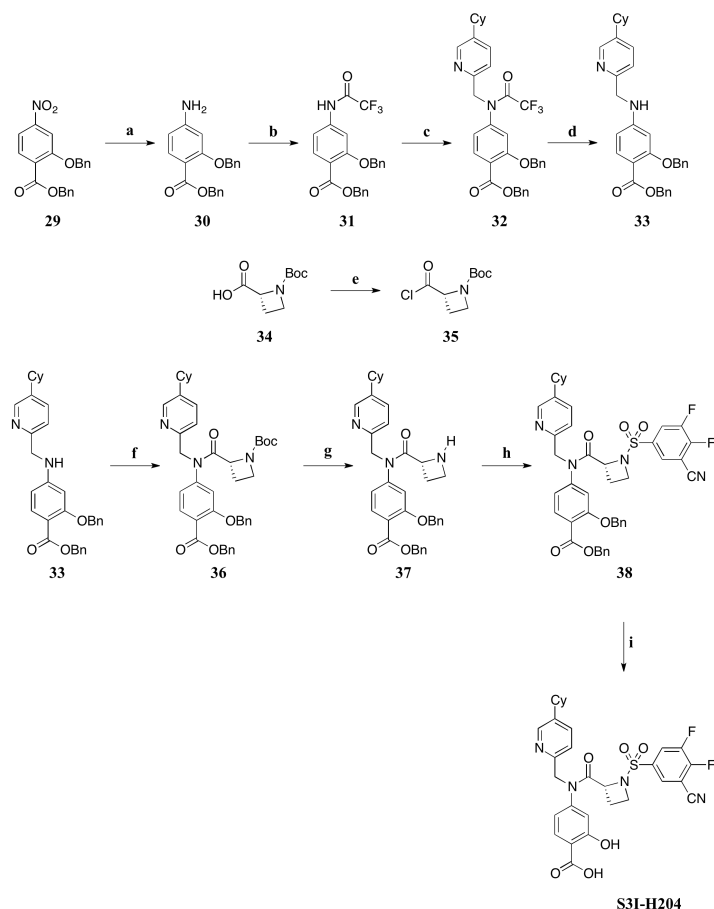


Figure 12. Mechanism for the Formation of Hydrazine with Magnesium and Structure of the Byproduct from Reaction (a), Scheme 4

Reaction of amine **30** with TFAA and pyridine gave trifluoroacetamide **31** in 84% yield (reaction b).^{22,23} A S_N2 reaction in the presence of catalytic NaI was used to convert **31** into trifluoroacetamide **32** in 64% yield (reaction c).²² Deprotection of **32** proceeded smoothly with K_2CO_3 giving amine **33** (reaction d).^{22,25}

For the synthesis of anilide **36**, precursor **35** needed to be synthesized first. Commercially available carboxylic acid **34** was converted to acid chloride **35** in quantitative yield using oxalyl chloride and catalytic DMF (reaction e).²² Reaction of amine **33** with freshly prepared **35** in the presence of MeMgBr produced anilide **36** in 75% yield (reaction f).²² Successive deprotection of **36** with TFA gave amine **37** (reaction g).^{22,28} Reaction of amine **37** with **17** in the presence of DIPEA produced sulfonamide **38** in 60% yield over two steps (reaction h).²² Finally, deprotection of **38** with 1:1 palladium on carbon/ $Pd(OH)_2$ under an atmosphere of hydrogen produced **S3I-H204** in 50% yield (reaction i).²² It should be noted that in reaction (i), palladium is acting as a catalyst, but it is being poisoned. The pyridyl and amine functionalities in intermediate **38** are likely interacting with palladium inhibiting turnover. The poor yield in reaction (i) can be attributed to the formation of unknown side-products which likely formed from the large amount of palladium used which is required to make this reaction go to completion.



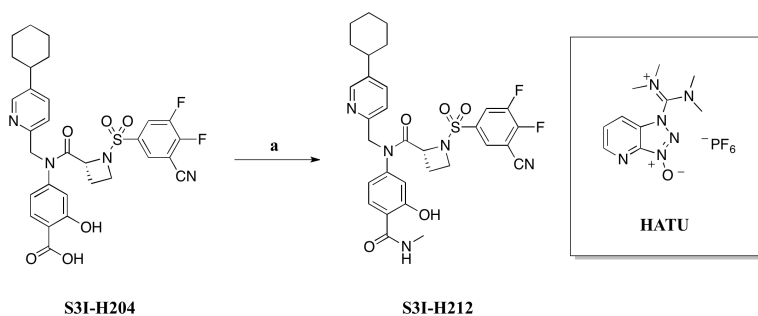
Scheme 4: Synthesis of S3I-H204^a

^aReagents and Conditions: (a) Iron powder (7.0 eq), NH₄Cl (10.2 eq), 2:1 EtOH/HPLC-grade H₂O, 66 °C, 16 h, 91%; (b) TFAA (1.1 eq), pyridine (2.2 eq), DCM, 0 to 25 °C, 3.5 h, 84%; (c) **3** (1.4 eq), NaI (0.2 eq), K₂CO₃ (2.0 eq), ACN, 65 °C, 24 h, 64%; (d) K₂CO₃ (2.0 eq), 1:1 THF/MeOH, 25 °C, 20 h, 98%; (e) (COCl)₂ (1.2 eq), cat. DMF, DCM, 25 °C, 1.5 h, quantitative yield; (f) MeMgBr (2.5 eq), **35** (2.1 eq), THF, 0 to 25 °C, 1.2 h, 75%; (g) TFA (37 eq), DCM, 25 °C, 1.5 h; (h) **17** (2.0 eq), DIPEA (5.0 eq), DCM, 0 to 25 °C, 2.2 h, 60% (yield over two steps); (i) H₂ (g), 42 wt% 1:1 Pd/C: Pd(OH)₂, 1:1 EtOAc/MeOH, 25 °C, 23 h, 50%

2.3 Synthesis of S3I-H212

To synthesize compound **S3I-H212**, **S3I-H204** was derivatized using typical peptide coupling conditions (reaction a, **Scheme 5**).³² Addition of HATU to a solution of **S3I-H204** in DCM in the presence of DIPEA generated the activated ester which was subsequently reacted with methylamine to form **S3I-H212** (reaction a). Unfortunately, this reaction gave the product

in a very low yield, 9%. One significant side-product confirmed by ^1H NMR and mass spectrometry analysis was **40**, formed from an $\text{S}_{\text{N}}\text{Ar}$ reaction of methylamine with the difluorocyanobenzenesulfonamide (**Figure 13**). Reducing the amount of methylamine in reaction (a) will most likely suppress the formation of side-product **40**, because methylamine should react faster with the activated ester than with difluorocyanobenzene (**Figure 13**). In the context of biological activity, side-product **40** illustrates the importance of the difluorocyanobenzene functionality which is labile to attack by cysteine residues in the DNA binding domain of STAT3. The $\text{S}_{\text{N}}\text{Ar}$ reaction of a cysteine residue with the difluorocyanobenzene functionality is crucial for inhibiting the interaction of STAT3 with DNA.



Scheme 5: Synthesis of **S3I-H212^a** and the Structure of HATU

^aReagents and Conditions: (a) HATU (1.0 eq), DIPEA (1.9 eq), methylamine (1.7 eq), DCM, 0 to 25 °C for 1.5 h then −10 °C for 3.8 h, 9%

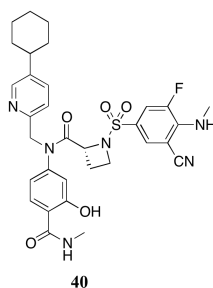
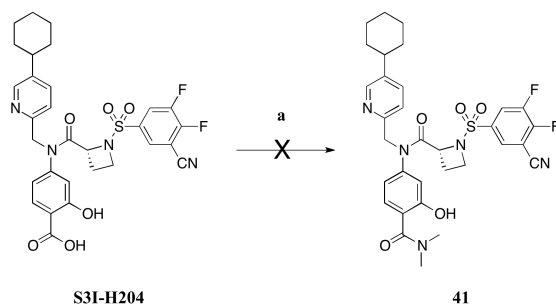


Figure 13. Side-product of Reaction (a), Scheme 5

2.4 Attempts at Synthesizing Compound 41

In an attempt to synthesize compound **41**, **S3I-H204** was activated using HATU and reacted with dimethylamine in the presence of DIPEA (reaction a, **Scheme 6**).²³ In the hope of suppressing the S_NAr side product, **42** (**Figure 14**), a substoichiometric amount of dimethylamine was used. Unfortunately, reaction (a) produced many side products as indicated by TLC and LCMS. Product **41** was detected by LCMS, but could not be isolated in pure form. Reaction (a) in **Scheme 6** was not optimized, because **S3I-H204** was used up in the initial attempt to synthesize **41**. Instead an alternative route (**Scheme 7**) for the synthesis of **41** was pursued.



Scheme 6: First Attempt at Synthesizing **41**^a

^aReagents and Conditions: HATU (1.0 eq), DIPEA (1.9 eq), HN(CH₃)₂ (0.86 eq), DCM, 0 to 25 °C for 1.5 h then −10 °C for 3.8 h, 0 %

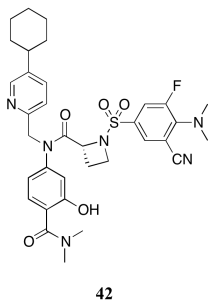


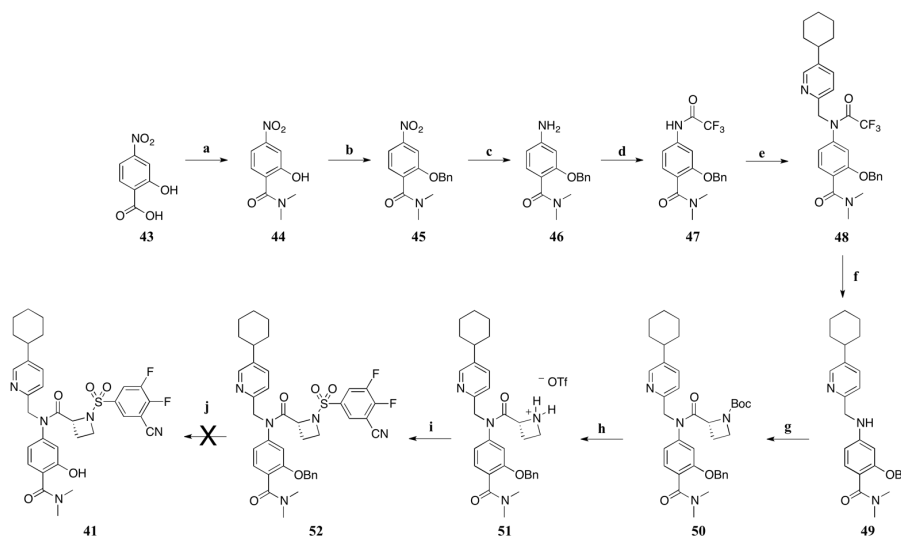
Figure 14. Side-product for Reaction (a), Scheme 6

The second route that was used in an attempt to synthesize **41** is shown in **Scheme 7**. The attempted synthesis of **41** began by first transforming **43** to its amide derivative **44** using standard peptide coupling conditions (reaction a).³² The phenol in intermediate **44** was protected using BnBr in the presence of K₂CO₃ giving **45** in good yield, 84% (reaction b).²² Reduction of **45** gave aniline **46** and was accomplished using iron powder and NH₄Cl as previously discussed (reaction c).^{22, 31} Aniline **46** was reacted with TFAA in the presence of pyridine producing **47** in 71% yield (reaction d).^{22,23} A S_N2 reaction in the presence of catalytic NaI was used to convert **47** into trifluoroacetamide **48** (reaction e).²² Deprotection of trifluoroacetamide **48** using K₂CO₃ gave amine **49** in 80% yield over two steps (reaction f).^{22,25} Reacting amine **49** with **35** in the presence of MeMgBr produced anilide **50** in 66% yield (reaction g).²² Deprotection of anilide **50** with TFA gave the trifluoroacetate salt of amine **51** (reaction h).^{22,28} Reacting **51** with **17** in the presence of DIPEA produced sulfonamide **52** in 76% yield over two steps from **50** (reaction i).²²

Unfortunately, deprotection of **52** using 40% by weight Pd/C and 30% by weight Pd(OH)₂ under a hydrogen atmosphere was problematic (reaction j1). Intermediate **52** was consumed completely and product **41** could not be detected by ¹H NMR or mass spectrometry. Unfortunately, the major product in reaction (j1) could not be determined by ¹H NMR analysis. A smaller amount of Pd(OH)₂ was used in reaction (j2) in the hope of suppressing the formation of the unknown compound. Satisfyingly, the desired product **41** was produced as a minor product as indicated by LCMS, but could not be isolated. Compound **41** could not be identified by ¹H NMR due to the large amount of impurities present in the sample. However, LCMS can be used to confirm the structure of **41** because the precursor **52** was fully characterized by ¹H NMR and HRMS.

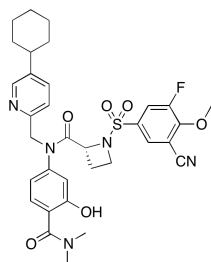
Additionally, the major product in reaction (j2) as detected by LCMS was again the unidentified compound. These results suggest that Pearlman's catalyst may be leading to the formation of the unidentified compound in reactions (j1) and (j2).

In reaction (j3), **52** was deprotected using 16% by weight Pd/C in the presence of a hydrogen atmosphere. Compound **41** was produced as the major product as indicated by LCMS. Unfortunately, **41** could not be isolated in pure form from reaction (j3). Purification by PTLC with methanol/ethyl acetate as the eluting solvent led to the formation of an inseparable byproduct, **53** (**Figure 15**). Byproduct **53** was formed from a S_NAr reaction on the difluorocyanobenzene ring of **41**. The effort to optimize the debenzylation reaction was abandoned and synthesis of the pyrazine analog (**S3I-H222**) of **41** was pursued.



Scheme 7: Second Attempt at Synthesizing **41^a**

^aReagents and Conditions: (a) HATU (1.0 eq), DIPEA (0.9 eq), $NHMe_2$ (1.5 eq), DCM, 0 to 25 °C, 26 h, 54%; (b) K_2CO_3 (1.2 eq), BnBr (1.1 eq), DMF, 25 °C, 32 h, 84%; (c) Iron powder (7.0 eq), NH_4Cl (10.2 eq), EtOH/HPLC-grade H_2O , 66 °C, 20 h, 87%; (d) TFAA (1.1 eq), pyridine (2.2 eq), DCM, 0 to 25 °C, 1.5 h, 71%; (e) **3** (2.0 eq), K_2CO_3 (2.0 eq), NaI (0.2 eq), ACN, 65 °C, 24 h; (f) K_2CO_3 (2.0 eq), 1:1 THF/MeOH, 25 °C, 16 h, 80% over two steps; (g) MeMgBr (2.5 eq), **35** (2.1 eq), THF, 0 to 25 °C, 1.2 h, 66%; (h) TFA (37 eq), DCM, 25 °C, 1.5 h; (i) **17** (2.0 eq), DIPEA (6.0 eq), DCM, 0 to 25 °C, 1.7 h, 76% over two steps; (j1) H_2 (g), 40 wt% Pd/C, 30 wt% $Pd(OH)_2$, 3:1 EtOAc/MeOH, 25 °C, 48 h, 0%; (j2) H_2 (g), 12 wt% $Pd(OH)_2$, 1:1 EtOAc/MeOH, 25 °C, 48 h, 0%; (j3) H_2 (g), 16 wt% Pd/C, 1:4 EtOAc/MeOH, 25 °C, 72 h, 0%



53

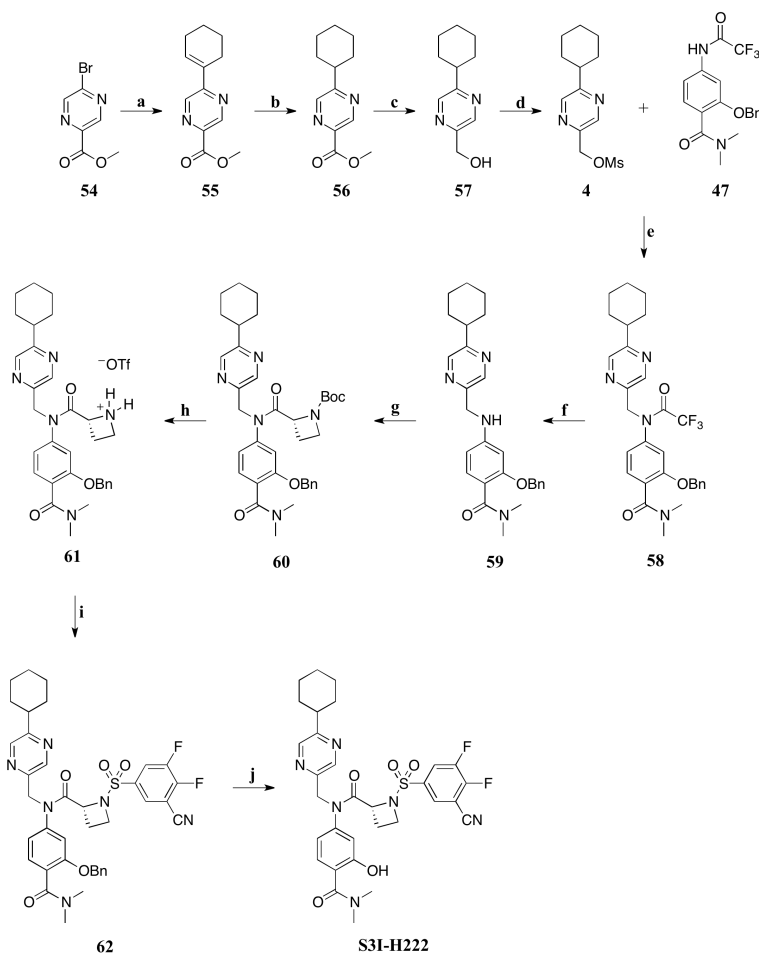
Figure 15. Structure of Byproduct **53** from Reaction (j3), Scheme 7

2.5 Synthesis of S3I-H222

The synthetic route to **S3I-H222** is shown in **Scheme 8**. Commercially available methyl 5-bromopyrazine-2-carboxylate **54** was coupled with cyclohex-1-en-1-ylboronic acid producing **55** using standard Suzuki reaction conditions (reaction a).²² Reduction of **55** using PtO₂ under a hydrogen atmosphere gave **56** in 52% yield (reaction b).²² The poor yield in reaction (b) is due to reduction of the pyrazine ring. Reduction of ester **56** using NaBH₄ furnished the alcohol **57** in good yield, 84% (reaction c).²² Alcohol **57** was transformed into **4** using MsCl in the presence of TEA (reaction d).²²

Due to the instability of compound **4** it was reacted immediately with trifluoroacetamide **47** using S_N2 reaction conditions to give **58** in excellent yield, 97% (reaction e).²² Facile deprotection of **58** using K₂CO₃ in methanol produced **59** in quantitative yield, 99% (reaction f).^{22,25} Anilide **60** was produced by reacting amine **59** with acid chloride **35** in the presence of MeMgBr (reaction g).²² Deprotection of anilide **60** produced trifluoroacetate salt **61** (reaction h).^{22,28} Reacting **61** with sulfonyl chloride **17** in the presence of base led to the formation of sulfonamide **62** in good yield, 78% over two steps from **60** (reaction i).²² Finally, debenzylation of **62** and subsequent purification via PTLC using methanol/ethyl acetate as an eluting solvent produced the desired compound **S3I-H222** in 44% yield (reaction j).²² The poor yield in reaction (j) is attributed to the formation of unknown side-products and the presence of

unreacted **62**. It is unclear why **S3I-H222** can be isolated using a PTLC purification method with methanol/ethyl acetate as an eluting solvent while its pyridine analog **41** cannot be.

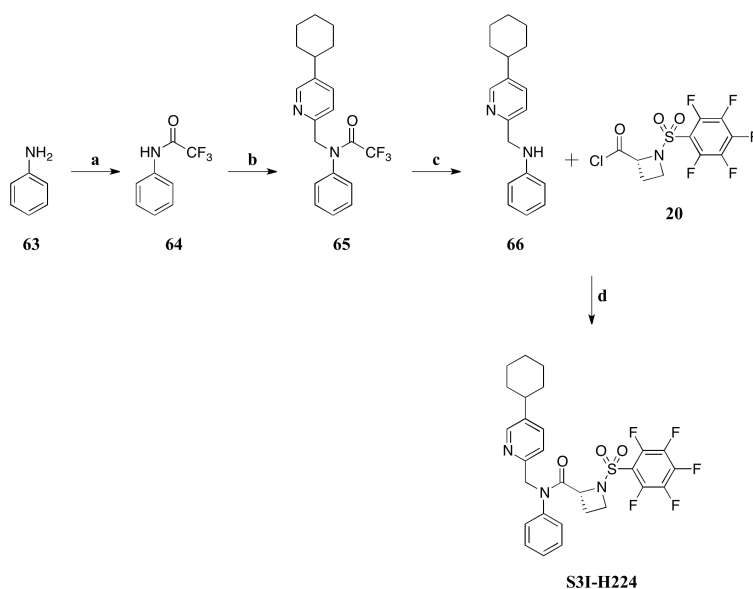


Scheme 8: Synthesis of S3I-H222^a

^aReagents and Conditions: (a) Pd(OAc)₂ (0.05 eq), SPhos (0.1 eq), K₃PO₄ (2.0 eq), cyclohex-1-en-1-ylboronic acid (1.5 eq), HPLC-grade H₂O (2.0 eq), THF, 40 °C, 22 h, 83%; (b) H₂ (g), PtO₂ (0.1 eq), 1:1 EtOAc/MeOH, 25 °C, 20.5 h, 52%; (c) NaBH₄ (3.0 eq), MeOH, 0 to 25 °C, 27 min, 84%; (d) MsCl (1.86 eq), TEA (3.0 eq), DCM, 0 °C, 32 min, 84%; (e) **4** (1.3 eq), K₂CO₃ (4.0 eq), NaI (0.38 eq), ACN, 60 °C, 14 h, 97%; (f) K₂CO₃ (2.0 eq), 1:1 THF/MeOH, 25 °C, 1.5 h, 99%; (g) MeMgBr (2.5 eq), **35** (2.1 eq), THF, 0 to 25 °C, 1.2 h, 75%; (h) TFA (37 eq), DCM, 25 °C, 1.5 h; (i) **17** (2.0 eq), DIPEA (8.0 eq), DCM, 0 to 25 °C, 1.7 h, 78% yield over two steps; (j) H₂ (g), 20 wt% Pd/C, 1:4 EtOAc/MeOH, 25 °C, 24 h, 44%

2.6. Synthesis of S3I-H224

For the synthesis of **S3I-H224** synthetic routes A (**Scheme 1**) and D (**Scheme 2**) were utilized. The synthetic route to **S3I-H224** is displayed in **Scheme 9**. Amidation of commercially available aniline **63** produced trifluoroacetamide **64** in 87% yield (reaction a).^{22,23} Exposure of trifluoroacetamide **64** to alkyl chloride **3** under S_N2 reaction conditions produced **65** in 57% yield (reaction b).²² The low yield in reaction (b) is attributed to starting material that was not consumed in the reaction. Deprotection of trifluoroacetamide **65** under basic conditions proceeded smoothly, forming aniline **66** in good yield (91%, reaction c).^{22,25} Reaction of aniline **66** with acid chloride **20** using standard peptide coupling conditions led to the formation of **S3I-H224** in moderate yield, 53% (reaction d).²² A potential side product in reaction (d) may be from aniline **66** reacting with the pentafluorobenzene moiety of **20** through a S_NAr reaction.



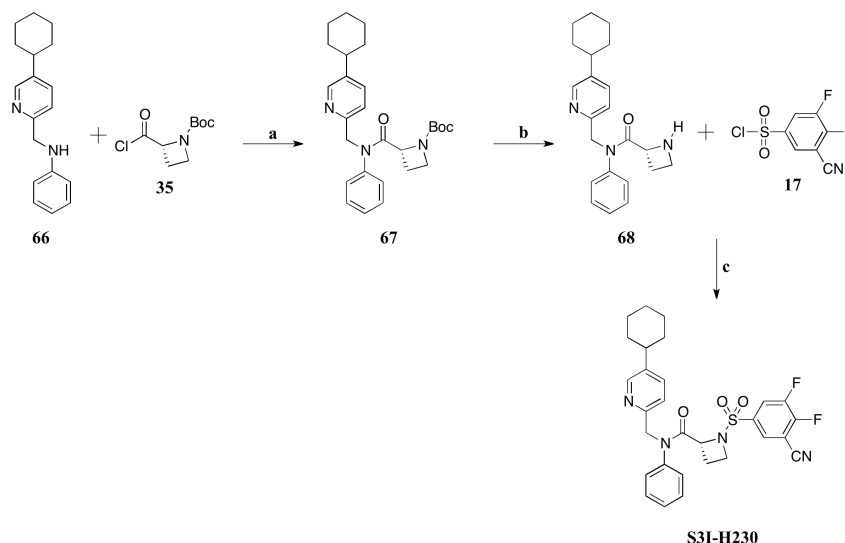
Scheme 9: Synthesis of **S3I-H224**^a

^aReagents and Conditions: (a) TFAA (1.3 eq), pyridine (2.2 eq), DCM, 0 to 25 °C, 1.5 h, 88%; (b) **3** (2.0 eq), NaI (0.2 eq), K₂CO₃ (2.0 eq), ACN, 65 °C, 24 h, 57%; (c) K₂CO₃ (2.0 eq), 1:1 THF/MeOH, 25 °C, 23 h, 91%; (d) **20** (1.5 eq), MeMgBr (2.5 eq), THF, 0 to 25 °C, 1 h, 53%

2.7 Synthesis of S3I-H230

Synthetic route C (Scheme 2) was followed to synthesize **S3I-H230** (Scheme 10).

Aniline **66**, previously synthesized as discussed in section 2.6, was reacted with acid chloride **35** under peptide coupling reaction conditions producing **67** (reaction a).²² Side-products from reaction (a) could not be fully separated from anilide **67**. Deprotection of impure anilide **67** in the presence of acid produced amine **68** in 42% over two steps from **66** (reaction b).^{22,28} Reaction of amine **68** with sulfonyl chloride **17** using DIPEA as a base produced the final product **S3I-H230** in 59% yield (reaction c).²² A potential side product contributing to the low yield in reaction (c) could again be from amine **68** reacting with the difluorocyanobenzene functionality of **17** through a S_NAr reaction.

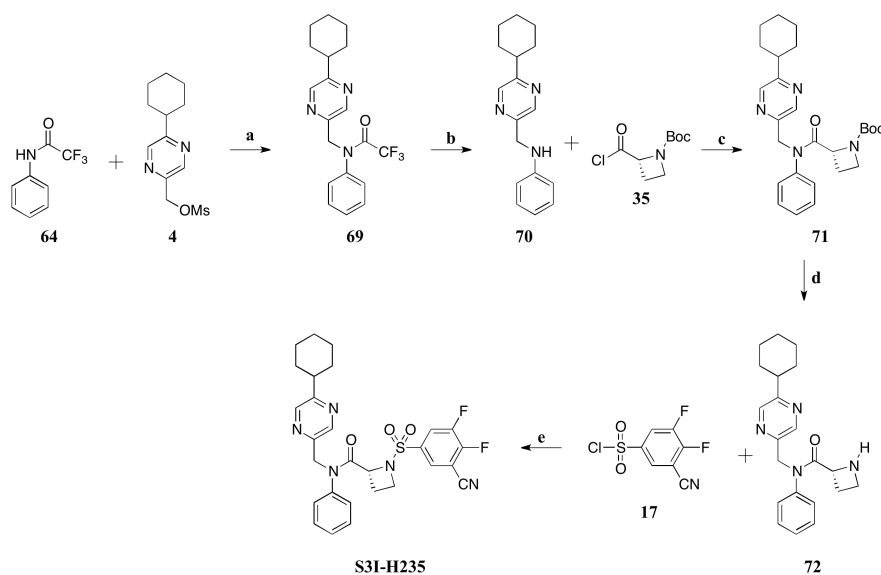


Scheme 10: Synthesis of **S3I-H230**^a

^aReagents and Conditions: (a) **35** (2.1 eq), MeMgBr (2.5 eq), THF, 0 to 25 °C, 1.2 h; (b) TFA (37 eq), DCM, 25 °C, 1.5 h, 42% over two steps from **66**; (c) **17** (2.0 eq), DIPEA (5.0 eq), DCM, 0 to 25 °C, 1.7 h, 59%

2.8 Synthesis of S3I-H235

For the synthesis of **S3I-H235** (Scheme 11) synthetic routes A (Scheme 1) and C (Scheme 2) were followed. Trifluoroacetamide **64** was exposed to **4** under S_N2 reaction conditions forming **69** in good yield, 85% (reaction a).²² Deprotection of **69** using K_2CO_3 produced **70** in 88% yield (reaction b).^{22,25} Anilide **71** was formed from the reaction of aniline **70** with acid chloride **35** using MeMgBr as a base (reaction c).²² Side-products from reaction (c) could not be fully separated from anilide **71** by column chromatography and acid/base washes. Impure anilide **71** was deprotected under acidic conditions giving amine **72** in 41% yield over two steps from **70** (reaction d).^{22,28} The final compound, **S3I-H235**, was produced in 78% yield from the reaction of amine **72** with sulfonyl chloride **17** in the presence of DIPEA (reaction e).²²

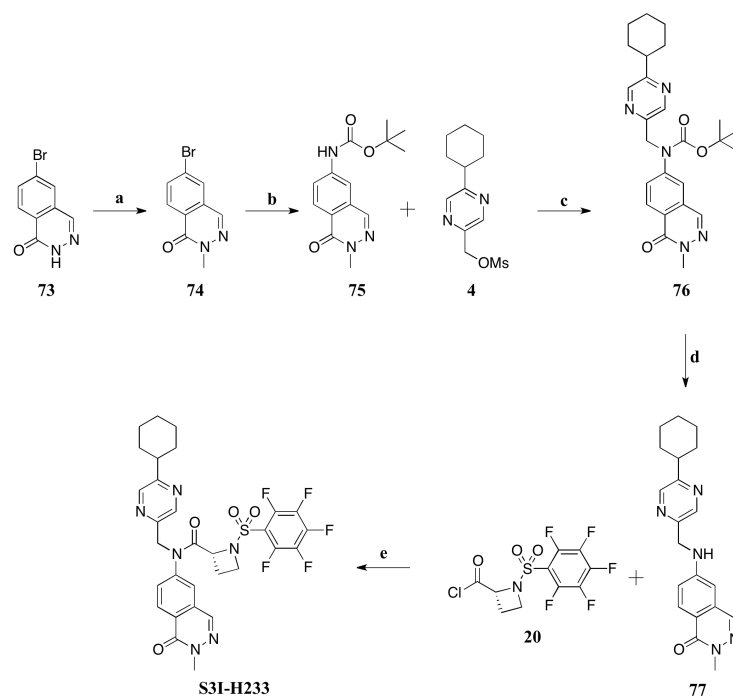


Scheme 11: Synthesis of S3I-H235^a

^aReagents and Conditions: (a) **4** (1.3 eq), K_2CO_3 (4.0 eq), NaI (0.38 eq), ACN, 60 °C, 18 h, 85%; (b) K_2CO_3 (2.0 eq), 1:1 THF/MeOH, 25 °C, 24 h, 88%; (c) **35** (2.1 eq), MeMgBr (2.5 eq), THF, 0 to 25 °C, 1.2 h; (d) TFA (37 eq), DCM, 25 °C, 1.5 h, 41% yield over two steps from **70**; (e) **17** (2.0 eq), DIPEA (5.0 eq), DCM, 0 to 25 °C, 1.7 h, 78%

2.9 Synthesis of S3I-H233

Target **S3I-H233** (**Scheme 12**) was synthesized by following routes B (**Scheme 1**) and D (**Scheme 2**). *N*-Methylation of commercially available phthalazinone **73** proceeded smoothly and produced **74** in 84% yield (reaction a).³³ The procedure reported in the literature for reaction (a) was followed although reaction times were slightly modified and the base was changed from NaH to KHMDS. Reaction of **74** with *t*-butyl carbamate using Buchwald-Hartwig amidation conditions produced carbamate **75** in good yield, 86% (reaction b).²² Carbamate **76** was formed in 85% yield by reacting **75** with **4** under standard S_N2 reaction conditions (reaction c).²² Deprotection of carbamate **76** using acid produced aniline **77** in 86% yield (reaction d).^{22,27} Reacting aniline **77** with acid chloride **20** using peptide coupling reaction conditions gave the final product **S3I-H233** in 38% yield (reaction e).²² Some side-products were formed in reaction (e) and aniline **77** was not fully consumed which contributed to the low yield. The phthalazinone functionality in aniline **77** may be withdrawing too much electron density from the nucleophilic nitrogen, thereby impeding the reaction of **77** with acid chloride **20**.



Scheme 12: Synthesis of S3I-H233^a

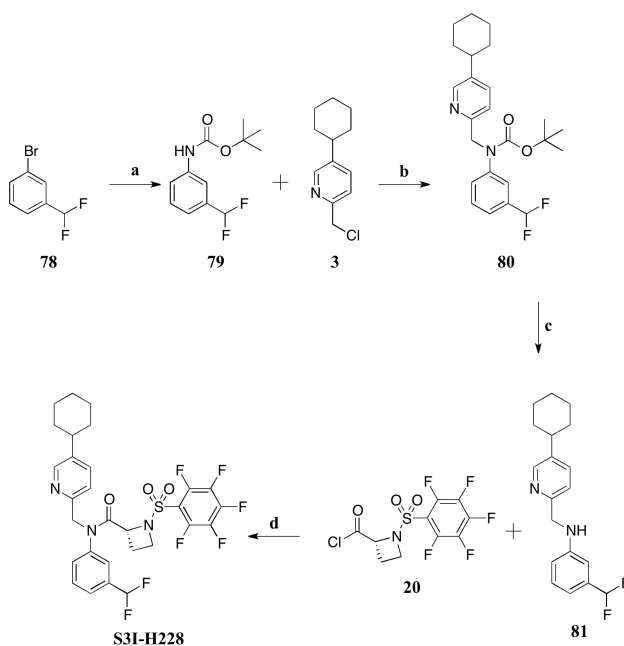
^aReagents and Conditions: (a) MeI (1.3 eq), KHMDS (1.2 eq), DMF, 0 to 25 °C, 23.2 h, 84%; (b) *t*-butyl carbamate (1.5 eq), Pd(OAc)₂ (0.05 eq), Xantphos (0.05 eq), Cs₂CO₃, dioxane, 100 °C, 23 h, 86%; (c) **4** (1.3 eq), KHMDS (1.3 eq), DMF, 0 to 25 °C, 15.5 h, 85%; (d) TFA (58 eq), DCM, 25 °C, 3 h, 86%; (e) **20** (1.5 eq), MeMgBr (1.3 eq), THF, 0 to 25 °C, 2.7 h, 38%

2.91 Synthesis of S3I-H228

The synthetic route for forming **S3I-H228** is displayed below in **Scheme 13**.

Commercially available 1-bromo-3-(difluoromethyl)benzene **78** was transformed into its carbamate derivative **79** in 63% yield using Buchwald-Hartwig coupling conditions (reaction a).²² Exposure of carbamate **79** to alkyl chloride **3** under S_N2 reaction conditions produced **80** in 86% yield (reaction b).²² Deprotection of carbamate **80** using TFA gave aniline **81** in 91% yield (reaction c).^{22,27} It was initially hypothesized that coupling aniline **81** with acid chloride **20** using a strong base like MeMgBr would lead to the formation of multiple products, because the pK_a of the amine and of the difluoromethyl methine proton in compound **81** are very similar.

To prevent the formation of multiple products in the final reaction, DMAP, an acyl transfer reagent, was utilized. Activation of acid chloride **20** with DMAP and subsequent reaction with aniline **81** led to the formation of the final product **S3I-H228** in good yield, 79% (reaction d).²²



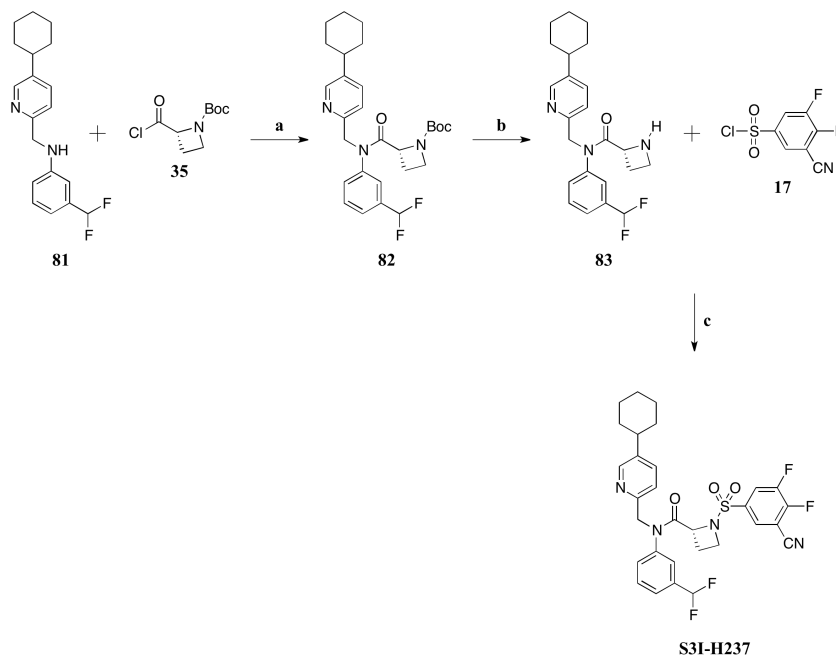
Scheme 13: Synthesis of **S3I-H228**^a

^aReagents and Conditions: (a) *t*-butyl carbamate (1.2 eq), Pd(OAc)₂ (0.05 eq), Xantphos (0.05 eq), Cs₂CO₃ (2.0 eq), dioxane, 100 °C, 18 h, 63%; (b) **3** (1.3 eq), KHMDS (1.3 eq), DMF, 0 to 25 °C, 24.2 h, 86%; (c) TFA (58 eq), DCM, 25 °C, 3 h, 91%; (d) **20** (1.1 eq), DMAP (1.1 eq), DCM, 0 to 25 °C, 24.2 h, 79%

2.92 Synthesis of S3I-H237

For the synthesis of **S3I-H237** (Scheme 14) synthetic route C (Scheme 2) was utilized. Aniline **81**, previously synthesized as discussed in section 2.91, was exposed to acid chloride **35** in the presence of MeMgBr producing anilide **82** in 63% yield (reaction a).²² Subsequent deprotection of **82** with TFA gave amine **83** (reaction b).^{22,28}

Unfortunately, reaction (b) led to the formation of many unidentified side products which could not be separated by column chromatography from amine **83**. Impure amine **83** was exposed to sulfonyl chloride **17** in the presence of DIPEA giving sulfonamide **S3I-H237** in 38% yield over two steps from **82** (reaction c).²²



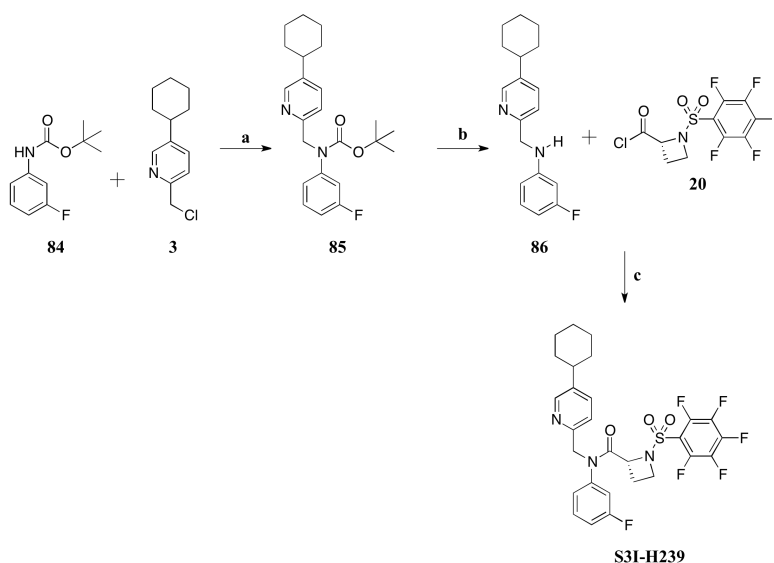
Scheme 14: Synthesis of **S3I-H237**^a

^aReagents and Conditions: (a) **35** (2.1 eq), MeMgBr (2.5 eq), THF, 0 to 25 °C, 1.2 h, 63%; (b) TFA (37 eq), DCM, 25 °C, 1.5 h; (c) **17** (2.0 eq), DIPEA (5.0 eq), DCM, 0 to 25 °C, 1.7 h, 38% yield over two steps from **82**

2.93 Synthesis of **S3I-H239**

Synthetic route B (**Scheme 1**) and a modified version of synthetic route D (**Scheme 2**) were used to prepare **S3I-H239** (**Scheme 15**). The synthesis of **S3I-H239** commenced by coupling carbamate **84** to alkyl chloride **3** using standard S_N2 reaction conditions to produce **85** in moderate yield 64% (reaction a).²² Subsequent deprotection of carbamate **85** in the presence of

acid led to the formation of aniline **86** in 72% yield (reaction b).^{22,27} It was initially thought that coupling aniline **86** with acid chloride **20** in the presence of a small strong nucleophilic base like MeMgBr might lead to the formation of unfavorable S_NAr side-products. To prevent the formation of any S_NAr side-products aniline **86** was coupled with acid chloride **20** in the presence of DMAP as a catalyst. This gave the final product **S3I-H239** in 46% yield (reaction c).²² Aniline **86** was not fully consumed in reaction (c) which contributed to the low yield.



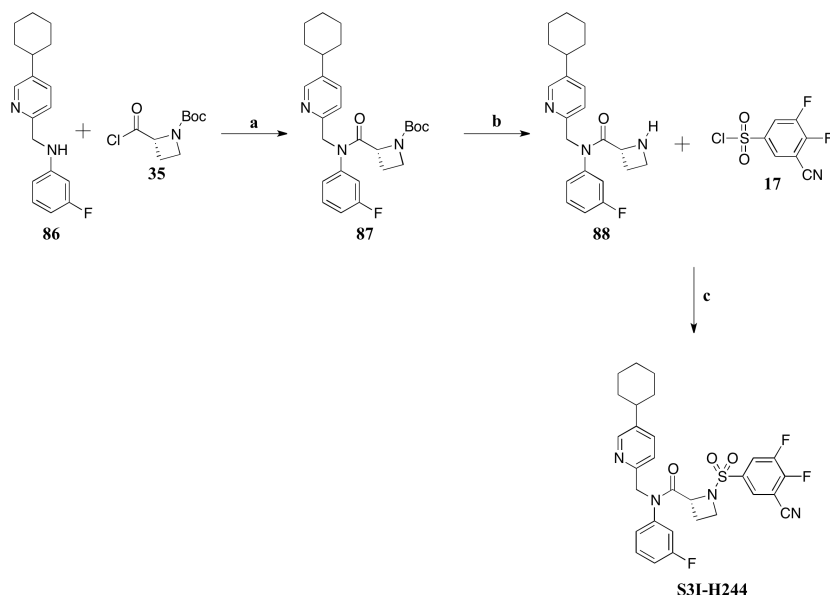
Scheme 15: Synthesis of S3I-H239^a

^aReagents and Conditions: (a) **3** (1.3 eq), KHMDS (1.3 eq), DMF, 0 to 25 °C, 20.2 h, 64%; (b) TFA (58 eq), DCM, 25 °C, 3 h, 72%; (c) **20** (1.1 eq), DMAP (1.1 eq), DCM, 0 to 25 °C, 24 h, 46%

2.94 Synthesis of S3I-H244

To prepare target **S3I-H244** (**Scheme 16**) synthetic route C (**Scheme 2**) was followed. Anilide **87** was formed in 60% yield using standard peptide coupling conditions (reaction a).²² The anionic form of **86** is much more reactive with acid chloride **35** compared to its neutral form (reaction c, **Scheme 15**). Removal of the Boc protecting group from intermediate **87** using TFA

resulted in a mixture of products that could not be fully separated from amine **88** by column chromatography (reaction b).^{22,28} Impure amine **88** was reacted with sulfonyl chloride **17** in the presence of Hünig's base producing the final compound **S3I-H244** in 57% yield over two steps from **87** (reaction c).²²



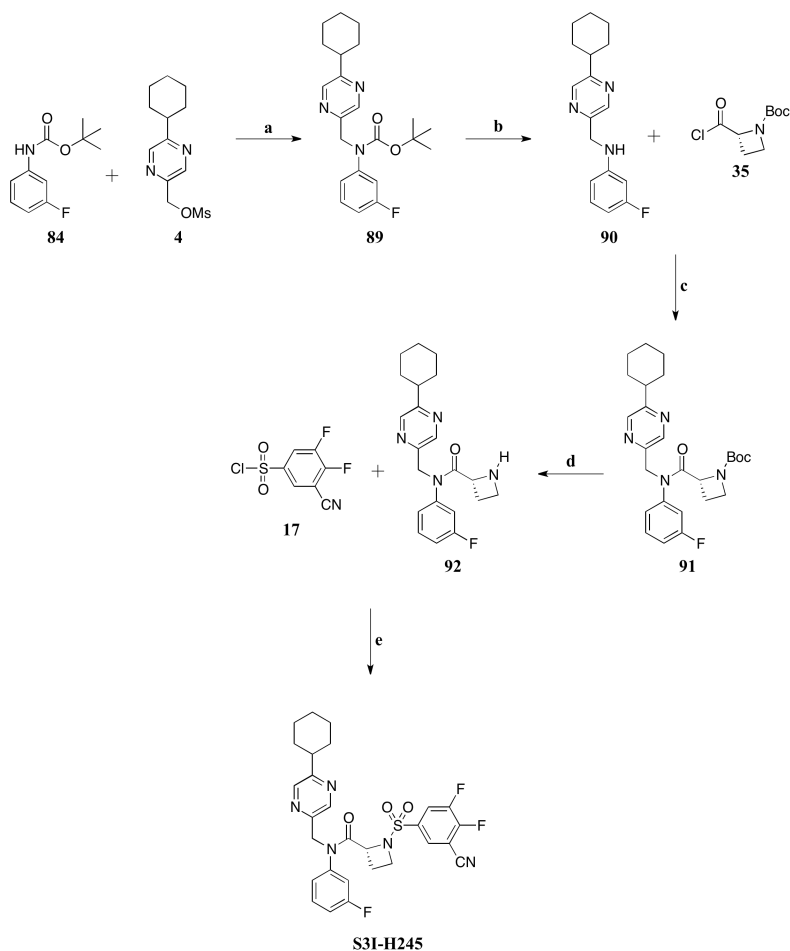
Scheme 16: Synthesis of **S3I-H244**^a

^aReagents and Conditions: (a) **35** (2.1 eq), MeMgBr (2.5 eq), THF, 0 to 25 °C, 1.2 h, 60%; (b) TFA (37 eq), DCM, 25 °C, 1.5 h; (c) **17** (2.0 eq), DIPEA (5.0 eq), DCM, 0 to 25 °C, 1.7 h, 57% yield over two steps from **87**

2.95 Synthesis of S3I-H245

Target **S3I-H245** (Scheme 17) was synthesized by following routes B (Scheme 1) and C (Scheme 2). Carbamate **84** was coupled with **4** under S_N2 reaction conditions producing **89** in 83% yield (reaction a).²² Deprotection of intermediate **89** with TFA resulted in the formation of aniline **90** in 83% yield (reaction b).^{22,27} Reaction of intermediate **90** with acid chloride **35** in the presence of MeMgBr produced anilide **91** in 45% yield (reaction c).²² The lower than usual yield in reaction (c) is due to unreacted starting aniline **90**, which was most likely quenched by the

presence of adventitious water. Removal of the Boc protecting group from intermediate **91** produced intermediate **92** (reaction d).^{22,28} Reaction (d) produced many side-products which could not be separated from amine **92** by column chromatography. Impure amine **92** was reacted with sulfonyl chloride **17** in the presence of DIPEA which led to the formation of the final product **S3I-H245** in 32% yield over two steps from **91** (reaction e).²²



Scheme 17: Synthesis of S3I-H245^a

^aReagents and Conditions: (a) **4** (1.3 eq), KHMDS (1.3 eq), DMF, 0 to 25 °C, 19.2 h, 83%; (b) TFA (58 eq), DCM, 25 °C, 3 h, 93%; (c) **35** (2.1 eq), MeMgBr (2.5 eq), THF, 0 to 25 °C, 1.2 h, 45%; (d) TFA (37 eq), DCM, 25 °C, 1.5 h; (e) **17** (2.0 eq), DIPEA (5.0 eq), DCM, 0 to 25 °C, 1.7 h, 32% yield over two steps from **91**

This concludes the synthesis of the STAT3 inhibitors **S3I-H204**, **S3I-H212**, **S3I-H222**, **S3I-H224**, **S3I-H230**, **S3I-H235**, **S3I-H233**, **S3I-H228**, **S3I-H237**, **S3I-H239**, **S3I-H244**, and **S3I-H245** (Chapter 1, **Figure 11**). Each compound was characterized by ^1H NMR and HRMS, purified to $\geq 95\%$ purity as determined by LCMS, and sent to the UH Cancer Center to test for STAT3 DNA-binding inhibitory activity using the EMSA assay. The biological results will be discussed in Chapter 3.

Each of the STAT3 inhibitors (**Figure 11**) were designed and synthesized using convergent synthetic routes previously developed by our group (Chapter 2, **Schemes 1 & 2**).²² These convergent synthetic routes have broad functional group tolerance which enables the development of a large library of molecules for screening. Most reactions with yields $< 70\%$ were not optimized, instead reaction intermediates and final compounds were carefully isolated and subjected to the next reaction step. In this medicinal chemistry project the goal was to isolate the desired molecules as fast as possible so relatively less time was spent on optimizing reaction conditions.

One important synthetic route that was modified was for the formation of alkyl chloride **3** (Chapter 2, **Scheme 3**). Alkyl chloride **3** is an important building block found in most of our STAT3 inhibitors. It is necessary to have a high yielding synthetic route so that gram quantities of alkyl chloride **3** can easily be obtained. Synthetic route A was modified by changing the substrate in the initial Suzuki reaction (Route A, reaction a). The substrate was changed from pyridyl alcohol **23** to pyridyl ester **26**. This prevented Pd^0 chelation by the substrate and increased the reaction yield by 37% (Route B, reaction d). An additional reaction step was needed to reduce ester **28** to alcohol **25** (Route B, reaction f).

A procedure from the literature was followed for reaction (f) which utilized the mild reducing agent NaBH₄ and catalytic NaOMe.³⁰ These synthetic modifications (Route B) increased the overall yield of alkyl chloride **3** by 21% compared to Route A.

In some circumstances, it can be more efficient to try a new reaction sequence rather than optimize a low yielding reaction when in pursuit of a target molecule. This was demonstrated in the attempted synthesis of compound **41** (**Schemes 6 & 7**). Derivatization of **S3I-H204** was initially attempted to form the *N,N*-dimethylsalicylamide derivative **41**, but this reaction produced many side-products and **41** could not be isolated (**Scheme 6**). To optimize this reaction, **S3I-H204** had to be resynthesized. Instead, an alternative synthetic route (**Scheme 7**) was utilized in the attempt to form **41**. Although **41** could not be isolated using this synthetic route, its pyrazine analog **S3I-H222** could be (**Scheme 8**).

Additionally, side-products **40**, **42**, and **53** isolated in the final reactions for forming **S3I-H212** and **41** demonstrate the reactivity of the difluorocyanobenzenesulfonamide functionality (**Figures 13, 14, and 15**). Side-products **40**, **42**, and **53** were formed by a S_NAr reaction on the difluorocyanobenzenesulfonamide function of **S3I-H212** and **41**. These side-products lend credence to the importance of the difluorocyanobenzenesulfonamide unit in terms of biological activity. Reaction of the difluorocyanobenzenesulfonamide functionality in our STAT3 inhibitors with cysteine residues in the DNA binding domain of STAT3 represents an important mechanism whereby STAT3 is prevented from interacting with the nucleus and simulating cell transcription.

Chapter 3

Results and Conclusions

To summarize, in Chapter 1 the importance of inhibiting STAT3 dimerization and the interaction of STAT3 with the DNA-binding domain to prevent the progression of cancerous transformations was discussed. Small molecule STAT3 inhibitors designed by our group were shown to disrupt STAT3 dimerization/DNA-binding and inhibited the growth of human breast and glioma tumor xenografts in mice. These results indicate that our small molecule STAT3 inhibitors show promise as anti-cancer drugs. However, if our STAT3 inhibitors are to be developed into anti-cancer drugs the potency and physicochemical properties of these molecules need to be improved.

Extensive SAR analysis was performed to improve the potency and physicochemical properties of these inhibitors and from this analysis a general scaffold for the STAT3 inhibitors was developed (Chapter 1, **Figure 7**). It was found that the most potent compounds incorporate a cyclohexane ring in R₁ and an azetidine in the linker region. It should be noted that the metabolic stability of the azetidine compounds still needs to be tested. The interplay between potency and the identity of the heteroarene ring, whether it is pyridine or pyrazine for the R₂ functionality, needs to be better understood through the testing of more analogs incorporating this change. Additionally, it was shown that more analogs comparing the pentafluorobenzenesulfonamide and difluorocyanobenzenesulfonamide in R₃ need to be examined to confirm that the difluorocyanobenzenesulfonamide functionality leads to the most potent compounds in the EMSA assay. It was established that functional groups that contain a carboxyl or hydroxamic acid in R₄ have good potency but poor cell membrane permeability. Therefore, functionalities in R₄ need to be varied to improve permeability and potency. In an effort to optimize R₂, R₃, and R₄ in terms of potency and physicochemical properties the targets shown below in **Figure 16** were designed and synthesized.

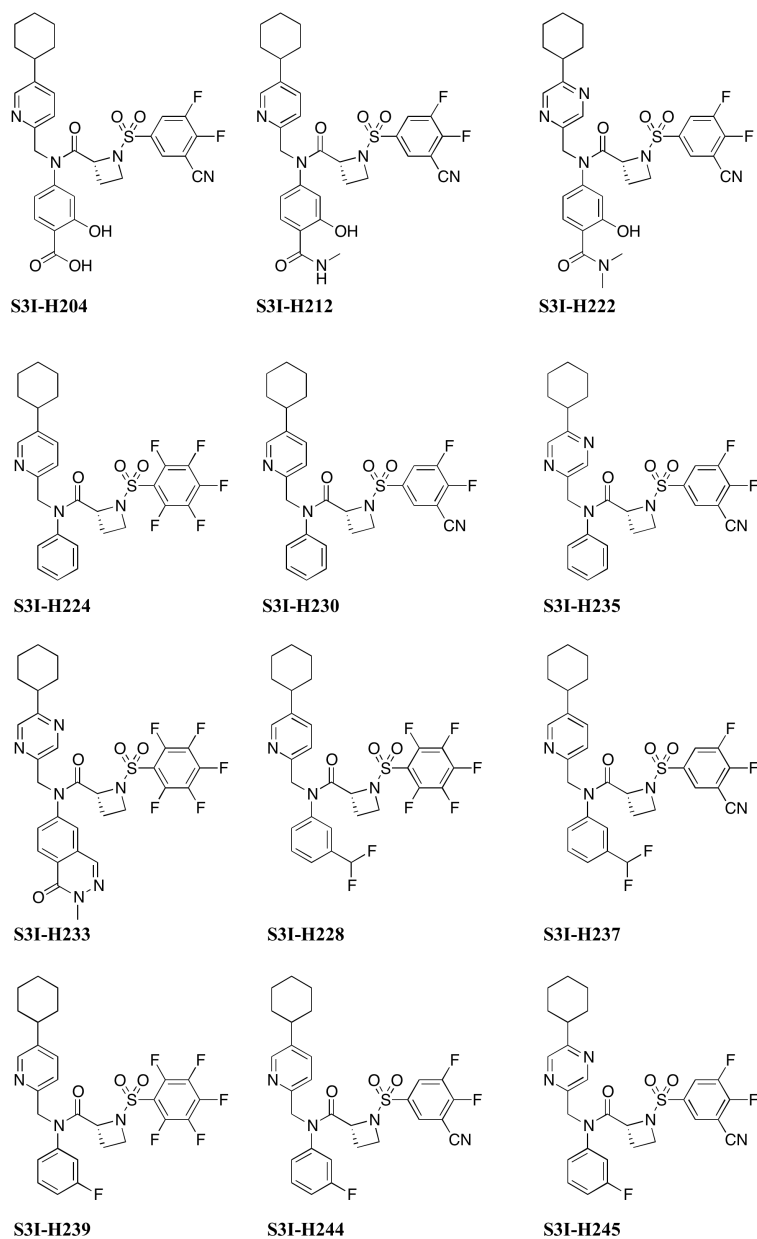


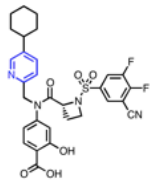
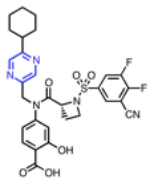
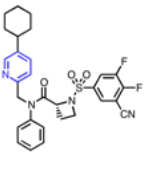
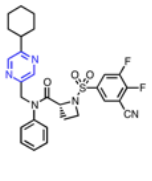
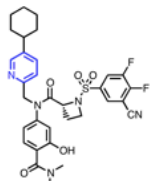
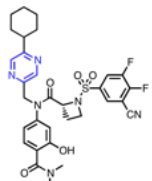
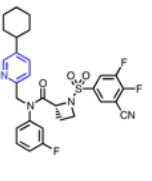
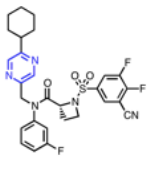
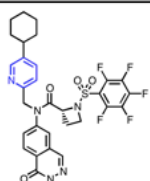
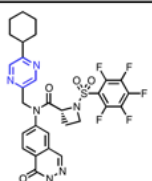
Figure 16. STAT3 Inhibitory Agents Synthesized

In Chapter 2 the synthesis of the target STAT3 inhibitors (**S3I-H204**, **S3I-H212**, **S3I-H222**, **S3I-H224**, **S3I-H230**, **S3I-H235**, **S3I-H233**, **S3I-H228**, **S3I-H237**, **S3I-H239**, **S3I-H244**, and **S3I-H245**) was discussed. Each of the targets shown in **Figure 16** is based on the azetidinamide scaffold and has two amine functionalities condensed with three different functionalities ($R_1 + R_2$, R_3 , and R_4 ; **Figure 7**). The targets were designed and synthesized using convergent synthetic routes previously developed by our group (Chapter 2, **Schemes 1 & 2**). These convergent routes allowed for facile derivatization making it easy to build a complex library of molecules for screening. Overall, these synthetic routes have broad functional group tolerance and a wide substrate scope. It should be noted that most reactions with low yields (< 70%) were not optimized, instead intermediates or final compounds were carefully isolated and subjected to the next reaction if necessary. This is the nature of synthesis in medical chemistry; little time is spent optimizing reactions so that the final compound can be synthesized as quickly as possible. Each target was synthesized, characterized, purified to $\geq 95\%$ purity as determined by LCMS, characterized spectroscopically, and sent to the UH Cancer Center to test for STAT3 DNA-binding inhibitory activity using the EMSA assay. The results from the EMSA assay are described below.

Earlier SAR experiments showed that when the heteroarene in R_2 is changed from pyridine to pyrazine the potency remains the same or slightly diminishes (Chapter 1, **Figures 7 & 8**). To determine which heteroarene, pyridine or pyrazine, produces the most potent compounds **S3I-H204**, **S3I-H222**, **S3I-H233**, **S3I-H230**, **S3I-H235**, **S3I-H244**, and **S3I-H245** were compared with their pyridine or pyrazine analogs (**Table 6**). Conflicting potency results were obtained. Replacing the pyridine functionality with pyrazine in **S3I-H207** and **S3I-H230**

to produce **S3I-H233** and **S3I-H235** led to a decrease in potency. However, when the pyridine functionality in **S3I-H204** is replaced by pyrazine to form **S3I-H203** potency is enhanced, $0.786 \pm 0.125 \mu\text{M}$ vs. $0.283 \pm 0.031 \mu\text{M}$. Unfortunately, **S3I-H222** could not be compared to its pyridine analog, **41**. Compound **41** could not be isolated, and once the low potency of **S3I-H222** was determined the synthesis of **41** was no longer pursued. Potency results for **S3I-H245** are currently pending, but once the results of the EMSA assay are received, the potency of **S3I-H245** will be compared to its pyridine analog, **S3I-H244**.

Table 6. Targeted STAT3 Compounds - SAR Variation in Region 2 (R₂)

Compounds with R ₂ = Pyridine	Compounds with R ₂ = Pyrazine	Compounds with R ₂ = Pyridine	Compounds with R ₂ = Pyrazine
 <p>S3I-H204 IC₅₀ (μM) = 0.786 ± 0.125</p>	 <p>S3I-H203 IC₅₀ (μM) = 0.283 ± 0.031</p>	 <p>S3I-H230 IC₅₀ (μM) = 0.632 ± 0.052</p>	 <p>S3I-H235 IC₅₀ (μM) = 1.42 ± 0.14</p>
 <p>41 IC₅₀ (μM) = N/A</p>	 <p>S3I-H222 IC₅₀ (μM) = 2.25 ± 0.04</p>	 <p>S3I-H244 IC₅₀ (μM) = 0.978 ± 0.203</p>	 <p>S3I-H245 IC₅₀ (μM) = Pending</p>
 <p>S3I-H207 IC₅₀ (μM) = 0.967</p>	 <p>S3I-H233 IC₅₀ (μM) = 4.32 ± 1.02</p>		

Note: R₂ in each compound is highlighted in blue, and all IC₅₀ values were obtained using the EMSA assay

Earlier SAR experiments done by our group on region 3 (Chapter 1, **Figure 7**) revealed that when the pentafluorobenzenesulfonamide in **S3I-H142** is replaced with difluorocyanobenzenesulfonamide to form **S3I-H203** a slight increase in *in vitro* STAT3 DNA-binding inhibition was observed, for example **S3I-H142** $IC_{50} = 0.42 \mu M$ vs. **S3I-H203** $IC_{50} = 0.283 \pm 0.031 \mu M$ (Chapter 1, **Figure 10**). To confirm that the difluorocyanobenzenesulfonamide is a better functionality to have in R_3 , compounds **S3I-H212**, **S3I-H224**, **S3I-H230**, **S3I-H228**, **S3I-H237**, **S3I-H239**, and **S3I-H244** were compared to their difluorocyanobenzenesulfonamide or pentafluorobenzenesulfonamide analogs in terms of potency (**Table 7**). When the pentafluorobenzenesulfonamide group in **S3I-H239** is replaced by difluorocyanobenzenesulfonamide to form **S3I-H244** a substantial increase in potency is observed, **S3I-H239** $IC_{50} = > 4.0 \mu M$ vs. **S3I-H244** $IC_{50} = 0.978 \pm 0.203 \mu M$. Likewise, replacing the pentafluorobenzenesulfonamide functionality in **S3I-H171** and **S3I-H224** with difluorocyanobenzenesulfonamide led to the formation of **S3I-H212** and **S3I-H230**, which slightly improved the STAT3 inhibitory potency (**S3I-H212** $IC_{50} = 0.711 \pm 0.074 \mu M$ & **S3I-H230** $IC_{50} = 0.632 \pm 0.052 \mu M$) compared to the parent compounds (**S3I-H171** $IC_{50} = 0.773 \mu M$ & **S3I-H224** $IC_{50} = 1.08 \pm 0.05 \mu M$). Interestingly, **S3I-H212** and **S3I-H230** had less potent half maximal effective concentrations (EC_{50}) values in the breast cancer cell viability assay compared to their pentafluorobenzenesulfonamide derivatives **S3I-H171** and **S3I-H224**, (**S3I-H212** MDA-231 $EC_{50} = 2.7 \mu M$ & **S3I-H230** MDA-231 $EC_{50} = 4.4 \mu M$ vs. **S3I-H171** MDA-231 $EC_{50} = 1.7 \mu M$ & **S3I-H224** MDA-231 $EC_{50} = 2.2 \mu M$). This could be a result of the increased polarity of the difluorocyanobenzenesulfonamide group, which may make it more difficult for compounds containing this functionality to permeate cells.

Contrary to the comparisons discussed above, compound **S3I-H237** containing the difluorocyanobenzenesulfonamide group suppressed STAT3 DNA-binding activity with lower activity compared to its pentafluorobenzenesulfonamide analog, **S3I-H228** (**S3I-H237** $IC_{50} = 2.58 \pm 0.07 \mu M$ vs. **S3I-H228** $IC_{50} = 1.78 \pm 0.28 \mu M$). These results do not fit with expected trends and in the near future **S3I-H228** and **S3I-H237** will be re-tested and the potency of these two compounds will be compared. Altogether the EMSA IC_{50} results from **S3I-H212**, **S3I-H230**, **S3I-H224**, **S3I-H244**, and **S3I-H239** confirm that when R_3 = difluorocyanobenzenesulfonamide compounds have better potency compared to compounds that have R_3 = pentafluorobenzenesulfonamide.

Table 7. Targeted STAT3 Compounds - SAR Variation of Region 3 (R_3)

Compounds with R_3 = Pentafluorobenzenesulfonamide	Compounds with R_3 = Difluorocyanobenzenesulfonamide	Compounds with R_3 = Pentafluorobenzenesulfonamide	Compounds with R_3 = Difluorocyanobenzenesulfonamide
 S3I-H239 $IC_{50} (\mu M) = > 4.0$	 S3I-H244 $IC_{50} (\mu M) = 0.978 \pm 0.203$	 S3I-H224 $IC_{50} (\mu M) = 1.08 \pm 0.05$	 S3I-H230 $IC_{50} (\mu M) = 0.632 \pm 0.052$
 S3I-H171 $IC_{50} (\mu M) = 0.773$	 S3I-H212 $IC_{50} (\mu M) = 0.711 \pm 0.074$	 S3I-H228 $IC_{50} (\mu M) = 1.78 \pm 0.28$	 S3I-H237 $IC_{50} (\mu M) = 2.58 \pm 0.07$

Note: R_3 in each compound is highlighted in red, and all IC_{50} values were obtained using the EMSA assay

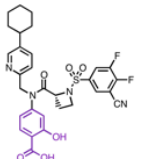
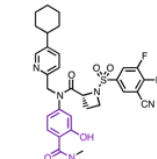
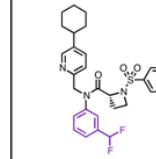
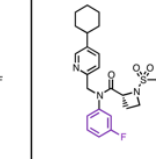
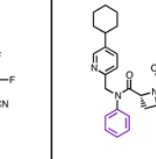
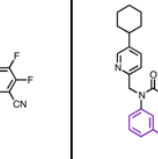
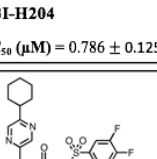
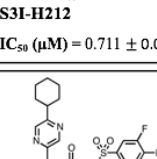
In Chapter 1 it was shown that STAT3 inhibitors that contain a carboxyl or hydroxamic acid on the benzene ring in region 4 (R_4) have good potency but poor permeability (**Figure 7**).

Compounds with a carboxyl or hydroxamic acid group in R₄ have poor cellular permeability, because these polar functional groups make it difficult for these molecules to traverse the non-polar cell membrane. In hopes of simultaneously increasing permeability and potency, various functionalities in the aromatic ring of R₄ were examined (**Figure 11, Table 8**). When the salicylic acid functionality in **S3I-H204** was converted to its less polar *N*-methylsalicylamide analog **S3I-H212** a slight increase in STAT3 DNA-binding inhibition was observed, **S3I-H204** IC₅₀ = 0.786 ± 0.125 μM vs. **S3I-H212** IC₅₀ = 0.711 ± 0.074 μM. However, *N,N*-dimethylsalicylamide **S3I-H222** performed worse in the EMSA assay compared to its salicylic analog **S3I-H203** (**S3I-H222** IC₅₀ = 2.25 ± 0.04 μM vs. **S3I-H203** IC₅₀ = 0.283 ± 0.031 μM). Similarly, meta-difluoromethylbenzene and meta-fluorobenzene (**S3I-H237** and **S3I-H244**) showed weaker *in vitro* activity compared to the parent compound, **S3I-H204** (**S3I-H237** IC₅₀ = 2.58 ± 0.07 μM & **S3I-H244** IC₅₀ = 0.978 ± 0.203 μM vs. **S3I-H204** IC₅₀ = 0.786 ± 0.125 μM). These results suggest that the salicylic acid functionality in R₄ can be replaced by the *N*-methylsalicylamide group for STAT3 inhibitory activity to be maintained. Permeability test results on **S3I-H212**, **S3I-H222**, **S3I-H237**, and **S3I-H244** were not obtained, because all of these compounds have similar or lower STAT3 inhibitory activity than the parent compounds, **S3I-H203** and **S3I-H204**.

Interestingly, removing all the functional groups on the benzene ring in R₄ enhanced *in vitro* activity. This was observed when comparing **S3I-H230** with its salicylic acid analog **S3I-H204** (**S3I-H230** IC₅₀ = 0.632 ± 0.052 μM vs. **S3I-H204** IC₅₀ = 0.786 ± 0.125 μM). Additionally, **S3I-H230** showed increased STAT3 DNA-binding inhibition compared to its meta-phenol analog **S3I-H226** (**S3I-H230** IC₅₀ = 0.632 ± 0.052 μM vs. **S3I-H226** IC₅₀ = 0.780 ±

0.132 μM). These results suggest that the salicylic acid functional group in **R4** is superfluous. Additional SAR experiments are underway to verify this statement. Furthermore, the less polar benzene group in **S3I-H230** should render this molecule more permeable than its salicylic acid analog, **S3I-H204**. Moreover, the low molecular weight of **S3I-H230** should make it easier for this molecule to traverse cells compared to its higher molecular weight analogs. Cellular permeability tests on **S3I-H230** will be obtained in the near future.

Table 8. Targeted STAT3 Compounds - SAR Variation of Region 4 (R₄)

 <p>S31-H204 IC_{50} (μM) = 0.786 ± 0.125</p>	 <p>S31-H212 IC_{50} (μM) = 0.711 ± 0.074</p>	 <p>S31-H237 IC_{50} (μM) = 2.58 ± 0.07</p>	 <p>S31-H244 IC_{50} (μM) = 0.978 ± 0.203</p>	 <p>S31-H230 IC_{50} (μM) = 0.632 ± 0.052</p>	 <p>S31-H226 IC_{50} (μM) = 0.780 ± 0.132</p>
 <p>S31-H203 IC_{50} (μM) = 0.283 ± 0.031</p>	 <p>S31-H222 IC_{50} (μM) = 2.25 ± 0.04</p>				

Note: R₄ in each compound is highlighted in purple, and all IC₅₀ values were obtained using the EMSA assay

To summarize, 12 small molecule STAT3 inhibitors were designed, synthesized, characterized spectroscopically, and sent to the UH Cancer Center to test for STAT3 DNA-binding inhibitory activity using the EMSA assay. The biological results for **S3I-H204**, **S3I-H222**, **S3I-H230**, **S3I-H235**, **S3I-H233**, **S3I-H244**, and **S3I-H245** indicate that more analogs comparing pyridine and pyrazine need to be explored to resolve which heterocycle in region 2 leads to the most potent compounds (**Figure 7, Table 6**). The EMSA IC₅₀ results from **S3I-**

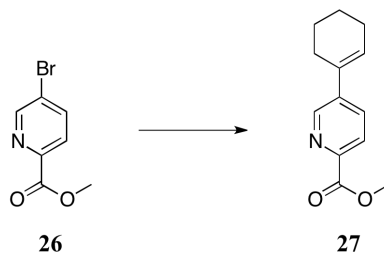
H212, S3I-H224, S3I-H230, S3I-H239, and S3I-H244 confirmed that compounds with $R_3 =$ difluorocyanobenzenesulfonamide have better potency compared to their analogs with $R_3 =$ pentafluorobenzenesulfonamide (**Figure 7, Table 7**). Compounds with $R_4 =$ *N*-methysalicylamide, *N,N*-dimethylsalicylamide, meta-difluoromethylbenzene, or meta-fluorobenzene (**S3I-H212, S3I-H222, S3I-H237, and S3I-H244**) had similar or lower STAT3 inhibitory activity than the parent compounds with $R_4 =$ salicylic acid (**Figure 7, Table 8**). Replacing the salicylic acid functionality with benzene led to enhanced *in vitro* activity (**S3I-H230** vs. **S3I-H204**). This suggests that functional groups on the benzene ring in R_4 are not necessary for enhancing potency.

Experimental

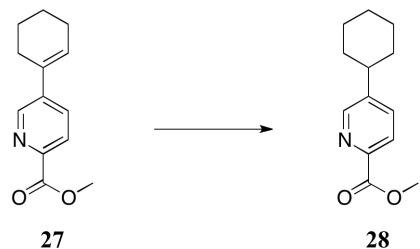
General

^1H NMR, and ^{19}F NMR were recorded on an Agilent DD2 spectrometer at 300 MHz (^1H), 75 MHz (^{13}C), 282 MHz (^{19}F) or on a Varian Unity Inova spectrometer at 500 MHz (^1H) and 125 MHz (^{13}C). Chemical shifts (δ) are reported in parts per million (ppm) and are referenced to the solvent, i.e., 7.26/77.2 for CDCl_3 and 2.50/39.5 for $\text{DMSO}-d_6$. Multiplicities are listed as: s (singlet), d (doublet), dd (doublet of doublets), ddd (doublet of doublet of doublets), t (triplet), q (quartet), quint (quintet), or m (multiplet). Coupling constants (J) are reported in Hertz (Hz).

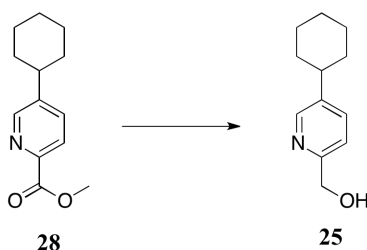
Thin-Layer Chromatography (TLC) was performed on Silicycle TLC glass plates, 250 μM , pore size 60 Å. Flash column chromatography was performed on Natland silica gel, 230-400 mesh. Preparative thin-layer chromatography was performed on Analtech uniplate prep TLC plates, 1000 μm . All moisture sensitive reactions were performed under a static atmosphere of argon in oven-dried or flame-dried glassware. Purity and homogeneity of all materials was determined to be at least 95% from TLC, ^1H NMR, LCMS, and ^{19}F NMR when applicable. Final compounds prepared for biological examination were purified to $\geq 95\%$ and evaluated at 254 nm by C18 reverse phase HPLC using an Agilent 6410 triple quadrupole LCMS. High resolution mass spectrometric data were obtained on an Agilent LC-MS TOF with ESI ionization in positive mode.



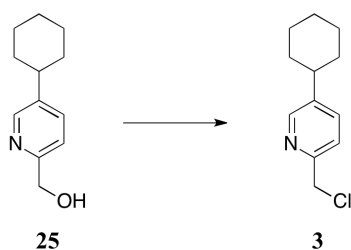
Synthesis of 27. To a two-neck round-bottom flask equipped with a stir bar was added methyl 5-bromopicolinate **26** (300 mg, 1.39 mmol, 1.0 eq), SPhos (57 mg, 0.139 mmol, 0.1 eq), 1-cyclohexenylboronic acid (350 mg, 2.78 mmol, 2.0 eq), and potassium phosphate tribasic (590 mg, 2.78 mmol, 2.0 eq). The flask was exchanged with Ar_(g) (x 3) before dry THF (6 mL) and HPLC Grade H₂O (0.05 mL, 2.78 mmol, 2.0 eq) were added. Then Pd(OAc)₂ (16 mg, .0695 mmol, 0.05 eq) was added to the mixture and the flask was exchanged with Ar_(g) (x 3). The mixture was stirred for 24 hours at 40 °C. After reaction completion, water was added to the mixture. The crude reaction mixture was extracted with ethyl acetate, and the combined ethyl acetate extracts were washed with water and brine and dried over anhydrous sodium sulfate. Purification via column chromatography (3:1 hexanes/ethyl acetate) gave the product **27** as a white solid (248 mg, 82% yield). Spectral data: ¹H NMR (300 MHz, Chloroform-*d*) δ 8.73 (d, *J* = 2.3 Hz, 1H), 8.05 (dd, *J* = 8.2, 0.8 Hz, 1H), 7.74 (dd, *J* = 8.2, 2.3 Hz, 1H), 6.42 – 6.15 (m, 1H), 3.98 (s, 3H), 2.47 – 2.34 (m, 2H), 2.27 – 2.18 (m, 2H), 1.86 – 1.73 (m, 2H), 1.72 – 1.61 (m, 2H); HRMS (ESI) *m/z* = 240.1001 [M+Na]⁺, HRMS (ESI⁺) calculated for C₁₃H₁₅NO₂: 217.1103, found 217.1108.



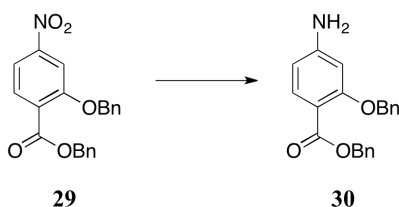
Synthesis of 28. To a round-bottom flask equipped with a stir bar was added alkene **27** (430 mg, 1.98 mmol, 1.0 eq) followed by platinum oxide (43 mg, 0.189 mmol, 0.1 eq). The flask was exchanged with Ar_(g) (x 3) before being exchanged with H₂ (g) (x 3). Ethyl acetate (3.5 mL) and methanol (3.5 mL) were then added. After stirring for four hours at room temperature, the mixture was filtered through a Celite[®] plug and solvent was evaporated under reduced pressure. This afforded product **28** as a white solid (417 mg, 96% yield). Spectral data: ¹H NMR (500 MHz, Chloroform-*d*) δ 8.59 (d, *J* = 2.2 Hz, 1H), 8.06 (d, *J* = 8.1 Hz, 1H), 7.66 (dd, *J* = 8.1, 2.2 Hz, 1H), 3.99 (s, 3H), 2.68 – 2.55 (m, 1H), 1.93 – 1.82 (m, 5H), 1.49 – 1.35 (m, 5H); HRMS (ESI) *m/z* = 242.1161 [M+Na]⁺, HRMS (ESI+) calculated for C₁₃H₁₇NO₂: 219.1259, found 219.1269.



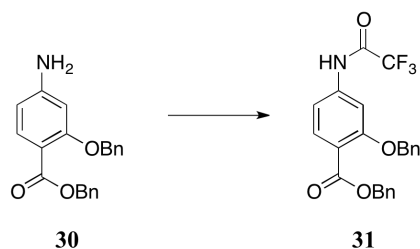
Synthesis of 25. To a round-bottom flask equipped with a stir bar was added a solution of ester **28** (636 mg, 2.90 mmol, 1.0 eq) in methanol (16 mL) followed by sodium methoxide (158 mg, 2.93 mmol, 1.01 eq). The reaction mixture was heated to 50 °C and powdered sodium borohydride was added (658 mg, 17.4 mmol, 6 eq). After one hour additional sodium methoxide (22 mg, .406 mmol, 0.14 eq) and sodium borohydride (110 mg, 2.90 mmol, 1.0 eq) were added to the mixture. After stirring for 2 hours at 50 °C the reaction was complete. After cooling to room temperature, the reaction mixture was quenched with saturated ammonium chloride (5 mL) and extracted with ethyl acetate. The combined organic extracts were washed with water and brine and dried with anhydrous sodium sulfate. Purification via column chromatography (1:1 hexanes/ethyl acetate) gave the product **25** as a clear oil (444 mg, 80% yield). Spectral data: ^1H NMR (300 MHz, Chloroform-*d*) δ 8.38 (d, J = 2.2 Hz, 1H), 7.50 (dd, J = 8.0, 2.2 Hz, 1H), 7.18 (d, J = 8.0 Hz, 1H), 4.71 (s, 2H), 2.62 – 2.41 (m, 1H), 1.97 – 1.68 (m, 5H), 1.51 – 1.13 (m, 5H); HRMS (ESI) m/z = 214.1170 $[\text{M}+\text{Na}]^+$, HRMS (ESI+) calculated for $\text{C}_{12}\text{H}_{17}\text{NO}$: 191.1310, found 191.1311.



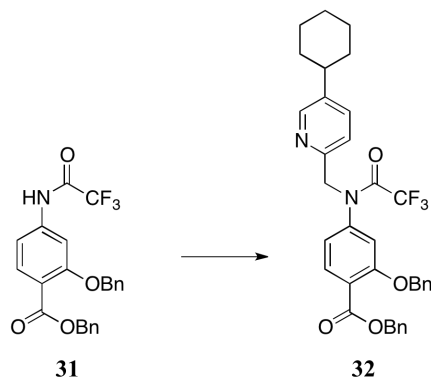
Synthesis of 3. To an oven-dried round-bottom flask equipped with a stir bar was added alcohol **25** (1 g, 5.23 mmol, 1.0 eq) followed by DCM (20.0 mL) under an atmosphere of argon. The solution was cooled and stirred for two minutes at 0 °C before SOCl₂ (0.58 mL, 7.80 mmol, 1.53 eq) was added. The solution was warmed to room temperature, stirred for 3 hours, and quenched with sat. NaHCO₃. DCM was used to extract the product which was washed with sat. NaHCO₃, dried over Na₂SO₄, and solvent was condensed *in vacuo*. This process gave the product **3** (1.10 g, 100% yield) as a yellow oil which was immediately diluted to 0.5M with dry toluene and stored in the freezer at −13 °C. No spectral data was acquired due to the instability of **3**.



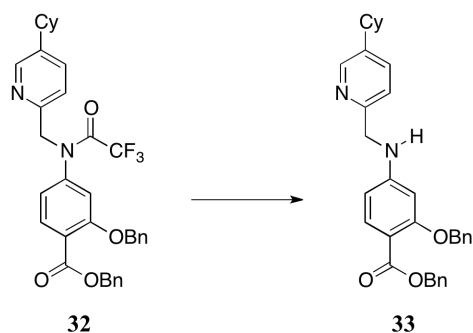
Synthesis of 30. To a round-bottom flask equipped with a stir bar was added **29** (2.0 g, 5.50 mmol, 1.0 eq) followed by NH₄Cl (3.0 g, 56.1 mmol, 10.2 eq), ethanol (20 mL), and HPLC-grade water (10 mL) under an argon atmosphere. Iron powder (1 g, 38.5 mmol, 7.0 eq) was added and the mixture was stirred rigorously overnight at 66 °C. After stirring for 16 hours the reaction was complete. The mixture was filtered through a Celite[®] plug and rinsed with ethyl acetate. The filtrate was washed with water and brine and dried with Na₂SO₄. The solvent was removed *in vacuo* to afford compound **30** as a white solid (1.66 g, 91% yield). Spectral data: ¹H NMR (300 MHz, Chloroform-*d*) δ 7.81 (d, *J* = 9.0 Hz, 1H), 7.54 – 7.27 (m, 10H), 6.28 – 6.22 (m, 2H), 5.30 (s, 2H), 5.12 (s, 2H), 4.01 (s, 2H); HRMS (ESI) *m/z* = 356.1266 [M+Na]⁺, HRMS (ESI⁺) calculated for C₂₁H₁₉NO₃: 333.1365, found 333.1375.



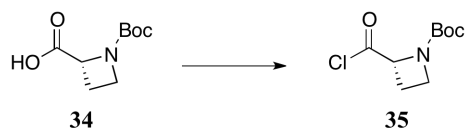
Synthesis of 31. To a solution of amine **30** (500 mg, 1.49 mmol, 1.0 eq) in DCM (8.0 mL) was added pyridine (0.26 mL, 3.26 mmol, 2.19 eq), followed by TFAA (0.23 mL, 1.64 mmol, 1.10 eq) under an argon atmosphere at 0 °C. The reaction mixture was warmed to 25 °C. After stirring for 3.5 hours, the reaction mixture was diluted with DCM and washed with sat. Na₂SO₄ and sat. NaHCO₃. The organic layer was dried with anhydrous Na₂SO₄ and the solvent was condensed in vacuo. Purification by flash chromatography (7:3 hexanes/ethyl acetate) yielded the product **31** (538 mg, 84% yield) as a white-orange solid. Spectral data: ¹H NMR (300 MHz, Chloroform-*d*) δ 8.00 (s, 1H), 7.92 (d, *J* = 8.4 Hz, 1H), 7.64 (d, *J* = 2.0 Hz, 1H), 7.49 – 7.29 (m, 10H), 6.97 (dd, *J* = 8.4, 2.0 Hz, 1H), 5.34 (s, 2H), 5.19 (s, 2H); HRMS (ESI) *m/z* = 452.1063 [M+Na]⁺, HRMS (ESI⁺) calculated for C₂₃H₁₈F₃NO₄: 429.1188, found 429.1171.



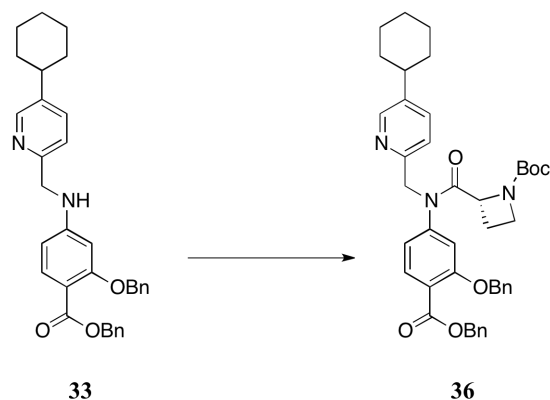
Synthesis of 32. To a round-bottom flask equipped with a stir bar was added NaI (21 mg, 0.140 mmol, 0.2 eq), K₂CO₃ (193 mg, 1.40 mmol, 2.0 eq), and trifluoroacetamide **31** (300 mg, 0.699 mmol, 1.0 eq) under an argon atmosphere. Dry acetonitrile (9 mL) was then added, followed by alkyl chloride **3** (2.0 mL, 0.978 mmol, 1.4 eq). The reaction mixture was warmed to 65 °C and stirred for 24 hours. After cooling to room temperature, the reaction mixture was quenched with water. The aqueous phase was extracted with ethyl acetate and the combined organic extracts were washed with brine and dried with anhydrous Na₂SO₄. The solvent was condensed *in vacuo* to yield the crude product. Purification by flash chromatography (10:1 to 8:2 hexanes/ethyl acetate) yielded the product **32** as a light-yellow oil (268 mg, 64% yield). Spectral data: ¹H NMR (300 MHz, Chloroform-*d*) δ 8.38 (d, *J* = 2.3 Hz, 1H), 7.83 (d, *J* = 8.2 Hz, 1H), 7.48 (dd, *J* = 8.0, 2.3 Hz, 1H), 7.42 – 7.28 (m, 10H), 7.17 (d, *J* = 8.0 Hz, 1H), 6.93 (d, *J* = 1.8 Hz, 1H), 6.87 (dd, *J* = 8.2, 1.8 Hz, 1H), 5.33 (s, 2H), 5.02 (s, 2H), 4.97 (s, 2H), 2.59 – 2.44 (m, 1H), 1.95 – 1.67 (m, 5H), 1.49 – 1.18 (m, 5H); HRMS (ESI) *m/z* = 625.2297 [M+Na]⁺, HRMS (ESI⁺) calculated for C₃₅H₃₃F₃N₂O₄: 602.2392, found 602.2409.



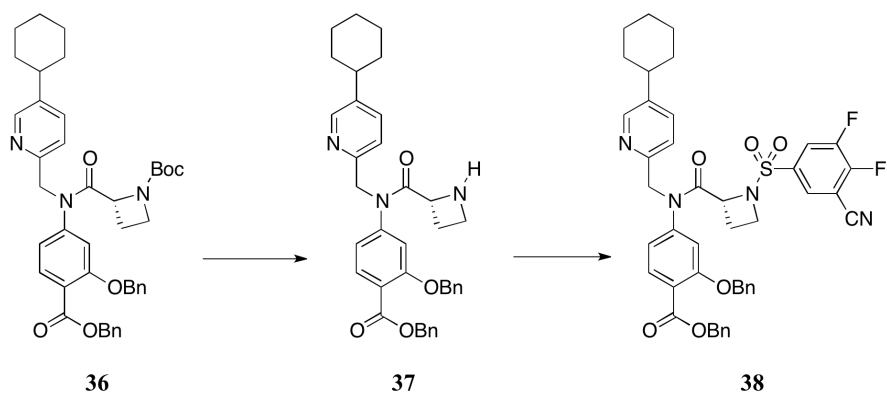
Synthesis of 33. To a solution of trifluoroacetamide **32** (136 mg, 0.225 mmol, 1.0 eq) in 1:1 THF/MeOH (1.0 mL) was added K_2CO_3 (62 mg, 0.450 mmol, 2.0 eq) under an argon atmosphere. After stirring for 20 hours at 25 °C the reaction was complete and was quenched with sat. NH_4Cl . The reaction mixture was extracted with ethyl acetate, washed with brine, dried over anhydrous Na_2SO_4 , and solvent was removed *in vacuo*. This process yielded the product **33** as a white solid (112 mg, 98% yield). Spectral data: ^1H NMR (300 MHz, Chloroform-*d*) δ 8.42 (d, $J = 2.2$ Hz, 1H), 7.85 (d, $J = 8.5$ Hz, 1H), 7.52 – 7.27 (m, 11H), 7.18 (d, $J = 8.0$ Hz, 1H), 6.41 – 6.14 (m, 2H), 5.38 – 5.18 (m, 3H), 5.11 (s, 2H), 4.42 (d, $J = 5.1$ Hz, 2H), 2.64 – 2.43 (m, 1H), 1.99 – 1.69 (m, 5H), 1.52 – 1.21 (m, 5H); HRMS (ESI) $m/z = 529.2469$ $[\text{M}+\text{Na}]^+$, HRMS (ESI+) calculated for $\text{C}_{33}\text{H}_{34}\text{N}_2\text{O}_3$: 506.2569, found 506.2578.



Synthesis of 35. To a round-bottom flask equipped with a stir bar was added carboxylic acid **34** (122 mg, 0.607 mmol, 1.0 eq) followed by DCM (3.0 mL) under an argon atmosphere. A bubbler was attached to the reaction flask and (COCl)₂ (60 uL, 0.709 mmol, 1.17 eq) and DMF (2 drops) were added. After stirring for 1.5 hours at 25 °C the reaction was complete. The stir bar was removed and the solvent was condensed *in vacuo*, the remaining oil was dried on the high vacuum for 1 hour. This process yielded the product **35** as a yellow oil (133 mg, 100% yield) which was used immediately. No spectral data was acquired due to the instability of compound **35**.

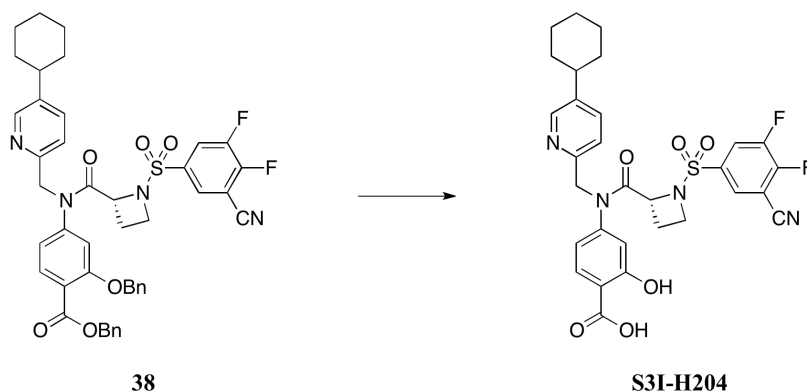


Synthesis of 36. Note: Water was removed azeotropically from amine **33** with anhydrous toluene prior to use. To an oven-dried round-bottom flask equipped with a stir bar was added amine **33** (147 mg, 0.289 mmol, 1.0 eq) followed by dry THF (3.0 mL) under an argon atmosphere. The solution was stirred at 0 °C for 2 minutes before MeMgBr (0.52 mL, 0.723 mmol, 2.5 eq) was added. The solution was allowed to stir at 0 °C for 10 minutes before acid chloride **35** (133 mg, 0.607 mmol, 2.1 eq) in THF (3.0 mL) was added. The solution was warmed to 25 °C, stirred for 1 hour, and quenched with water. The reaction mixture was extracted with ethyl acetate, washed with brine, dried over anhydrous Na₂SO₄, and solvent was removed *in vacuo*. Purification by flash chromatography using 1:1 hexanes/ethyl acetate gave the product **36** as a clear oil (150 mg, 75% yield). Spectral data: ¹H NMR (300 MHz, Chloroform-*d*) δ 8.31 (d, *J* = 2.0 Hz, 1H), 7.80 (d, *J* = 8.3 Hz, 1H), 7.46 (dd, *J* = 8.0, 2.0 Hz, 1H), 7.41 – 7.28 (m, 10H), 7.21 – 7.06 (m, 1H), 6.97 – 6.68 (m, 2H), 5.33 (s, 2H), 5.18 – 4.86 (m, 4H), 4.70 – 4.43 (m, 1H), 4.11 – 3.94 (m, 1H), 3.81 – 3.62 (m, 1H), 2.56 – 2.42 (m, 1H), 2.13 – 1.90 (m, 2H), 1.90 – 1.75 (m, 5H), 1.57 – 1.19 (m, 14H); HRMS (ESI) *m/z* = 712.3364 [M+Na]⁺, HRMS (ESI+) calculated for C₄₂H₄₇N₃O₆: 689.3465, found 689.3473.

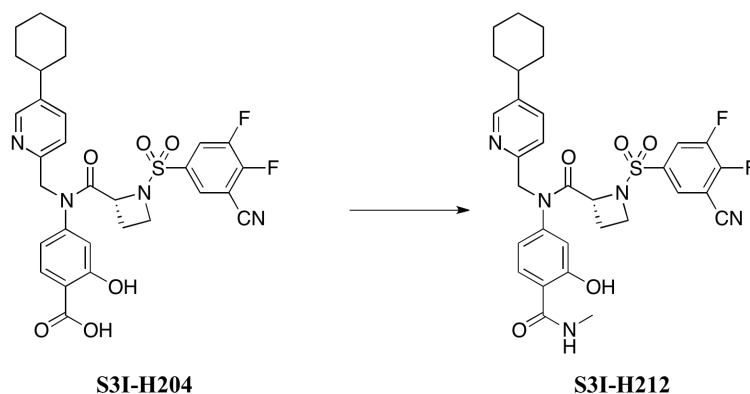


Synthesis of 38. To a solution of carbamate **36** (141 mg, 0.204 mmol, 1.0 eq) in DCM (2.0 mL) was added TFA (0.58 mL, 7.55 mmol, 37.0 eq) at 25 °C under an argon atmosphere. After stirring for 1.5 hours the reaction was complete. Solvent was removed on the rotary evaporator and then water and ethyl acetate were added to the residue. The ethyl acetate layer was washed with brine, dried over anhydrous Na₂SO₄, and solvent was removed *in vacuo*. Purification via flash chromatography yielded amine **37** (105 mg) which was used in the following reaction. To a round-bottom flask equipped with a stir bar was added **37** (105 mg, 0.178 mmol, 1.0 eq) followed by DCM (1.9 mL) under an atmosphere of argon. The solution was allowed to stir at 0 °C for 2 minutes before DIPEA (0.16 mL, 0.891 mmol, 5.0 eq) was added. The solution was stirred at 0 °C for 10 minutes before sulfonyl chloride **17** (85 mg, 0.356 mmol, 2.0 eq) in DCM (1.8 mL) was added. After stirring for 2 hours at 25 °C the reaction was complete. The reaction was quenched with water, extracted with DCM, washed with brine, and dried over anhydrous Na₂SO₄. Solvent was condensed on the rotary evaporator and purification by flash chromatography gave the product **38** (97 mg, 60% yield over two steps) as a clear oil.

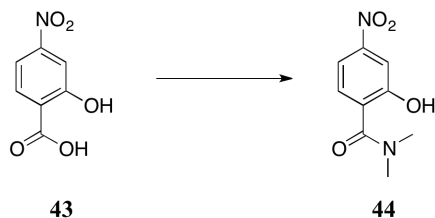
^1H NMR (300 MHz, Chloroform-*d*) δ 8.36 (d, $J = 2.3$ Hz, 1H), 8.21 – 8.11 (m, 1H), 8.09 – 8.03 (m, 1H), 7.82 (d, $J = 8.2$ Hz, 1H), 7.48 (dd, $J = 8.0, 2.3$ Hz, 1H), 7.43 – 7.28 (m, 10H), 7.19 (d, $J = 8.0$ Hz, 1H), 6.88 (d, $J = 1.9$ Hz, 1H), 6.80 (dd, $J = 8.2, 1.9$ Hz, 1H), 5.42 – 4.74 (m, 7H), 3.99 – 3.83 (m, 1H), 3.63 – 3.44 (m, 1H), 2.57 – 2.44 (m, 1H), 2.15 – 1.99 (m, 1H), 1.95 – 1.66 (m, 6H), 1.50 – 1.14 (m, 5H); HRMS (ESI) $m/z = 813.2532$ $[\text{M}+\text{Na}]^+$, HRMS (ESI+) calculated for $\text{C}_{44}\text{H}_{40}\text{F}_2\text{N}_4\text{O}_6\text{S}$: 790.2637, found 790.2641.



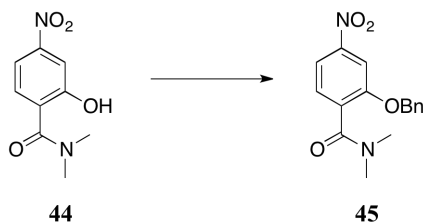
Synthesis of S3I-H204. To a round-bottom flask equipped with a stir bar was added sulfonamide **38** (97 mg, 0.122 mmol, 1.0 eq) followed by 15% by weight 1:1 Pd/C and Pd(OH)₂ (.015 g each) and 1:1 ethyl acetate/methanol (2.2 mL). The mixture was exchanged with hydrogen gas three times before stirring at 25 °C. After 5 hours, an additional 10% by weight Pd/C and Pd(OH)₂ (.006 g each) was added and the flask was exchanged with hydrogen gas three times before being allowed to stir at 25 °C. After stirring for 18 hours at 25 °C the reaction was complete. The mixture was flushed through a Celite[®] plug with ethyl acetate containing 10% methanol. The filtrate was concentrated and the crude material was purified via prep-TLC. This process gave the product **S3I-H204** (37 mg, 50% yield) as a white solid. ¹H NMR (300 MHz, DMSO-*d*₆) δ 8.34 (d, *J* = 2.2 Hz, 1H), 8.29 – 8.20 (m, 1H), 8.18 – 8.04 (m, 1H), 7.73 – 7.51 (m, 2H), 7.24 (d, *J* = 8.1 Hz, 1H), 6.60 – 6.39 (m, 2H), 4.99 – 4.49 (m, 3H), 3.87 – 3.56 (m, 2H), 2.36 – 2.18 (m, 1H), 1.98 – 1.57 (m, 6H), 1.52 – 1.16 (m, 5H); HPLC purity: 100 %; HRMS (ESI) *m/z* = 611.1768 [M+H]⁺, HRMS (ESI⁺) calculated for C₃₀H₂₈F₂N₄O₆S: 610.1698, found 610.1695; EMSA IC₅₀ = .786 ± .125 μM.



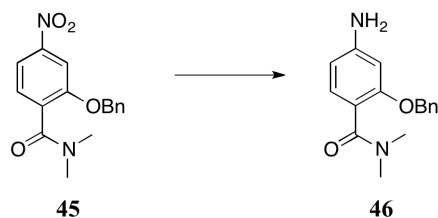
Synthesis of S3I-H212. To a round-bottom flask equipped with a stir bar was added **S3I-H204** (51 mg, 0.0829 mmol, 1.0 eq) in DCM (2.3 mL). The mixture was allowed to stir at 0 °C for 2 minutes before DIPEA (13 μ L, 0.0746 mmol, 0.9 eq) and HATU (32 mg, 0.0829 mmol, 1.0 eq) were added. This solution was allowed to stir for 1.5 hours at 25 °C before being cooled to –10 °C. After stirring for 2 minutes at –10 °C, methylamine (72 μ L, 0.144 mmol, 1.74 eq) and DIPEA (14.4 μ L, 0.0829 mmol, 1.0 eq) were added and the solution was allowed to stir at –10 °C. After stirring for 3 hours and 45 minutes at –10 °C the reaction was complete. The reaction mixture was quenched with sat. NH_4Cl , extracted with DCM, dried with anhydrous Na_2SO_4 , and concentrated *in vacuo*. The crude product was purified via prep-TLC yielding the product **S3I-H212** (4 mg, 9.0% yield) as a white powder. ^1H NMR (300 MHz, Chloroform-*d*) δ 12.64 (s, 1H), 8.34 (s, 1H), 8.18 – 8.07 (m, 1H), 8.03 – 7.95 (m, 1H), 7.50 (dd, J = 8.1, 2.2 Hz, 1H), 7.41 (d, J = 8.9 Hz, 1H), 7.26 – 7.23 (m, 1H), 6.79 – 6.70 (m, 2H), 6.61 – 6.51 (m, 1H), 5.07 – 4.82 (m, 3H), 4.02 – 3.85 (m, 1H), 3.78 – 3.60 (m, 1H), 3.01 (d, J = 4.8 Hz, 3H), 2.57 – 2.31 (m, 2H), 2.09 – 1.90 (m, 1H), 1.90 – 1.55 (m, 5H), 1.51 – 1.15 (m, 5H); HPLC purity: 100 %; HRMS (ESI) m/z = 646.1933 $[\text{M}+\text{Na}]^+$, HRMS (ESI+) calculated for $\text{C}_{31}\text{H}_{31}\text{F}_2\text{N}_5\text{O}_5\text{S}$: 623.2014, found 623.2041; EMSA IC_{50} = $0.711 \pm .074$ μM .



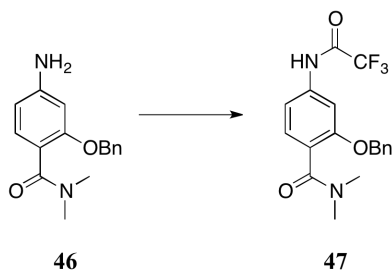
Synthesis of 44. To a suspension of 2-hydroxy-4-nitrobenzoic acid **43** (500 mg, 2.730 mmol, 1.0 eq) in DCM (25.0 mL) was added DIPEA (0.43 mL, 2.451 mmol, 0.9 eq) at 25 °C under an argon atmosphere. This solution was stirred for 2 minutes 0 °C before HATU (1.04 g, 2.730 mmol, 1.0 eq) was added. The solution was warmed to 25 °C and stirred for 1.5 hours before NHMe_2 (2.0 mL, 4.0 mmol, 1.5 eq) was added. After 24.3 hours, the reaction was quenched with water, extracted with DCM, dried over anhydrous Na_2SO_4 , and solvent was condensed *in vacuo*. Purification by flash chromatography (2:1 hexanes/ethyl acetate) yielded the product **44** (310 mg, 54% yield) as a white solid. ^1H NMR (300 MHz, Chloroform-*d*) δ 7.85 (d, J = 2.3 Hz, 1H), 7.73 (dd, J = 8.6, 2.3 Hz, 1H), 7.49 (d, J = 8.6 Hz, 1H), 3.21 (s, 6H). HRMS (ESI) m/z = 212.0745 $[\text{M}+\text{H}]^+$, HRMS (ESI+) calculated for $\text{C}_9\text{H}_{10}\text{N}_2\text{O}_4$: 210.0641, found 210.0638.



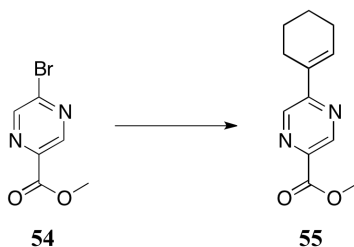
Synthesis of 45. To a round-bottom flask equipped with a stir bar was added 2-hydroxy-*N,N*-dimethyl-4-nitrobenzamide **44** (761 mg, 3.62 mmol, 1.0 eq) followed by K₂CO₃ (601 mg, 4.35 mmol, 1.2 eq) under an atmosphere of argon. DMF (22.0 mL) was added and suspension was stirred for 10 minutes at 25 °C before BnBr (0.47 mL, 3.98 mmol, 1.1 eq) was added. The reaction was stirred for 32 hours, quenched with water, extracted with ethyl acetate, washed with brine, dried over anhydrous Na₂SO₄, and solvent was condensed *in vacuo*. Purification by flash chromatography (1:1 hexanes/ethyl acetate) gave the product **45** (918 mg, 84% yield) as a white solid. ¹H NMR (300 MHz, Chloroform-*d*) δ 7.92 – 7.86 (m, 1H), 7.83 (d, *J* = 2.0 Hz, 1H), 7.47 – 7.30 (m, 6H), 5.21 (s, 2H), 3.11 (s, 3H), 2.83 (s, 3H); HRMS (ESI) *m/z* = 323.1000 [M+Na]⁺, HRMS (ESI+) calculated for C₁₆H₁₆N₂O₄: 300.1110, found 300.1109.



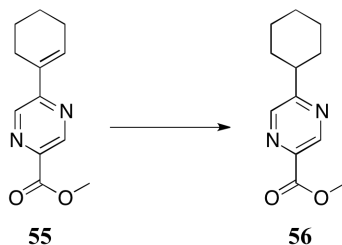
Synthesis of 46. To a solution of 2-(benzyloxy)-*N,N*-dimethyl-4-nitrobenzamide **45** (181 mg, 0.601 mmol, 1.0 eq) and NH₄Cl (328 mg, 6.12 mmol, 10.2 eq) in ethanol (2.2 mL) and HPLC-grade water (1.1 mL) was added iron powder (109 mg, 4.21 mmol, 7.0 eq) under an argon atmosphere. The suspension was allowed to stir vigorously for 20 hours at 66 °C. The suspension was cooled to room temperature and filtered through a Celite[®] plug which was rinsed with ethyl acetate. The ethyl acetate layer was washed with water and brine, dried over anhydrous Na₂SO₄, and the solvent was condensed *in vacuo*. This process yielded the product **46** (141 mg, 87% yield) as a light orange solid. ¹H NMR (300 MHz, Chloroform-*d*) δ 7.39 – 7.27 (m, 5H), 7.09 (d, *J* = 8.1 Hz, 1H), 6.30 (dd, *J* = 8.1, 2.0 Hz, 1H), 6.24 (d, *J* = 2.0 Hz, 1H), 5.05 (s, 2H), 3.78 (s, 2H), 3.07 (s, 3H), 2.87 (s, 3H); HRMS (ESI) *m/z* = 293.1260 [M+Na]⁺, HRMS (ESI+) calculated for C₁₆H₁₈N₂O₂: 270.1368, found 270.1369.



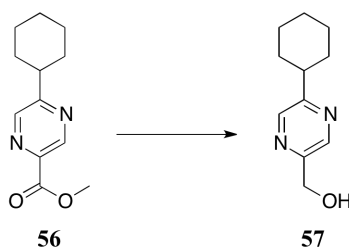
Synthesis of 47. To a solution of amine **46** (120 mg, 0.444 mmol, 1.0 eq) in DCM (2.5 mL) was added pyridine (87 μ L, 1.08 mmol, 2.2 eq) under an atmosphere of argon. The solution was stirred at 0 °C for 2 minutes before TFAA (68 μ L, 0.489 mmol, 1.1 eq) was added and then warmed to room temperature. After stirring for 1.5 hours the reaction was complete. The solution was diluted with DCM, washed with Sat. Na₂SO₄, washed with Sat. NaHCO₃, dried over anhydrous Na₂SO₄, and solvent was condensed *in vacuo*. Purification by flash chromatography (2:1 hexanes/ethyl acetate) gave the product **47** (115 mg, 71% yield) as a light orange white solid. ¹H NMR (300 MHz, Chloroform-*d*) δ 10.31 (s, 1H), 7.35 – 7.15 (m, 6H), 7.02 – 6.90 (m, 2H), 4.86 – 4.57 (m, 2H), 3.08 (s, 3H), 2.79 (s, 3H); HRMS (ESI) m/z = 389.1082 [M+Na]⁺, HRMS (ESI⁺) calculated for C₁₈H₁₇F₃N₂O₃: 366.1191, found 366.1193.



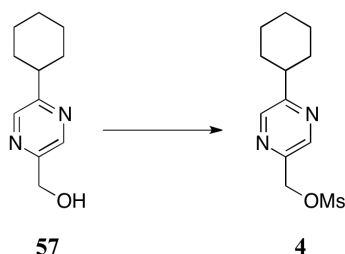
Synthesis of 55. To a round-bottom flask equipped with a stir bar was added methyl 5-bromopyrazine-2-carboxylate **54** (1.25 g, 5.76 mmol, 1.0 eq), cyclohex-1-en-1-ylboronic acid (1.09 g, 8.64 mmol, 1.5 eq), K_3PO_4 (2.45 g, 11.5 mmol, 2.0 eq), $Pd(OAc)_2$ (65 mg, 0.288 mmol, 0.05 eq), and SPhos (237 mg, 0.576 mmol, 0.1 eq) under an argon atmosphere. The solids were then exchanged with an argon atmosphere (x 3) before dry THF (19.2 mL) and HPLC-grade water (0.21 mL) were added. The solution was exchanged with argon (x 3) before being stirred for 22 hours at 40 °C. The reaction was quenched with water and extracted with ethyl acetate. The combined organic extracts were washed with brine, dried over anhydrous Na_2SO_4 , and solvent was condensed *in vacuo*. Purification by flash chromatography (17:3 hexanes/ethyl acetate) gave the product **55** (1.04 g, 83% yield). 1H NMR (500 MHz, Chloroform-*d*) δ 9.17 (d, J = 1.5 Hz, 1H), 8.76 (d, J = 1.5 Hz, 1H), 6.98 – 6.92 (m, 1H), 4.01 (s, 3H), 2.57 – 2.49 (m, 2H), 2.37 – 2.25 (m, 2H), 1.86 – 1.76 (m, 2H), 1.73 – 1.64 (m, 2H); HRMS (ESI) m/z = 241.0956 $[M+Na]^+$, HRMS (ESI+) calculated for $C_{12}H_{14}N_2O_2$: 218.1055, found 218.1066.



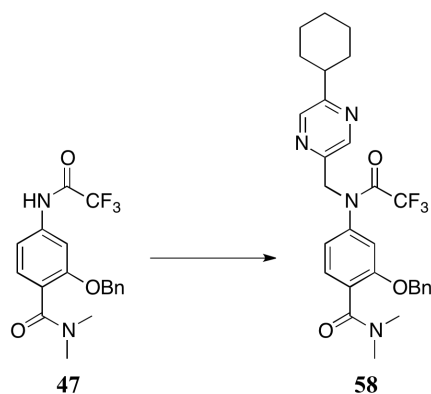
Synthesis of 56. To a solution of alkene **55** (3.30 g, 15.2 mmol, 1.0 eq) in 1:1 ethyl acetate/methanol (52.0 mL) was added PtO₂ (330 mg, 1.45 mmol, 10% by weight). The suspension was exchanged with hydrogen gas (x 3) before being stirred for 20.5 hours at 25 °C. The suspension was filtered through a Celite[®] plug, the Celite[®] plug was rinsed with ethyl acetate, and solvent was condensed *in vacuo*. Purification by flash chromatography (4:1 hexanes/ethyl acetate to 100% ethyl acetate) gave the product **56** (1.72 g, 52% yield). ¹H NMR (300 MHz, Chloroform-*d*) δ 9.17 (d, *J* = 1.5 Hz, 1H), 8.53 (d, *J* = 1.5 Hz, 1H), 3.99 (s, 3H), 2.91 – 2.73 (m, 1H), 2.01 – 1.17 (m, 10H); HRMS (ESI) *m/z* = 243.1112 [M+Na]⁺, HRMS (ESI+) calculated for C₁₂H₁₆N₂O₂: 220.1212, found 220.1214.



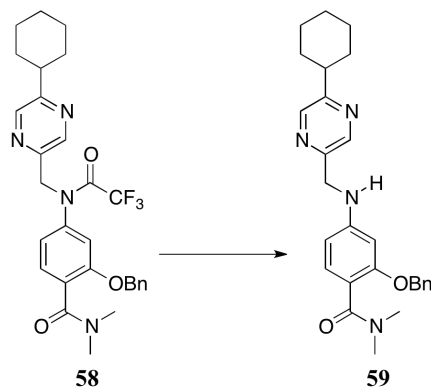
Synthesis of 57. To a round-bottom flask equipped with a stir bar was added ester **56** (1.72 g, 7.81 mmol, 1.0 eq) followed by methanol (40.0 mL) under an atmosphere of argon. The solution was stirred for 2 minutes at 0 °C before powdered NaBH₄ (886 mg, 23.4 mmol, 3.0 eq) was added. The solution was warmed to room temperature, stirred for 25 minutes, and solvent was condensed *in vacuo*. The crude product was extracted with ethyl acetate, washed with brine, dried over anhydrous Na₂SO₄, and solvent was condensed *in vacuo*. Purification by flash chromatography (9:11 hexanes/ethyl acetate) gave the product **57** (1.26 g, 84% yield) as a yellow oil. ¹H NMR (300 MHz, Chloroform-*d*) δ 8.52 (d, *J* = 1.5 Hz, 1H), 8.38 (d, *J* = 1.5 Hz, 1H), 4.78 (s, 2H), 3.65 (s, 1H), 2.82 – 2.63 (m, 1H), 1.98 – 1.16 (m, 10H); HRMS (ESI) *m/z* = 385.2504 [2M+H]⁺, HRMS (ESI+) calculated for C₁₁H₁₆N₂O: 192.1263, found 192.1267.



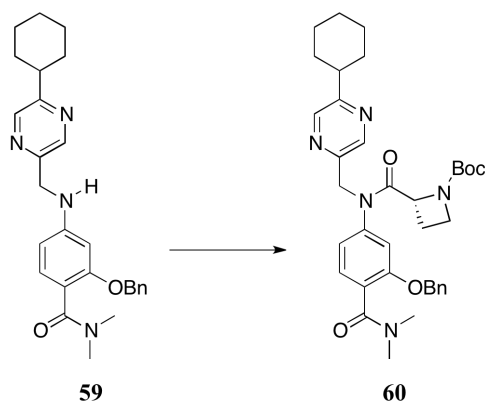
Synthesis of 4. To a solution of alcohol **57** (200 mg, 1.04 mmol, 1.0 eq) in DCM (5.2 mL) was added trimethylamine (0.43 mL, 3.12 mmol, 3.0 eq) under an argon atmosphere. The solution was stirred at 0 °C for 2 minutes before MsCl (0.15 mL, 1.93 mmol, 1.86 eq) was added. The remaining solution was stirred for 30 minutes at 0 °C before being quenched with Sat. NaHCO₃. The crude product was extracted with ethyl acetate, washed with brine, dried over anhydrous Na₂SO₄, and solvent was condensed *in vacuo*. Purification by flash chromatography gave the product **4** (237 mg, 84% yield) as a pink solid. ¹H NMR (300 MHz, Chloroform-*d*) δ 8.55 (d, *J* = 1.5 Hz, 1H), 8.39 (d, *J* = 1.5 Hz, 1H), 5.26 (s, 2H), 3.05 (s, 3H), 2.76 – 2.64 (m, 1H), 1.91 – 1.13 (m, 10H); HRMS (ESI) *m/z* = 293.0956 [M+Na]⁺, HRMS (ESI+) calculated for C₁₂H₁₈N₂O₃S: 270.1038, found 270.1043.



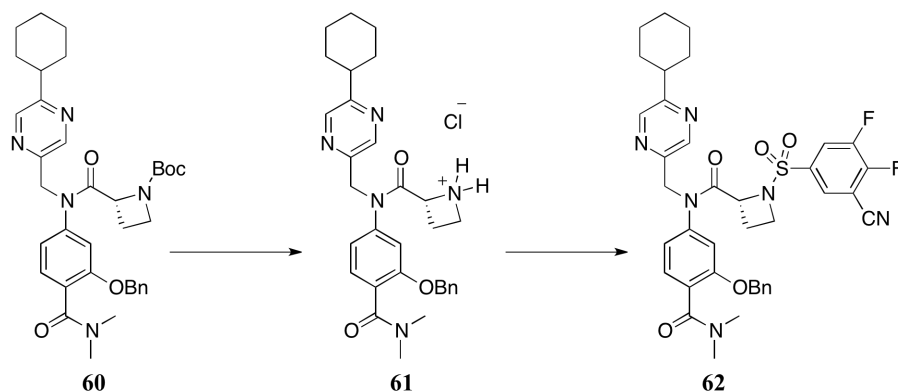
Synthesis of 58. To a solution of trifluoroacetamide **47** (207 mg, 0.565 mmol, 1.0 eq) and **4** (199 mg, 0.735 mmol, 1.3 eq) in acetonitrile (4.4 mL) was added K_2CO_3 (313 mg, 2.26 mmol, 4.0 eq) and NaI (32 mg, 0.215 mmol, 0.38 eq) under an atmosphere of argon. The suspension was heated to 60 °C, stirred for 14 hours, and quenched with water. The reaction mixture was extracted with ethyl acetate, washed with brine, dried over anhydrous Na_2SO_4 , and solvent was condensed *in vacuo*. Purification by flash chromatography (1:1 hexanes/ethyl acetate) gave the product **58** (296 mg, 97% yield) as a clear oil. ^1H NMR (300 MHz, Chloroform-*d*) δ 8.44 (d, $J = 1.5$ Hz, 1H), 8.35 (d, $J = 1.5$ Hz, 1H), 7.41 – 7.21 (m, 6H), 6.99 – 6.85 (m, 2H), 5.02 (s, 2H), 4.95 (s, 2H), 3.08 (s, 3H), 2.81 (s, 3H), 2.78 – 2.65 (m, 1H), 1.97 – 1.70 (m, 5H), 1.63 – 1.20 (m, 5H); ^{19}F NMR (282 MHz, Chloroform-*d*) δ -67.03; HRMS (ESI) $m/z = 563.2224$ $[\text{M}+\text{Na}]^+$, HRMS (ESI+) calculated for $\text{C}_{29}\text{H}_{31}\text{F}_3\text{N}_4\text{O}_3$: 540.2348, found 540.2329.



Synthesis of 59. To a solution of trifluoroacetamide **58** (296 mg, 0.548 mmol, 1.0 eq) in 1:1 THF/MeOH (2.7 mL) was added K_2CO_3 (152 mg, 1.10 mmol, 2.0 eq) under an argon atmosphere. The reaction mixture was stirred for 1.5 hours at room temperature, quenched with Sat. NH_4Cl , extracted with ethyl acetate, washed with brine, dried over anhydrous Na_2SO_4 , and solvent was condensed *in vacuo*. This process yielded the product **59** (240 mg, 99% yield) as a white solid. ^1H NMR (300 MHz, Chloroform-*d*) δ 8.48 (d, $J = 1.5$ Hz, 1H), 8.39 (d, $J = 1.5$ Hz, 1H), 7.41 – 7.24 (m, 5H), 7.11 (d, $J = 8.2$ Hz, 1H), 6.28 (dd, $J = 8.2, 2.1$ Hz, 1H), 6.24 (d, $J = 2.1$ Hz, 1H), 5.02 (s, 2H), 4.91 (s, 1H), 4.41 (s, 2H), 3.05 (s, 3H), 2.86 (s, 3H), 2.80 – 2.65 (m, 1H), 2.01 – 1.69 (m, 5H), 1.66 – 1.21 (m, 5H); HRMS (ESI) $m/z = 467.2419[\text{M}+\text{Na}]^+$, HRMS (ESI+) calculated for $\text{C}_{27}\text{H}_{32}\text{N}_4\text{O}_2$: 444.2525, found 444.2526.

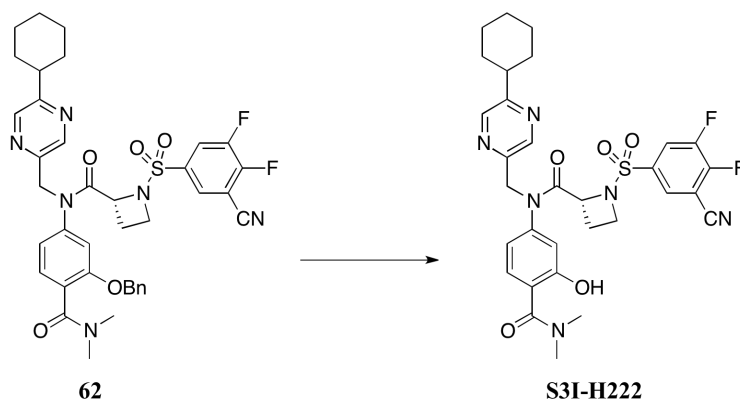


Synthesis of 60. Note: Water was removed azeotropically from amine **59** with anhydrous toluene prior to use. To an oven-dried round-bottom flask equipped with a stir bar was added amine **59** (221 mg, 0.498 mmol, 1.0 eq) followed by dry THF (5.3 mL) under an atmosphere of argon. The solution was stirred at 0 °C for 2 minutes before MeMgBr (0.89 mL, 1.24 mmol, 2.5 eq) was added. The solution was allowed to stir at 0 °C for 10 minutes before acid chloride **35** (203 mg, 1.05 mmol, 2.1 eq) in dry THF (5.3 mL) was added. The solution was warmed to room temperature, stirred for 1 hour, quenched with water, and extracted with ethyl acetate. The ethyl acetate layer was washed with brine, dried over anhydrous Na₂SO₄, and solvent was condensed *in vacuo*. Purification by flash chromatography (100% ethyl acetate) gave the product **60** (236 mg, 75% yield) as a clear oil. ¹H NMR (300 MHz, Chloroform-*d*) δ 8.53 (s, 1H), 8.27 (d, *J* = 1.5 Hz, 1H), 7.35 – 7.16 (m, 6H), 6.92 – 6.72 (m, 2H), 5.15 – 4.84 (m, 4H), 4.63 – 4.41 (m, 1H), 4.04 – 3.87 (m, 1H), 3.74 – 3.60 (m, 1H), 3.06 (s, 3H), 2.81 (s, 3H), 2.75 – 2.59 (m, 1H), 2.10 – 1.64 (m, 7H), 1.60 – 1.10 (m, 14H); HRMS (ESI) *m/z* = 650.8310 [M+Na]⁺, HRMS (ESI+) calculated for C₃₆H₄₅N₅O₅: 627.3421, found 627.3418.

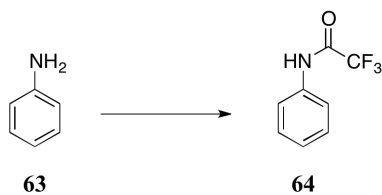


Synthesis of 62. To a solution of carbamate **60** (236 mg, 0.376 mmol, 1.0 eq) in DCM (4.0 mL) was added TFA (1.06 mL, 13.9 mmol, 37.0 eq) under an argon atmosphere. After stirring for 1.5 hours at room temperature, solvent was condensed, giving the product **61** (241 mg, 100% yield) in quantitative yield. To a round-bottom flask was added **61** (241 mg, 0.376 mmol, 1.0 eq) followed by DCM (4.0 mL) under an atmosphere of argon. The solution was stirred at 0 °C for 2 minutes prior to the addition of DIPEA (0.52 mL, 2.98 mmol, 8.0 eq). The solution was stirred at 0 °C for 10 minutes then sulfonyl chloride **17** (179 mg, 0.751 mmol, 2.0 eq) in dry DCM (3.8 mL) was added. The solution was warmed to room temperature, stirred for 1.5 hours, and quenched with water. The aqueous phase was extracted with ethyl acetate, and the combined organic extracts were washed with brine, dried over anhydrous Na₂SO₄, and solvent was condensed *in vacuo*. Purification by flash chromatography (5:1 hexanes/ethyl acetate to 100% ethyl acetate) gave the product **62** (214 mg, 78% yield over two steps) as a clear oil.

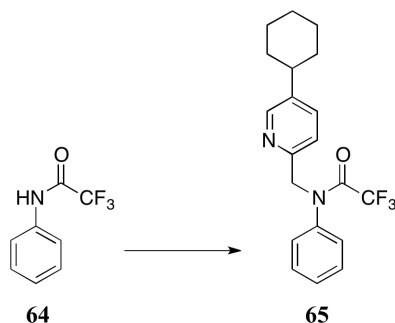
^1H NMR (300 MHz, Chloroform-*d*) δ 8.40 (d, $J = 1.5$ Hz, 1H), 8.32 (d, $J = 1.5$ Hz, 1H), 8.18 – 8.07 (m, 1H), 8.07 – 7.98 (m, 1H), 7.38 – 7.20 (m, 6H), 6.85 – 6.76 (m, 2H), 5.18 – 4.70 (m, 5H), 3.98 – 3.80 (m, 1H), 3.57 – 3.43 (m, 1H), 3.07 (s, 3H), 2.83 (s, 3H), 2.76 – 2.61 (m, 1H), 2.13 – 1.96 (m, 1H), 1.94 – 1.13 (m, 11H); ^{19}F NMR (282 MHz, Chloroform-*d*) δ -122.40 – -124.01 (m), -129.48 – -131.06 (m); HRMS (ESI) $m/z = 751.252$ $[\text{M}+\text{Na}]^+$, HRMS (ESI+) calculated for $\text{C}_{38}\text{H}_{38}\text{F}_2\text{N}_6\text{O}_5\text{S}$: 728.2593, found 728.2627.



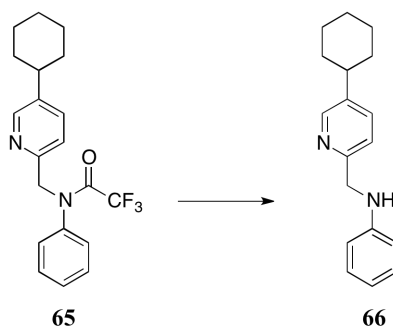
Synthesis of S3I-H222. To a round-bottom flask containing a stir bar was added **62** (155 mg, 0.213 mmol, 1.0 eq) in 1:4 ethyl acetate/methanol (8.8 mL). The mixture was exchanged with nitrogen gas three times before Pd/C (31 mg, 20% by weight) was added. The mixture was then exchanged with nitrogen gas three times before being exchanged with hydrogen gas three times and was then allowed to stir at 25 °C. After 24 hours the reaction was complete, the mixture was flushed through a Celite® plug with ethyl acetate and concentrated *in vacuo*. Purification via prep-TLC yielded the product **S3I-H222** (60 mg, 44% yield) as a white solid. ¹H NMR (300 MHz, Chloroform-*d*) δ 10.36 (s, 1H), 8.46 (d, *J* = 1.5 Hz, 1H), 8.37 (d, *J* = 1.5 Hz, 1H), 8.22 – 8.10 (m, 1H), 8.10 – 7.99 (m, 1H), 7.37 (d, *J* = 8.3 Hz, 1H), 6.84 (d, *J* = 2.1 Hz, 1H), 6.77 (dd, *J* = 8.3, 2.1 Hz, 1H), 5.21 – 4.78 (m, 3H), 4.09 – 3.93 (m, 1H), 3.75 – 3.56 (m, 1H), 3.17 (s, 6H), 2.81 – 2.64 (m, 1H), 2.44 – 2.27 (m, 1H), 2.07 – 1.66 (m, 6H), 1.63 – 1.19 (m, 5H); ¹⁹F NMR (282 MHz, Chloroform-*d*) δ -122.73 (ddd, *J* = 20.0, 7.0, 4.9 Hz), -129.78 (ddd, *J* = 20.0, 8.9, 1.8 Hz); HPLC Purity = 100%; HRMS (ESI) *m/z* = 661.2015 [*M*+Na]⁺, HRMS (ESI+) calculated for C₃₁H₃₂F₂N₆O₅S: 638.2123, found 638.2125; EMSA IC₅₀ = 2.25 ± 0.04 μM.



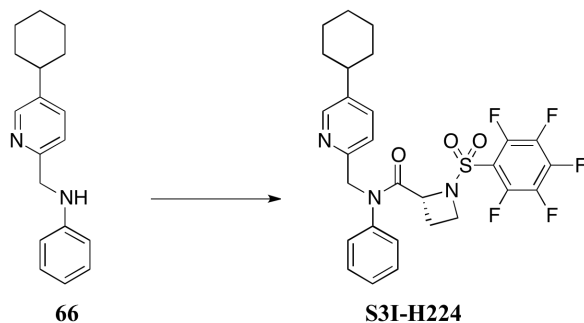
Synthesis of 64. To a round-bottom flask equipped with a stir bar was added aniline **63** (0.69 mL, 7.52 mmol, 1.0 eq) followed by DCM (25.0 mL) under an atmosphere of argon. The solution was cooled and stirred for 2 minutes at 0 °C before pyridine (1.33 mL, 16.5 mmol, 2.2 eq) and TFAA (1.35 mL, 9.71 mmol, 1.3 eq) were added. The solution was warmed to room temperature, stirred for 1.5 hours, diluted with DCM, washed with Sat. Na₂SO₄, washed with Sat. NaHCO₃, washed with 1M HCl, dried over anhydrous Na₂SO₄, and solvent was condensed *in vacuo*. Purification by flash chromatography (7:3 hexanes/ethyl acetate) gave the product **64** (1.24 g, 88% yield) as a white solid. ¹H NMR (300 MHz, Chloroform-*d*) δ 8.01 (s, 1H), 7.61 – 7.52 (m, 2H), 7.45 – 7.35 (m, 2H), 7.30 – 7.19 (m, 1H); ¹⁹F NMR (282 MHz, Chloroform-*d*) δ -75.73 (d, *J* = 1.3 Hz); HRMS (ESI) *m/z* = 190.0482 [M+H]⁺, HRMS (ESI+) calculated for C₈H₆F₃NO: 189.0401, found 189.0406.



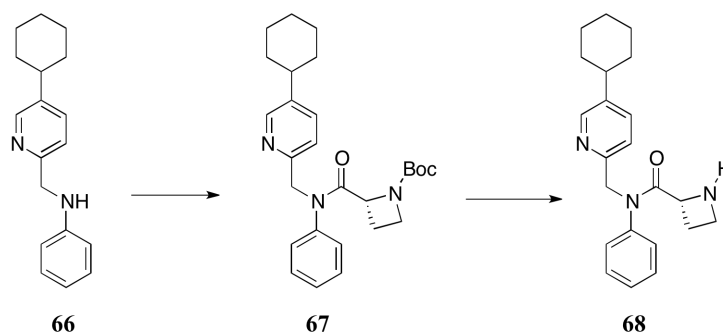
Synthesis of 65. To a round-bottom flask equipped with a stir bar was added NaI (32 mg, 0.211 mmol, 0.2 eq), K₂CO₃ (292 mg, 2.11 mmol, 2.0 eq), 2,2,2-trifluoro-*N*-phenylacetamide **64** (200 mg, 1.06 mmol, 1.0 eq), dry acetonitrile (13.6 mL), and 2-(chloromethyl)-5-cyclohexylpyridine **3** (2.11 mL, 1.05 mmol, 1.0 eq) under an atmosphere of argon. The suspension was warmed to 65 °C, and stirred for 6 hours before the second addition of 2-(chloromethyl)-5-cyclohexylpyridine **3** (2.11 mL, 1.05 mmol, 1.0 eq). The suspension was stirred for 18 hours at 65 °C, quenched with water, extracted with ethyl acetate, washed with brine, dried over anhydrous Na₂SO₄, and solvent was condensed *in vacuo*. Purification by flash chromatography (10:1 hexanes/ethyl acetate) gave the product **65** (218 mg, 57% yield) as a clear oil. ¹H NMR (300 MHz, Chloroform-*d*) δ 8.36 (d, *J* = 2.3 Hz, 1H), 7.48 (dd, *J* = 8.1, 2.3 Hz, 1H), 7.38 – 7.28 (m, 3H), 7.28 – 7.13 (m, 3H), 5.00 (s, 2H), 2.59 – 2.38 (m, 1H), 1.95 – 1.66 (m, 5H), 1.55 – 1.13 (m, 5H); ¹⁹F NMR (282 MHz, Chloroform-*d*) δ -66.95; HRMS (ESI) *m/z* = 364.1718 [M+H]⁺, HRMS (ESI⁺) calculated for C₂₀H₂₁F₃N₂O: 362.1606, found 362.1606.



Synthesis of 66. To a solution of trifluoroacetamide **65** (214 mg, 0.591 mmol, 1.0 eq) in 1:1 THF/MeOH (2.0 mL) was added K_2CO_3 (163 mg, 1.18 mmol, 2.0 eq) under an atmosphere of argon. The suspension was stirred at room temperature for 23 hours, quenched with Sat. NH_4Cl , extracted with ethyl acetate, washed with brine, dried over anhydrous Na_2SO_4 , and solvent was condensed *in vacuo*. Purification by flash chromatography (3:1 hexanes/ethyl acetate) gave the product **66** (143 mg, 91% yield). 1H NMR (300 MHz, Chloroform-*d*) δ 8.46 (d, J = 2.3 Hz, 1H), 7.47 (dd, J = 8.0, 2.3 Hz, 1H), 7.31 – 7.12 (m, 3H), 6.81 – 6.60 (m, 3H), 4.79 (s, 1H), 4.43 (s, 2H), 2.62 – 2.44 (m, 1H), 2.00 – 1.71 (m, 5H), 1.53 – 1.20 (m, 5H); HRMS (ESI) m/z = 267.1854 $[M+H]^+$, HRMS (ESI+) calculated for $C_{18}H_{22}N_2$: 266.1783, found 266.1783.

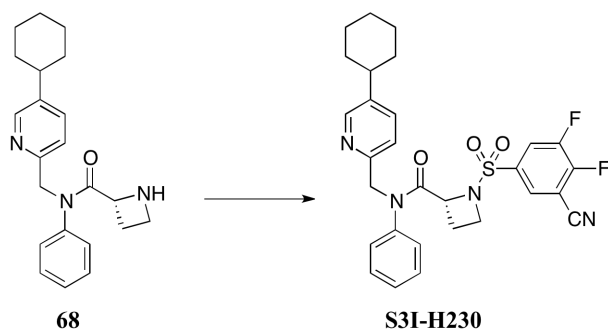


Synthesis of S3I-H224. Note: Water was removed azeotropically from aniline **66** with anhydrous toluene prior to use. To an oven-dried round-bottom flask equipped with a stir bar was added aniline **66** (151 mg, 0.565 mmol, 1.0 eq) followed by dry THF (4.5 mL) under an atmosphere of argon. The solution was cooled to 0 °C and stirred for 2 minutes prior to the addition of MeMgBr (1.01 mL, 1.41 mmol, 2.5 eq). The solution was stirred for 10 minutes at 0 °C prior to the addition of acid chloride **20** (297 mg, 0.848 mmol, 1.5 eq). The solution was warmed to room temperature, stirred for 1 hour, quenched with cold Sat. NH₄Cl and H₂O, extracted with ethyl acetate, washed with brine, dried over anhydrous MgSO₄, and solvent was condensed *in vacuo*. Purification by flash chromatography (3:1 hexanes/ethyl acetate) gave the product **S3I-H224** (181 mg, 53% yield). ¹H NMR (300 MHz, Chloroform-*d*) δ 8.31 (d, *J* = 2.3 Hz, 1H), 7.48 (dd, *J* = 8.1, 2.3 Hz, 1H), 7.40 – 7.31 (m, 3H), 7.19 (d, *J* = 8.1 Hz, 1H), 7.16 – 7.08 (m, 2H), 5.08 – 4.76 (m, 3H), 4.18 – 3.95 (m, 2H), 2.59 – 2.41 (m, 1H), 2.38 – 2.20 (m, 1H), 2.06 – 1.70 (m, 6H), 1.51 – 1.20 (m, 5H); ¹⁹F NMR (282 MHz, Chloroform-*d*) δ -135.44 – -136.27 (m), -146.78 – -147.56 (m), -159.27 – -160.33 (m); HPLC Purity: 99%; HRMS (ESI) *m/z* = 602.1505 [M+Na]⁺, HRMS (ESI⁺) calculated for C₂₈H₂₆F₅N₃O₃S: 579.1615, found 579.1614; EMSA IC₅₀ = 1.08 ± 0.05 μM.

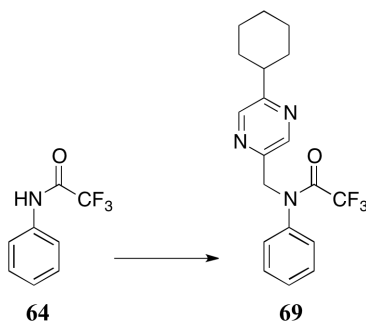


Synthesis of 68. Note: Water was removed azeotropically from aniline **66** with anhydrous toluene prior to use. To an oven dried round-bottom flask equipped with a stir bar was added aniline **66** (157 mg, 0.588 mmol, 1.0 eq) followed by dry THF (6.3 mL). The solution was cooled to 0 °C and stirred for 2 minutes prior to the addition of MeMgBr (1.05 mL, 1.47 mmol, 2.5 eq). The solution was stirred for 10 minutes prior to the addition of acid chloride **35** (271 mg, 1.23 mmol, 2.1 eq) in dry THF (6.3 mL). The solution was warmed to room temperature, stirred for 1 hour, and quenched with water. Ethyl acetate was used to extract the product. The ethyl acetate layer was washed with brine, dried over Na₂SO₄, and solvent was condensed *in vacuo*. Purification by column chromatography (1:1 hexanes/ethyl acetate) gave the product **67** (172 mg) which was used in the following reaction. To a solution of carbamate **67** (172 mg, 0.382 mmol, 1.0 eq) in DCM (4.5 mL) was added TFA (1.1 mL, 14.4 mmol, 37.0 eq) under an atmosphere of argon. The solution was stirred for 1.5 hours at room temperature, quenched with Sat. NaHCO₃, and extracted with DCM. The DCM layer was washed with brine, dried over anhydrous Na₂SO₄, and solvent was removed *in vacuo*. Purification by flash chromatography (24:1 CHCl₃/MeOH) gave the product **68** (86.0 mg, 42% yield over two steps) as a clear oil.

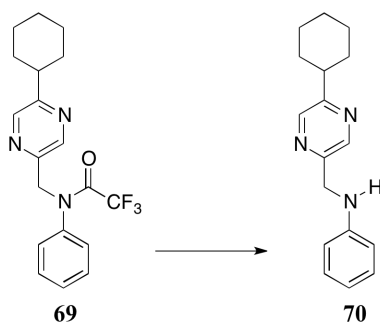
^1H NMR (300 MHz, Chloroform-*d*) δ 8.29 (d, $J = 2.3$ Hz, 1H), 7.43 (dd, $J = 8.0, 2.3$ Hz, 1H), 7.34 – 7.19 (m, 4H), 7.10 – 6.97 (m, 2H), 5.07 – 4.87 (m, 2H), 4.29 – 4.11 (m, 1H), 3.60 – 3.45 (m, 1H), 3.37 – 3.20 (m, 1H), 3.05 (s, 1H), 2.52 – 2.26 (m, 2H), 2.24 – 2.09 (m, 1H), 1.89 – 1.62 (m, 5H), 1.49 – 1.09 (m, 5H); HRMS (ESI) $m/z = 350.2228$ $[\text{M}+\text{H}]^+$, HRMS (ESI+) calculated for $\text{C}_{22}\text{H}_{27}\text{N}_3\text{O}$: 349.2154, found 349.2156.



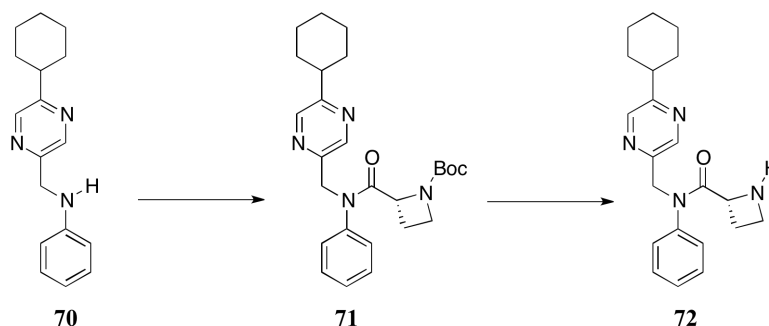
Synthesis of S3I-H230. To a round-bottom flask equipped with a stir bar was added amine **68** (87 mg, 0.248 mmol, 1.0 eq), followed by DCM (5.2 mL). The solution was cooled to 0 °C and stirred for 2 minutes prior to the addition of DIPEA (0.22 mL, 1.24 mmol, 5.0 eq). The solution was stirred for an additional 10 minutes at 0 °C before sulfonyl chloride **17** (118 mg, 0.496 mmol, 2.0 eq) was added. The solution was warmed to room temperature, stirred for 1.5 hours, and quenched with water. The crude product was extracted with DCM, washed with brine, dried over anhydrous Na₂SO₄, and solvent was condensed *in vacuo*. Purification by flash chromatography (2:3 ethyl acetate/hexanes) gave the product **S3I-H230** (80 mg, 59% yield) as a white solid. ¹H NMR (300 MHz, Chloroform-*d*) δ 8.33 (d, *J* = 2.3 Hz, 1H), 8.21 – 8.12 (m, 1H), 8.05 – 7.98 (m, 1H), 7.48 (dd, *J* = 8.1, 2.3 Hz, 1H), 7.41 – 7.31 (m, 3H), 7.25 (d, *J* = 8.1 Hz, 1H), 7.19 – 7.09 (m, 2H), 5.03 – 4.87 (m, 3H), 4.02 – 3.85 (m, 1H), 3.73 – 3.54 (m, 1H), 2.57 – 2.42 (m, 1H), 2.42 – 2.23 (m, 1H), 1.96 – 1.63 (m, 6H), 1.50 – 1.15 (m, 5H); ¹⁹F NMR (282 MHz, Chloroform-*d*) δ -123.05 (ddd, *J* = 20.1, 7.0, 5.0 Hz), -129.95 (ddd, *J* = 20.1, 9.0, 1.8 Hz); HPLC Purity: 100%; HRMS (ESI) *m/z* = 573.1740 [M+Na]⁺, HRMS (ESI+) calculated for C₂₉H₂₈F₂N₄O₃S: 550.1850, found 550.1849; EMSA IC₅₀ = 0.632 ± 0.052 μM.



Synthesis of 69. To a solution of **4** (199 mg, 0.7372 mmol, 1.3 eq) in dry ACN (4.4 mL) was added 2,2,2-trifluoro-*N*-phenylacetamide **64** (107 mg, 0.5671 mmol, 1.0 eq), K₂CO₃ (314 mg, 2.269 mmol, 4.0 eq), and NaI (32 mg, 0.2135 mmol, 0.38 eq) under an atmosphere of argon. The suspension was warmed to 60 °C, stirred for 18 hours, quenched with water, and extracted with ethyl acetate. The ethyl acetate layer was washed with brine, dried over anhydrous Na₂SO₄, and solvent was removed *in vacuo*. Purification by flash chromatography (10:1 hexanes/ethyl acetate) gave the product **69** (175 mg, 85% yield) as a clear oil. ¹H NMR (300 MHz, Chloroform-*d*) δ 8.44 (d, *J* = 1.5 Hz, 1H), 8.37 (d, *J* = 1.5 Hz, 1H), 7.37 – 7.29 (m, 3H), 7.27 – 7.18 (m, 2H), 4.99 (s, 2H), 2.80 – 2.58 (m, 1H), 1.98 – 1.64 (m, 5H), 1.61 – 1.14 (m, 5H); ¹⁹F NMR (282 MHz, Chloroform-*d*) δ -67.09; HRMS (ESI) *m/z* = 386.1466 [M+Na]⁺, HRMS (ESI⁺) calculated for C₁₉H₂₀F₃N₃O: 363.1559, found 363.1562.

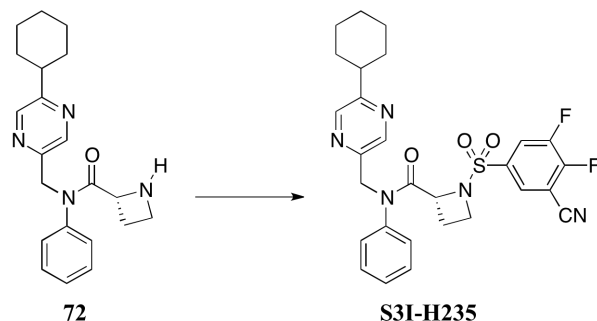


Synthesis of 70. To a solution of trifluoroacetamide **69** (175 mg, 0.4805 mmol, 1.0 eq) in 1:1 THF/MeOH (2.0 mL) was added K_2CO_3 (133 mg, 0.9609 mmol, 2.0 eq) under an atmosphere of argon. The solution was stirred for 24 hours at room temperature and quenched with Sat. NH_4Cl . The crude product was extracted with ethyl acetate, washed with brine, dried over anhydrous Na_2SO_4 , and solvent was condensed *in vacuo*. Purification by flash chromatography (4:1 hexanes/ethyl acetate) gave the product **70** (113 mg, 88% yield) as a white solid. 1H NMR (300 MHz, Chloroform-*d*) δ 8.53 (d, $J = 1.5$ Hz, 1H), 8.41 (d, $J = 1.5$ Hz, 1H), 7.23 – 7.12 (m, 2H), 6.78 – 6.64 (m, 3H), 4.71 (s, 1H), 4.44 (s, 2H), 2.86 – 2.64 (m, 1H), 2.01 – 1.69 (m, 5H), 1.68 – 1.19 (m, 5H); HRMS (ESI) $m/z = 268.1810$ $[M+H]^+$, HRMS (ESI+) calculated for $C_{17}H_{21}N_3$: 267.1735, found 267.1737.

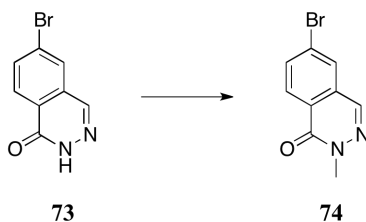


Synthesis of 72. Note: Water was removed azeotropically from aniline **70** with anhydrous toluene prior to use. To a round-bottom flask equipped with a stir bar was added aniline **70** (113 mg, 0.4241 mmol, 1.0 eq) followed by dry THF (4.6 mL) under an atmosphere of argon. The solution was cooled to 0 °C and stirred for 2 minutes before MeMgBr (0.76 mL, 1.060 mmol, 12.5 eq) was added. The solution was stirred for an additional 10 minutes at 0 °C before acid chloride **35** (196 mg, 0.8906 mmol, 2.1 eq) in dry THF (4.6 mL) was added. The solution was warmed to room temperature, stirred for 1 hour, quenched with water, and the crude product was extracted with ethyl acetate. The ethyl acetate layer was washed with brine, dried over anhydrous Na₂SO₄, and solvent was condensed *in vacuo*. Purification by flash chromatography (2:1 hexanes/ethyl acetate) gave the product **71** (113 mg) as a clear oil. To a solution of carbamate **71** (105 mg, 0.2339 mmol, 1.0 eq) in DCM (2.8 mL) was added TFA (0.66 mL, 8.655 mmol, 37.0 eq). The solution was allowed to stir at room temperature for 1.5 hours. The reaction mixture was quenched with Sat. NaHCO₃, extracted with DCM, washed with brine, dried over Na₂SO₄, and solvent was condensed *in vacuo*. Purification by flash chromatography (24:1 CHCl₃/MeOH) gave the product **72** as a clear oil (60 mg, 41% yield).

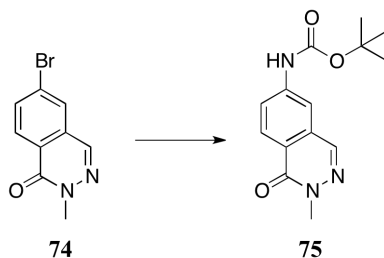
^1H NMR (300 MHz, Chloroform-*d*) δ 8.47 (d, $J = 1.5$ Hz, 1H), 8.32 (d, $J = 1.5$ Hz, 1H), 7.38 – 7.23 (m, 3H), 7.15 – 7.03 (m, 2H), 5.12 – 4.84 (m, 2H), 4.33 – 4.14 (m, 1H), 3.62 – 3.43 (m, 1H), 3.38 – 3.25 (m, 1H), 3.21 (s, 1H), 2.75 – 2.59 (m, 1H), 2.41 – 2.27 (m, 1H), 2.24 – 2.13 (m, 1H), 1.95 – 1.66 (m, 5H), 1.60 – 1.15 (m, 5H); HRMS (ESI) $m/z = 373.1998$ $[\text{M}+\text{Na}]^+$, HRMS (ESI+) calculated for $\text{C}_{21}\text{H}_{26}\text{N}_4\text{O}$: 350.2107, found 350.2101.



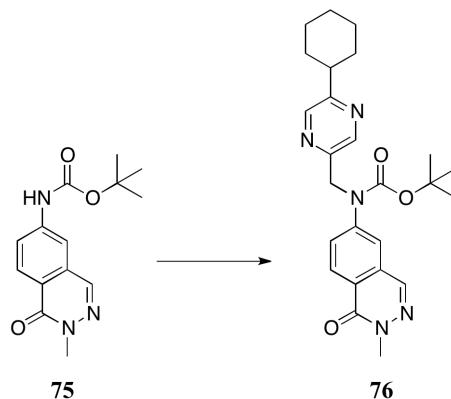
Synthesis of S3I-H235. To a round-bottom flask equipped with a stir bar was added amine **72** (61 mg, 0.1729 mmol, 1.0 eq) followed by DCM (3.6 mL). The solution was cooled to 0 °C and stirred for 2 minutes before DIPEA (0.15 mL, 0.8646 mmol, 5.0 eq) was added. The solution was stirred for an additional 10 minutes at 0 °C before sulfonyl chloride **17** (82 mg, 0.3458 mmol, 2.0 eq) was added. The solution was warmed to room temperature, stirred for 1.5 hours, and quenched with water. The crude product was extracted with DCM, and the DCM layer was washed with brine, dried over anhydrous Na₂SO₄, and solvent was condensed *in vacuo*. Purification by flash chromatography (2:1 hexanes/ethyl acetate) gave the product **S3I-H235** (75 mg, 78% yield) as a white solid. ¹H NMR (300 MHz, Chloroform-*d*) δ 8.46 (d, *J* = 1.5 Hz, 1H), 8.37 (d, *J* = 1.5 Hz, 1H), 8.23 – 8.12 (m, 1H), 8.08 – 7.99 (m, 1H), 7.45 – 7.36 (m, 3H), 7.24 – 7.16 (m, 2H), 5.19 – 4.81 (m, 3H), 4.04 – 3.88 (m, 1H), 3.72 – 3.57 (m, 1H), 2.80 – 2.63 (m, 1H), 2.41 – 2.22 (m, 1H), 1.99 – 1.70 (m, 6H), 1.58 – 1.19 (m, 5H); ¹⁹F NMR (282 MHz, Chloroform-*d*) δ -122.82 (ddd, *J* = 20.0, 7.0, 4.8 Hz), -129.83 (ddd, *J* = 20.0, 8.8, 1.8 Hz); HPLC Purity = 100%; HRMS (ESI) *m/z* = 574.1698 [M+Na]⁺, HRMS (ESI⁺) calculated for C₂₈H₂₇F₂N₅O₃S: 551.1803, found 551.1808; EMSA IC₅₀ = 1.42 ± 0.14 μM.



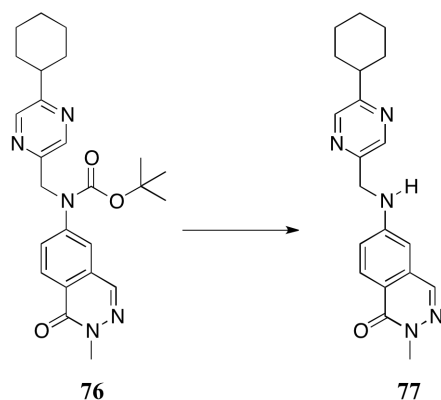
Synthesis of 74. To a round-bottom flask equipped with a stir bar was added 6-bromophthalazin-1(2*H*)-one **73** (2.5 g, 11.11 mmol, 1.0 eq) followed by DMF (45.0 mL) under an atmosphere of argon. The reaction mixture was cooled to 0 °C and stirred for 2 minutes prior to the addition of KHMDS (13.3 mL, 13.33 mmol, 1.2 eq). The reaction mixture was stirred for an additional 10 minutes at 0 °C before MeI (0.90 mL, 14.44 mmol, 1.3 eq) was added. The reaction mixture was warmed to room temperature, stirred for 23 hours, and quenched by addition to a Sat. NH₄Cl solution. The solids were filtered and washed with water and hexanes. This process gave the product **74** (2.2 g, 84% yield) as a white solid. ¹H NMR (300 MHz, DMSO-*d*₆) δ 8.50 – 8.41 (m, 1H), 8.29 – 8.24 (m, 1H), 8.07 – 7.97 (m, 2H), 4.01 (s, 3H).; HRMS (ESI) *m/z* = 240.9795 [M+H]⁺, HRMS (ESI⁺) calculated for C₉H₇BrN₂O: 237.9742, found 237.9740.



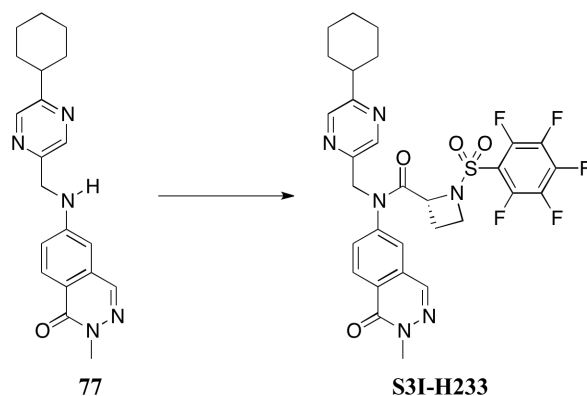
Synthesis of 75. To a round-bottom flask equipped with a stir bar was added 6-bromo-2-methylphthalazin-1(2*H*)-one **74** (2.16 g, 8.317 mmol, 1.0 eq), *t*-butyl carbamate (1.46 g, 12.47 mmol, 1.5 eq), Pd(OAc)₂ (93 mg, 0.4158 mmol, 0.05 eq), Xantphos (240 mg, 0.4158 mmol, .05 eq), and Cs₂CO₃ (5.42 g, 16.63 mmol, 2.0 eq) under an atmosphere of argon. The solids were exchanged with an argon atmosphere (x 3) before dioxane (82.0 mL) was added. The suspension was exchanged with argon (x 3) before being stirred at 100 °C for 23 hours. The reaction mixture was quenched with water, and extracted with ethyl acetate and DCM. The organic layers were washed with brine, combined, dried over anhydrous Na₂SO₄, and solvent was removed *in vacuo*. Purification by recrystallization (2:1 ethyl acetate/hexanes) gave the product **75** (1.97 g, 86% yield) as a yellow solid. ¹H NMR (300 MHz, Chloroform-*d*) δ 8.31 (d, *J* = 8.7 Hz, 1H), 8.12 – 8.01 (m, 2H), 7.45 (dd, *J* = 8.7, 2.2 Hz, 1H), 7.10 (s, 1H), 3.83 (s, 3H), 1.53 (s, 9H); HRMS (ESI) *m/z* = 298.1179 [M+Na]⁺, HRMS (ESI⁺) calculated for C₁₄H₁₇N₃O₃: 275.1270, found 275.1275.



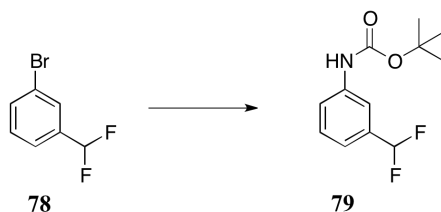
Synthesis of 76. To a round-bottom flask equipped with a stir bar was added carbamate **75** (269 mg, 0.9765 mmol, 1.0 eq) followed by DMF (5.5 mL). The reaction mixture was cooled to 0 °C prior to the addition of KHMDS (1.27 mL, 1.269 mmol, 1.3 eq). The reaction mixture was stirred for an additional 10 minutes at 0 °C before **4** (343 mg, 1.269 mmol, 1.3 eq) in DMF (2.5 mL) was added. The reaction mixture was warmed to room temperature, stirred for 15.5 hours, quenched with Sat. NH₄Cl, and extracted with ethyl acetate. The ethyl acetate layer was washed with brine, dried over anhydrous Na₂SO₄, and solvent was condensed *in vacuo*. Purification by flash chromatography (column #1: 3:1 hexanes/acetone, column #2: 5:1 hexanes/acetone) gave the product **76** (373 mg, 85% yield). ¹H NMR (300 MHz, Chloroform-*d*) δ 8.52 (d, *J* = 1.5 Hz, 1H), 8.40 (d, *J* = 1.5 Hz, 1H), 8.34 (d, *J* = 8.7 Hz, 1H), 8.05 (d, *J* = 0.7 Hz, 1H), 7.81 – 7.68 (m, 2H), 5.02 (s, 2H), 3.81 (s, 3H), 2.82 – 2.64 (m, 1H), 2.02 – 1.70 (m, 5H), 1.65 – 1.16 (m, 14H); HRMS (ESI) *m/z* = 472.2316 [M+Na]⁺, HRMS (ESI⁺) calculated for C₂₅H₃₁N₅O₃: 449.2427, found 449.2428.



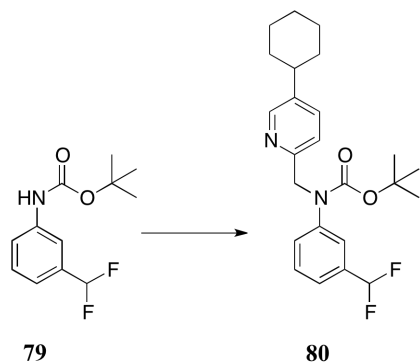
Synthesis of 77. To a solution of carbamate **76** (373 mg, 0.8290 mmol, 1.0 eq) in DCM (9.5 mL) was added TFA (3.7 mL, 48.08 mmol, 58.0 eq) under an atmosphere of argon. The solution was stirred at room temperature for 3 hours, quenched with Sat. NaHCO₃, and extracted with DCM. The DCM layer was washed with brine, dried over anhydrous Na₂SO₄, and solvent was condensed *in vacuo*. This process yielded the product **77** (248 mg, 86% yield). ¹H NMR (300 MHz, Chloroform-*d*) δ 8.53 (d, *J* = 1.5 Hz, 1H), 8.42 (d, *J* = 1.5 Hz, 1H), 8.18 (d, *J* = 8.8 Hz, 1H), 7.94 (s, 1H), 7.07 (dd, *J* = 8.8, 2.4 Hz, 1H), 6.65 (d, *J* = 2.4 Hz, 1H), 5.57 (t, *J* = 5.2 Hz, 1H), 4.54 (d, *J* = 5.2 Hz, 2H), 3.77 (s, 3H), 2.89 – 2.60 (m, 1H), 2.05 – 1.69 (m, 5H), 1.65 – 1.18 (m, 5H); HRMS (ESI) *m/z* = 372.1791 [M+Na]⁺, HRMS (ESI+) calculated for C₂₀H₂₃N₅O: 349.1903, found 349.1901.



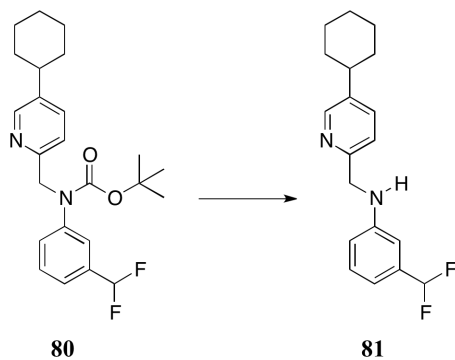
Synthesis of S3I-H233. Note: Water was removed azeotropically from aniline **77** with anhydrous toluene prior to use. To a round-bottom flask equipped with a stir bar was added amine **77** (96 mg, 0.2747 mmol, 1.0 eq) followed by dry THF (3.1 mL) under an atmosphere of argon. The solution was cooled to 0 °C and stirred for 2 minutes prior to the addition of MeMgBr (0.25 mL, 0.3572 mmol, 1.3 eq). The solution was stirred for an additional 10 minutes at 0 °C before acid chloride **20** (144 mg, 0.4121 mmol, 1.5 eq) was added. The solution was warmed to room temperature, stirred for 2.5 hours, quenched with Sat. NH₄Cl, and extracted with ethyl acetate. The ethyl acetate layer was washed with brine, dried over anhydrous Na₂SO₄, and solvent was condensed *in vacuo*. Purification by preparative TLC (1:1 hexanes/acetone) gave the product **S3I-H233** (66 mg, 38% yield) as a white solid. ¹H NMR (300 MHz, Chloroform-*d*) δ 8.47 – 8.40 (m, 2H), 8.35 (s, 1H), 8.10 (s, 1H), 7.71 – 7.57 (m, 2H), 5.16 – 4.73 (m, 3H), 4.17 – 3.93 (m, 2H), 3.84 (s, 3H), 2.80 – 2.61 (m, 1H), 2.38 – 2.19 (m, 1H), 2.04 – 1.67 (m, 6H), 1.61 – 1.19 (m, 5H); ¹⁹F NMR (282 MHz, Chloroform-*d*) δ -135.77 – -136.12 (m), -146.34 – -146.65 (m), -159.18 – -159.46 (m); HPLC Purity = 100%; HRMS (ESI) *m/z* = 685.1653 [M+Na]⁺, HRMS (ESI⁺) calculated for C₃₀H₂₇F₅N₆O₄S: 662.1735, found 662.1751; EMSA IC₅₀ = 4.32 ± 1.02 μM.



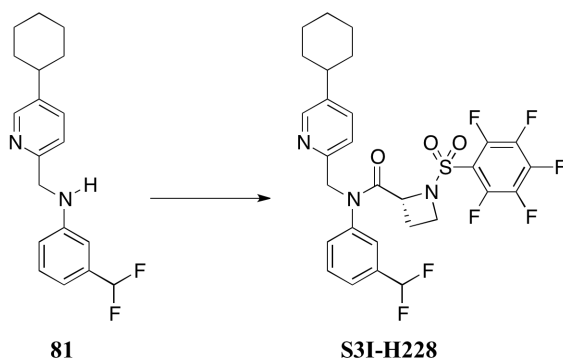
Synthesis of 79. To a round-bottom flask equipped with a stir bar was added 1-bromo-3-(difluoromethyl)benzene **78** (0.32 mL, 2.415 mmol, 1.0 eq), Xantphos (70 mg, 0.1208 mmol, 0.05 eq), *t*-butyl carbamate (339 mg, 2.898 mmol, 1.2 eq), Cs₂CO₃ (1.57 g, 4.830 mmol, 2.0 eq), and Pd(OAc)₂ (27 mg, 0.1208 mmol, 0.05 eq) under an atmosphere of argon. The solids were exchanged with argon (x 3) before dioxane (28.0 mL) was added. The suspension was exchanged with argon (x 3) before being heated to 100 °C. The suspension was stirred for 18 hours at 100 °C, quenched with Sat. NH₄Cl, and the crude product was extracted with ethyl acetate. The organic extracts were washed with brine, dried over anhydrous Na₂SO₄, and solvent was condensed *in vacuo*. Purification by flash chromatography (100% hexanes to 9:1 hexanes/ethyl acetate) gave the product **79** (368 mg, 63% yield) as a white solid. ¹H NMR (300 MHz, Chloroform-*d*) δ 7.61 (s, 1H), 7.46 – 7.30 (m, 2H), 7.23 – 7.13 (m, 1H), 6.82 – 6.39 (m, 2H), 1.52 (s, 9H); ¹⁹F NMR (282 MHz, Chloroform-*d*) δ -110.81 (d, *J* = 56.6 Hz); HRMS (ESI) *m/z* = 242.0975 [M+H]⁺, HRMS (ESI⁺) calculated for C₁₂H₁₅F₂NO₂: 243.1071, found 243.1059.



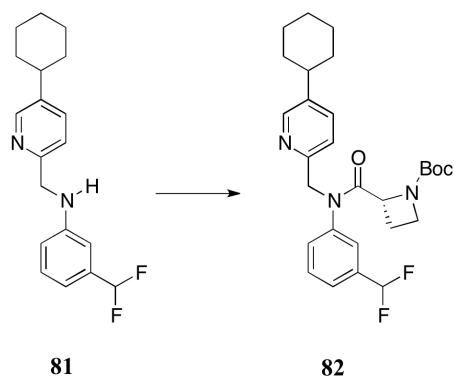
Synthesis of 80. To a round-bottom flask equipped with a stir bar was added carbamate **79** (100 mg, 0.4111 mmol, 1.0 eq) followed by DMF (2.32 mL). The solution was cooled to 0 °C before KHMDS (0.53 mL, 0.5344 mmol, 1.3 eq) was added. The solution was stirred for an additional 10 minutes at 0 °C before alkyl chloride **3** (1.07 mL, 0.5344 mmol, 1.3 eq) was added. The solution was warmed to room temperature, stirred for 24 hours, quenched with Sat. NH₄Cl, and extracted with ethyl acetate. The ethyl acetate layer was washed with brine, dried over anhydrous Na₂SO₄, and solvent was condensed *in vacuo*. Purification by flash chromatography (9:1 hexanes/ethyl acetate to 8:2 hexanes/ethyl acetate) gave the product **80** (147 mg, 86% yield). ¹H NMR (300 MHz, Chloroform-*d*) δ 8.37 (d, *J* = 2.3 Hz, 1H), 7.53 – 7.43 (m, 2H), 7.42 – 7.29 (m, 2H), 7.28 – 7.18 (m, 2H), 6.56 (t, *J* = 56.4 Hz, 1H), 4.92 (s, 2H), 2.57 – 2.42 (m, 1H), 1.91 – 1.66 (m, 5H), 1.51 – 1.15 (m, 14H); ¹⁹F NMR (282 MHz, Chloroform-*d*) δ -110.92 (d, *J* = 56.4 Hz); HRMS (ESI) *m/z* = 417.2354 [M+H]⁺, HRMS (ESI⁺) calculated for C₂₄H₃₀F₂N₂O₂: 416.2275, found 416.2280.



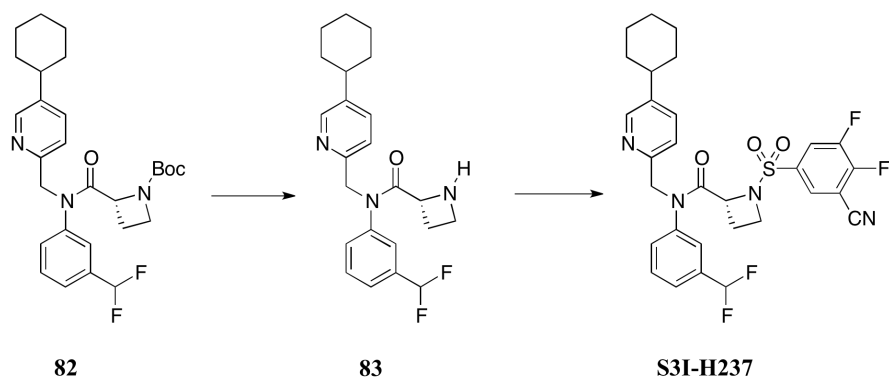
Synthesis of 81. To a solution of carbamate **80** (147 mg, 0.3517 mmol, 1.0 eq) in DCM (4.1 mL) was added TFA (1.56 mL, 20.38 mmol, 58.0 eq) under an atmosphere of argon. The solution was stirred for 3 hours at room temperature, quenched with Sat. NaHCO₃, and extracted with DCM. The DCM layer was washed with brine, dried over anhydrous Na₂SO₄, and solvent was condensed *in vacuo*. Purification by flash chromatography (2:1 hexanes/ethyl acetate) gave the product **81** (101 mg, 91% yield). ¹H NMR (300 MHz, Chloroform-*d*) δ 8.44 (d, *J* = 2.2 Hz, 1H), 7.47 (dd, *J* = 8.0, 2.2 Hz, 1H), 7.30 – 7.12 (m, 2H), 6.88 – 6.30 (m, 4H), 5.08 (s, 1H), 4.41 (s, 2H), 2.62 – 2.44 (m, 1H), 1.96 – 1.70 (m, 5H), 1.51 – 1.16 (m, 5H); ¹⁹F NMR (282 MHz, Chloroform-*d*) δ -110.45 (d, *J* = 56.7 Hz); HRMS (ESI) *m/z* = 317.1825 [M+H]⁺, HRMS (ESI+) calculated for C₁₉H₂₂F₂N₂: 316.1751, found 316.1753.



Synthesis of S3I-H228. To a solution of aniline **81** (101 mg, 0.3189 mmol, 1.0 eq) in DCM (3.0 mL) was added acid chloride **20** (122.7 mg, 0.3508 mmol, 1.1 eq) under an atmosphere of argon. The solution was cooled to 0 °C and stirred for 2 minutes before DMAP (42.9 mg, 0.3508 mmol, 1.1 eq) was added. The solution was warmed to room temperature and stirred for 24 hours. The reaction was quenched with water, extracted with DCM, washed with brine, dried over anhydrous Na₂SO₄, and solvent was condensed *in vacuo*. Purification by flash chromatography (3:1 hexanes/ethyl acetate) gave the product **S3I-H228** (159 mg, 79% yield) as a white solid. ¹H NMR (300 MHz, Chloroform-*d*) δ 8.30 (d, *J* = 2.2 Hz, 1H), 7.53 – 7.39 (m, 3H), 7.35 – 7.12 (m, 3H), 6.58 (t, *J* = 56.1 Hz, 1H), 5.01 – 4.78 (m, 3H), 4.17 – 3.92 (m, 2H), 2.57 – 2.41 (m, 1H), 2.39 – 2.20 (m, 1H), 2.06 – 1.65 (m, 6H), 1.54 – 1.14 (m, 5H); ¹⁹F NMR (282 MHz, Chloroform-*d*) δ -111.51 (m), -135.75 – -136.14 (m), -146.85 – -147.48 (m), -159.40 – -160.09 (m); HPLC Purity = 100%; HRMS (ESI) *m/z* = 652.1476 [M+Na]⁺, HRMS (ESI+) calculated for C₂₉H₂₆F₇N₃O₃S: 629.1583, found 629.1585; EMSA IC₅₀ = 1.78 ± 0.28 μM.

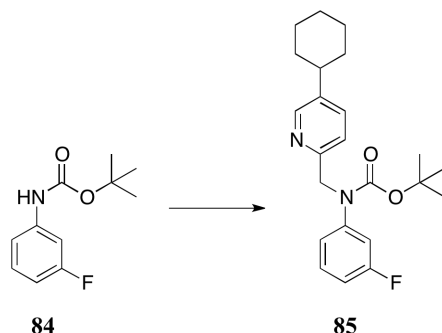


Synthesis of 82. Note: Water was removed azeotropically from aniline **81** with anhydrous toluene prior to use. To a round-bottom flask equipped with a stir bar was added aniline **81** (199 mg, 0.6293 mmol, 1.0 eq) followed by dry THF (6.8 mL) under an atmosphere of argon. The solution was cooled to 0 °C and stirred for 2 minutes before MeMgBr (1.12 mL, 1.573 mmol, 2.5 eq) was added. The solution was stirred for an additional 10 minutes at 0 °C before acid chloride **35** (290 mg, 1.321 mmol, 2.1 eq) in dry THF (6.8 mL) was added. The solution was warmed to room temperature, stirred for 1 hour, and quenched with water. The crude product was extracted with ethyl acetate, washed with brine, dried over anhydrous Na₂SO₄, and solvent was condensed *in vacuo*. Purification by flash chromatography (1:1 hexanes/ethyl acetate) gave the product **82** (200 mg, 63% yield) as a clear oil. ¹H NMR (300 MHz, Chloroform-*d*) δ 8.24 (d, *J* = 2.2 Hz, 1H), 7.48 – 7.19 (m, 6H), 6.54 (t, *J* = 56.2 Hz, 1H), 5.06 – 4.77 (m, 2H), 4.56 – 4.37 (m, 1H), 4.05 – 3.91 (m, 1H), 3.73 – 3.62 (m, 1H), 2.51 – 2.35 (m, 1H), 2.20 – 1.95 (m, 2H), 1.84 – 1.60 (m, 5H), 1.43 – 1.10 (m, 14H); ¹⁹F NMR (282 MHz, Chloroform-*d*) δ -110.49 – -112.13 (m); HRMS (ESI) *m/z* = 522.2543 [M+Na]⁺, HRMS (ESI⁺) calculated for C₂₈H₃₅F₂N₃O₃: 499.2646, found 499.2650.

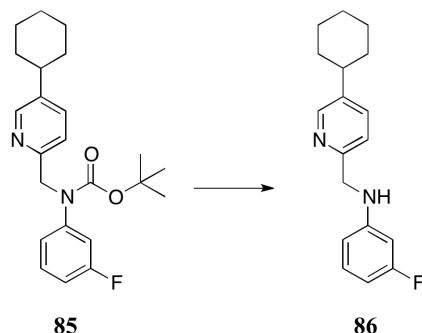


Synthesis of S3I-H237. To a solution of carbamate **82** (200 mg, 0.3995 mmol, 1.0 eq) in DCM (4.8 mL) was added TFA (1.1 mL, 14.78 mmol, 37.0 eq). The solution was stirred at room temperature for 1.5 hours, quenched with Sat. NaHCO₃, and extracted with DCM. The DCM layer was washed with brine, dried over anhydrous Na₂SO₄, and solvent was condensed *in vacuo*. Purification by flash chromatography (24:1 CHCl₃/MeOH) gave the product **83** (100 mg). To a round-bottom flask equipped with a stir bar was added amine **83** (100 mg, 0.2418 mmol, 1.0 eq) followed by DCM (5.0 mL) under an argon atmosphere. The solution was cooled to 0 °C and stirred for 2 minutes before DIPEA (0.21 mL, 1.209 mmol, 5.0 eq) was added. The solution was stirred for an additional 10 minutes at 0 °C before sulfonyl chloride **17** (115 mg, 0.4836 mmol, 2.0 eq) was added. The solution was warmed to room temperature, stirred for 1.5 hours, and quenched with water. The crude product was extracted with DCM, washed with brine, dried over anhydrous Na₂SO₄, and solvent was condensed *in vacuo*. Purification by flash chromatography (3:1 to 2:1 hexanes/ethyl acetate) gave the product **S3I-H237** (92 mg, 38% yield) as a white solid.

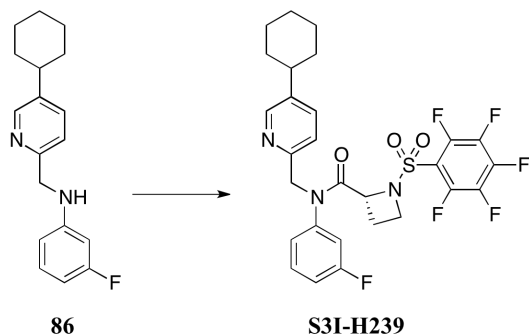
^1H NMR (300 MHz, Chloroform-*d*) δ 8.35 (d, $J = 2.2$ Hz, 1H), 8.23 – 8.10 (m, 1H), 8.10 – 7.99 (m, 1H), 7.59 – 7.43 (m, 3H), 7.41 – 7.19 (m, 3H), 6.61 (t, $J = 56.1$ Hz, 1H), 5.11 – 4.78 (m, 3H), 4.09 – 3.86 (m, 1H), 3.78 – 3.49 (m, 1H), 2.66 – 2.23 (m, 2H), 2.13 – 1.62 (m, 6H), 1.54 – 1.05 (m, 5H); ^{19}F NMR (282 MHz, Chloroform-*d*) δ -111.16 – -111.63 (m), -122.57 – -123.62 (m), -129.41 – -130.59 (m); HPLC Purity = 100%; HRMS (ESI) m/z = 623.1710 $[\text{M}+\text{Na}]^+$, HRMS (ESI+) calculated for $\text{C}_{30}\text{H}_{28}\text{F}_4\text{N}_4\text{O}_3\text{S}$: 600.1818, found 600.1819; EMSA $\text{IC}_{50} = 2.58 \pm 0.07$ μM .



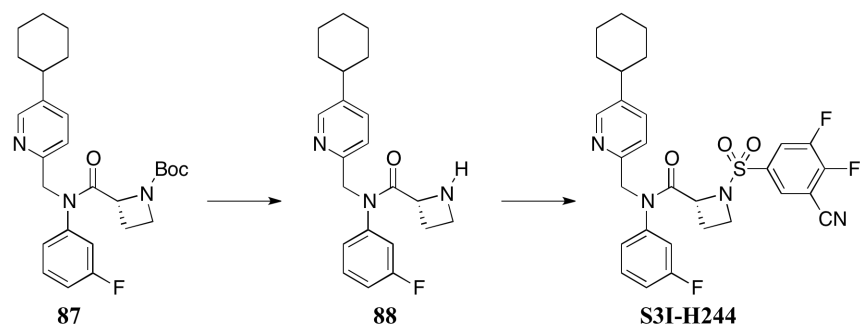
Synthesis of 85. To a round-bottom flask equipped with a stir bar was added *tert*-butyl (3-fluorophenyl)carbamate **84** (500 mg, 2.367 mmol, 1.0 eq) was added DMF (13.0 mL) under an atmosphere of argon. The solution was cooled to 0 °C and stirred for 2 minutes before the addition of KHMDS (3.08 mL, 3.077 mmol, 1.3 eq). The solution was stirred for an additional 10 minutes at 0 °C before alkyl chloride **3** (6.15 mL, 3.077 mmol, 1.3 eq) was added. The solution was warmed to room temperature and stirred for 20 hours. The reaction mixture was quenched with Sat. NH₄Cl, extracted with ethyl acetate, washed with brine, dried over anhydrous Na₂SO₄, and solvent was condensed *in vacuo*. Purification by flash chromatography (9:1 hexanes/ethyl acetate) gave the product **85** (582 mg, 64% yield). ¹H NMR (300 MHz, Chloroform-*d*) δ 8.33 (d, *J* = 2.2 Hz, 1H), 7.42 (dd, *J* = 8.1, 2.2 Hz, 1H), 7.21 – 6.97 (m, 4H), 6.74 (m, 1H), 4.86 (s, 2H), 2.52 – 2.36 (m, 1H), 1.86 – 1.59 (m, 5H), 1.44 – 1.08 (m, 14H); ¹⁹F NMR (282 MHz, Chloroform-*d*) δ -112.29 – -112.74 (m); HRMS (ESI) *m/z* = 407.2109 [M+Na]⁺, HRMS (ESI+) calculated for C₂₃H₂₉FN₂O₂: 384.2213, found 384.2217.



Synthesis of 86. To a solution of carbamate **85** (582 mg, 1.513 mmol, 1.0 eq) in DCM (17.6 mL) was added TFA (6.71 mL, 87.7 mmol, 58.0 eq). The solution was stirred for 3 hours at room temperature, quenched with Sat. NaHCO₃, extracted with DCM, washed with brine, dried over anhydrous Na₂SO₄, and solvent was condensed *in vacuo*. Purification by flash chromatography (3:1 hexanes/ethyl acetate) gave the product **86** (309 mg, 72% yield). ¹H NMR (300 MHz, Chloroform-*d*) δ 8.43 (d, *J* = 2.3 Hz, 1H), 7.49 (dd, *J* = 8.0, 2.3 Hz, 1H), 7.32 – 7.17 (m, 1H), 7.16 – 7.01 (m, 1H), 6.49 – 6.28 (m, 3H), 4.94 (s, 1H), 4.39 (s, 2H), 2.64 – 2.38 (m, 1H), 1.98 – 1.68 (m, 5H), 1.56 – 1.16 (m, 5H); ¹⁹F NMR (282 MHz, Chloroform-*d*) δ -112.97 (ddd, *J* = 11.5, 8.8, 6.8 Hz); HRMS (ESI) *m/z* = 285.1766 [M+H]⁺, HRMS (ESI+) calculated for C₁₈H₂₁FN₂: 284.1689, found 284.1694.

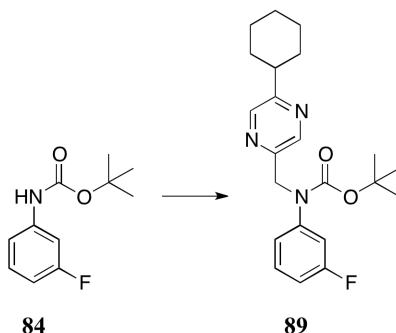


Synthesis of S3I-H239. To a solution of aniline **86** (100 mg, 0.352 mmol, 1.0 eq) in DCM (3.3 mL) was added acid chloride **20** (135 mg, 0.3868 mmol, 1.1 eq) under an atmosphere of argon. The solution was cooled to 0 °C and stirred for 2 minutes before DMAP (47 mg, 0.3868 mmol, 1.1 eq) was added. The solution was warmed to room temperature and stirred for 24 hours. The reaction mixture was quenched with water, extracted with DCM, washed with brine, dried over anhydrous Na₂SO₄, and solvent condensed *in vacuo*. Purification by flash chromatography (3:1 hexanes/ethyl acetate) gave the product **S3I-H239** (97 mg, 46% yield) as a white solid. ¹H NMR (300 MHz, Chloroform-*d*) δ 8.32 (d, *J* = 2.3 Hz, 1H), 7.48 (dd, *J* = 8.1, 2.3 Hz, 1H), 7.40 – 7.28 (m, 1H), 7.17 (d, *J* = 8.1 Hz, 1H), 7.12 – 7.02 (m, 1H), 7.01 – 6.88 (m, 2H), 5.07 – 4.96 (m, 1H), 4.91 – 4.84 (m, 2H), 4.23 – 3.94 (m, 2H), 2.62 – 2.41 (m, 1H), 2.40 – 2.19 (m, 1H), 2.12 – 1.93 (m, 1H), 1.93 – 1.70 (m, 5H), 1.52 – 1.17 (m, 5H); ¹⁹F NMR (282 MHz, Chloroform-*d*) δ -108.75 – -110.83 (m), -135.00 – -137.53 (m), -146.10 – -148.18 (m), -158.37 – -161.07 (m); HPLC Purity = 100%; HRMS (ESI) *m/z* = 620.1420 [M+Na]⁺, HRMS (ESI+) calculated for C₂₈H₂₅F₆N₃O₃S: 597.1521, found 597.1527; EMSA IC₅₀ = > 4 μM.

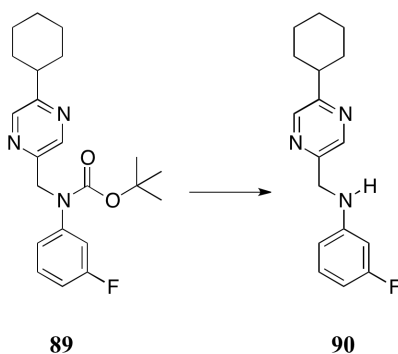


Synthesis of S3I-H244. To a solution of carbamate **87** (85 mg, 0.1824 mmol, 1.0 eq) in DCM (2.2 mL) was added TFA (0.51 mL, 6.750 mmol, 37.0 eq) under an atmosphere of argon. The solution was stirred at room temperature for 1.5 hours. The reaction mixture was quenched with Sat. NaHCO₃, extracted with DCM, washed with brine, dried over anhydrous Na₂SO₄, and solvent was condensed *in vacuo*. Purification by flash chromatography (24:1 CHCl₃/MeOH) gave the product **88** (52 mg). To a round-bottom flask equipped with a stir bar was added amine **88** (52 mg, 0.1426 mmol, 1.0 eq) followed by DCM (3.0 mL) under an atmosphere of argon. The solution was cooled to 0 °C and stirred for 2 minutes before DIPEA (0.12 mL, 0.713 mmol, 5.0 eq) was added. The solution was stirred for an additional 10 minutes at 0 °C before sulfonyl chloride **17** (68 mg, 0.2852 mmol, 2.0 eq) was added. The solution was warmed to room temperature and stirred for 1.5 hours. The reaction mixture was quenched with water, extracted with DCM, washed with brine, dried over anhydrous Na₂SO₄, and solvent was condensed *in vacuo*. Purification by flash chromatography (3:1 hexanes/ethyl acetate) gave the product **S3I-H244** (59 mg, 57% yield over two steps) as a white solid.

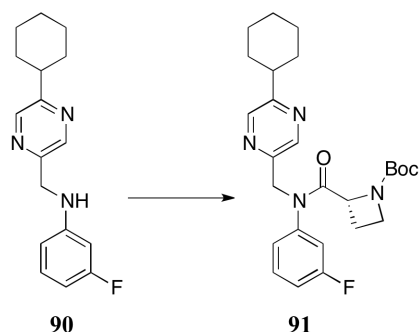
^1H NMR (300 MHz, Chloroform-*d*) δ 8.35 (d, $J = 2.3$ Hz, 1H), 8.21 – 8.10 (m, 1H), 8.08 – 8.00 (m, 1H), 7.49 (dd, $J = 8.0, 2.3$ Hz, 1H), 7.42 – 7.30 (m, 1H), 7.23 (d, $J = 8.0$ Hz, 1H), 7.14 – 6.90 (m, 3H), 5.11 – 4.81 (m, 3H), 4.11 – 3.85 (m, 1H), 3.77 – 3.56 (m, 1H), 2.58 – 2.44 (m, 1H), 2.43 – 2.24 (m, 1H), 2.09 – 1.61 (m, 6H), 1.52 – 1.10 (m, 5H); ^{19}F NMR (282 MHz, Chloroform-*d*) δ -108.76 – -110.07 (m), -122.96 (ddd, $J = 19.9, 7.0, 4.9$ Hz), -129.95 (ddd, $J = 19.9, 8.8, 1.8$ Hz); HPLC Purity = 100%; HRMS (ESI) $m/z = 591.1640$ $[\text{M}+\text{Na}]^+$, HRMS (ESI+) calculated for $\text{C}_{29}\text{H}_{27}\text{F}_3\text{N}_4\text{O}_3\text{S}$: 568.1756, found 568.1747; EMSA $\text{IC}_{50} = 0.978 \pm 0.203$



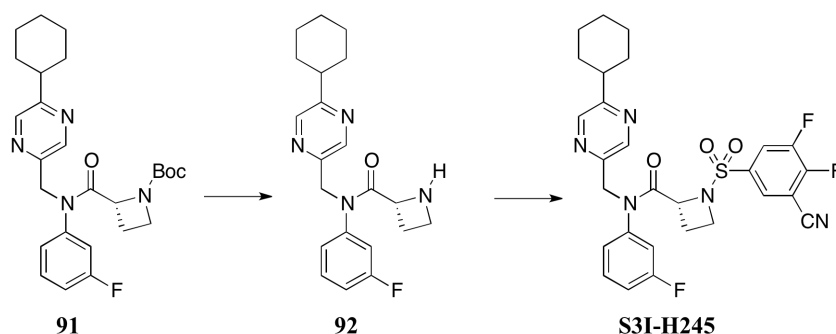
Synthesis of 89. To a round-bottom flask equipped with a stir bar was added *tert*-butyl (3-fluorophenyl)carbamate **84** (142 mg, 0.6743 mmol, 1.0 eq) followed by DMF (3.8 mL) under an atmosphere of argon. The solution was cooled to 0 °C prior to the addition of KHMDS (0.88 mL, 0.8766 mmol, 1.3 eq). The solution was stirred at 0 °C for an additional 10 minutes before **4** (237 mg, 0.8766 mmol, 1.3 eq) in DMF (1.7 mL) was added. The solution was warmed to room temperature and stirred for 19 hours. The reaction mixture was quenched with water, extracted with ethyl acetate, washed with brine, dried over anhydrous Na₂SO₄, and solvent was condensed *in vacuo*. Purification by flash chromatography (9:1 hexanes/ethyl acetate) gave the product **89** (217 mg, 83% yield). ¹H NMR (300 MHz, Chloroform-*d*) δ 8.47 (s, 1H), 8.34 (s, 1H), 7.24 – 7.12 (m, 1H), 7.10 – 6.98 (m, 2H), 6.87 – 6.72 (m, 1H), 4.88 (s, 2H), 2.80 – 2.59 (m, 1H), 2.00 – 1.62 (m, 5H), 1.62 – 1.08 (m, 14H); ¹⁹F NMR (282 MHz, Chloroform-*d*) δ -112.10 – -112.39 (m); HRMS (ESI) *m/z* = 408.2064 [M+Na]⁺, HRMS (ESI⁺) calculated for C₂₂H₂₈FN₃O₂: 385.2166, found 385.2171.



Synthesis of 90. To a solution of carbamate **89** (217 mg, 0.5619 mmol, 1.0 eq) in DCM (6.0 mL) was added TFA (2.5 mL, 32.67 mmol, 58.0 eq) under an atmosphere of argon. The solution was stirred for 3 hours at room temperature, quenched with Sat. NaHCO₃, and extracted with DCM. The DCM layer was washed with brine, dried over anhydrous Na₂SO₄, and solvent was condensed *in vacuo*. Purification by flash chromatography (5:1 hexanes/ethyl acetate) gave the product **90** (149 mg, 93% yield). ¹H NMR (300 MHz, Chloroform-*d*) δ 8.49 (s, 1H), 8.39 (s, 1H), 7.14 – 6.99 (m, 1H), 6.47 – 6.27 (m, 3H), 4.89 (t, *J* = 5.4 Hz, 1H), 4.39 (d, *J* = 5.4 Hz, 2H), 2.80 – 2.57 (m, 1H), 1.99 – 1.68 (m, 5H), 1.64 – 1.15 (m, 5H); ¹⁹F NMR (282 MHz, Chloroform-*d*) δ -112.57 (ddd, *J* = 11.3, 8.6, 6.7 Hz); HRMS (ESI) *m/z* = 286.1718 [M+H]⁺, HRMS (ESI+) calculated for C₁₇H₂₀FN₃: 285.1641, found 285.1646.



Synthesis of 91. Water was removed azeotropically from aniline **90** with anhydrous toluene prior to use. To an oven-dried round-bottom flask equipped with a stir bar was added aniline **90** (149 mg, 0.5253 mmol, 1.0 eq) followed by dry THF (5.7 mL) under an argon atmosphere. The solution was stirred at 0 °C for 2 minutes prior to the addition of MeMgBr (0.93 mL, 1.31 mmol, 2.5 eq). The solution was stirred for an additional 10 minutes at 0 °C before acid chloride **35** (241 mg, 1.099 mmol, 2.1 eq) in dry THF (5.7 mL) was added. The solution was warmed to room temperature and stirred for 1 hour. The reaction mixture was quenched with water, extracted with ethyl acetate, washed with brine, dried over anhydrous Na₂SO₄, and solvent was condensed *in vacuo*. Purification by flash chromatography (7:1 hexanes/ethyl acetate) followed by a 1M HCl and Sat. NaHCO₃ wash gave the product **91** (111 mg, 45% yield). ¹H NMR (300 MHz, Chloroform-*d*) δ 8.54 (s, 1H), 8.29 (d, *J* = 1.1 Hz, 1H), 7.36 – 7.23 (m, 1H), 7.07 – 6.90 (m, 3H), 5.29 – 4.64 (m, 2H), 4.61 – 4.43 (m, 1H), 4.06 – 3.92 (m, 1H), 3.76 – 3.63 (m, 1H), 2.72 – 2.59 (m, 1H), 2.18 – 2.01 (m, 2H), 1.92 – 1.63 (m, 5H), 1.58 – 1.12 (m, 14H); ¹⁹F NMR (282 MHz, Chloroform-*d*) δ -109.68 – -110.36 (m); HRMS (ESI) *m/z* = 491.2433 [M+Na]⁺, HRMS (ESI+) calculated for C₂₆H₃₃FN₄O₃: 468.2537, found 468.2541.



Synthesis of S3I-H245. To a solution of carbamate **91** (111 mg, 0.2365 mmol, 1.0 eq) in DCM (2.9 mL) was added TFA (0.67 mL, 8.750 mmol, 37.0 eq) under an atmosphere of argon. The solution was stirred for 1.5 hours at room temperature, quenched with Sat. NaHCO₃, and extracted with DCM. The DCM layer was washed with brine, dried over anhydrous Na₂SO₄, and solvent was condensed *in vacuo*. Purification by flash chromatography (24:1 CHCl₃/MeOH) gave the product **92** (63 mg). To a round-bottom flask equipped with a stir bar was added amine **92** (63 mg, 0.1723 mmol, 1.0 eq) followed by DCM (3.6 mL). The solution was cooled to 0 °C and stirred for 2 minutes prior to the addition of DIPEA (0.15 mL, 0.8615 mmol, 5.0 eq). The solution was stirred for an additional 10 minutes at 0 °C before sulfonyl chloride **17** (82 mg, 0.3447 mmol, 2.0 eq) was added. The solution was warmed to room temperature and stirred for 1.5 hours. The reaction was quenched with water, extracted with DCM, washed with brine, dried over anhydrous Na₂SO₄, and solvent was condensed *in vacuo*. Purification by flash chromatography (3:1 hexanes/ethyl acetate) gave the product **S3I-H245** (43 mg, 32% yield over two steps) as a white solid.

^1H NMR (300 MHz, Chloroform-*d*) δ 8.46 (s, 1H), 8.37 (s, 1H), 8.20 – 8.09 (m, 1H), 8.07 – 7.99 (m, 1H), 7.47 – 7.32 (m, 1H), 7.19 – 6.94 (m, 3H), 5.22 – 4.77 (m, 3H), 4.12 – 3.87 (m, 1H), 3.76 – 3.54 (m, 1H), 2.83 – 2.60 (m, 1H), 2.44 – 2.22 (m, 1H), 2.03 – 1.66 (m, 6H), 1.66 – 1.14 (m, 5H); ^{19}F NMR (282 MHz, Chloroform-*d*) δ -108.78 – -109.32 (m), -122.84 (ddd, J = 20.0, 7.1, 4.9 Hz), -129.87 (ddd, J = 20.0, 9.0, 1.8 Hz); HPLC Purity = 95%; HRMS (ESI) m/z = 592.1603 $[\text{M}+\text{Na}]^+$, HRMS (ESI+) calculated for $\text{C}_{28}\text{H}_{26}\text{F}_3\text{N}_5\text{O}_3\text{S}$: 569.1709, found 569.1710; EMSA IC_{50} = pending.

Appendix I

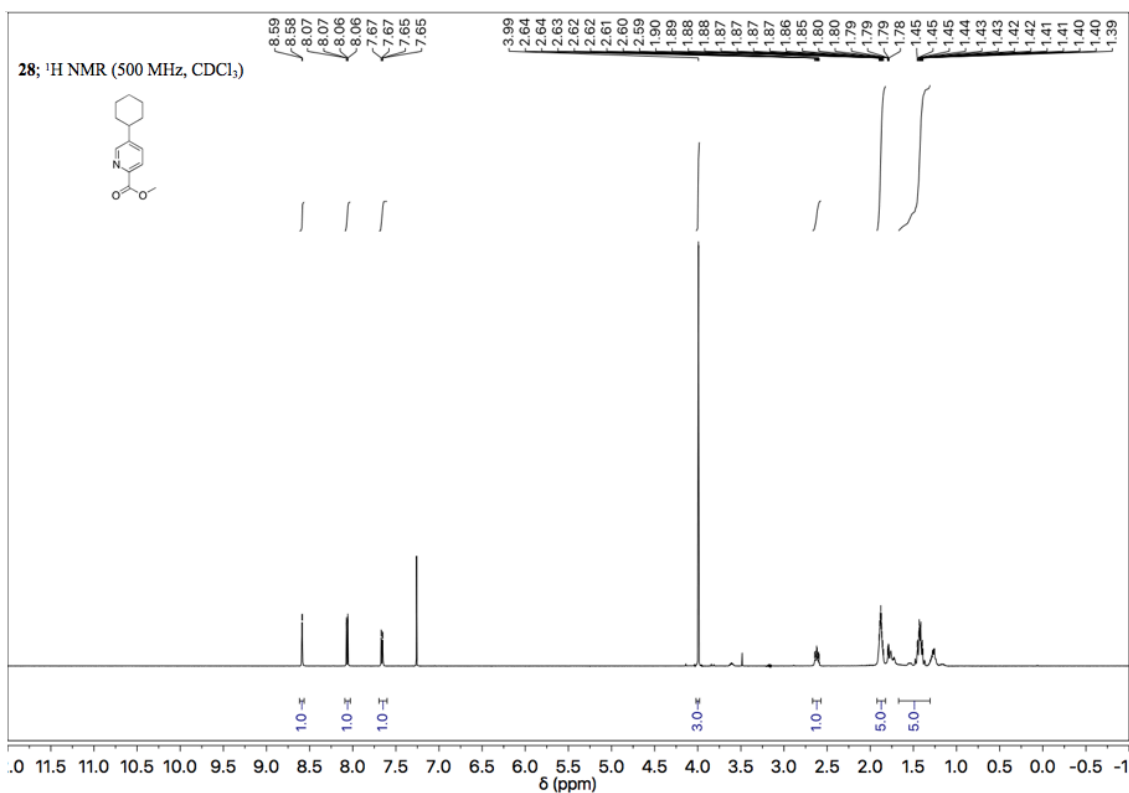
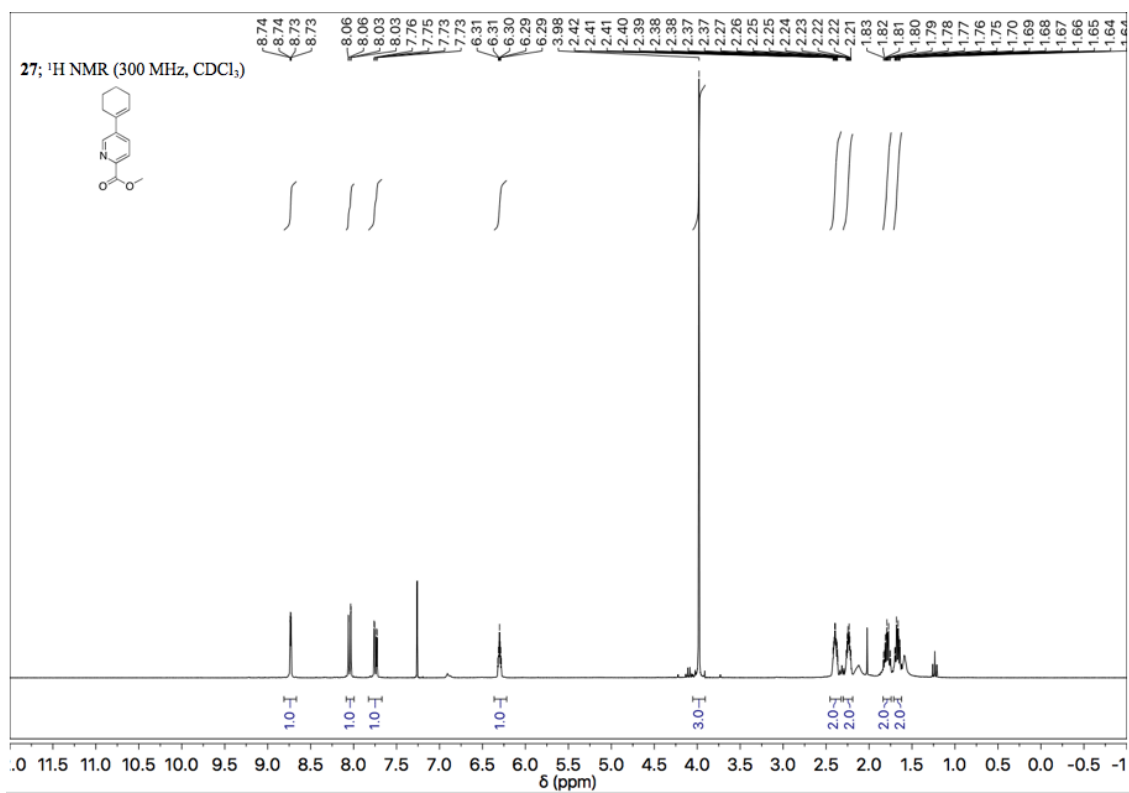
Spectra for Selected Compounds in Chapter 2

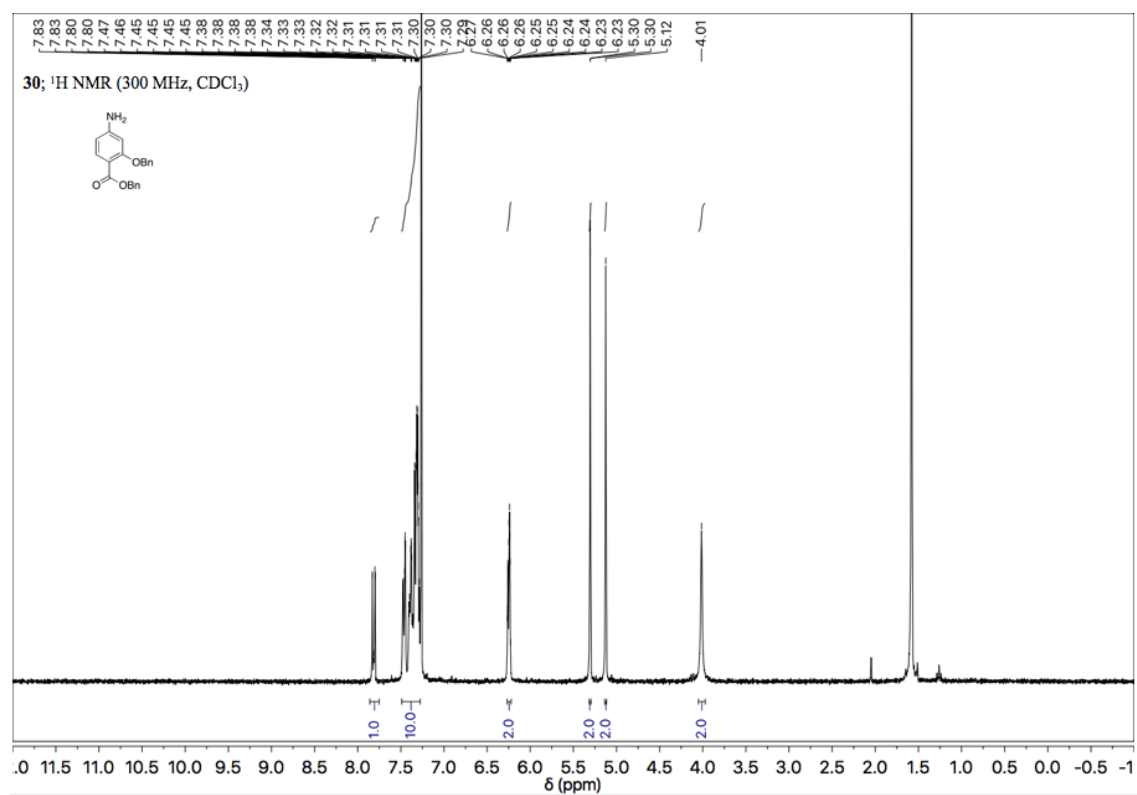
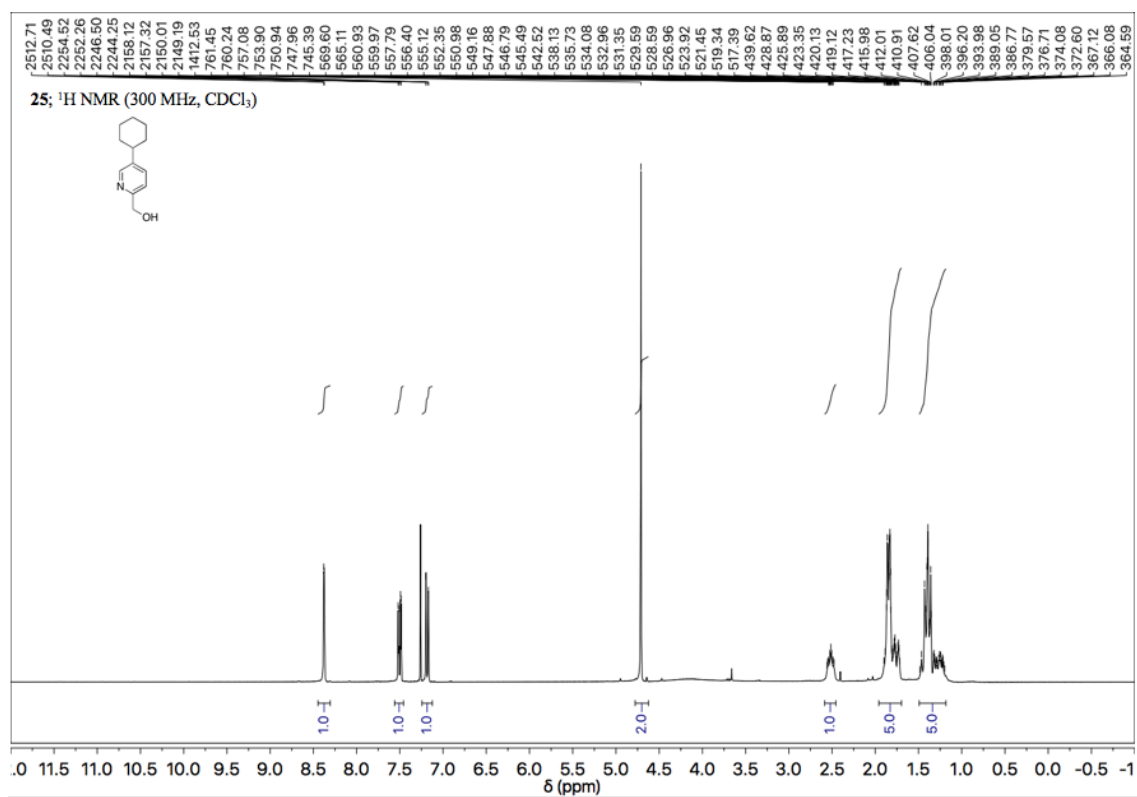
Table of Contents for Appendix I

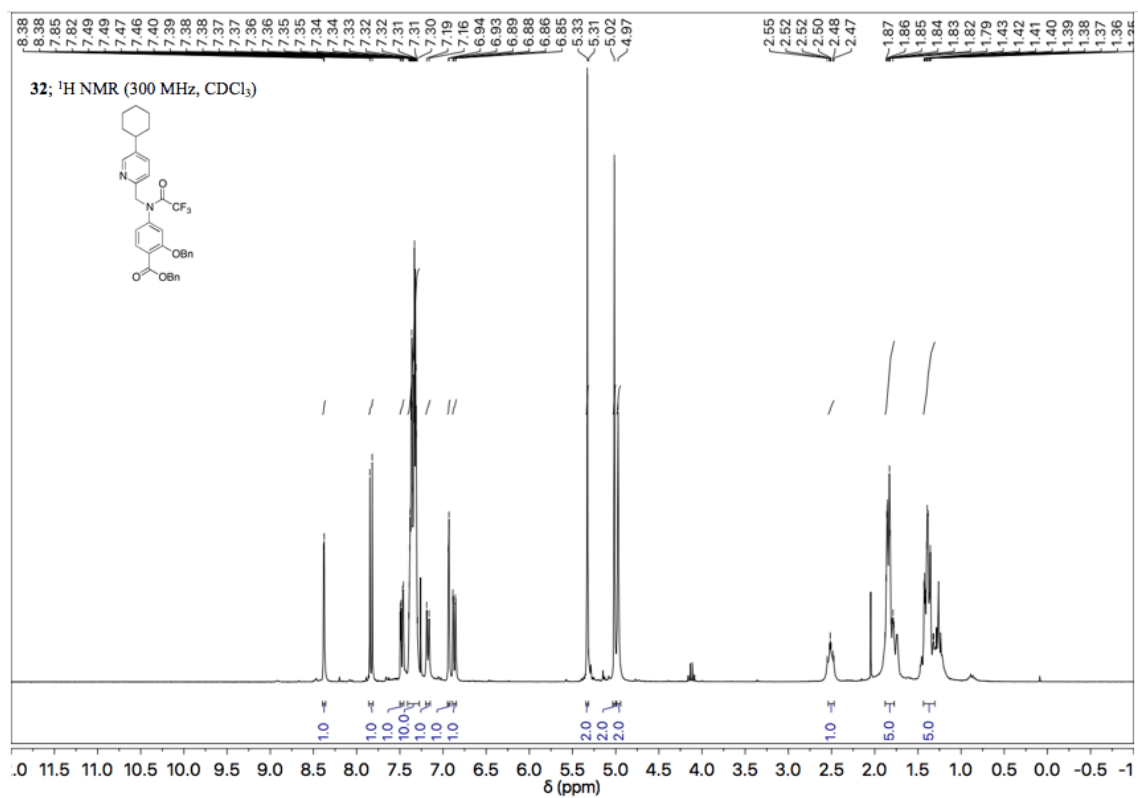
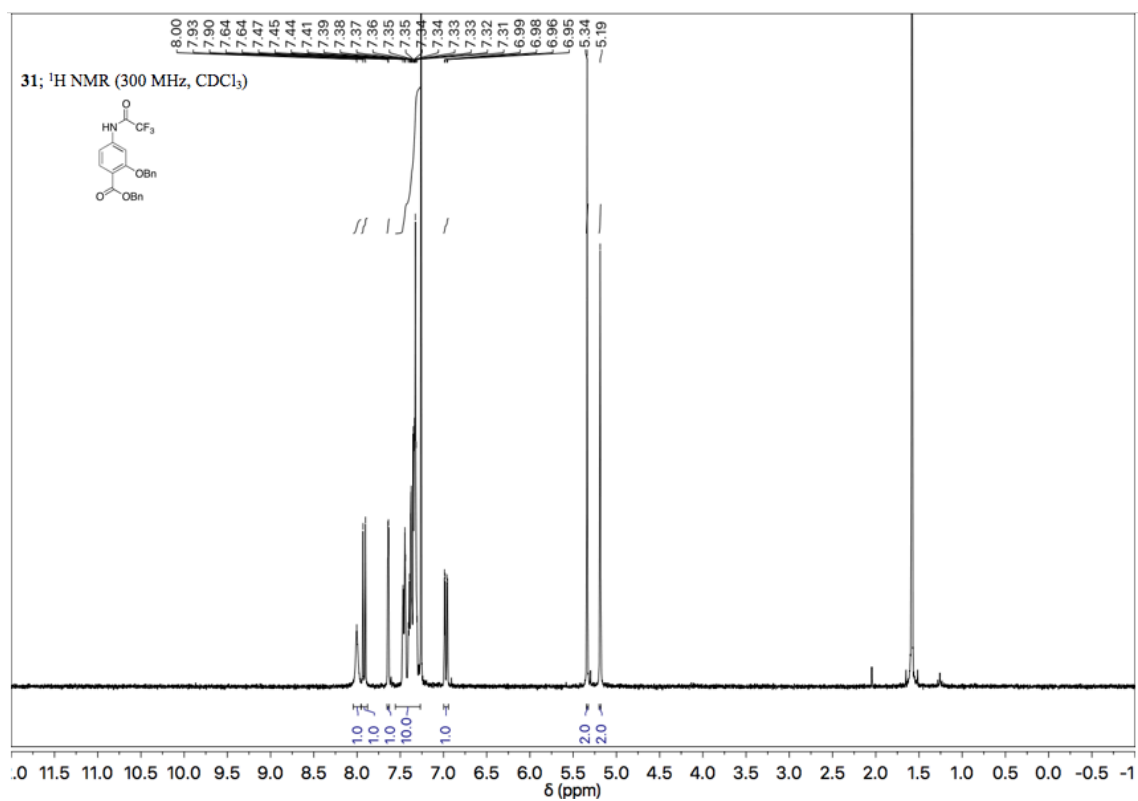
1. Selected Compounds from Chapter 2

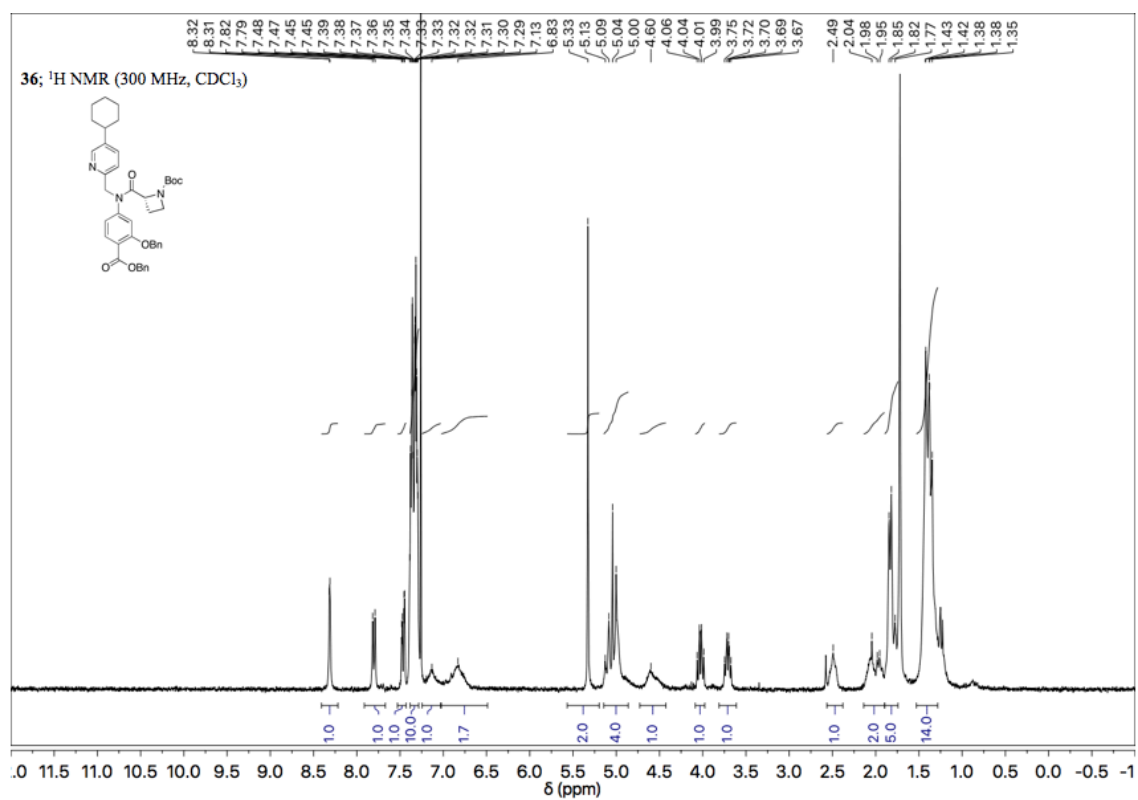
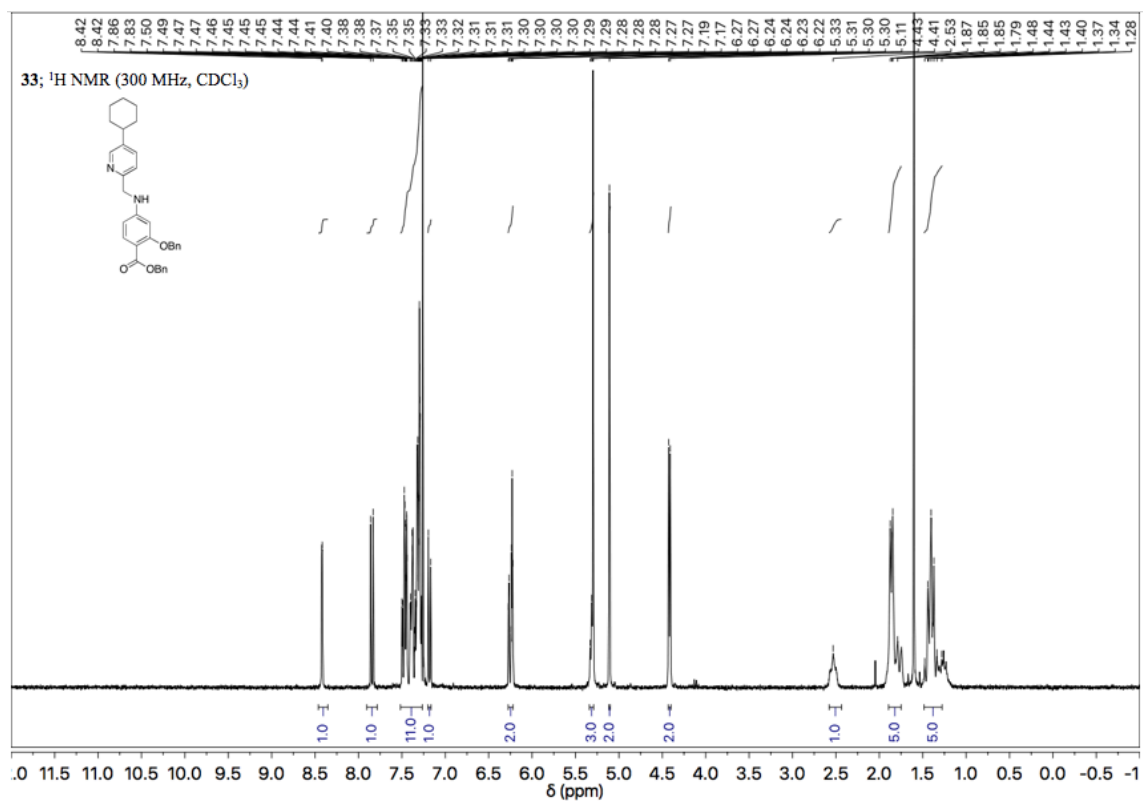
27 (¹H), 28 (¹H)	121
25 (¹H), 30 (¹H)	122
31 (¹H), 32 (¹H)	123
33 (¹H), 36 (¹H)	124
38 (¹H), S3I-H204 (¹H)	125
S3I-H212 (¹H), 44 (¹H)	126
45 (¹H), 46 (¹H)	127
47 (¹H), 55 (¹H)	128
56 (¹H), 57 (¹H)	129
4 (¹H), 58 (¹H)	130
58 (¹⁹F), 59 (¹H)	131
60 (¹H), 62 (¹H)	132
62 (¹⁹F), S3I-H222 (¹H)	133
S3I-H222 (¹⁹F), 64 (¹H)	134
64 (¹⁹F), 65 (¹H)	135
65 (¹⁹F), 66 (¹H)	136
S3I-H224 (¹H, ¹⁹F)	137
68 (¹H), S3I-H230 (¹H)	138
S3I-H230 (¹⁹F), 69 (¹H)	139
69 (¹⁹F), 70 (¹H)	140

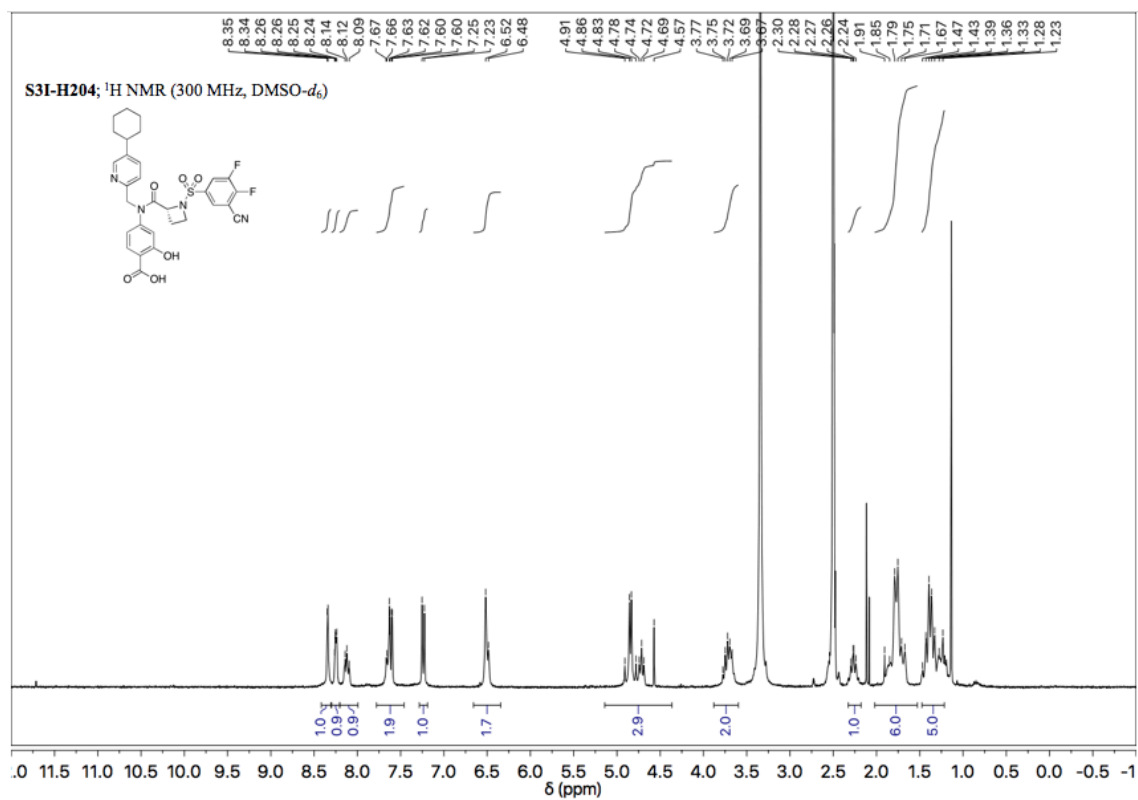
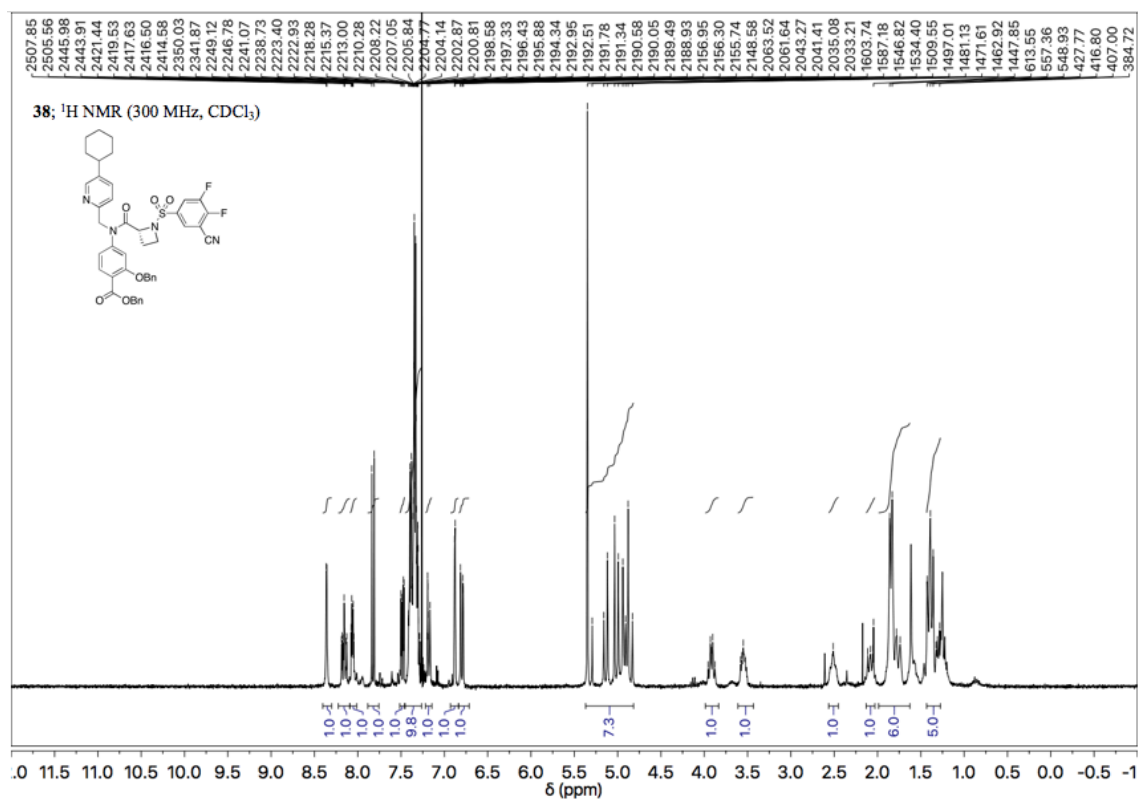
72 (¹H), S3I-H235 (¹H)	141
S3I-H235 (¹⁹F), 74 (¹H)	142
75 (¹H), 76 (¹H)	143
77 (¹H), S3I-H233 (¹H)	144
S3I-H233 (¹⁹F), 79 (¹H)	145
79 (¹⁹F), 80 (¹H)	146
80 (¹⁹F), 81 (¹H)	147
81 (¹⁹F), S3I-H228 (¹H)	148
S3I-H228 (¹⁹F), 82 (¹H)	149
82 (¹⁹F), S3I-H237 (¹H)	150
S3I-H237 (¹⁹F), 85 (¹H)	151
85 (¹⁹F), 86 (¹H)	152
86 (¹⁹F), S3I-H239 (¹H)	153
S3I-H239 (¹⁹F), 87 (¹H)	154
87 (¹⁹F), S3I-H244 (¹H)	155
S3I-H244 (¹⁹F), 89 (¹H)	156
89 (¹⁹F), 90 (¹H)	157
90 (¹⁹F), 91 (¹H)	158
91 (¹⁹F), S3I-H245 (¹H)	159
S3I-H245 (¹⁹F)	160

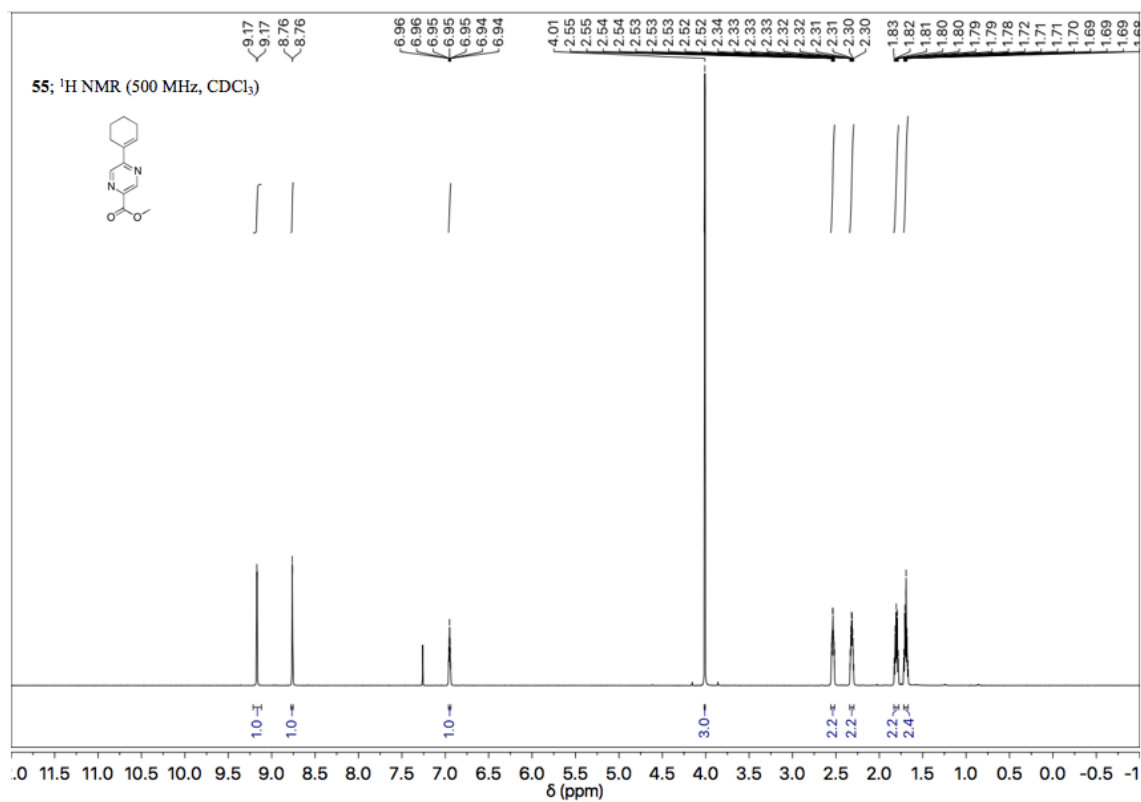
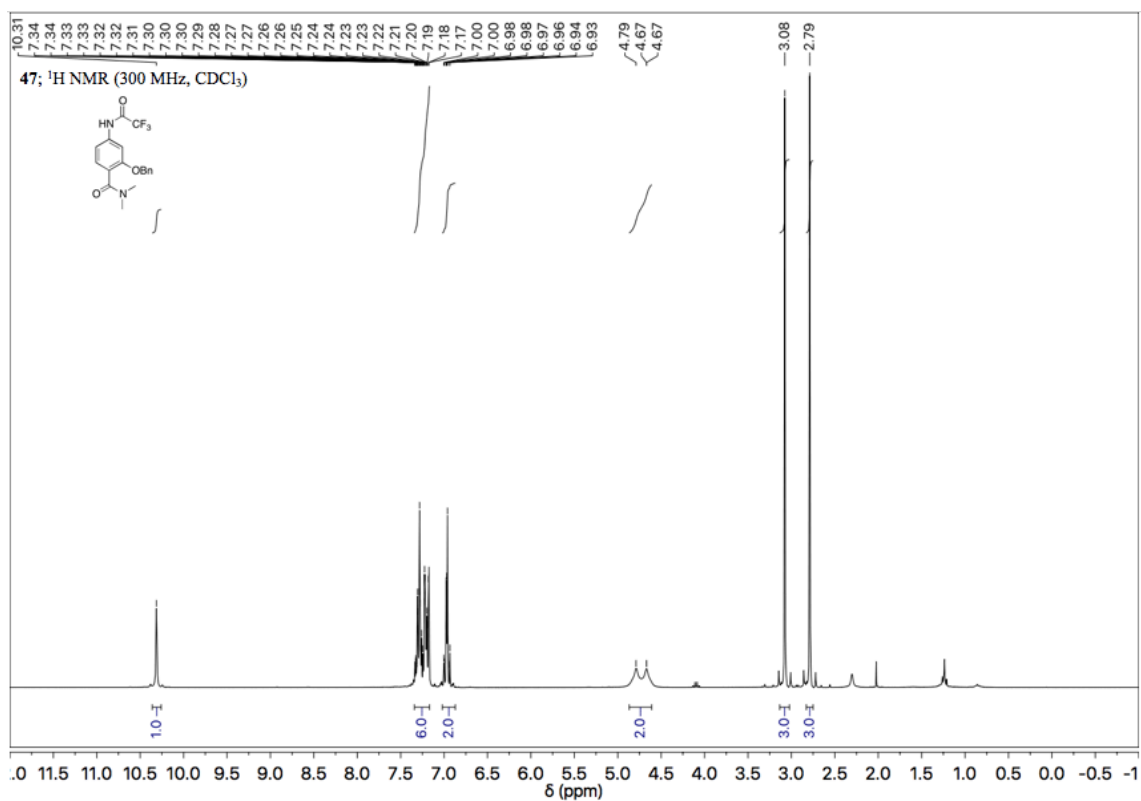


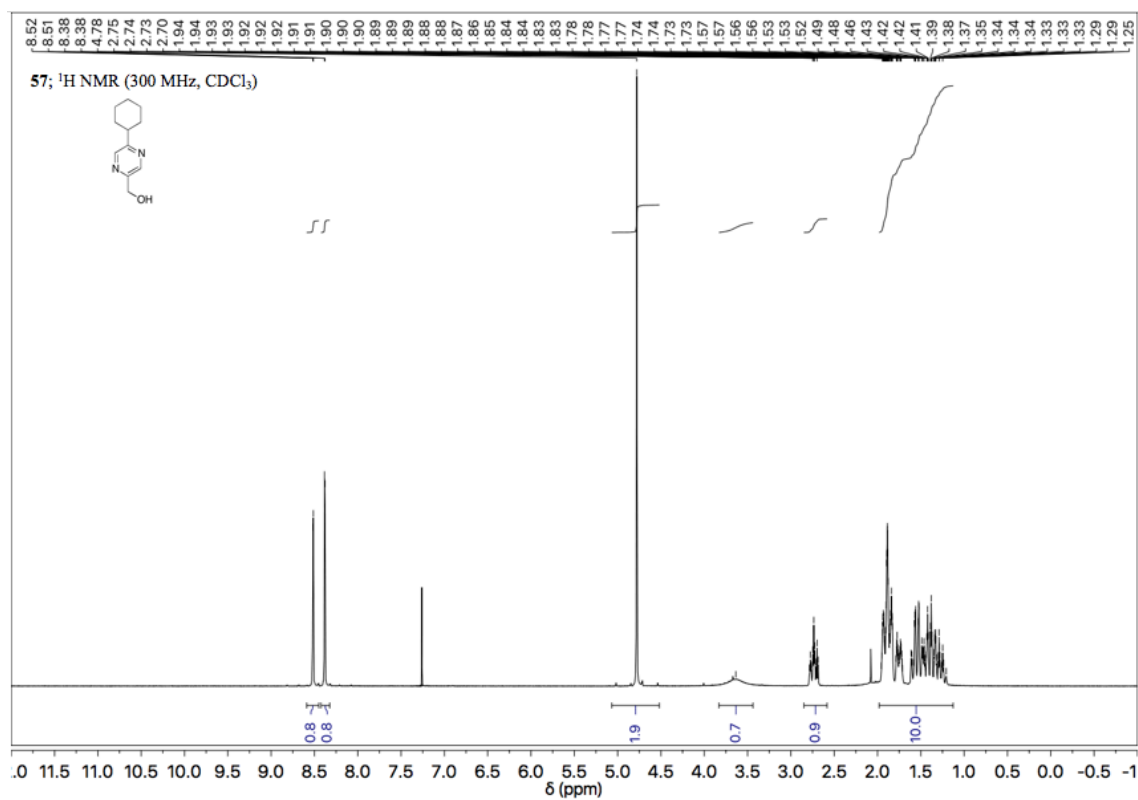
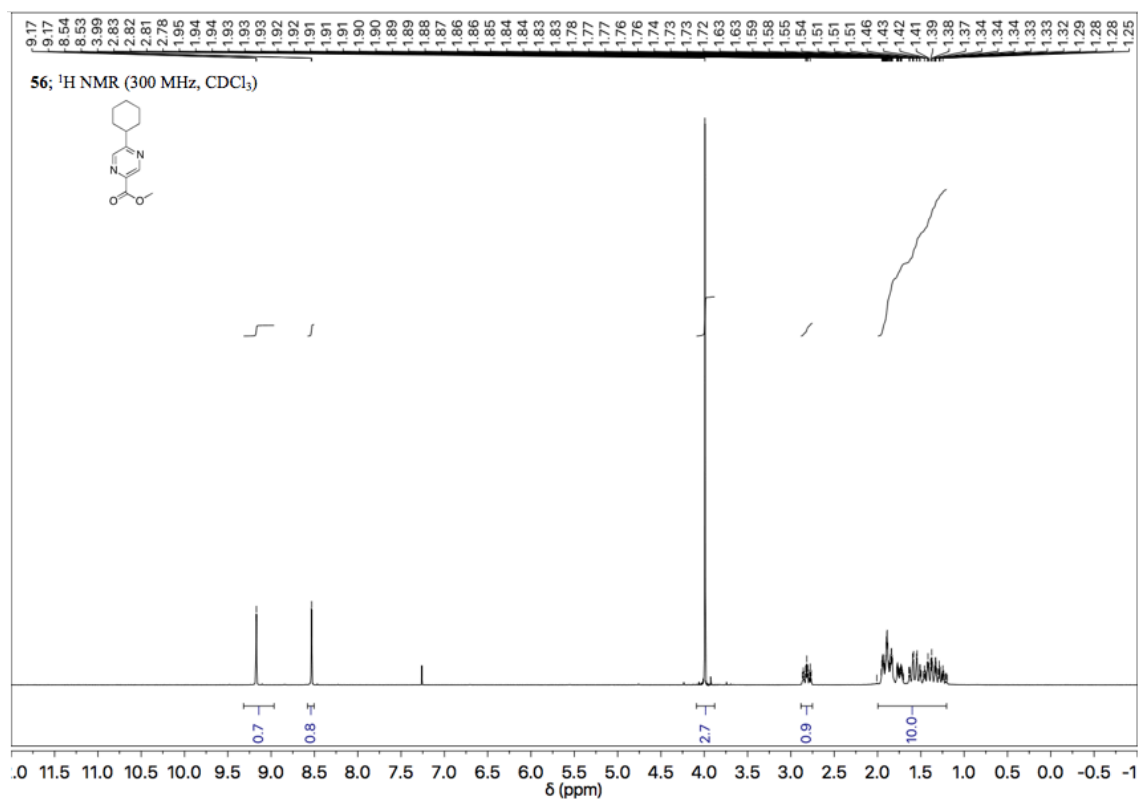


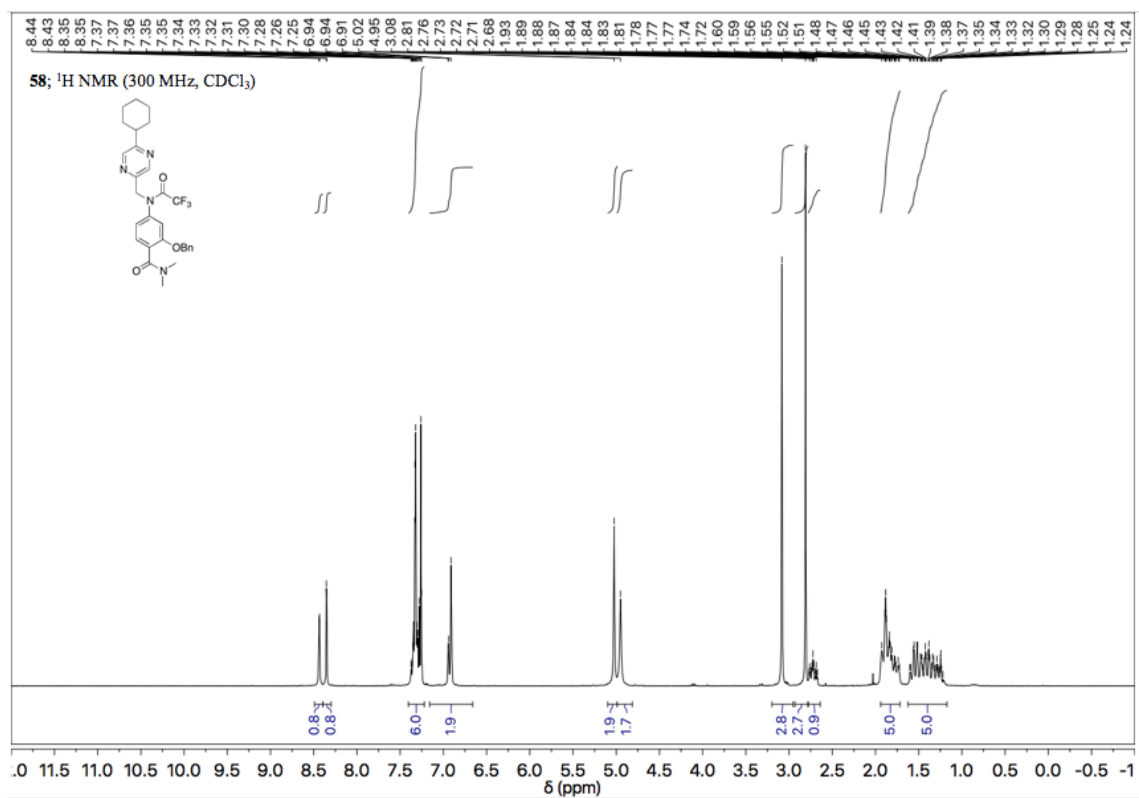
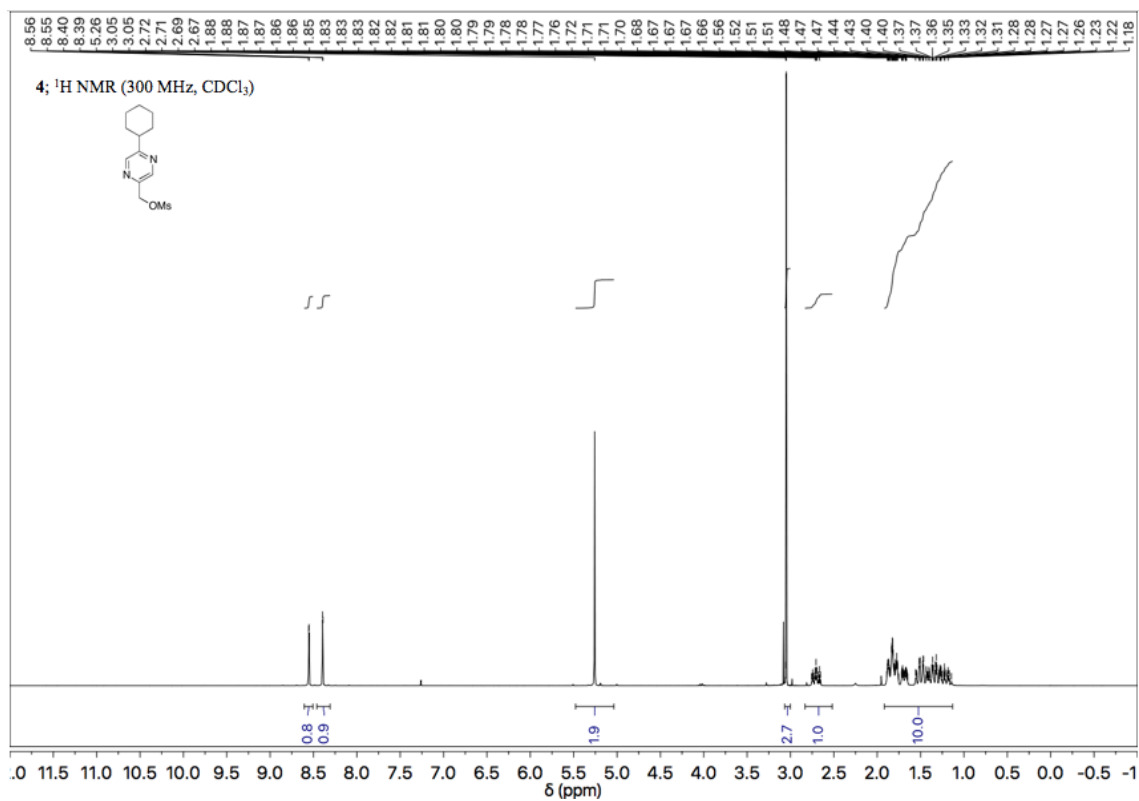


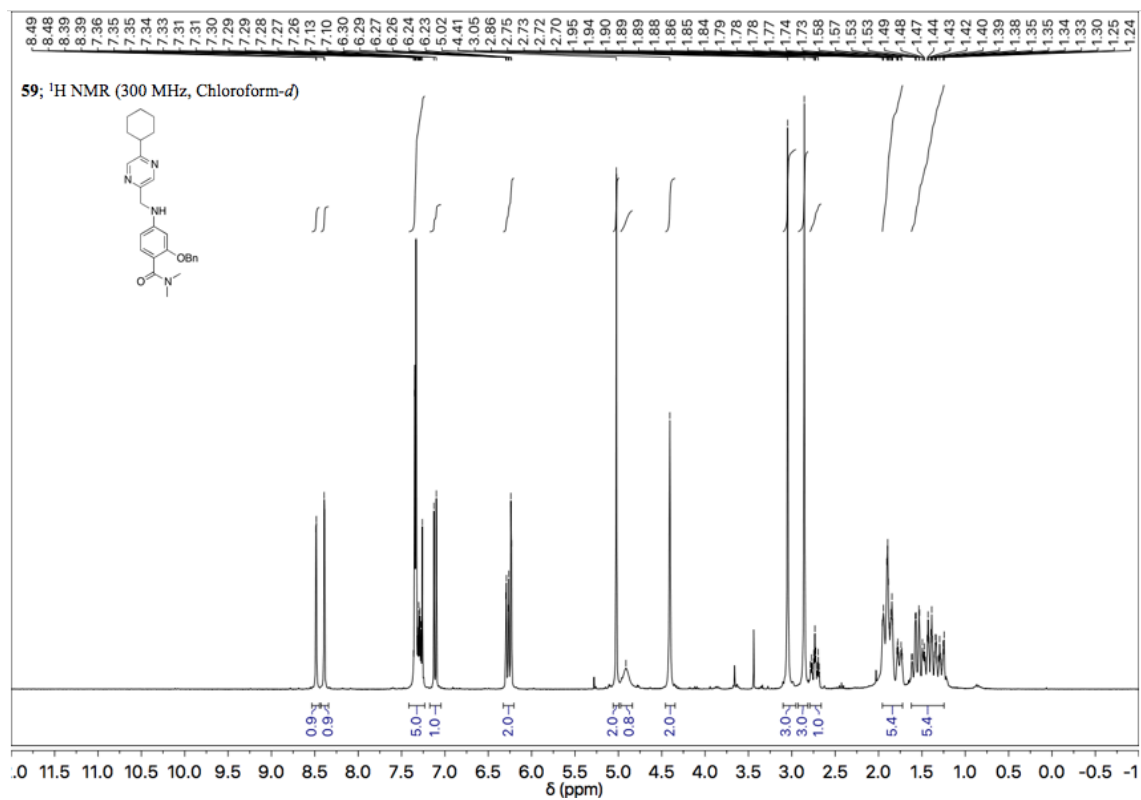
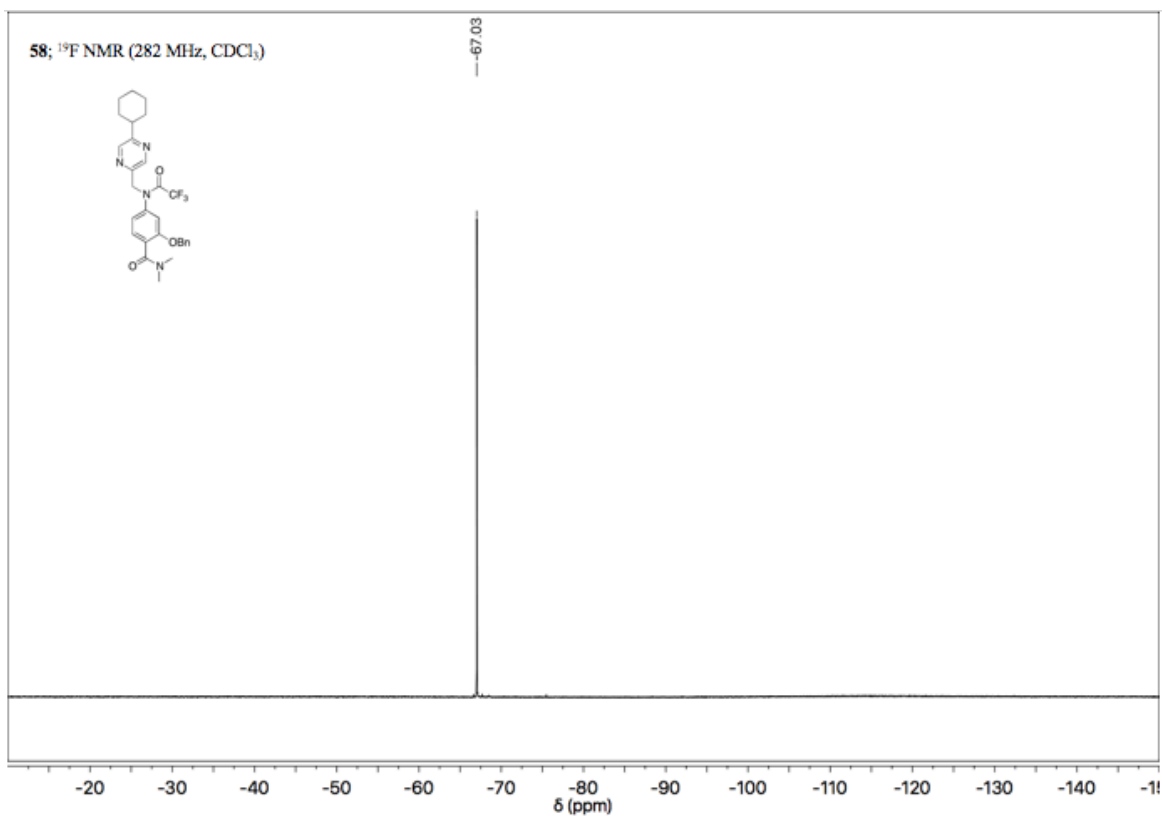


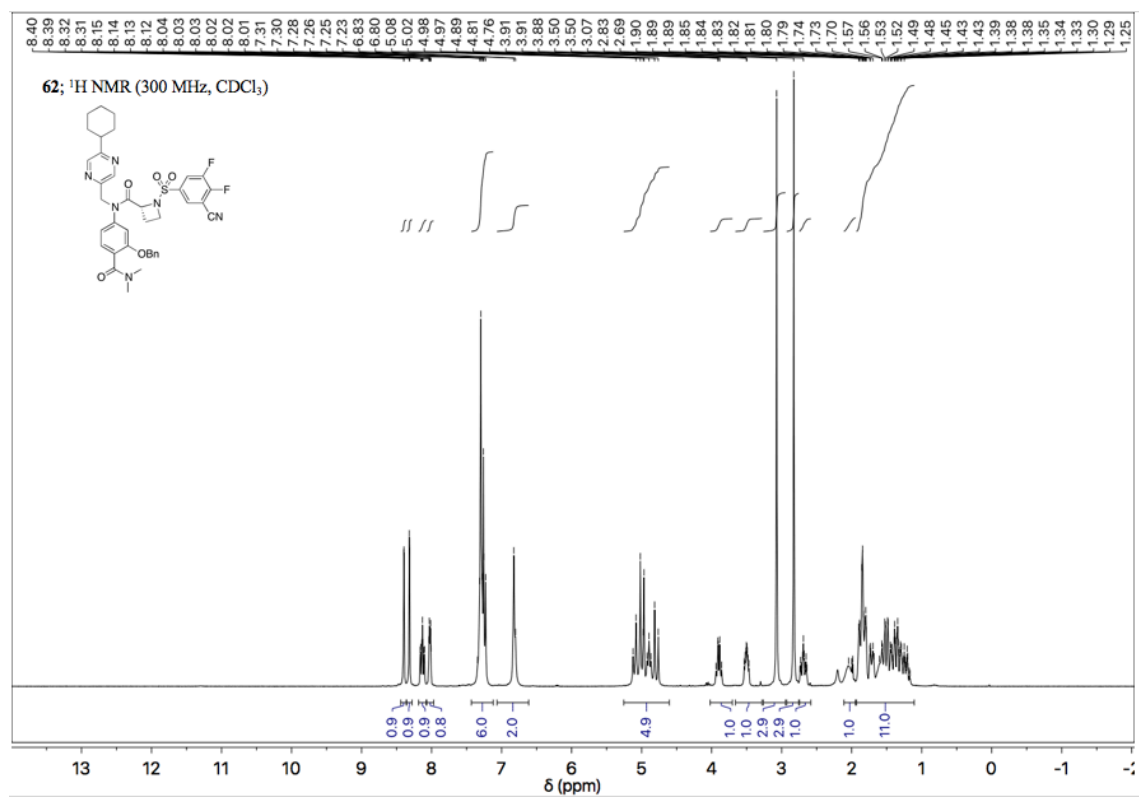
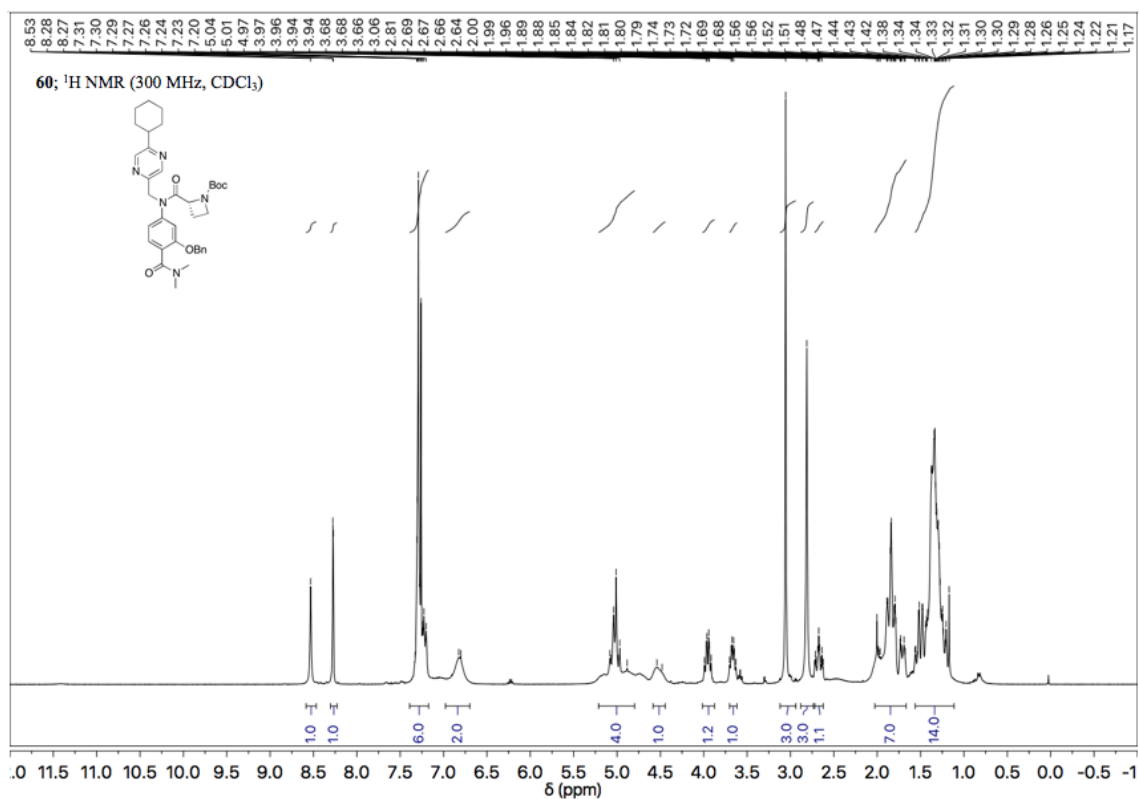


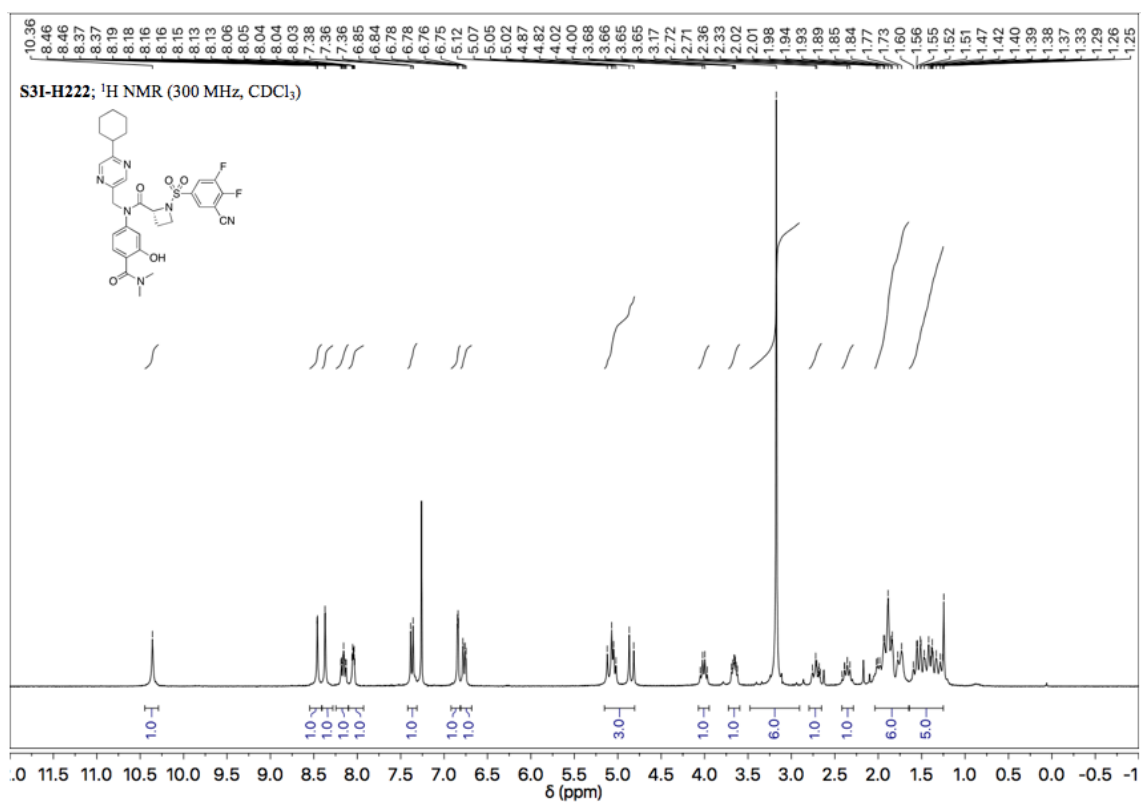
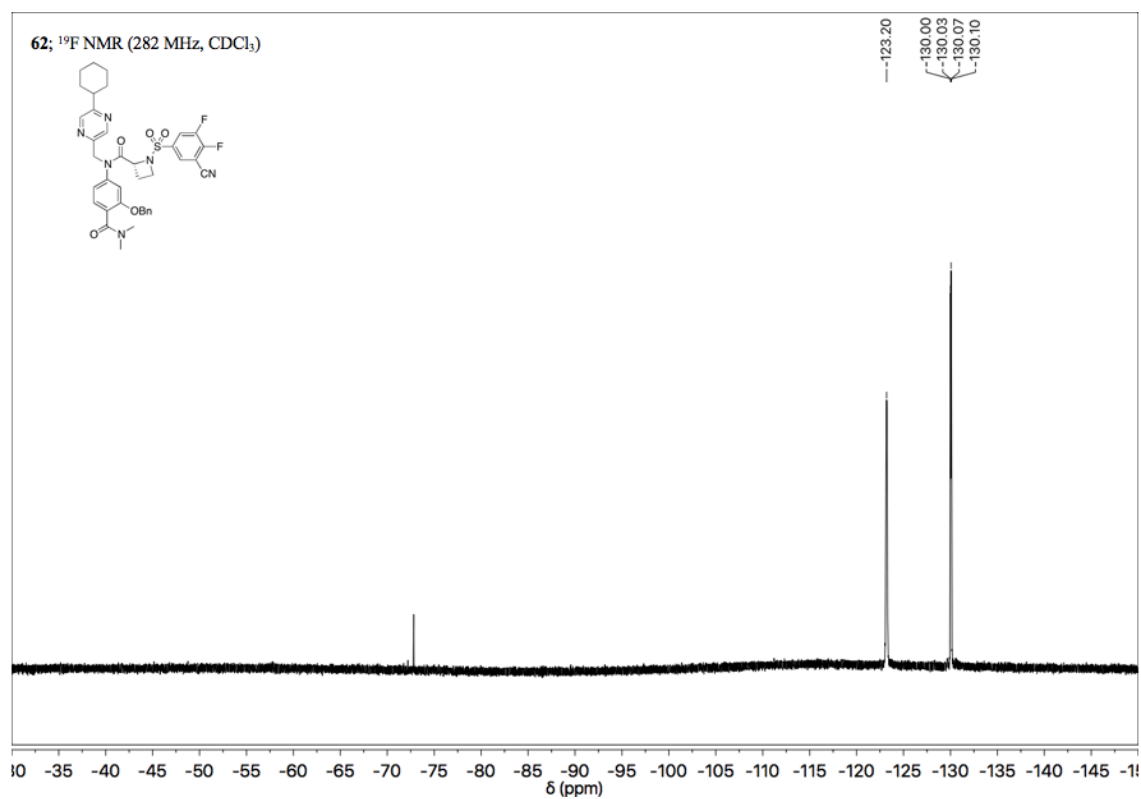


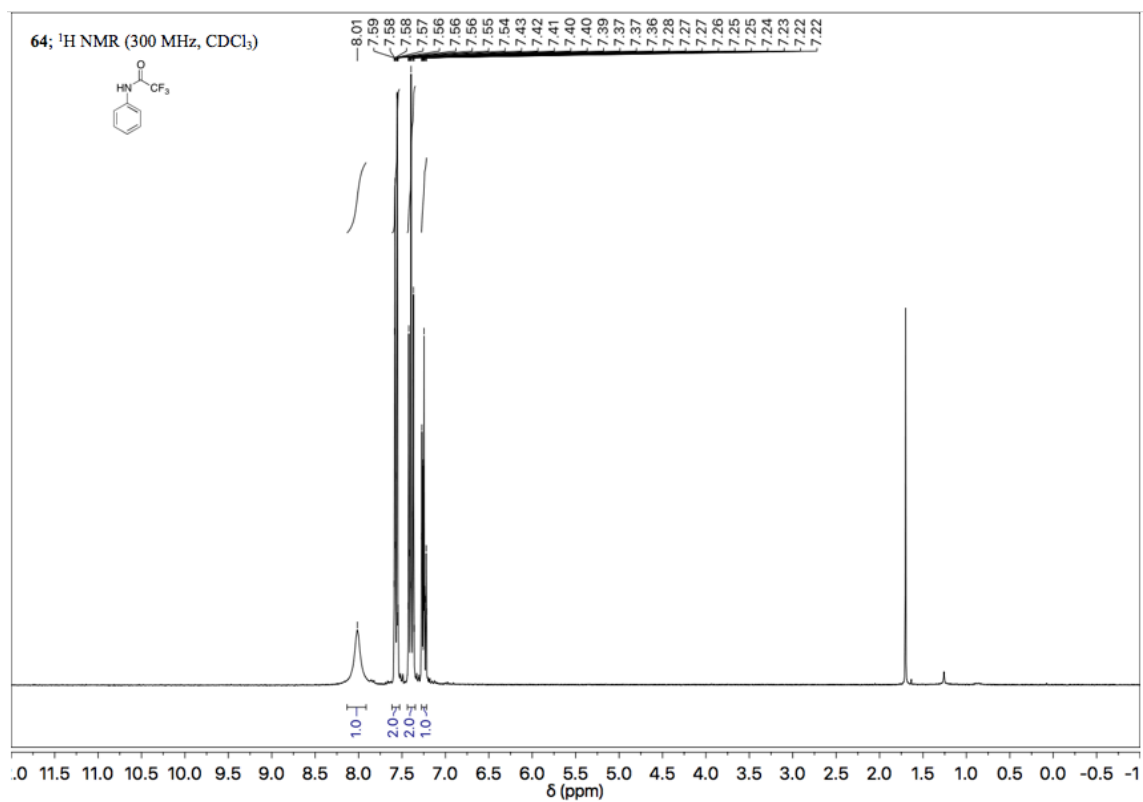
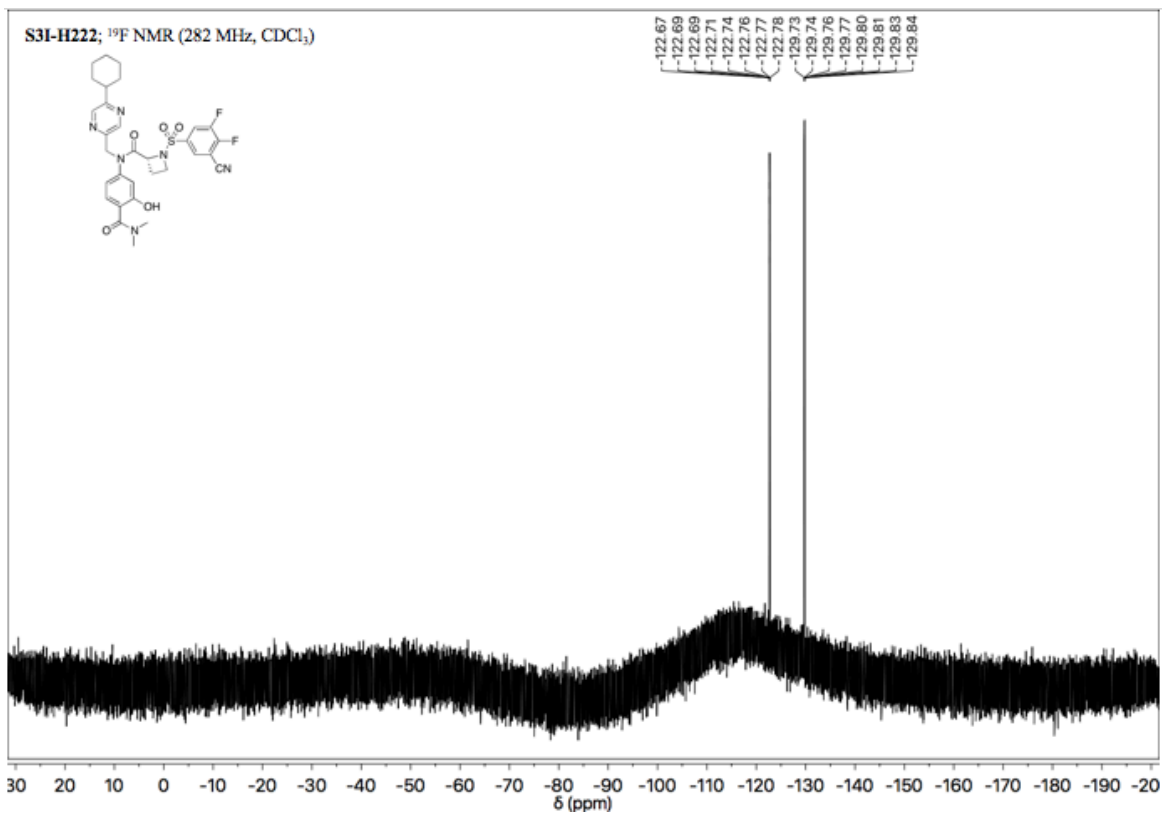


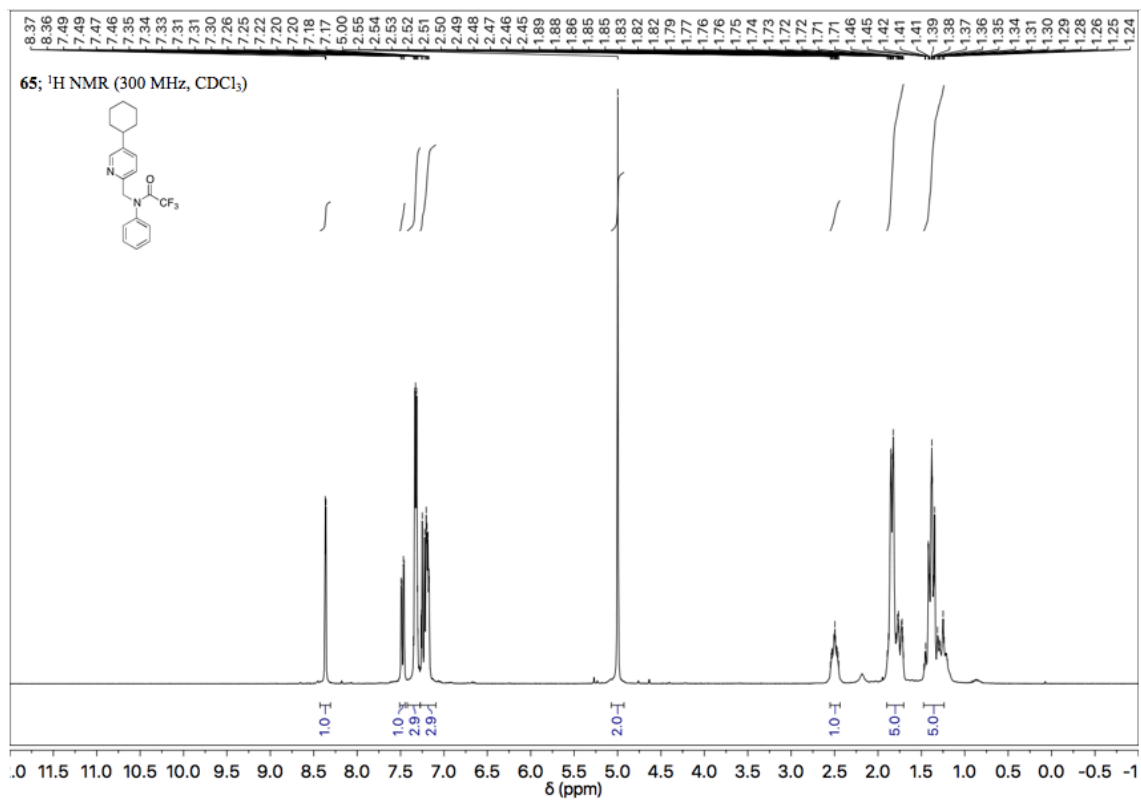
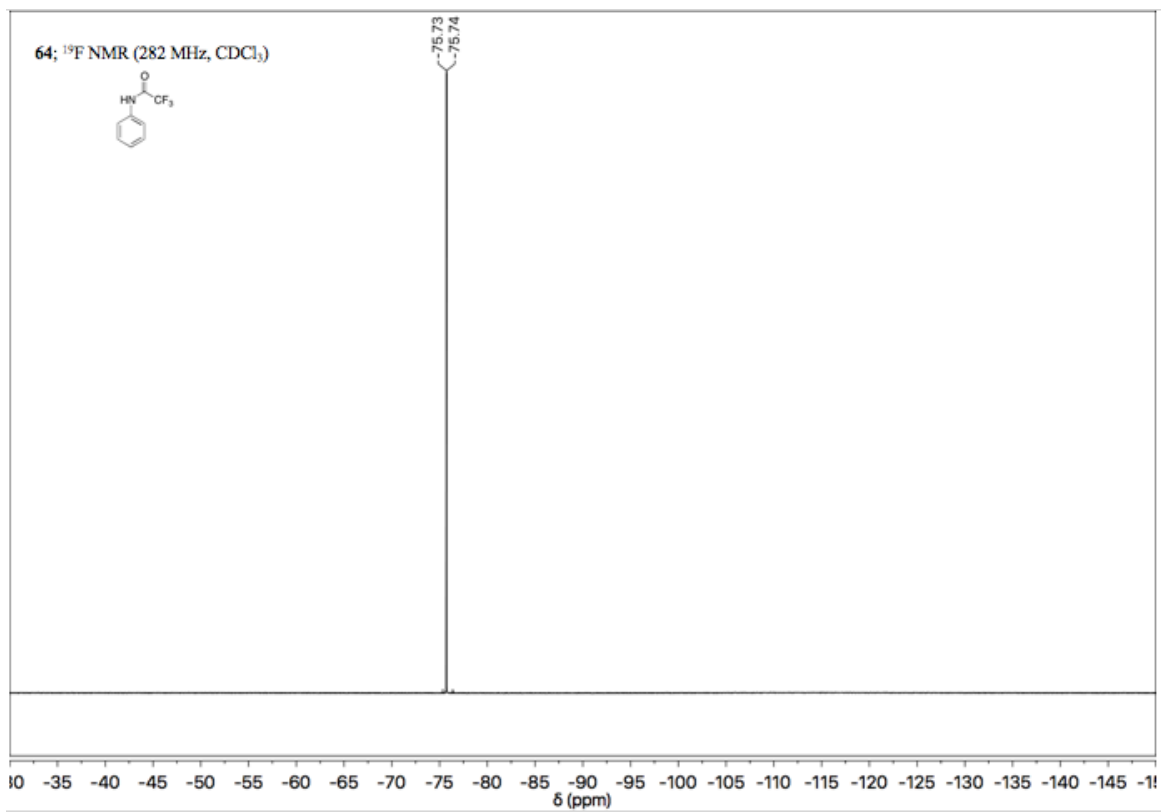


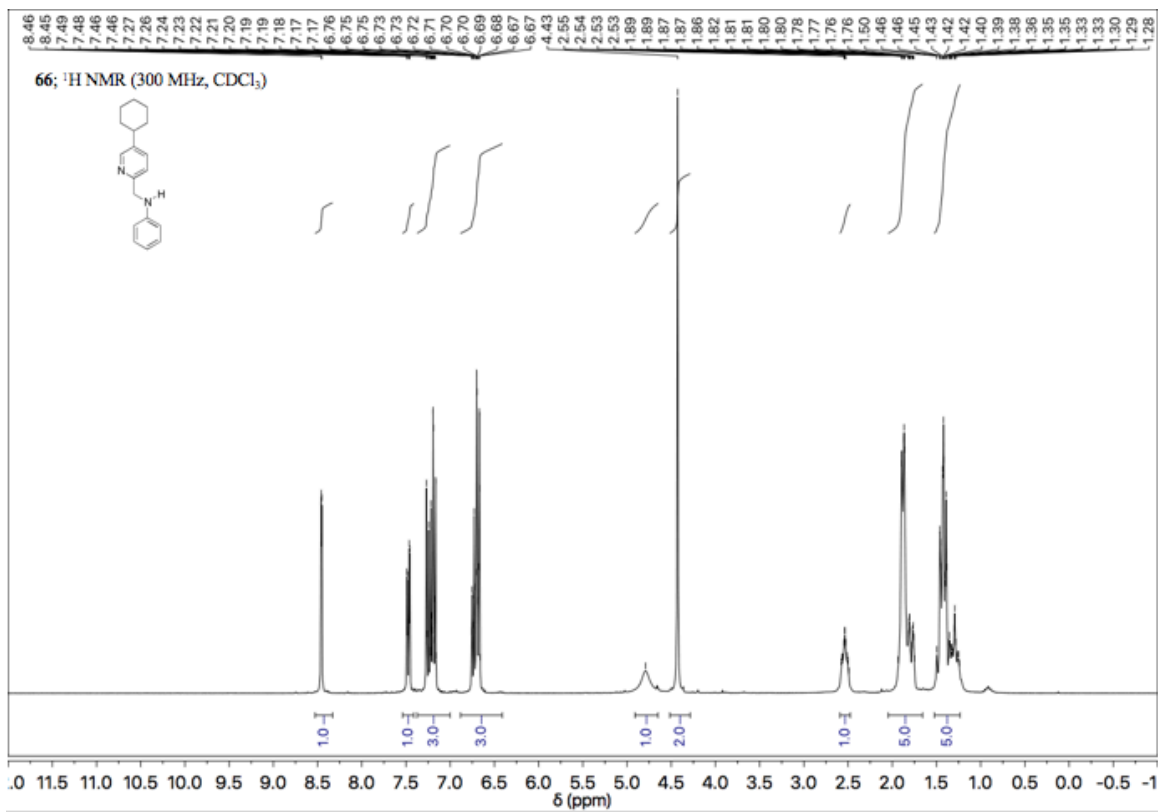
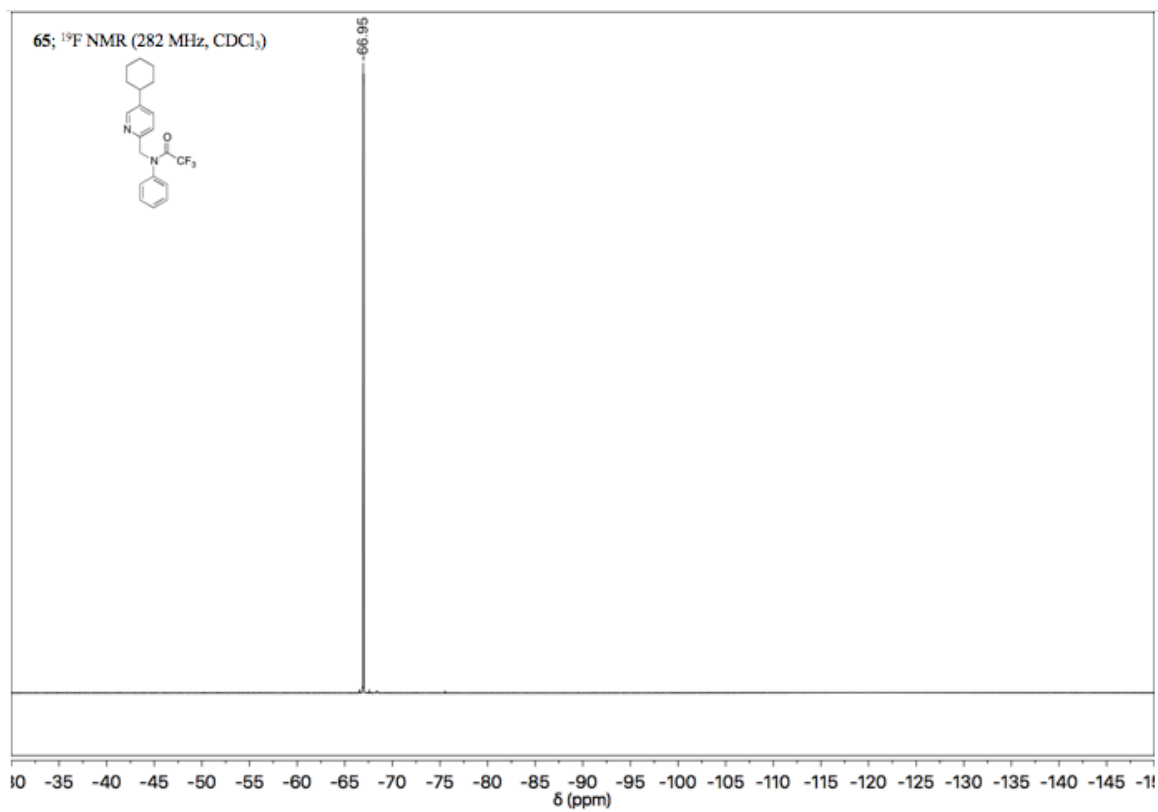


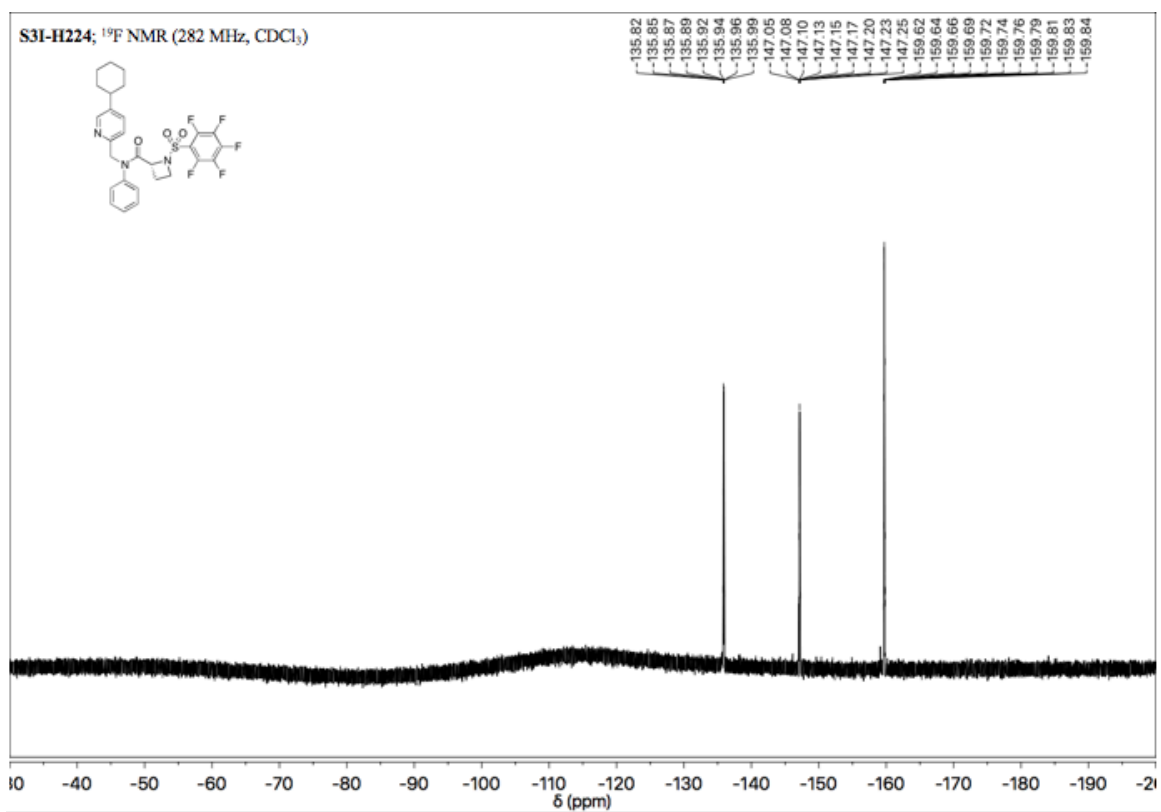
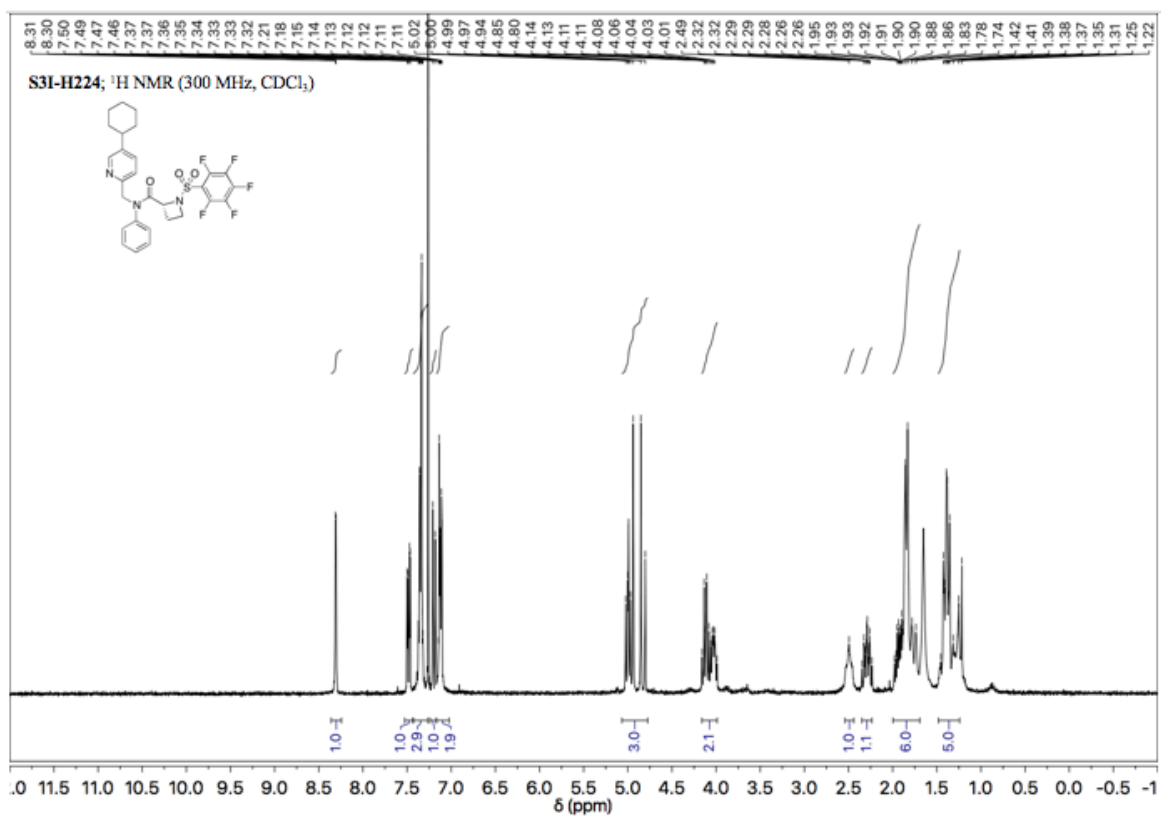


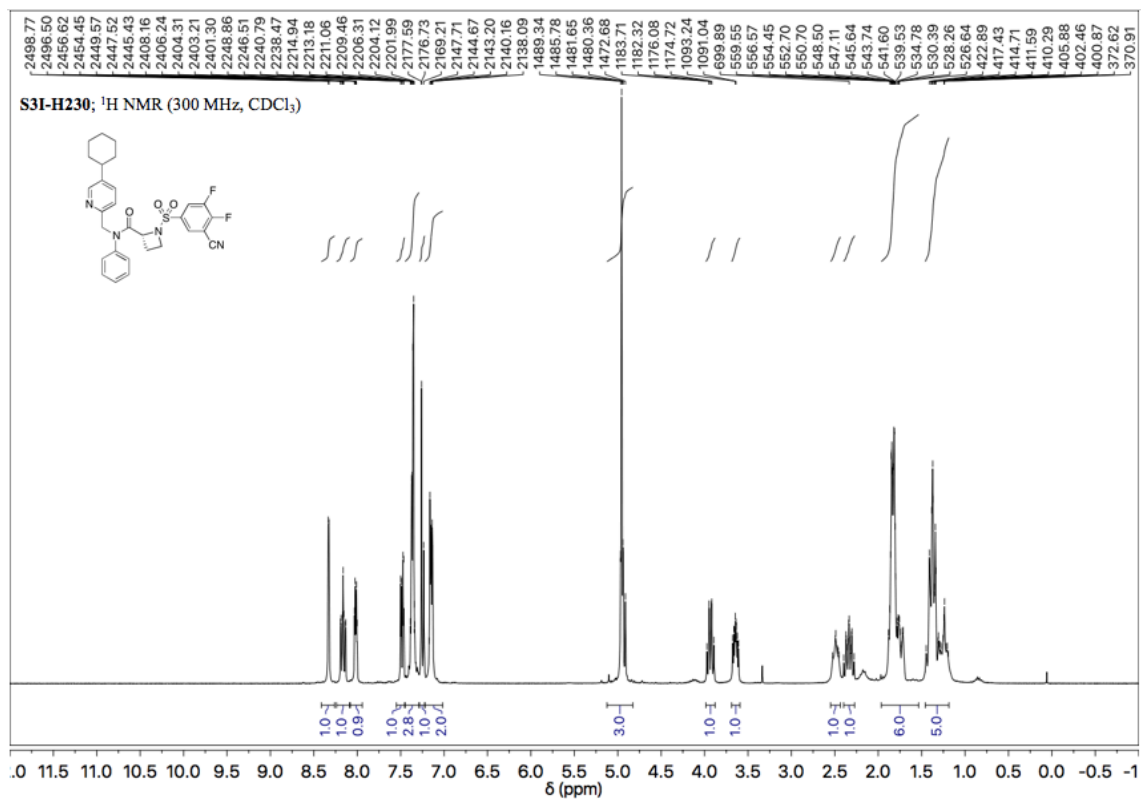
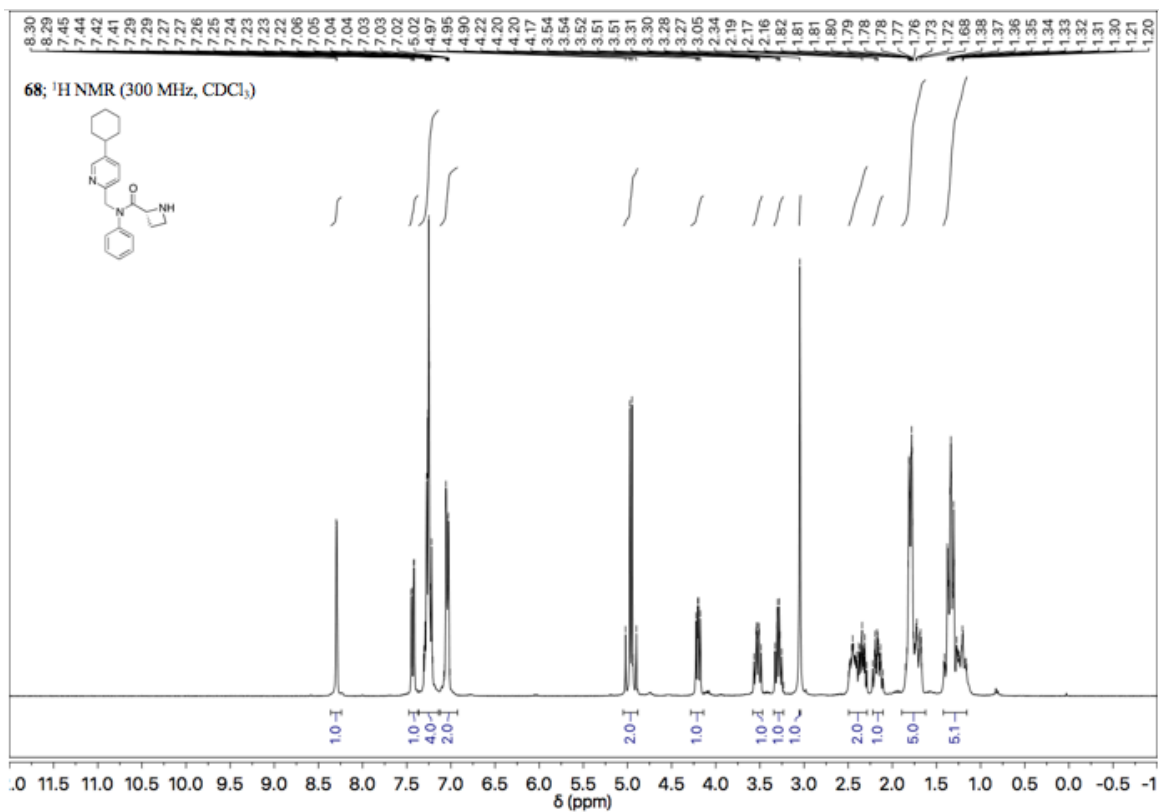


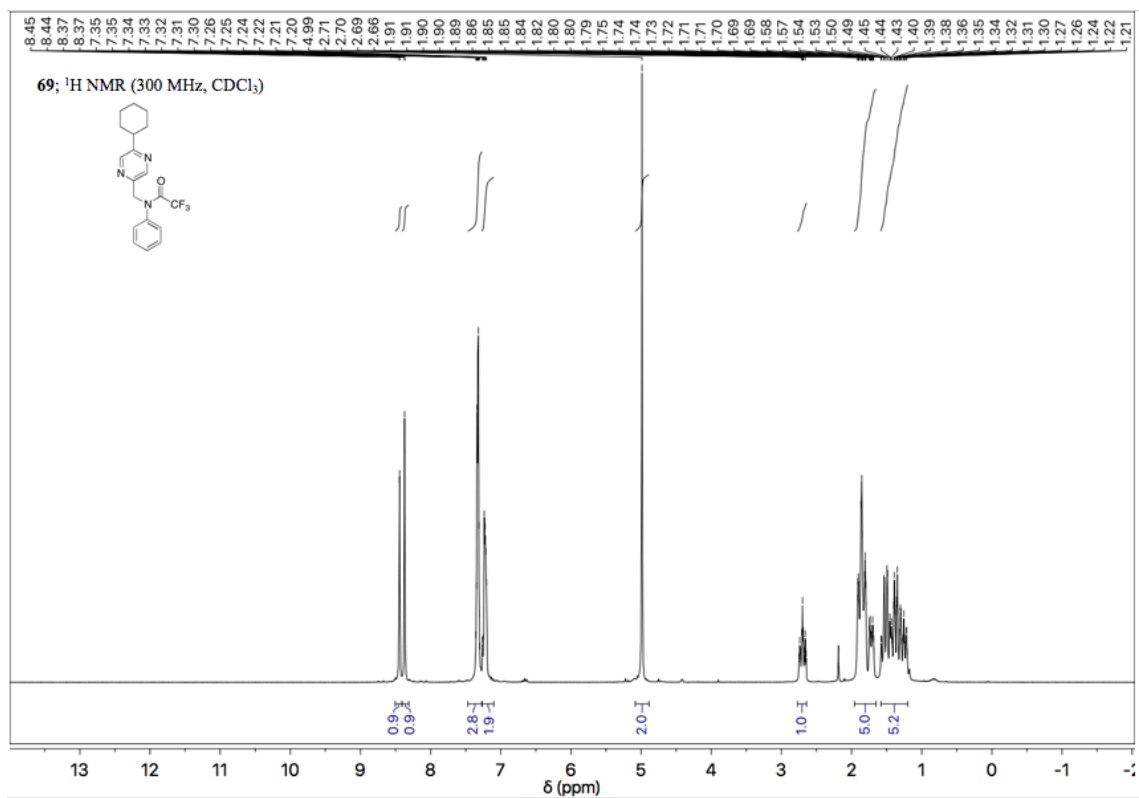
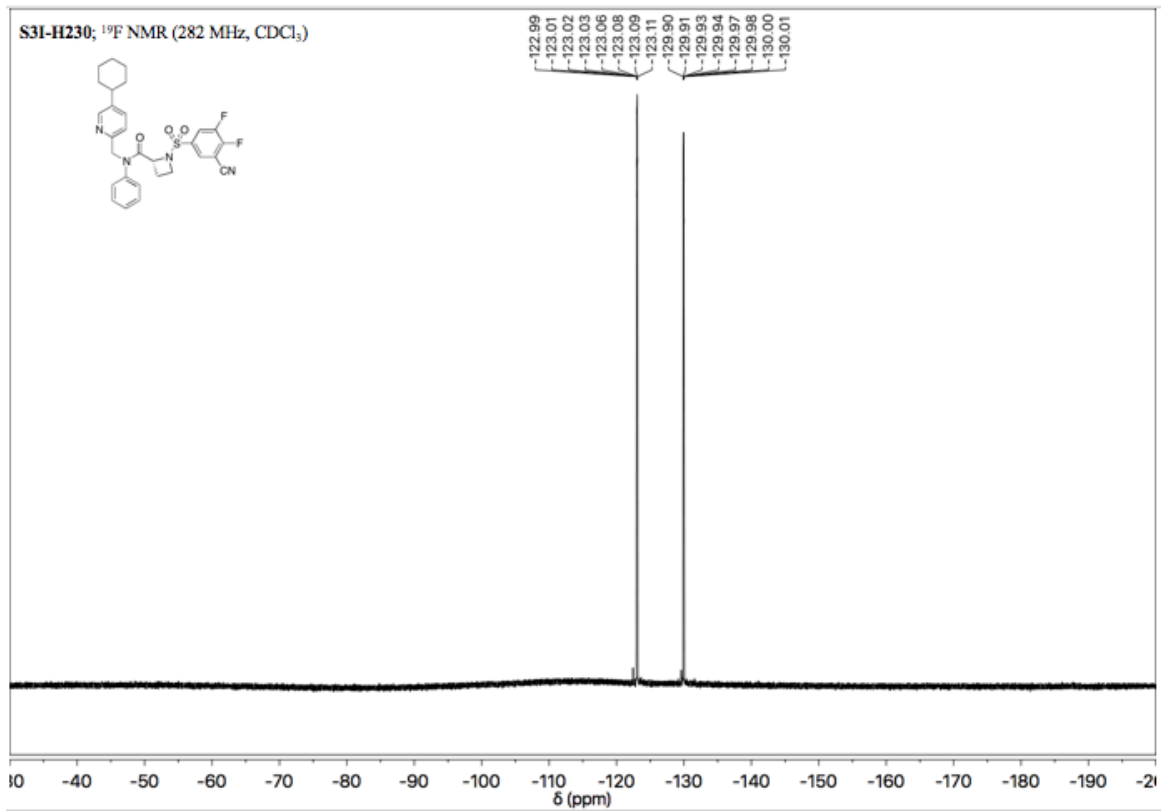


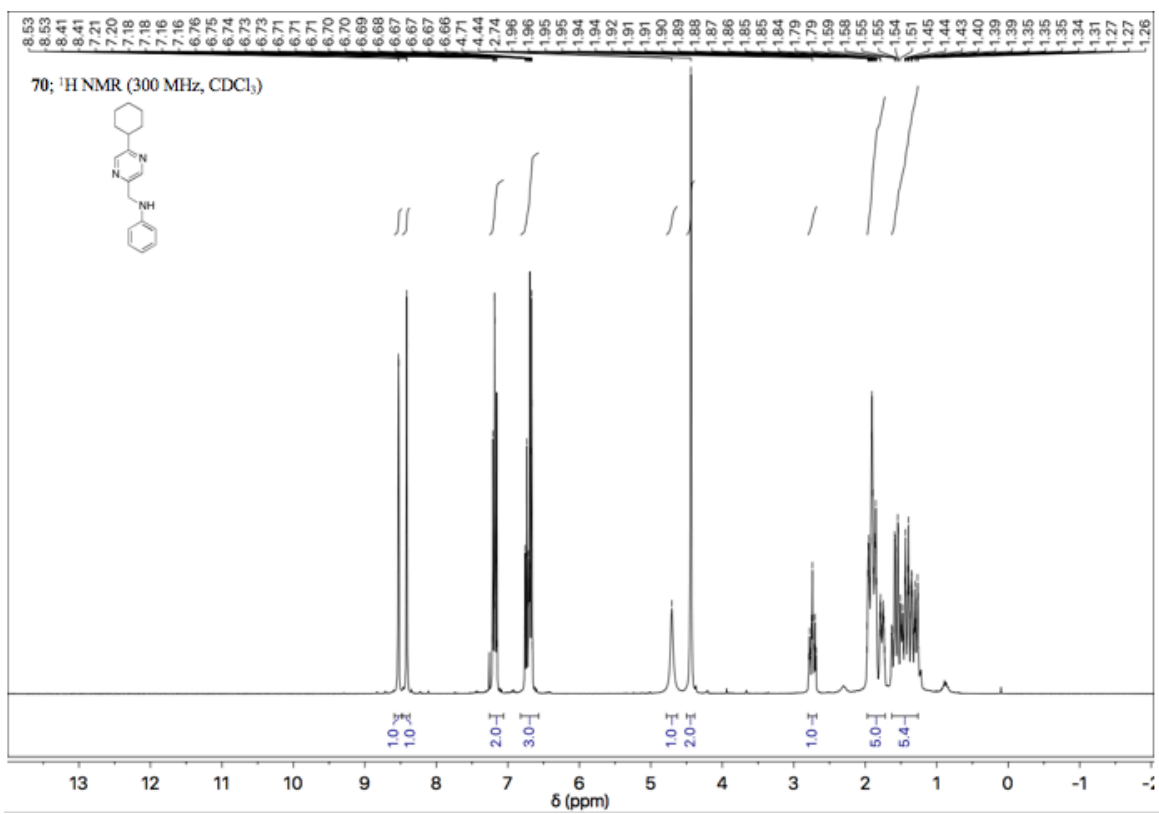
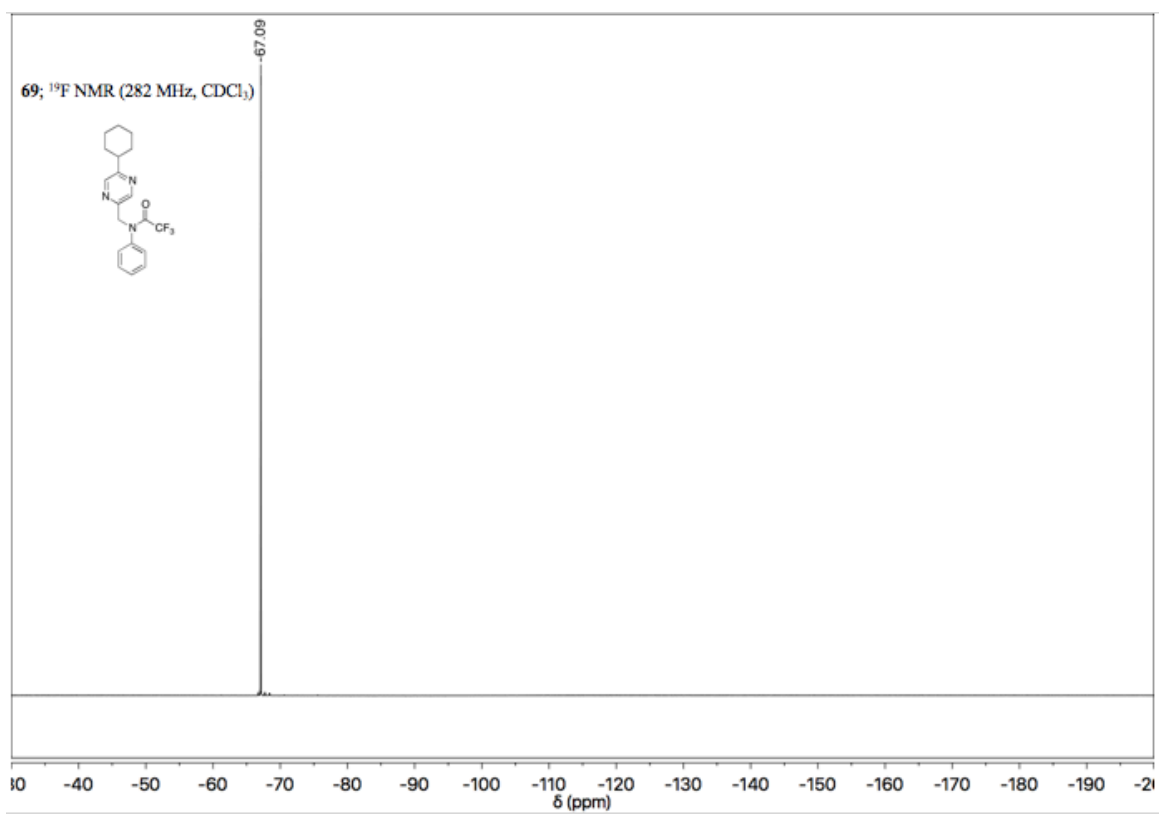


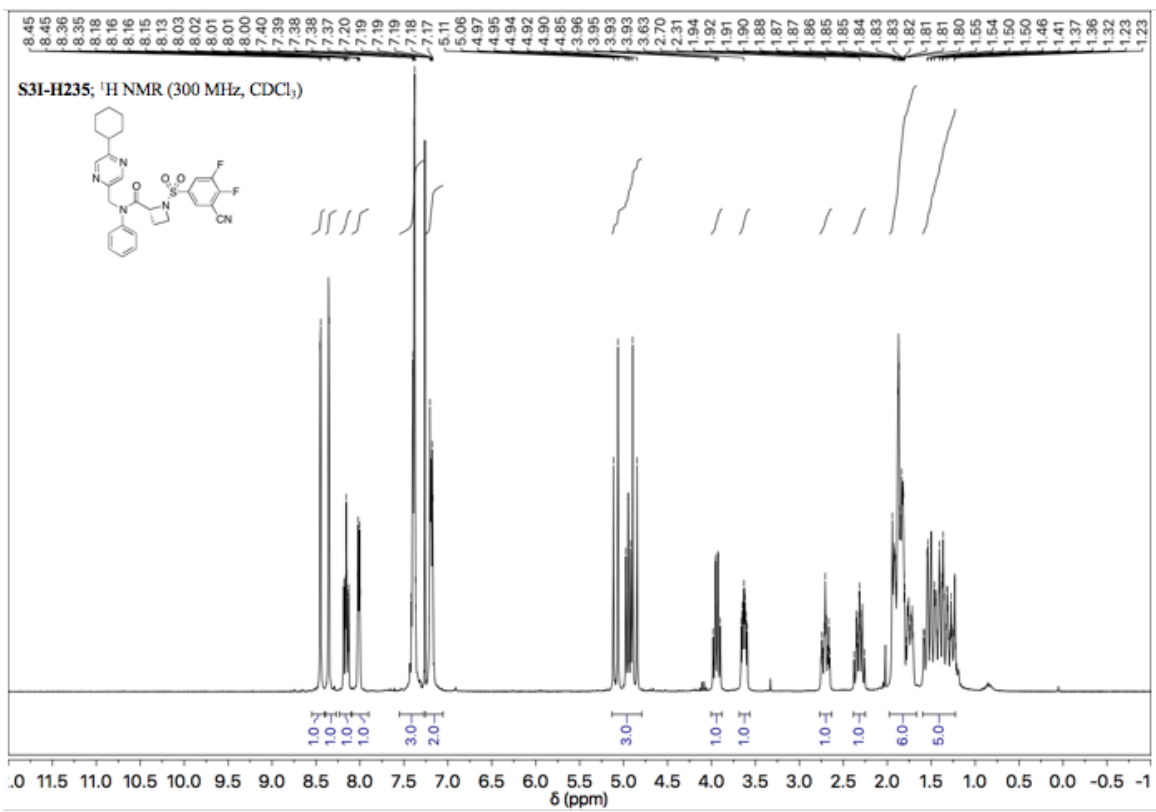
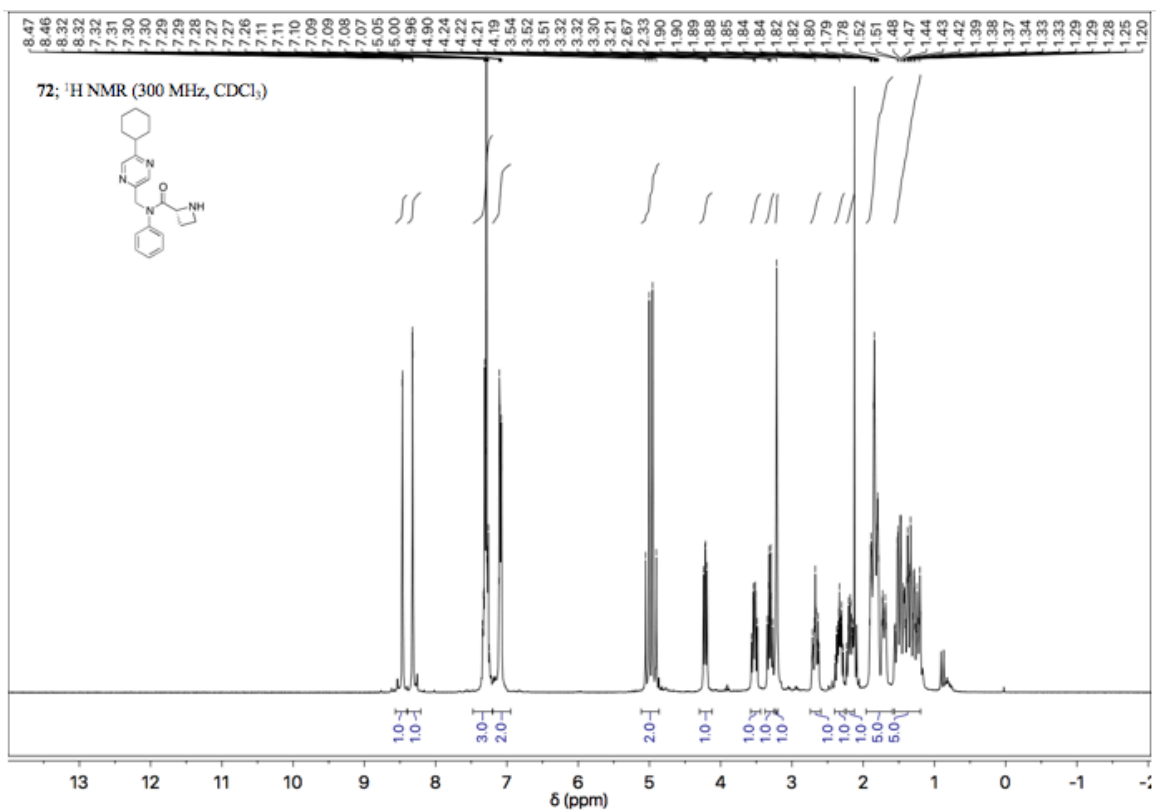


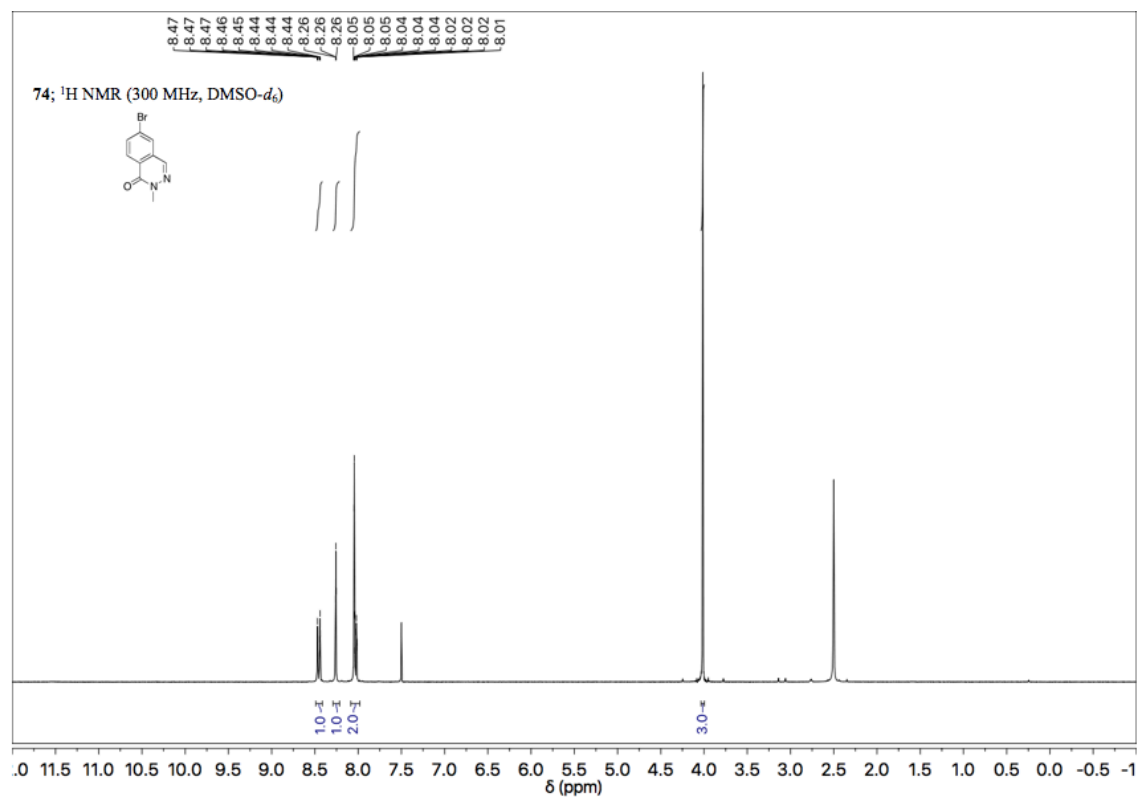
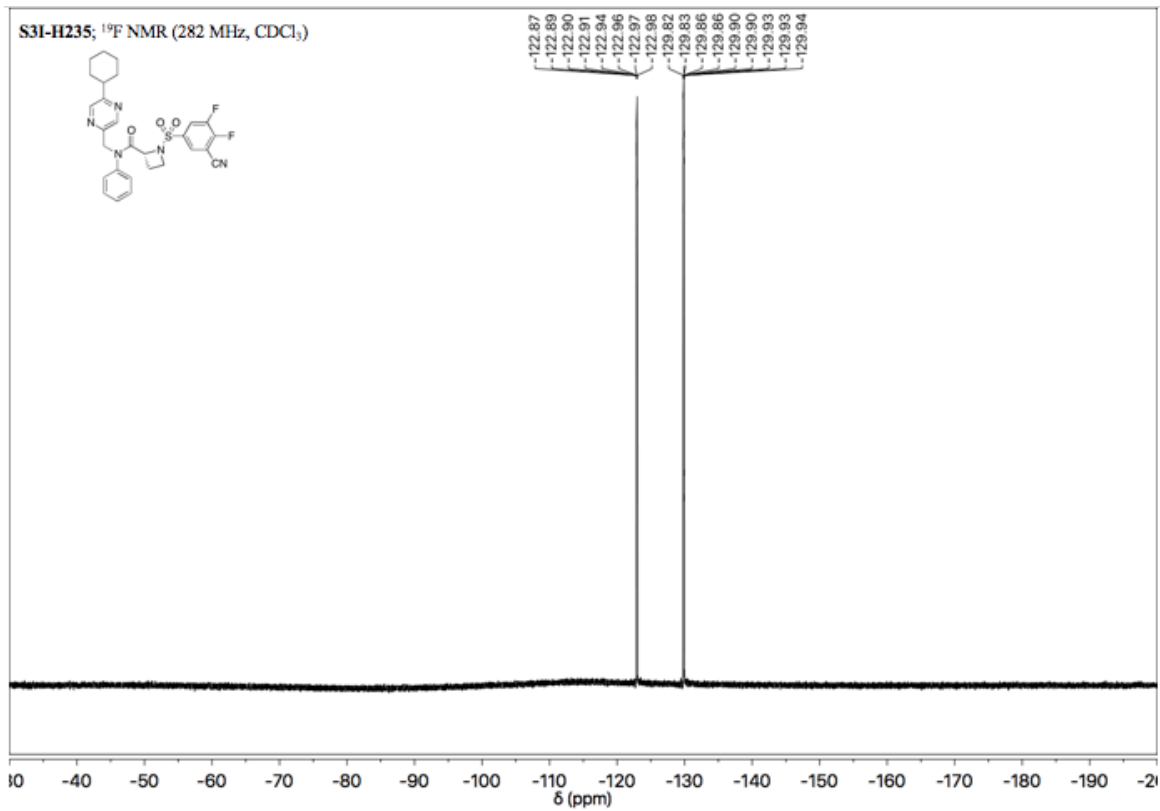


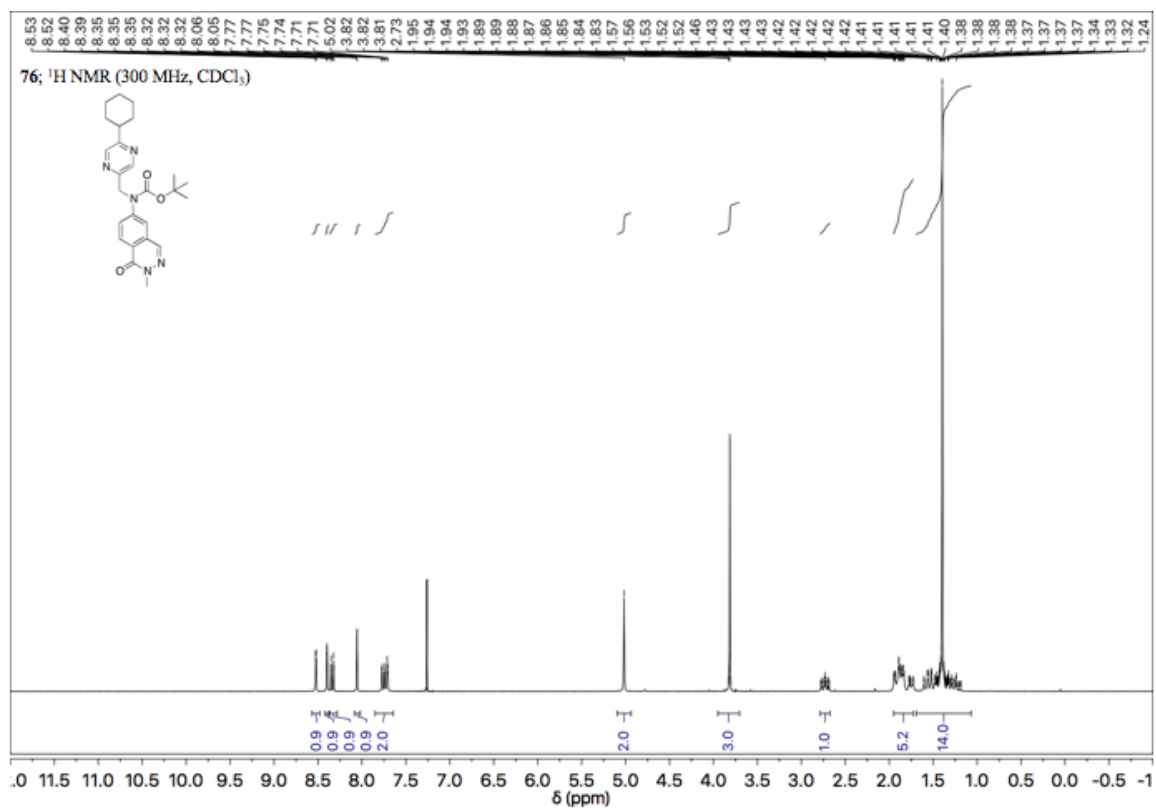
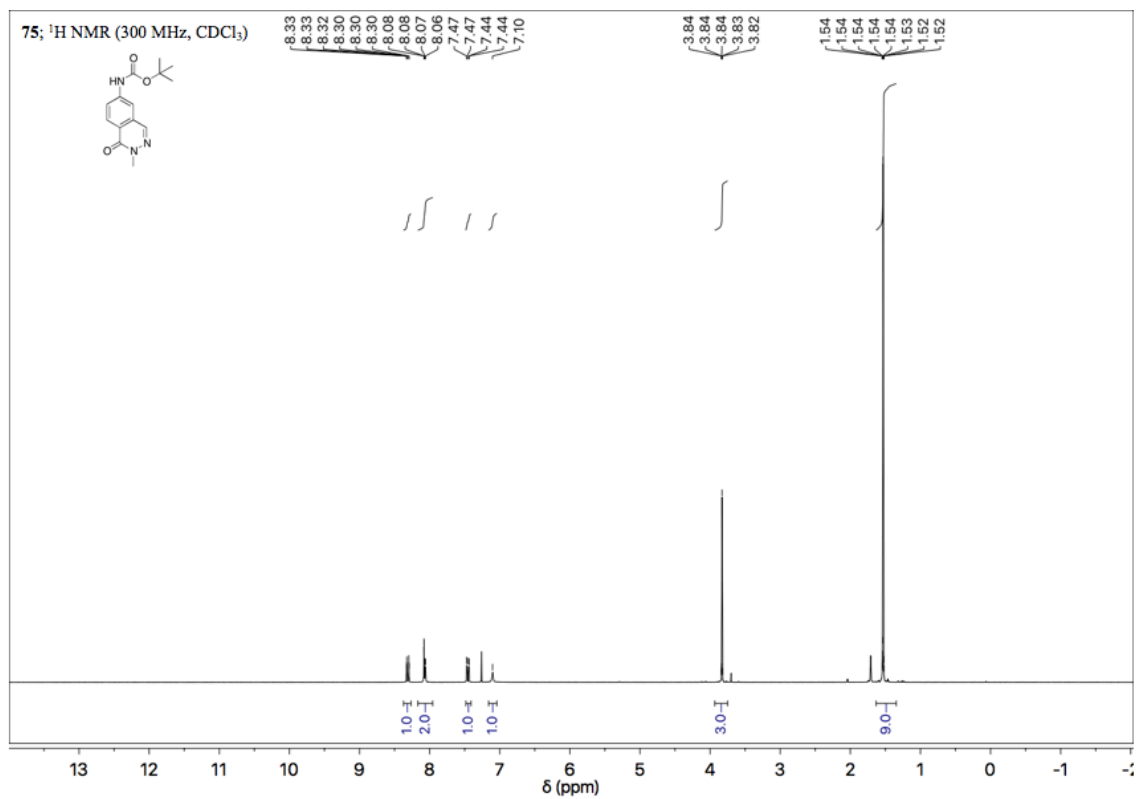


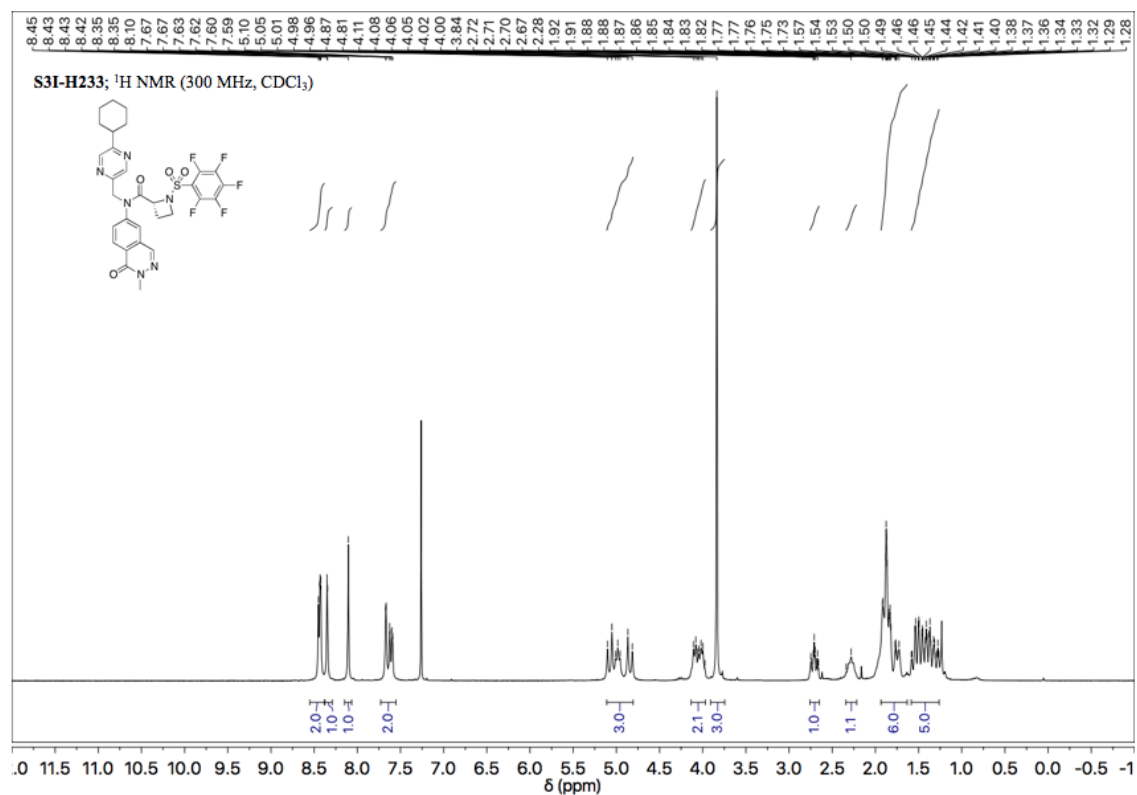
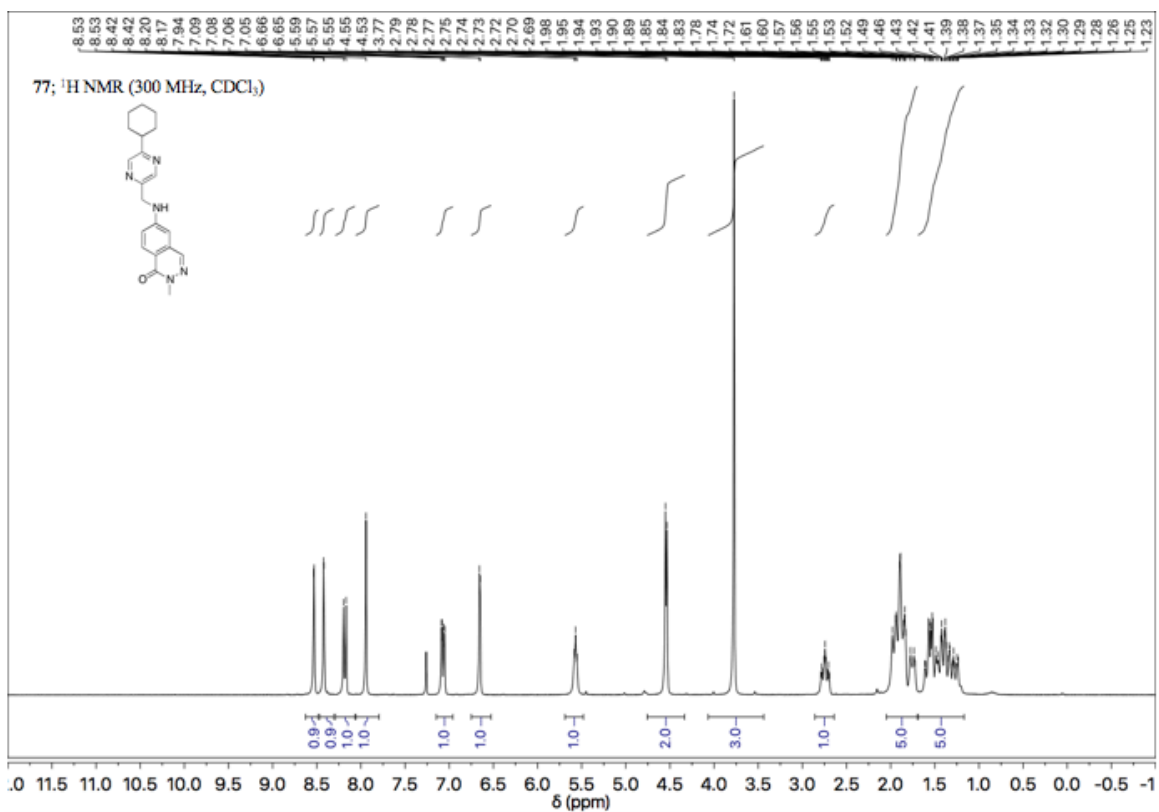


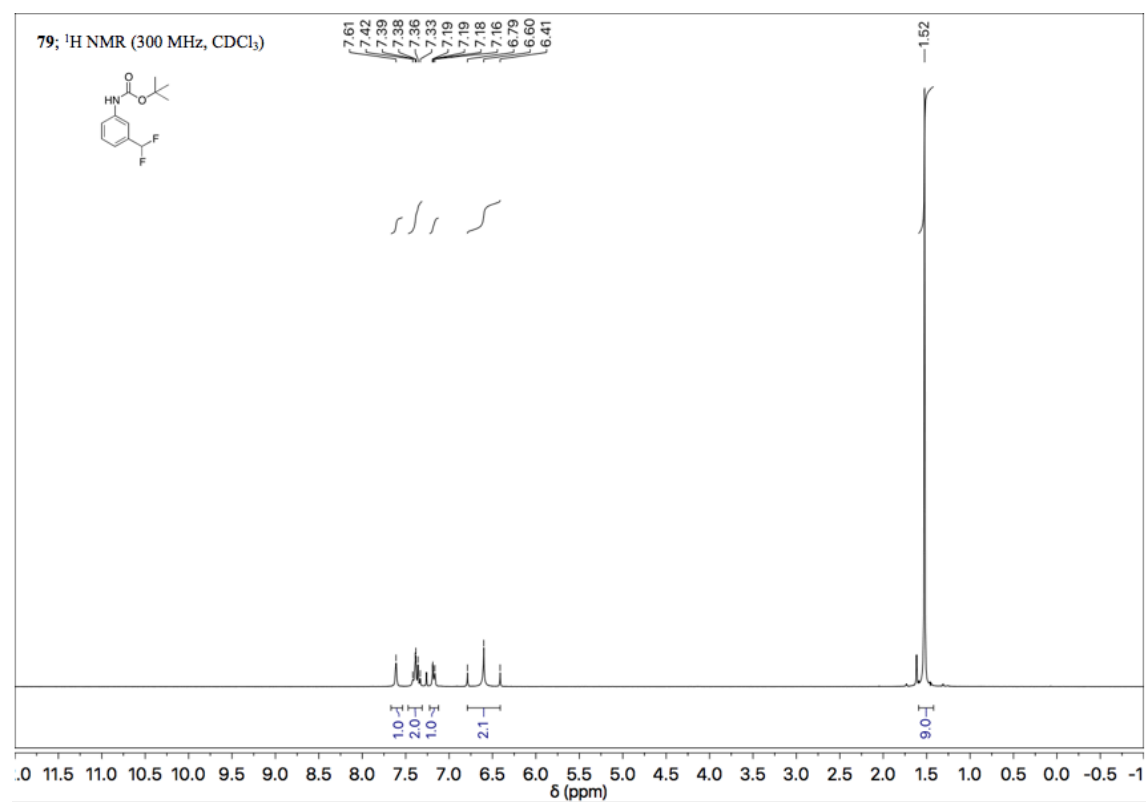
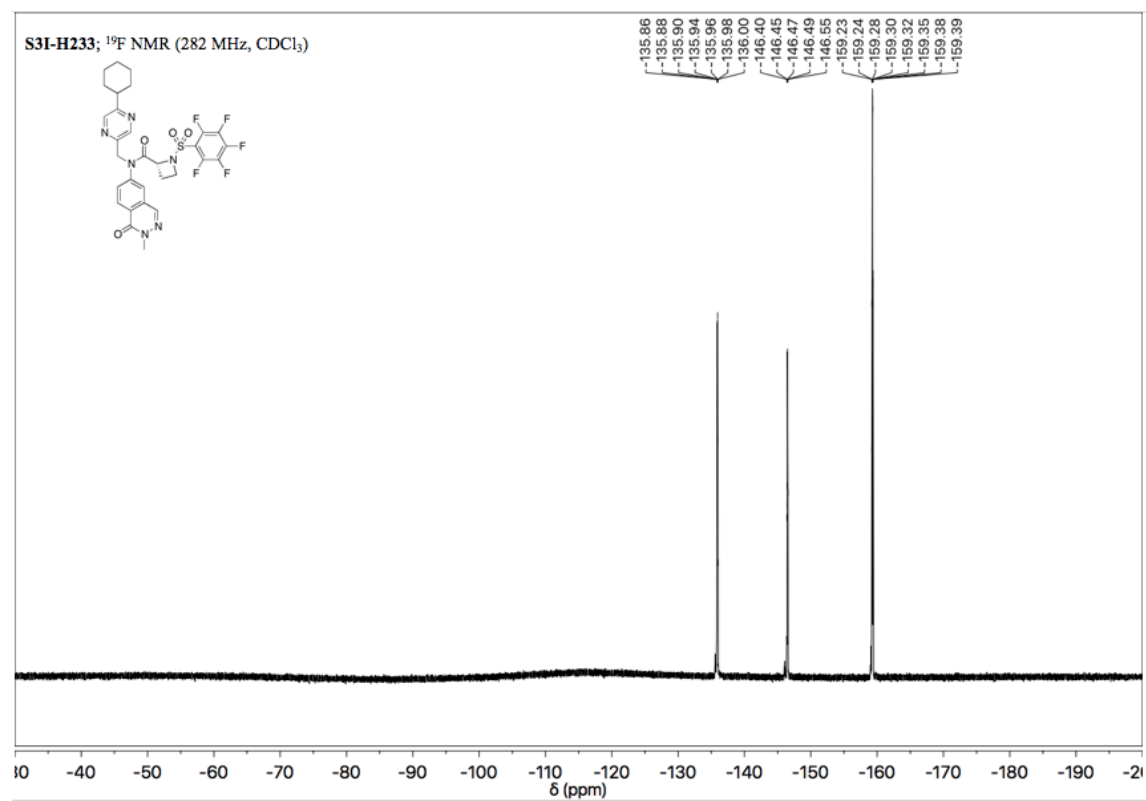


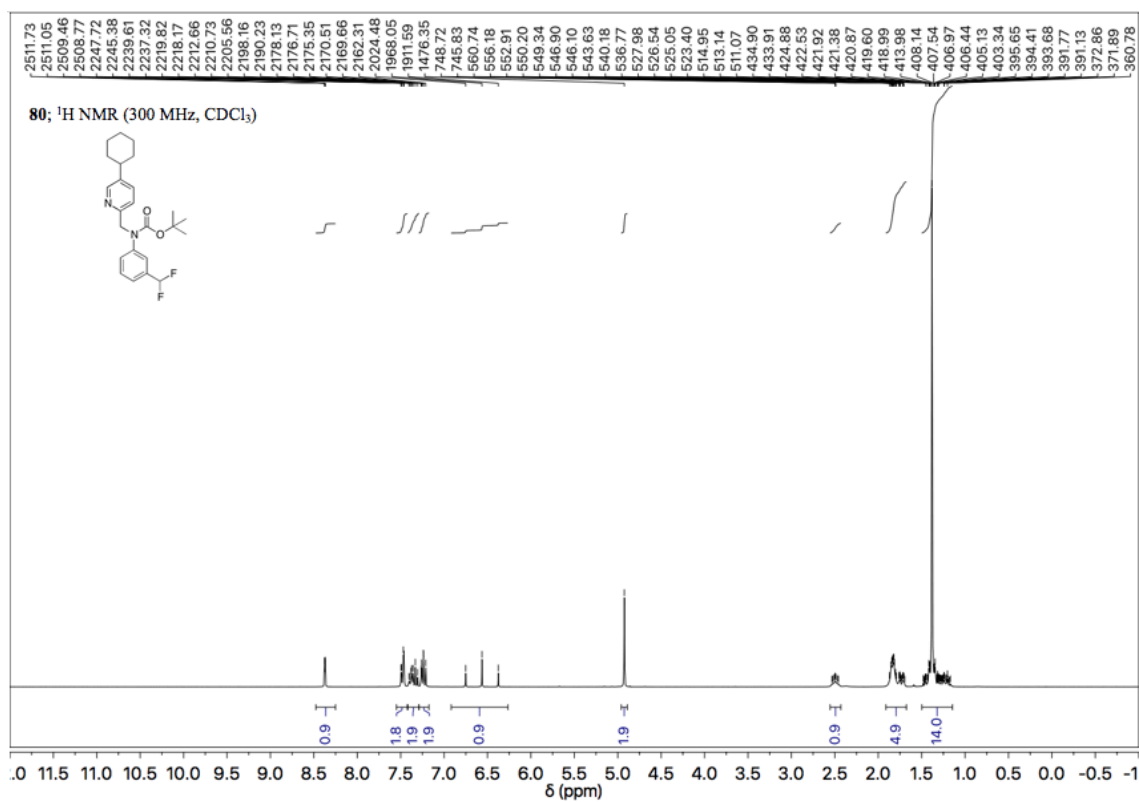
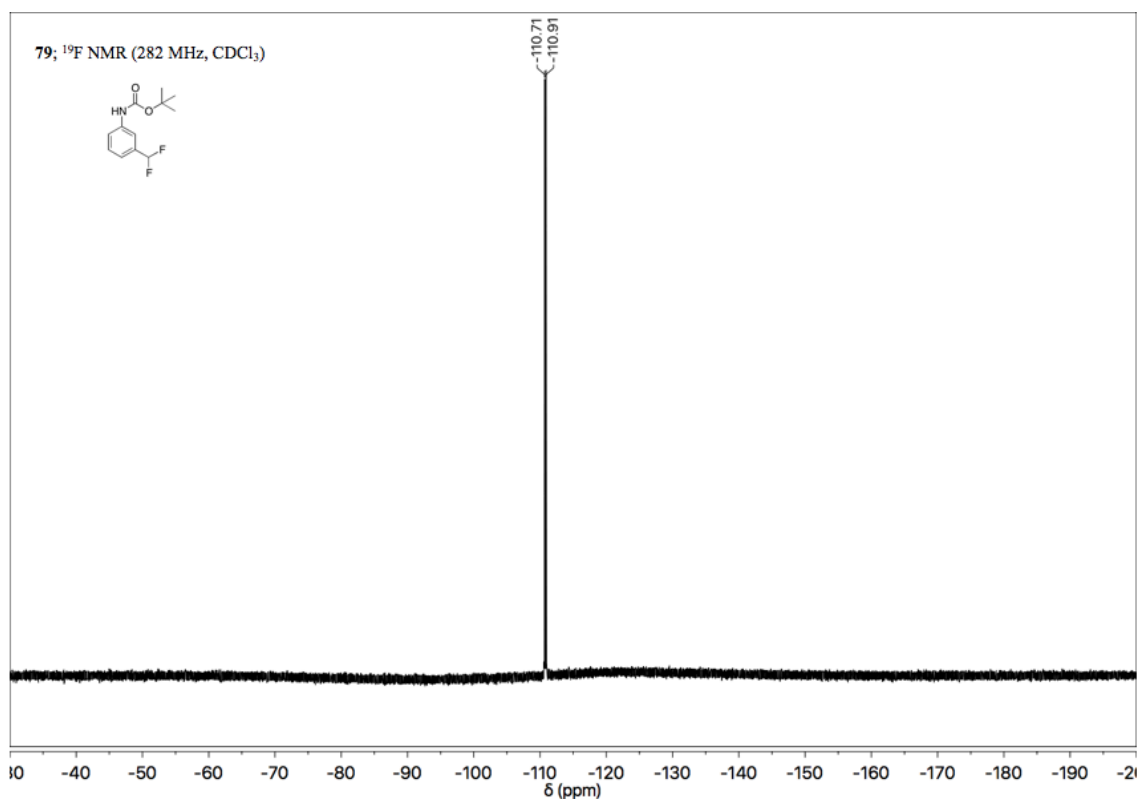


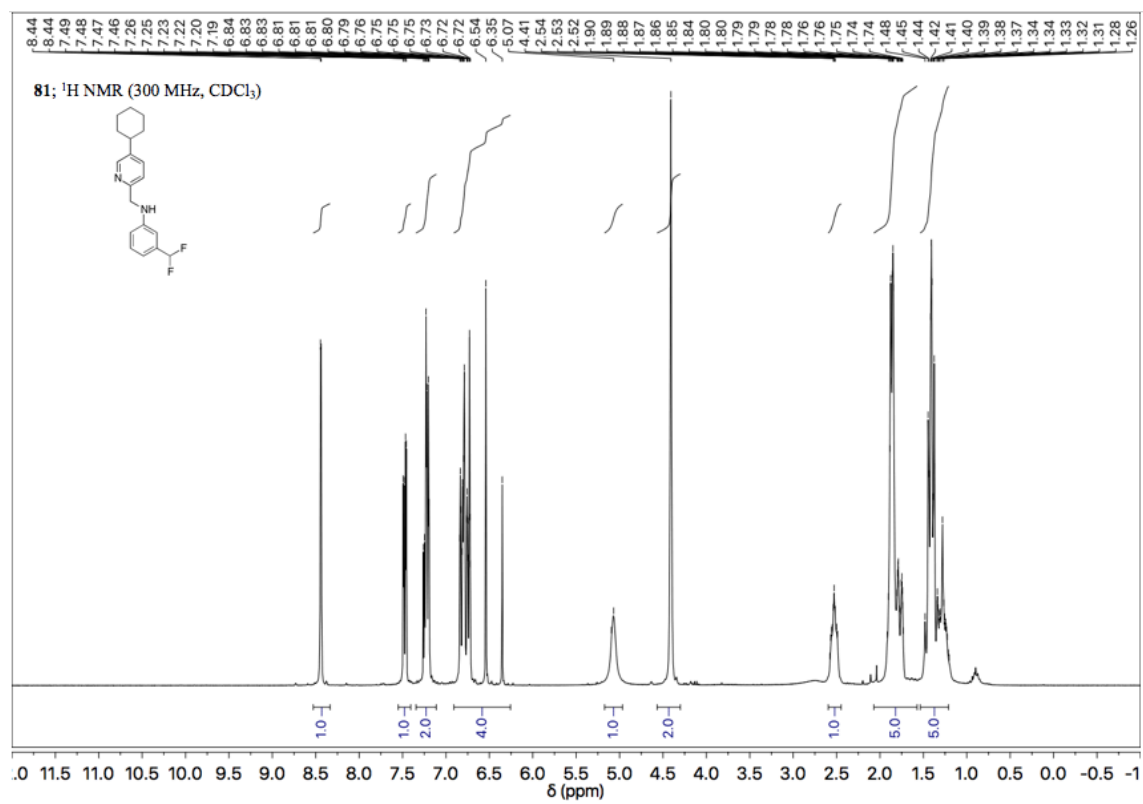
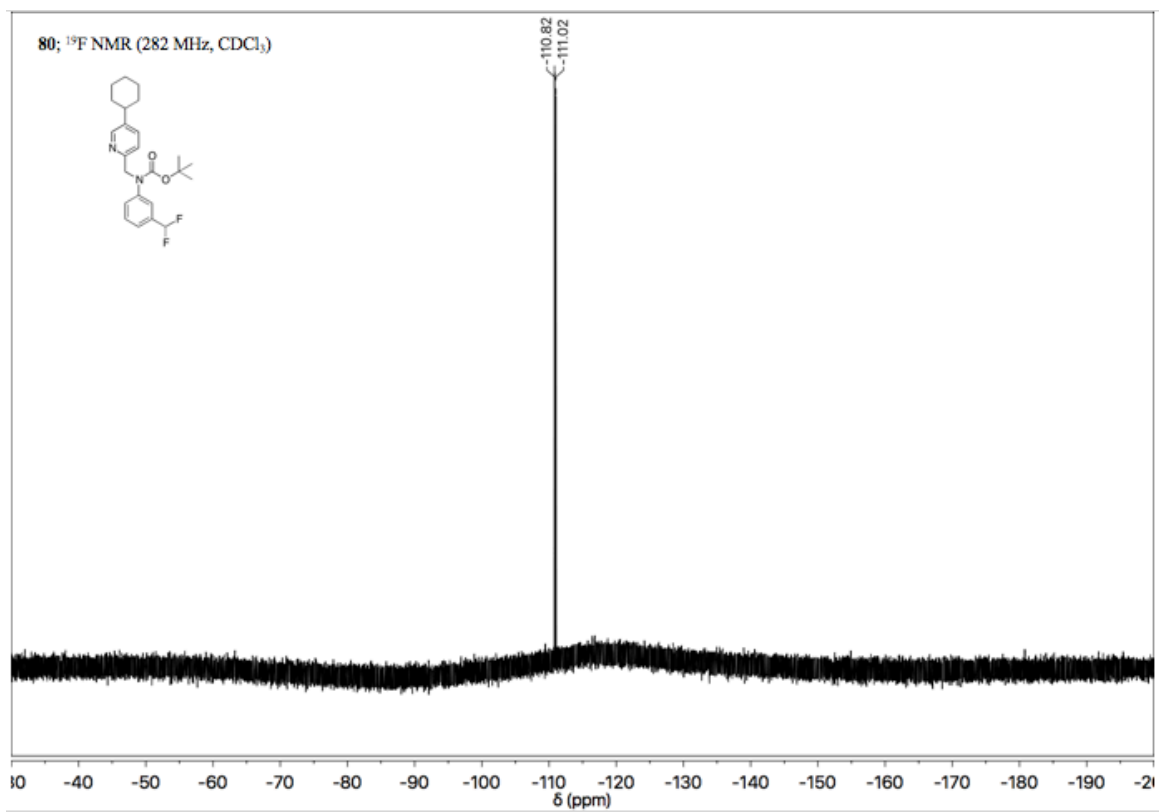


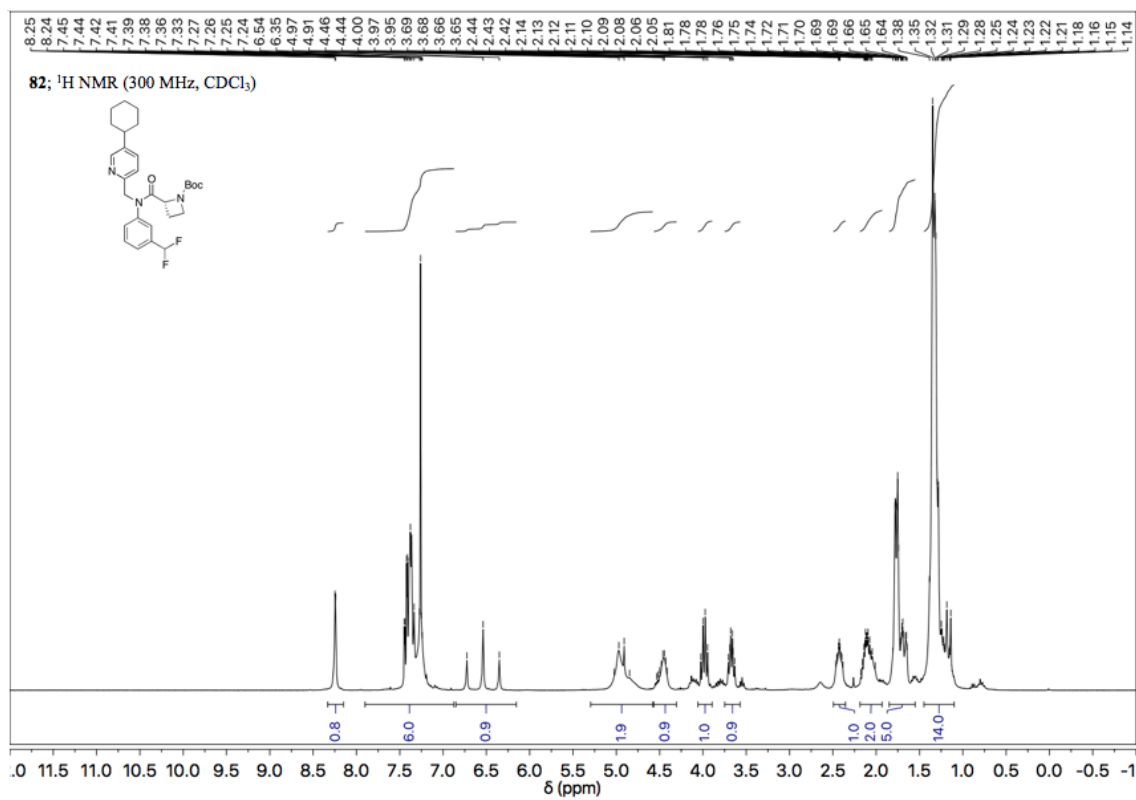
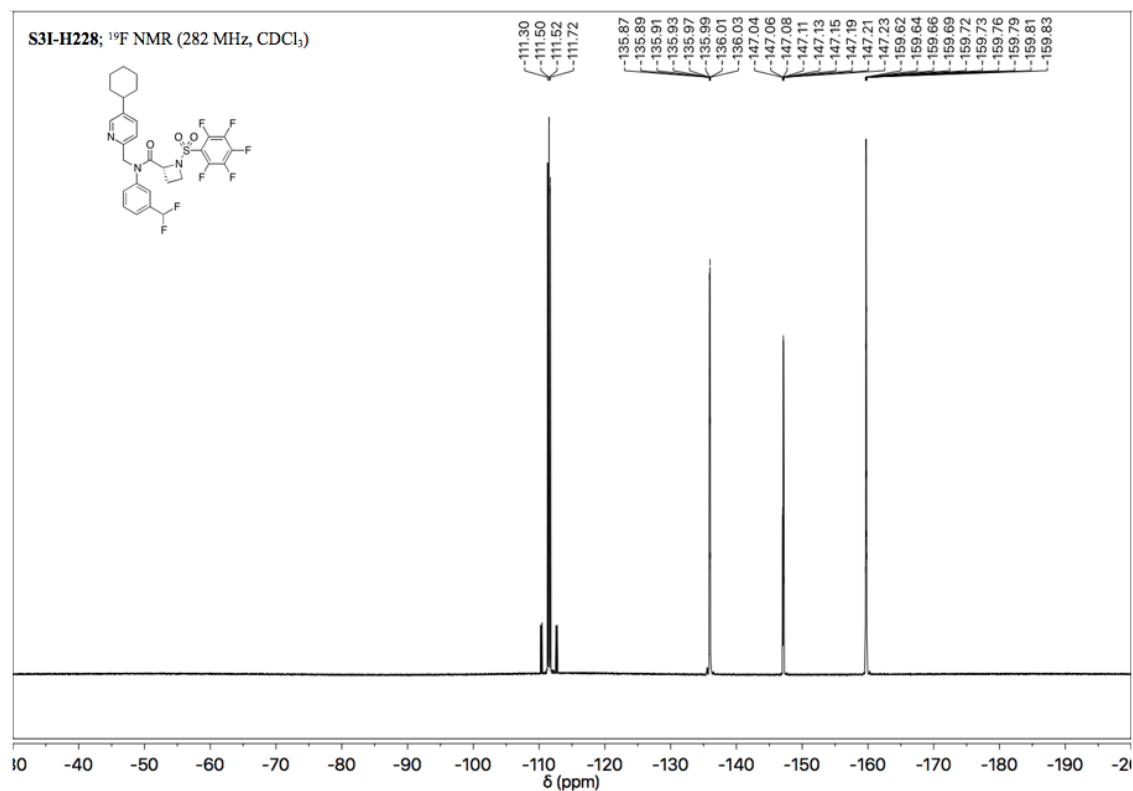


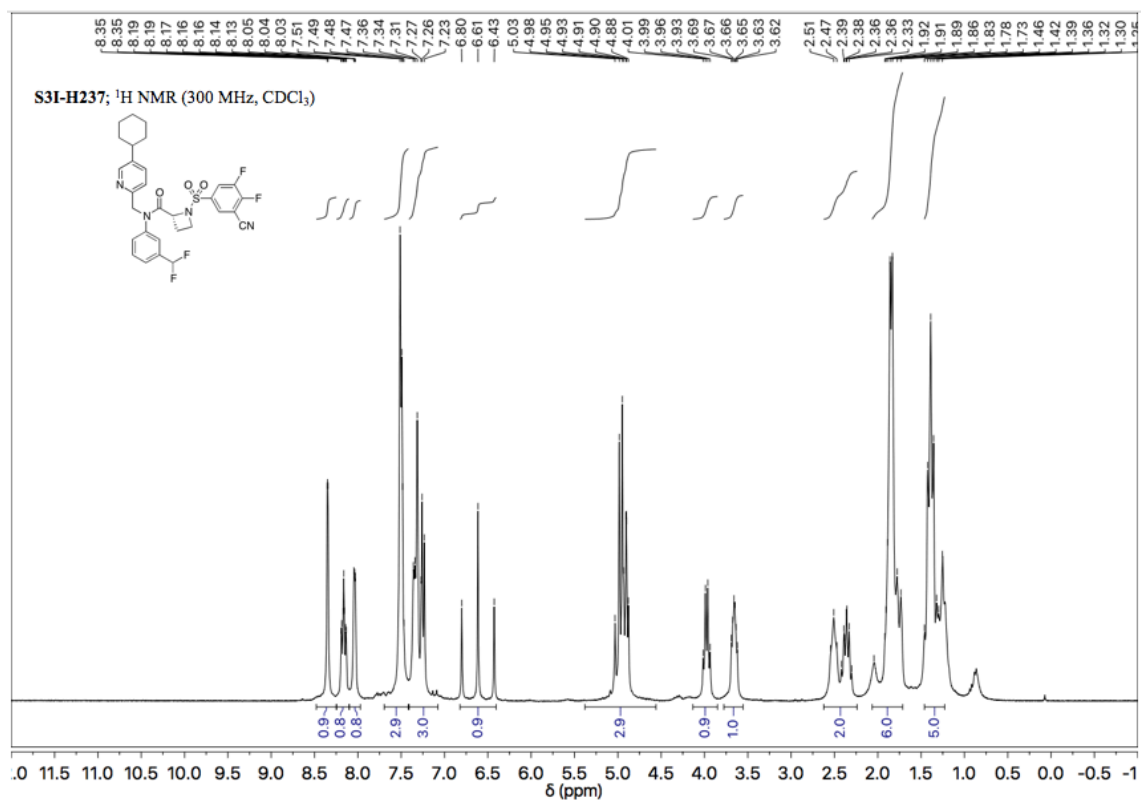
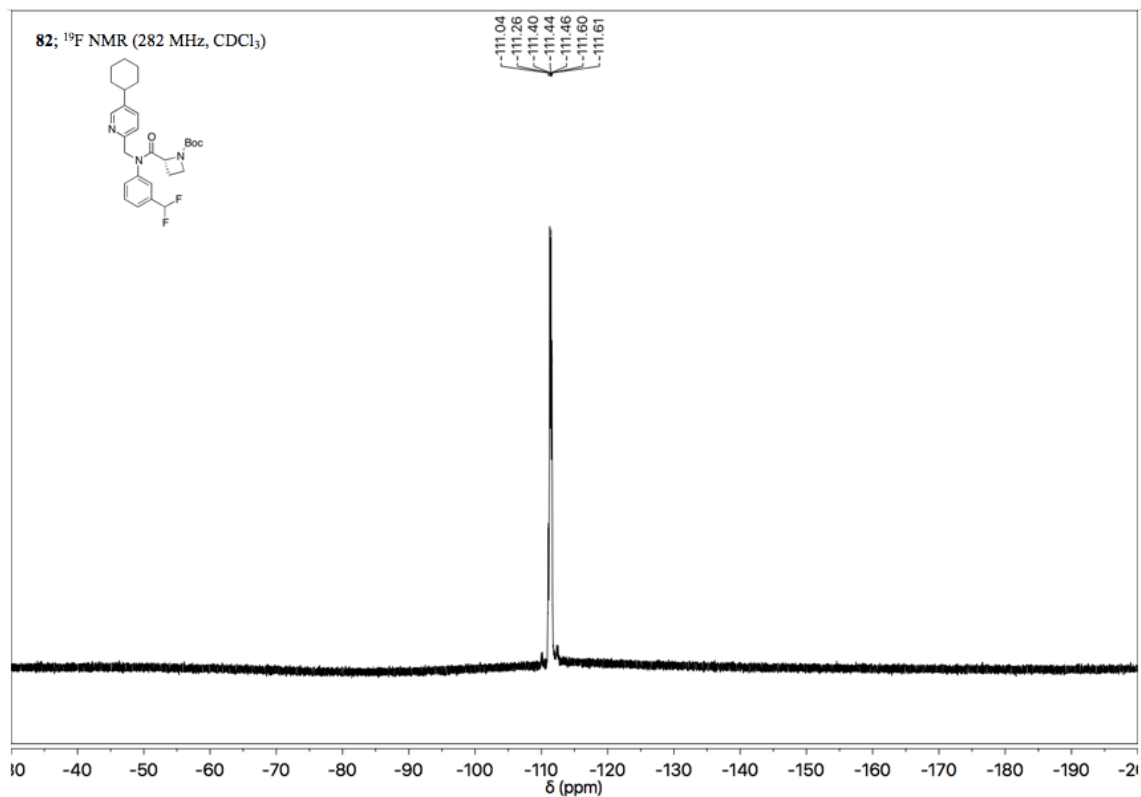


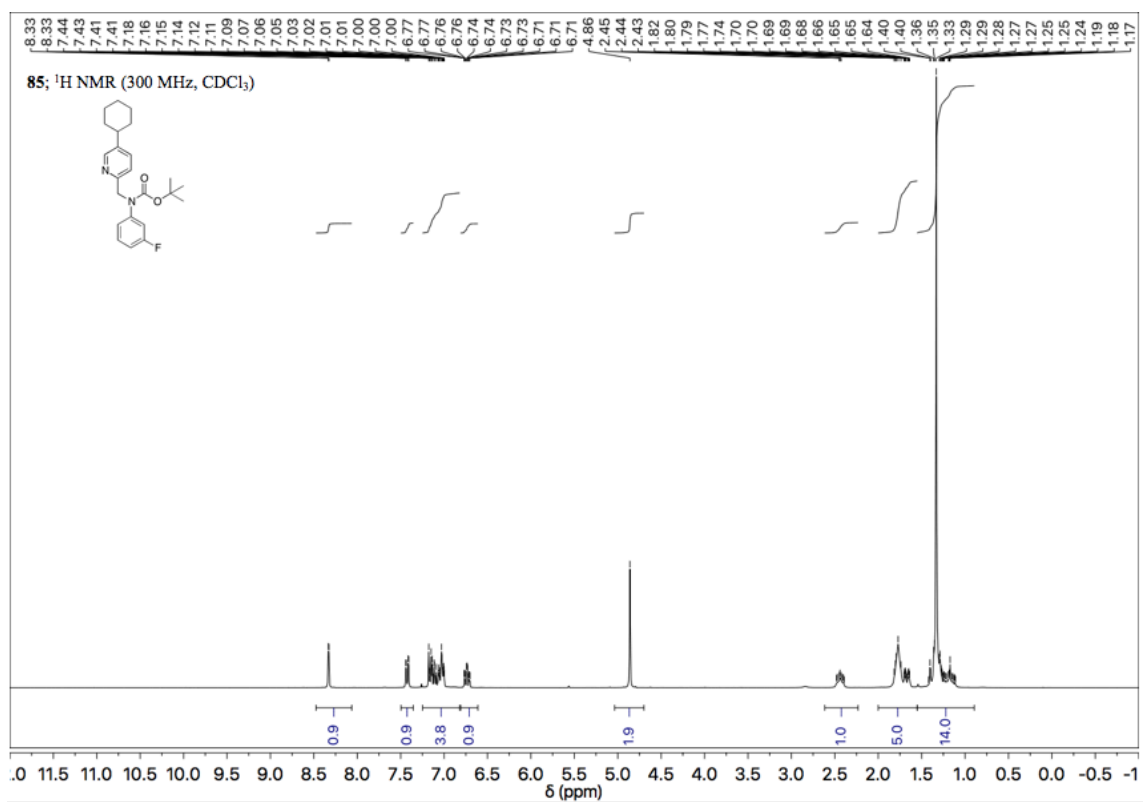
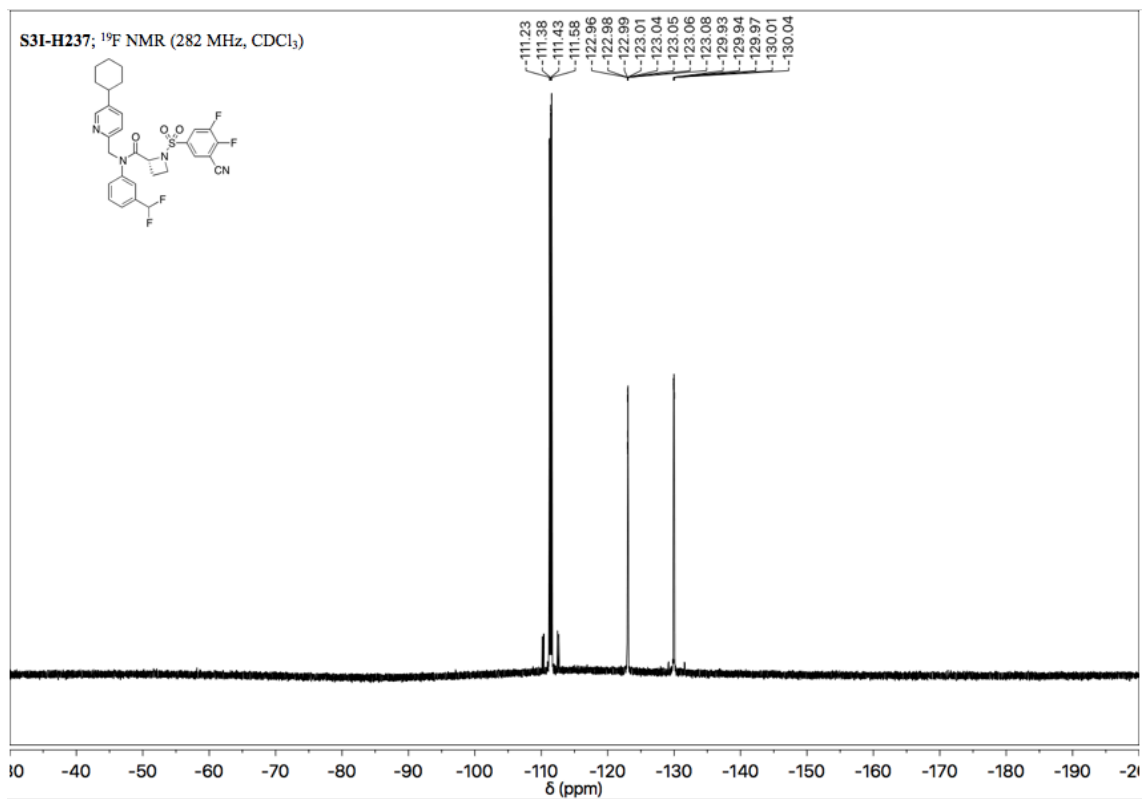


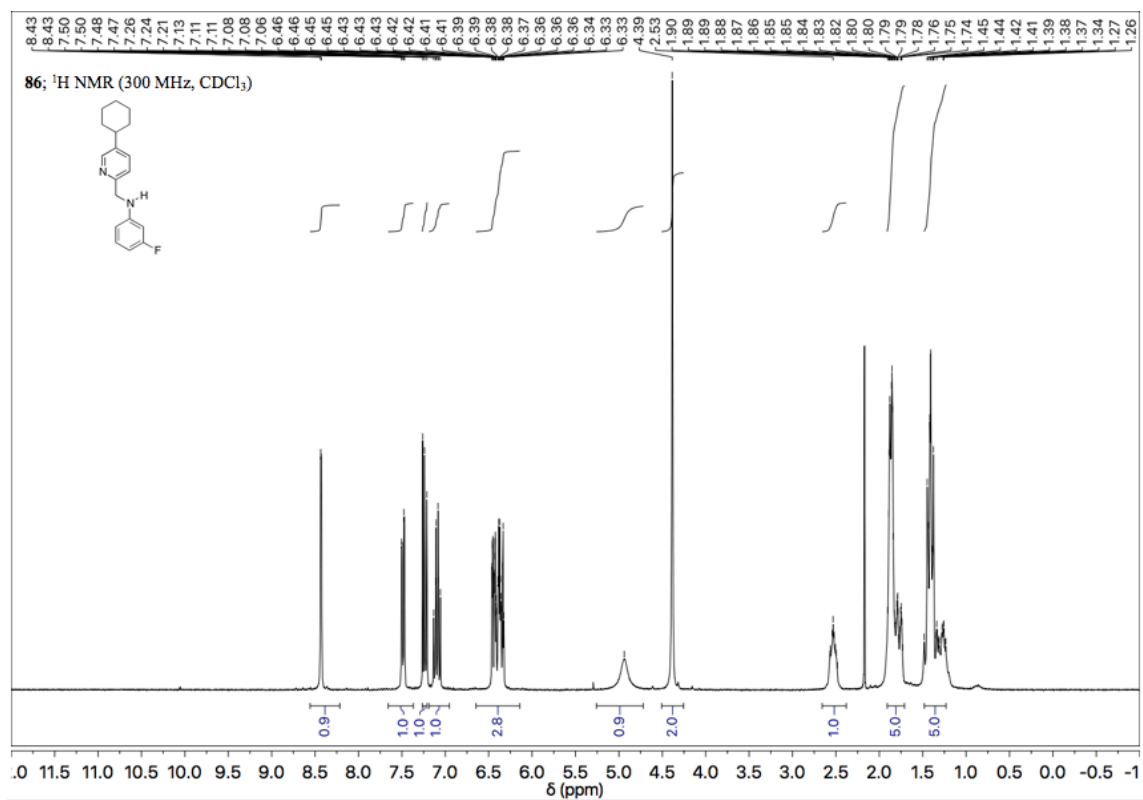
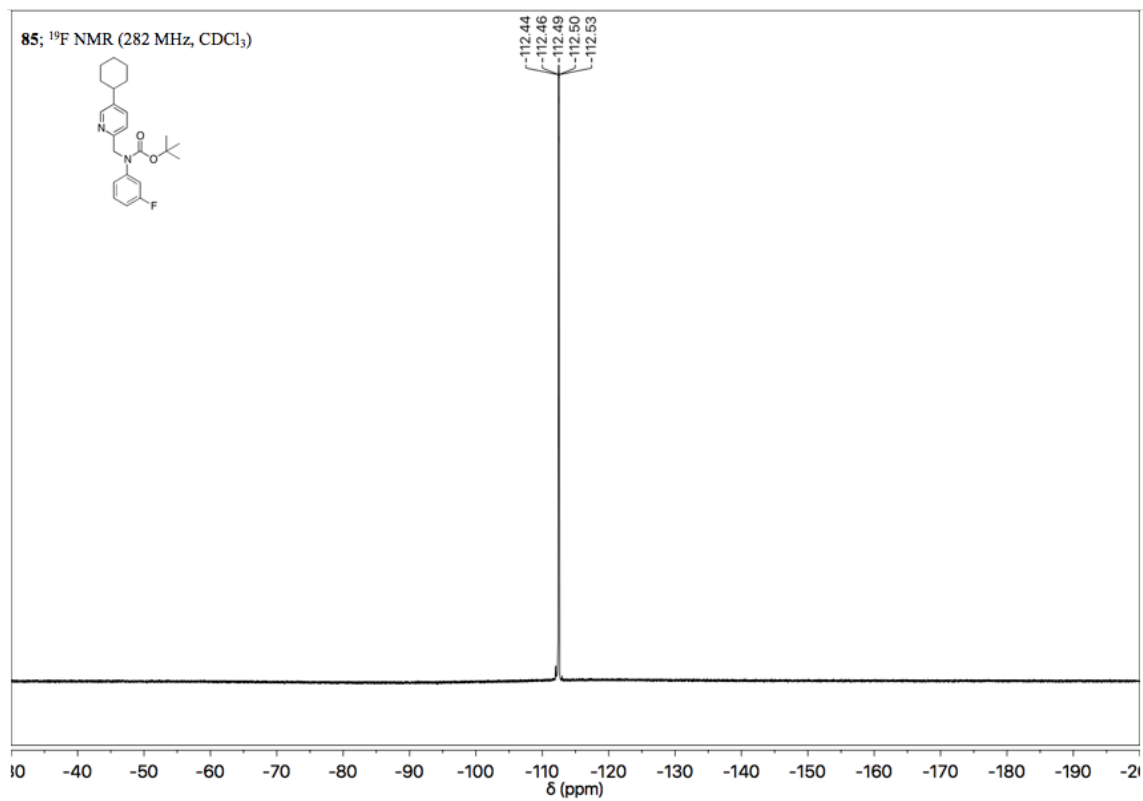


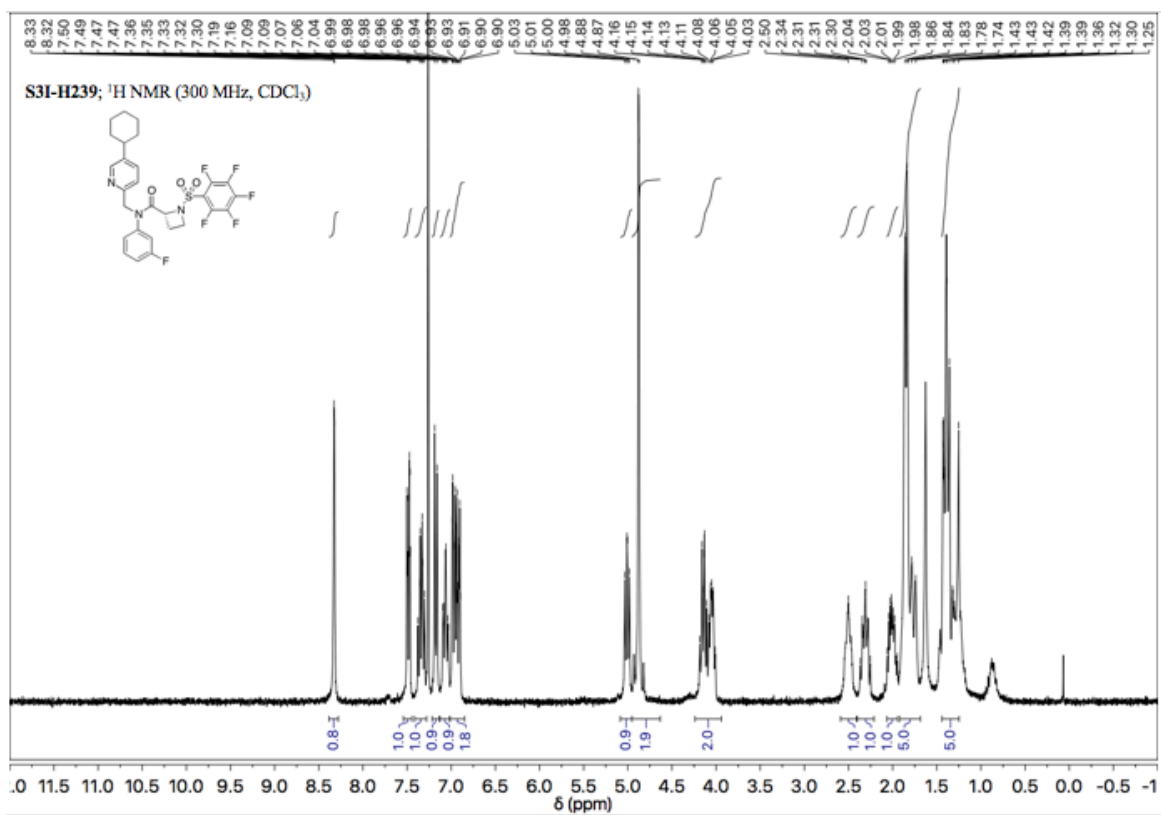
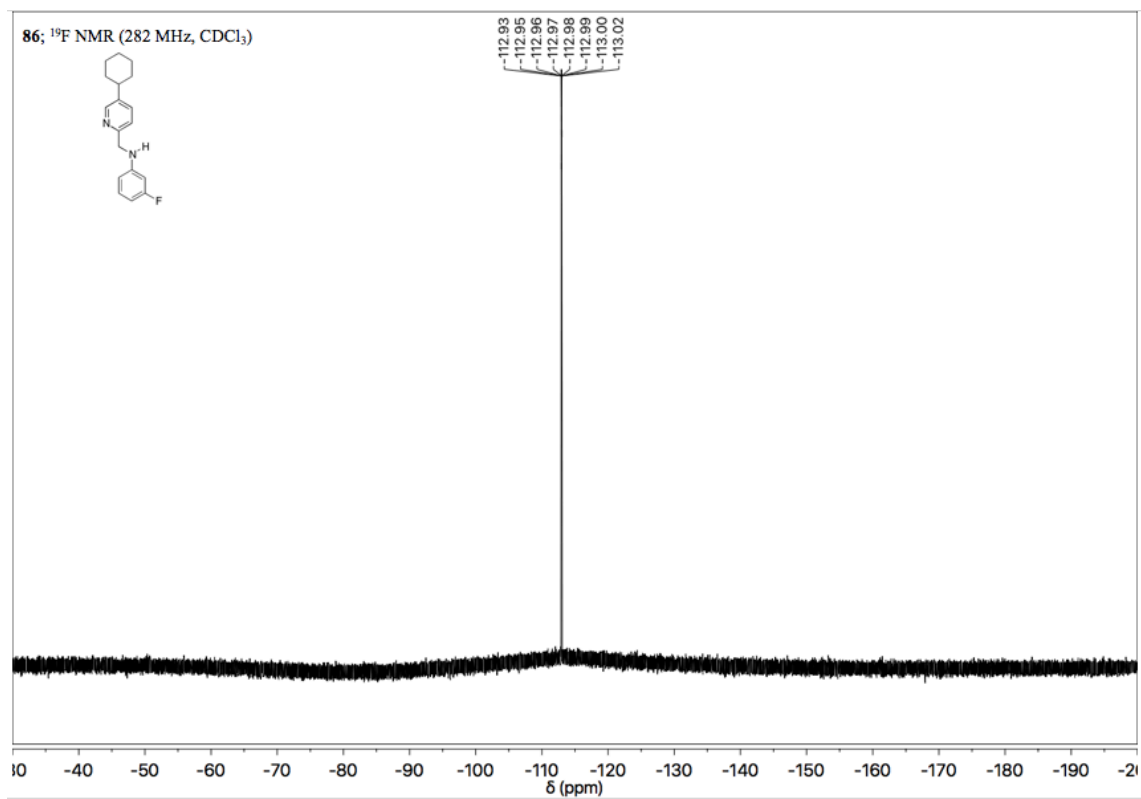


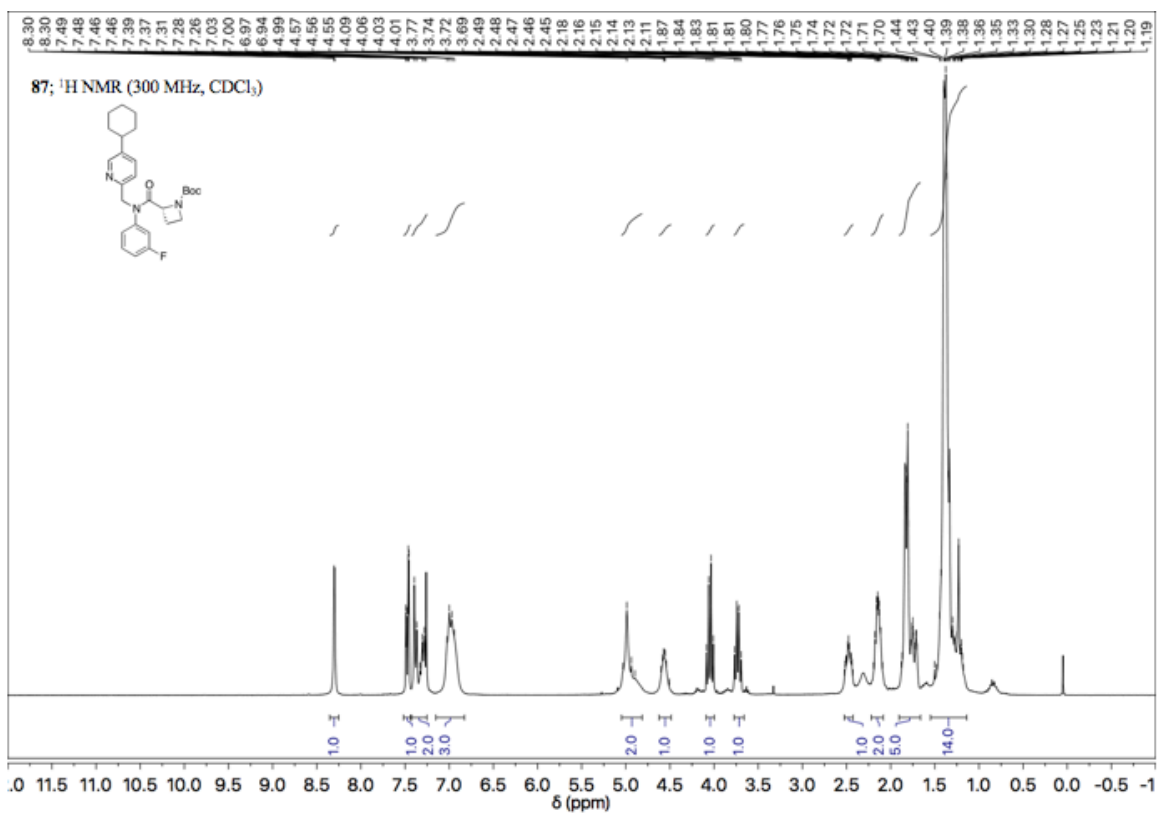
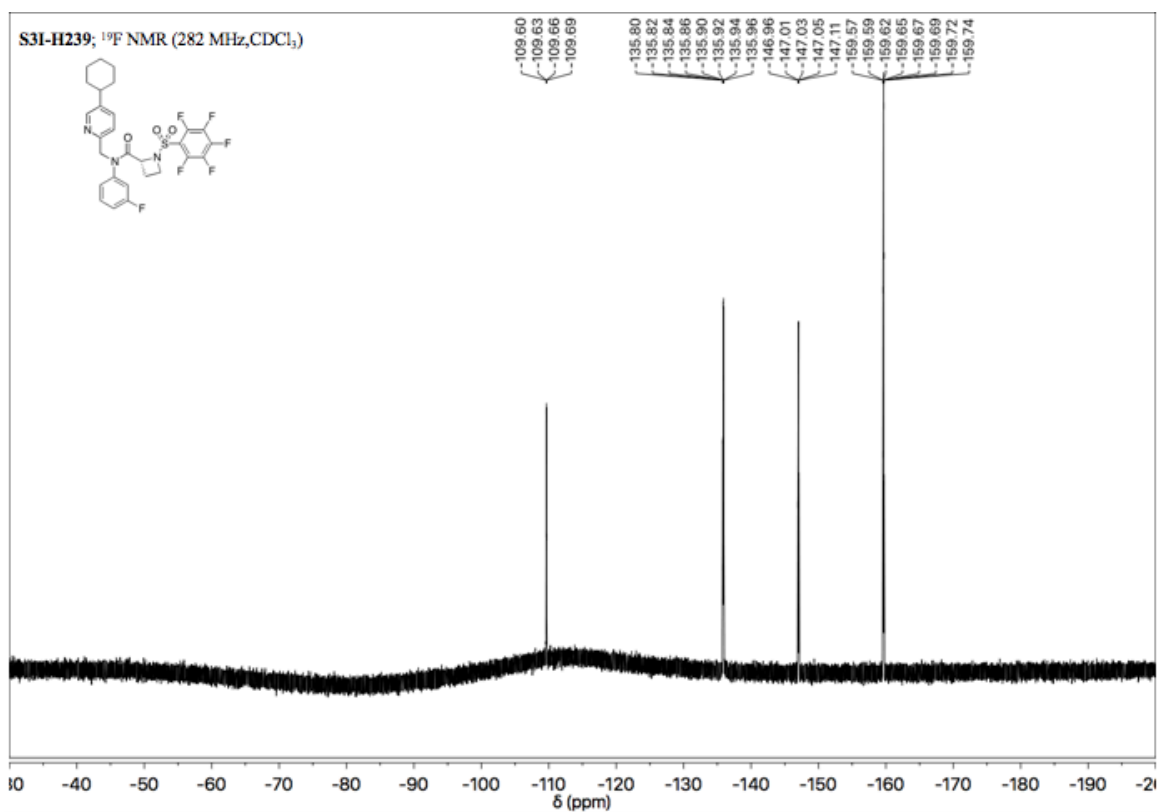


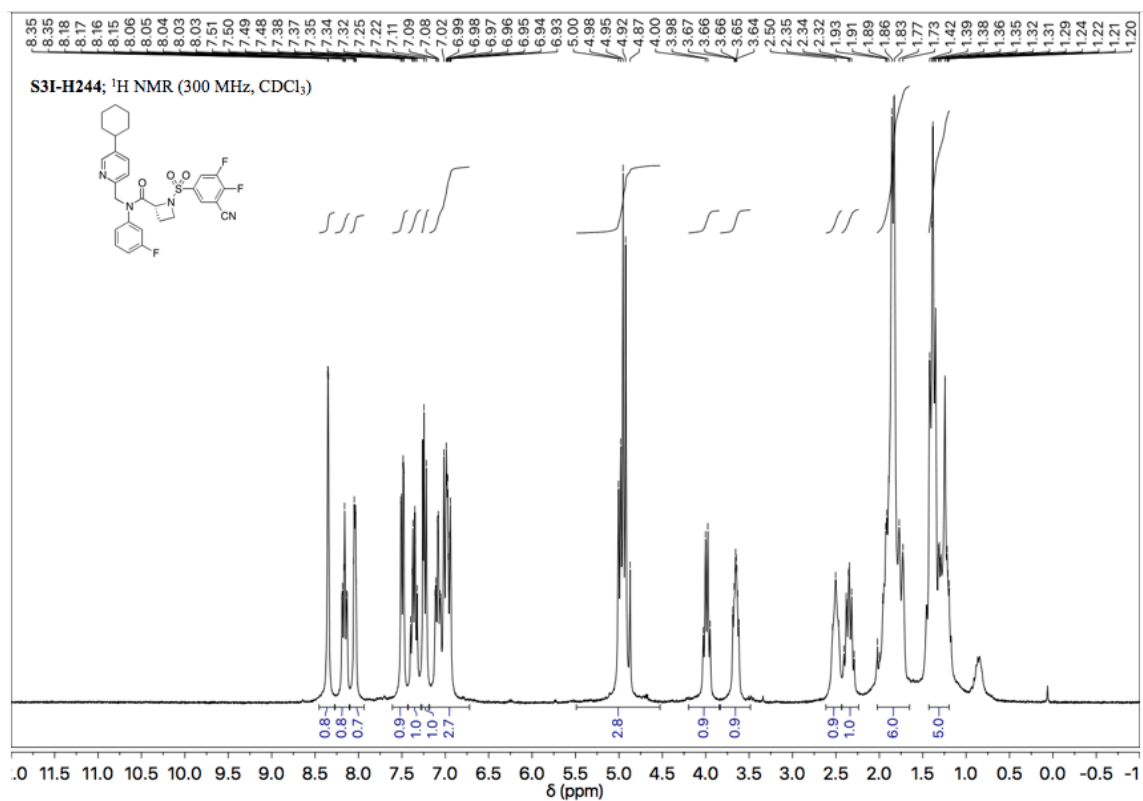
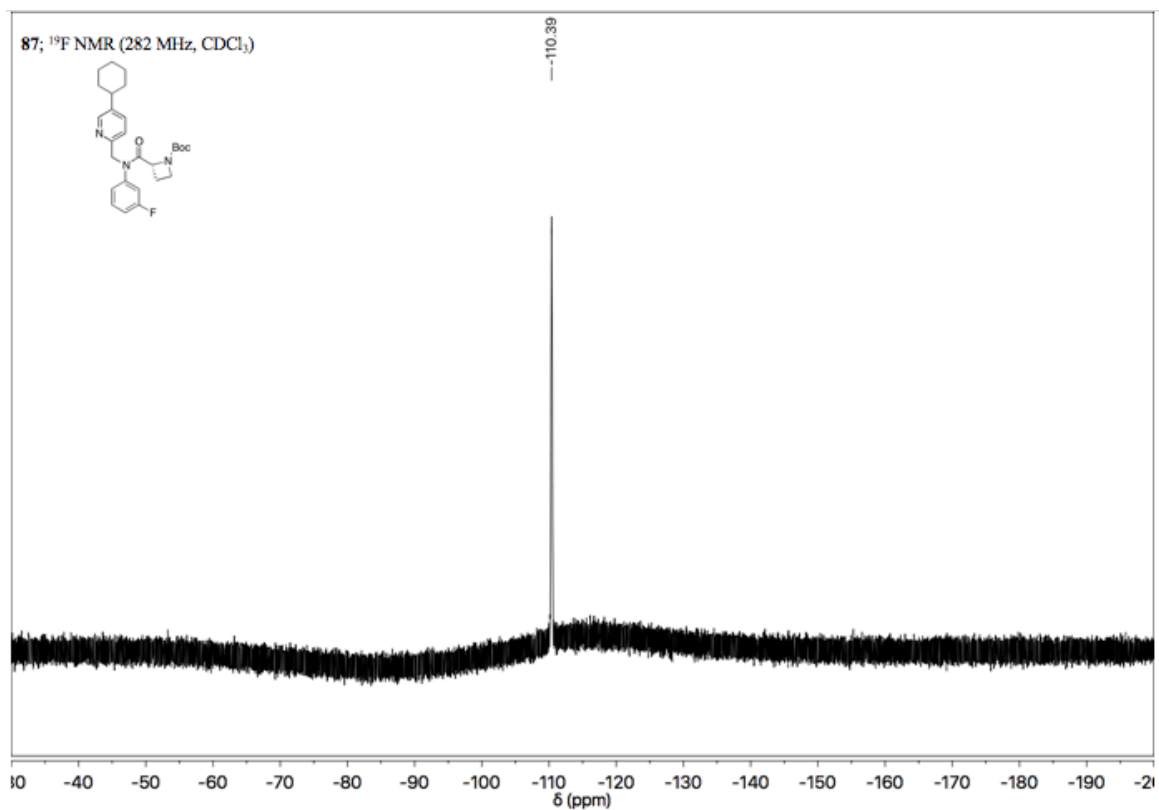


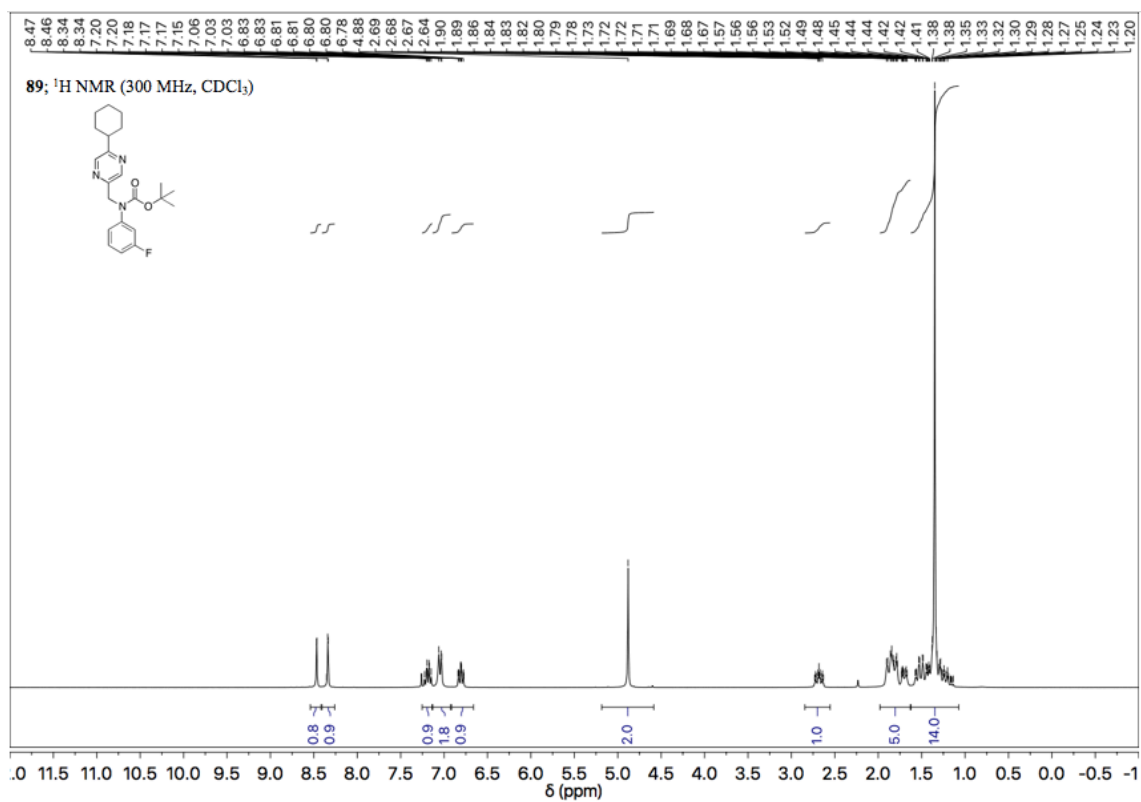
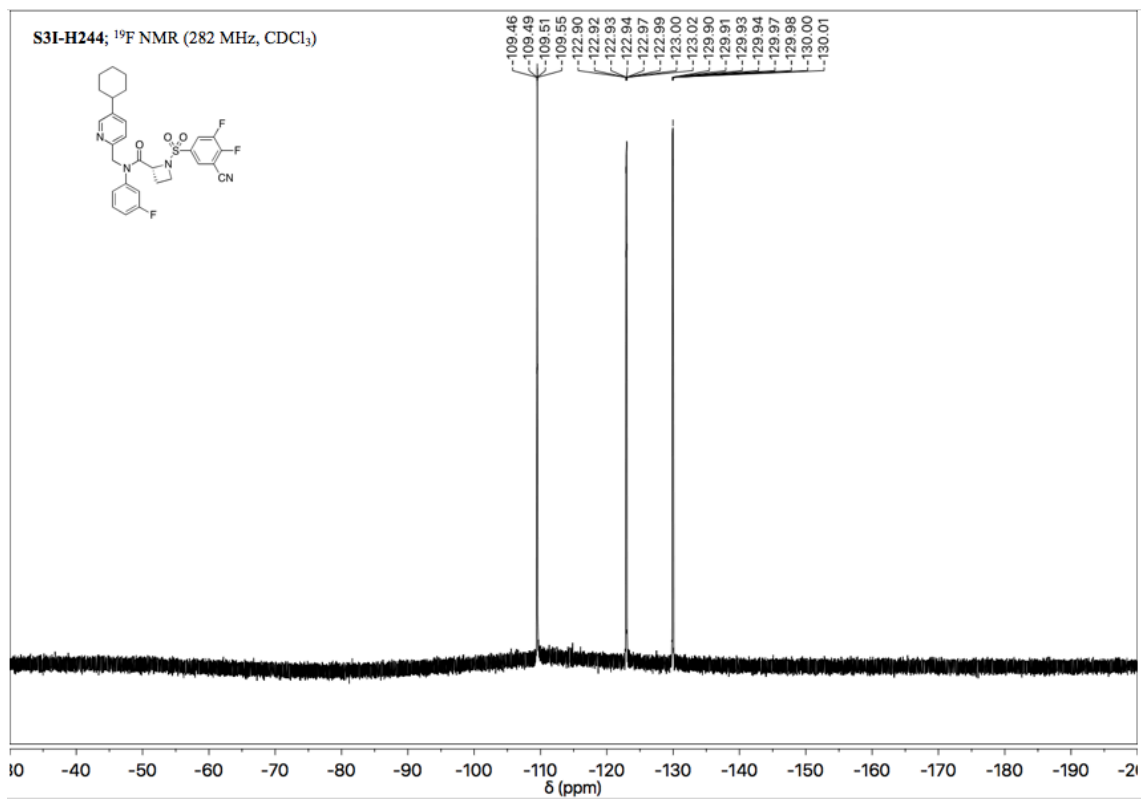


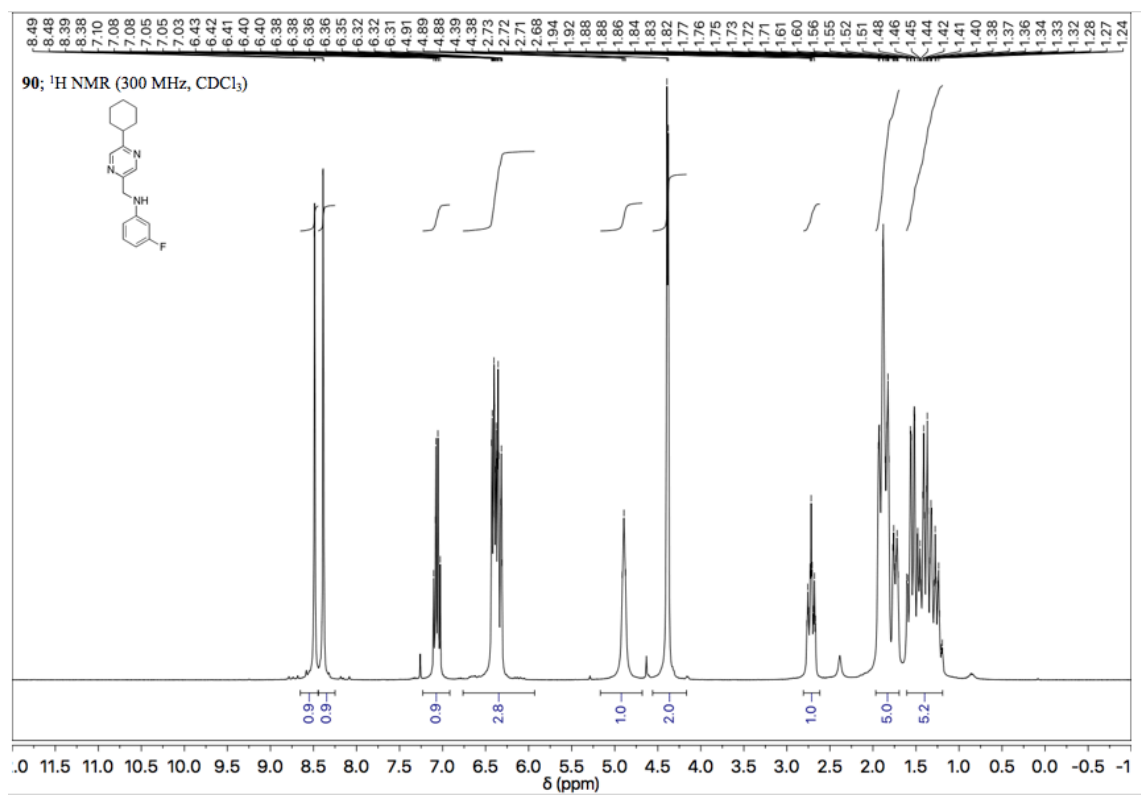
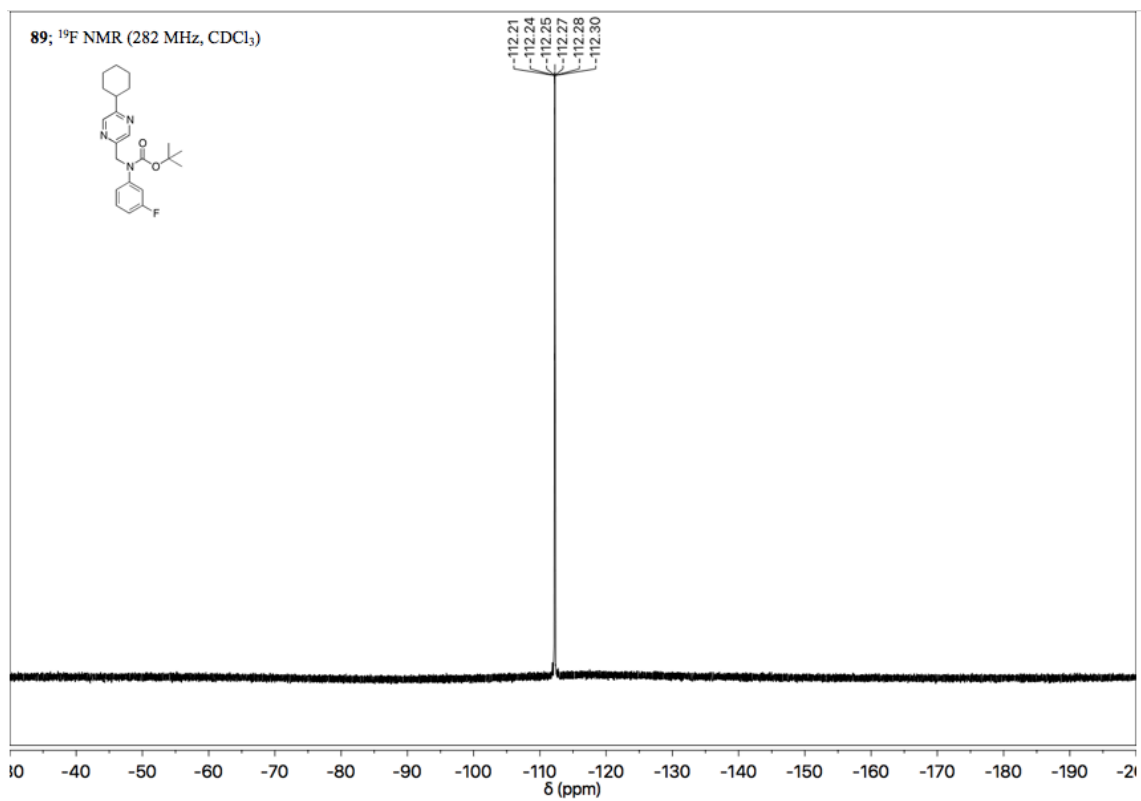


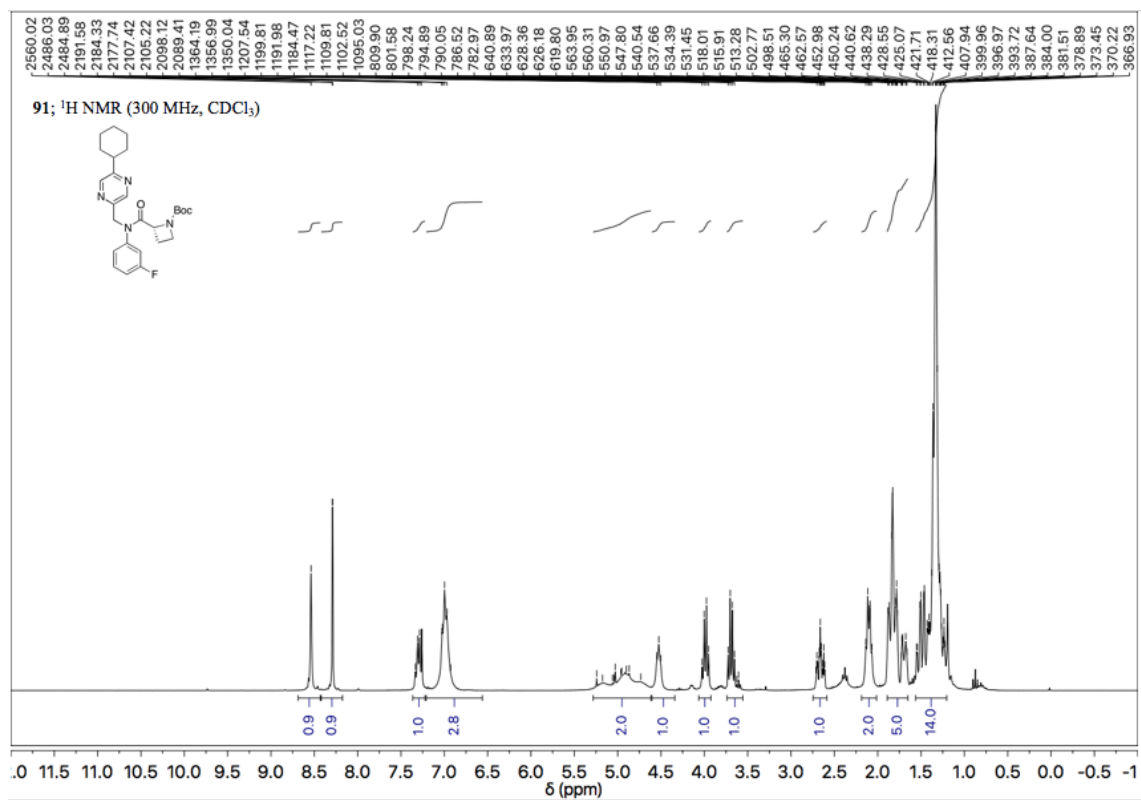
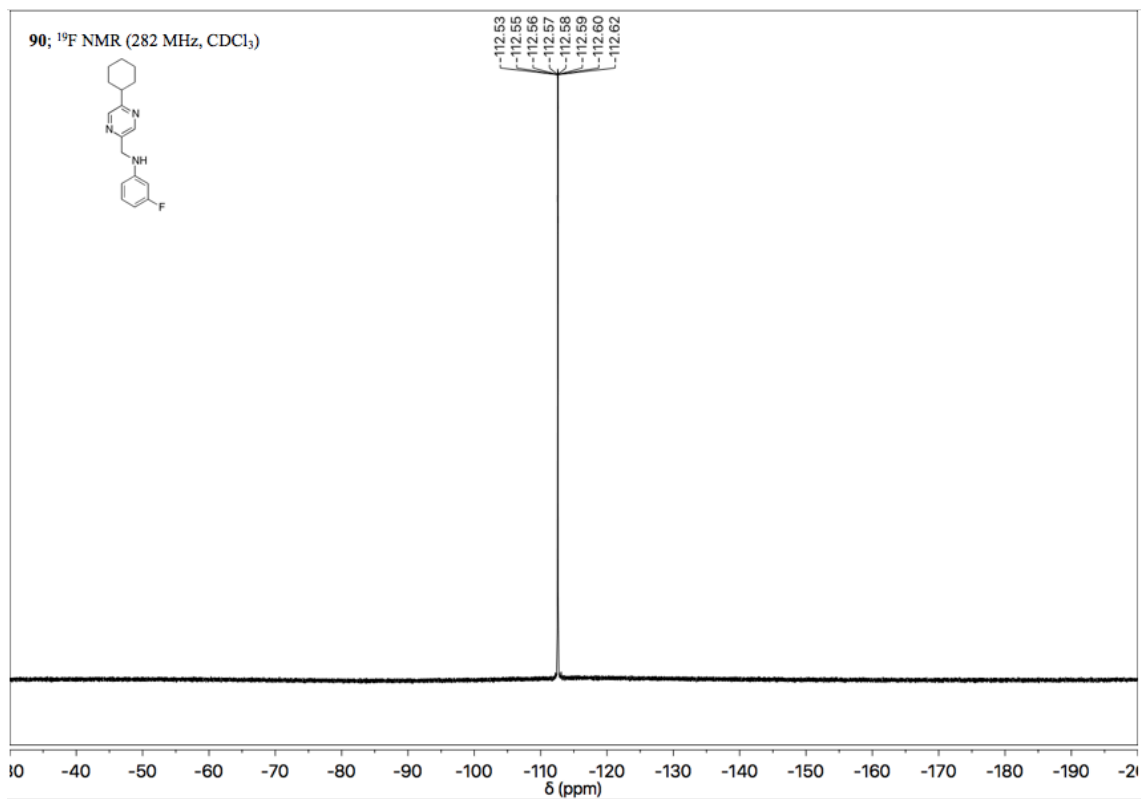


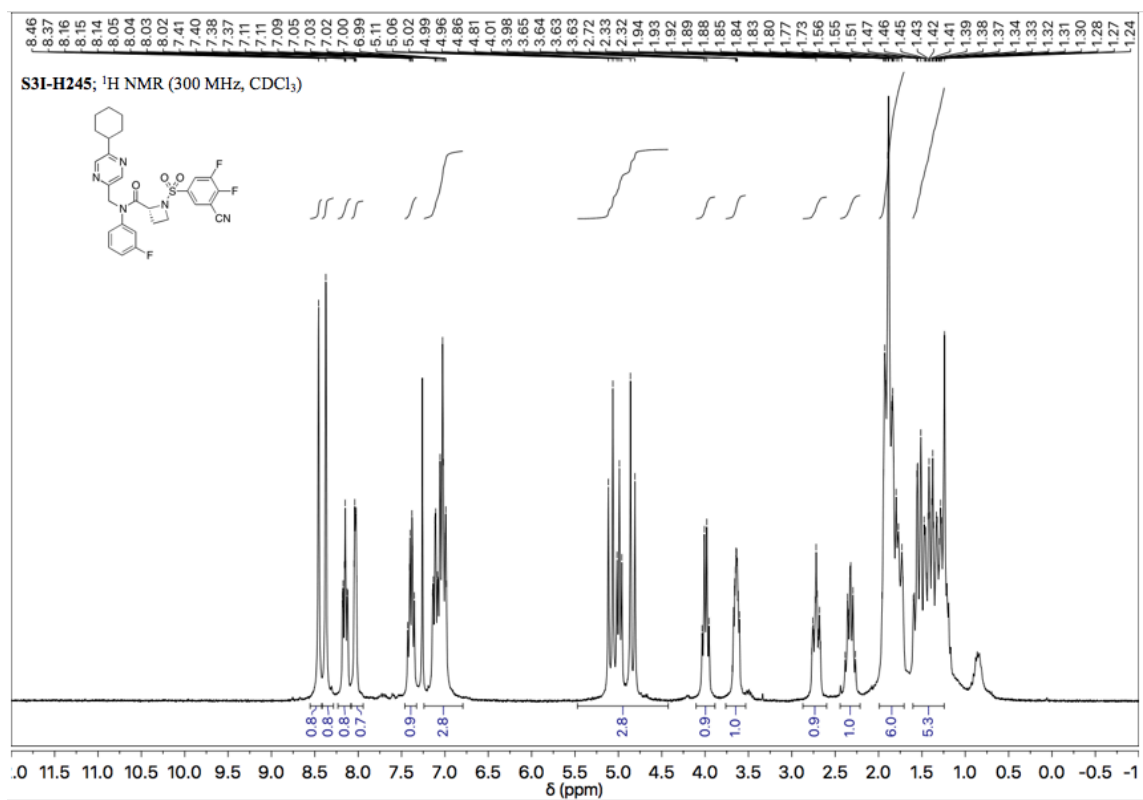
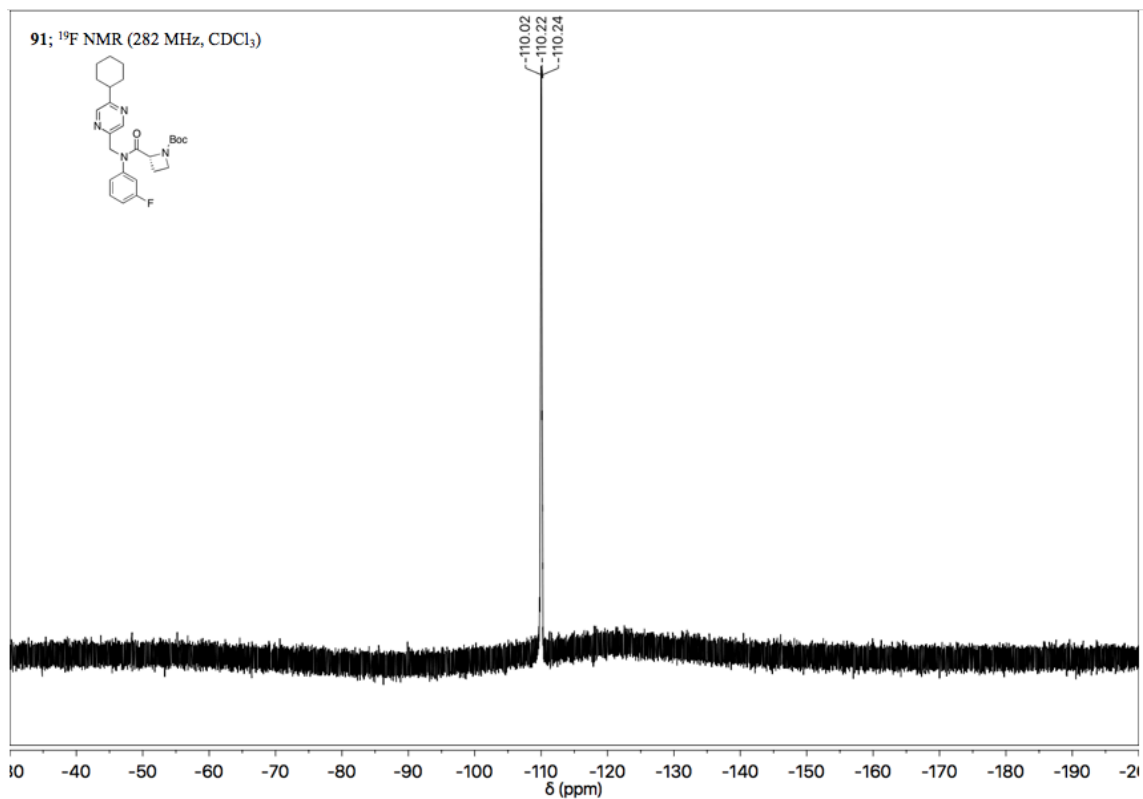


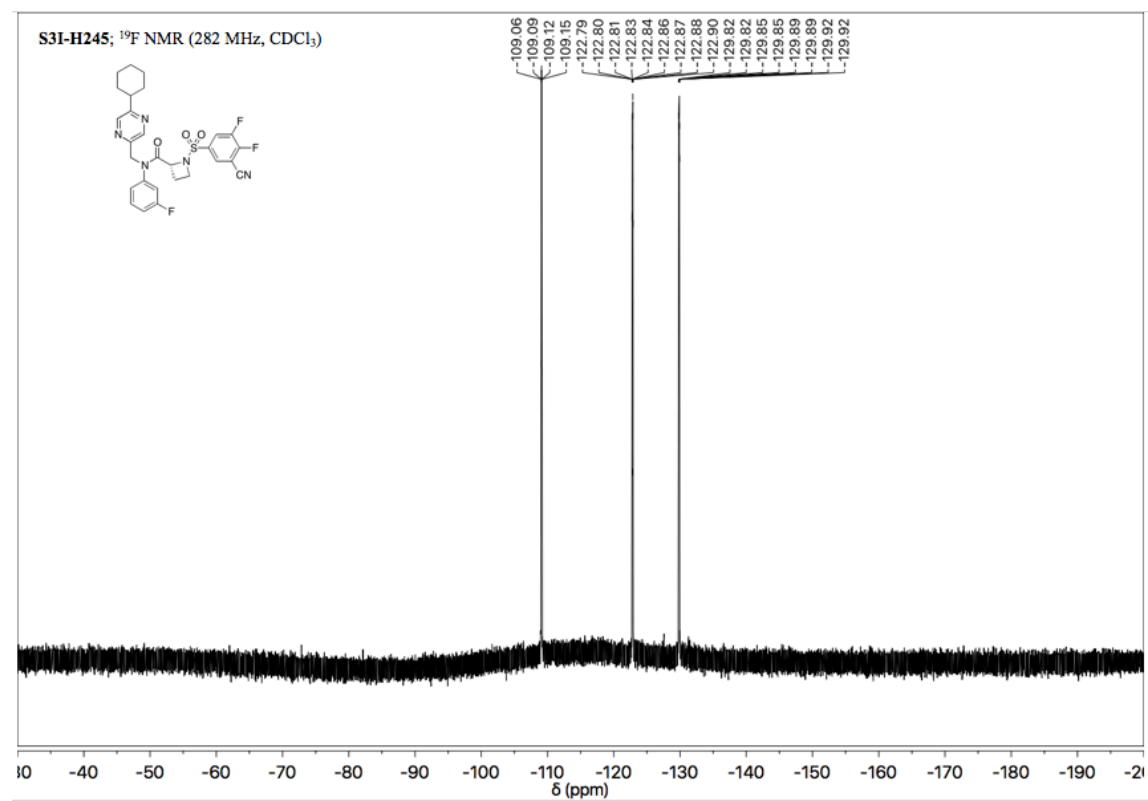












Appendix II

References

References:

1. Bromberg, J.; Darnell, J. E., Jr. The role of STATs in transcriptional control and their impact on cellular function. *Oncogene* **2000**, *19*, 2468-2473.
2. Darnell, J. E., Jr. Validating Stat3 in cancer therapy. *Nat. Med.* **2005**, *11*, 595-596.
3. Yue, P.; Turkson, J. Targeting STAT3 in cancer: how successful are we? *Expert Opin. Invest. Drugs* **2009**, *18*, 45-56.
4. Yu, H.; Jove, R. The STATs of cancer-new molecular targets come of age. *Nat. Rev. Cancer* **2004**, *4*, 97-105.
5. Miklossy, G.; Hilliard, T. S.; Turkson, J. Therapeutic modulators of STAT signaling for human diseases. *Nat. Rev. Drug Discov.* **2013**, *12*, 611-629.
6. Yue, P.; Lopez-Tapia, F.; Paladino, D.; Li, Y.; Chen, C.; Namanja, A. T.; Hilliard, T.; Chen, Y.; Tius, M. A.; Turkson, J. Hydroxamic Acid and Benzoic Acid-Based STAT3 Inhibitors Suppress Human Glioma and Breast Cancer Phenotypes *In Vitro* and *In Vivo*. *Cancer Res.* **2016**, *76*, 652-663.
7. Bowman, T.; Garcia, R.; Turkson, J.; Jove, R. STATs in oncogenesis. *Oncogene* **2000**, *19*, 2474-2488.
8. Turkson, J.; Jove, R. STAT proteins: novel molecular targets for cancer drug discovery. *Oncogene* **2000**, *19*, 6613-6626.
9. Turkson, J. STAT proteins as novel targets for cancer drug discovery. *Expert Opin. Ther. Targets* **2004**, *8*, 409-422.
10. Wang, T.; Niu, G.; Kortylewski, M.; Burdelya, L.; Shain, K.; Zhang, S.; Bhattacharya, R.; Gabrilovich, D.; Heller, R.; Coppola, D.; Dalton, W.; Jove, R.; Pardoll, D.; Yu, H. Regulation of the innate and adaptive immune responses by Stat-3 signaling in tumor cells. *Nat. Med.* **2004**, *10*, 48-54.
11. Siddiquee, K. A.; Gunning, P. T.; Glenn, M.; Katt, W. P.; Zhang, S.; Schroeck, C.; Sebt, S. M.; Jove, R.; Hamilton, A. D.; Turkson, J. An Oxazole-Based Small-Molecule Stat3 Inhibitor Modulates Stat3 Stability and Processing and Induces Antitumor Cell Effects. *ACS Chem. Biol.* **2007**, *2*, 787-798.

12. Siddiquee, K.; Zhang, S.; Guida, W. C.; Blaskovich, M. A.; Greedy, B.; Lawrence, H. R.; Yip, M. L.; Jove, R.; McLaughlin, M. M.; Lawrence, N. J.; Sebt, S. M.; Turkson, J. Selective chemical probe inhibitor of Stat3, identified through structure-based virtual screening, induces antitumor activity. *Proc. Natl. Acad. Sci. U.S.A.* **2007**, *104*, 7391–7396.
13. Zhang, X.; Yue, P.; Page, B. D. G.; Li, T.; Zhao, W.; Namanja, A. T.; Paladino, D.; Zhao, J.; Chen, Y.; Gunning, P. T.; Turkson, J. Orally bioavailable small-molecule inhibitor of transcription factor Stat3 regresses human breast and lung cancer xenografts. *Proc. Natl. Acad. Sci. U.S.A.* **2012**, *109*, 9623–9628.
14. Zhang, X.; Sun, Y.; Pireddu, R.; Yang, H.; Urlam, M. K.; Lawrence, H. R.; Guida, W. C.; Lawrence, N. J.; Sebt, S. M. A Novel Inhibitor of STAT3 Homodimerization Selectively Suppresses STAT3 Activity and Malignant Transformation. *Cancer Res.* **2013**, *73*, 1922–1933.
15. Turkson, J.; Kim, J. S.; Zhang, S.; Yuan, J.; Huang, M.; Glenn, M.; Haura, E.; Sebt, S.; Hamilton, A. D.; Jove, R. Novel peptidomimetic inhibitors of signal transducer and activator of transcription 3 dimerization and biological activity. *Mol. Cancer Ther.* **2004**, *3*, 261–269.
16. Turkson, J.; Ryan, D.; Kim, J. S.; Zhang, Y.; Chen, Z.; Haura, E.; Laudano, A.; Sebt, S.; Hamilton, A. D.; Jove, R. Phosphotyrosyl Peptides Block Stat3-mediated DNA Binding Activity, Gene Regulation, and Cell Transformation. *J. Biol. Chem.* **2001**, *276*, 45443–45455.
17. Coleman, D. R., IV; Ren, Z.; Mandal, P. K.; Cameron, A. G.; Dyer, G. A.; Muranjan, S.; Campbell, M.; Chen, X.; McMurray, J. S. Investigation of the Binding Determinants of Phosphopeptides Targeted to the Src Homology 2 Domain of the Signal Transducer and Activator of Transcription 3. Development of a High-Affinity Peptide Inhibitor. *J. Med. Chem.* **2005**, *48*, 6661–6670.
18. Song, H.; Wang, R.; Wang, S.; Lin, J.; Stark, G. R. A Low-Molecular-Weight Compound Discovered through Virtual Database Screening Inhibits Stat3 Function in Breast Cancer Cells. *Proc. Natl. Acad. Sci. U.S.A.* **2005**, *102*, 4700–4705.
19. Lopez-Tapia, F.; Brotherton-Pleiss, C.; Yue, P.; Murakami, H.; Costa Araujo, A. C.; Reis dos Santos, B.; Ichinotsubo, E.; Rabkin, A.; Shah, R.; Lantz, M.; Chen, S.; Tius, M. A.; Turkson, J. Linker Variation and Structure-Activity Relationship Analyses of Carboxylic Acid-based Small Molecule STAT3 Inhibitors. *ACS Med. Chem. Lett.* **2018**, *9*, 250–255.
20. De Groot, M. J.; Ackland, M. J.; Horne, V. A.; Alexander, A. A.; Jones, B. C. A Novel Approach to Predicting P450 Mediated Drug Metabolism. CYP2D6 Catalyzed N-Dealkylation Reactions and Qualitative Metabolite Predictions Using a Combined Protein and Pharmacophore Model for CYP2D6. *J. Med. Chem.* **1999**, *42*, 4062–4070.

21. Klein, S. The Use of Biorelevant Dissolution Media to Forecast the In Vivo Performance of a Drug. *AAPS J.* **2010**, *12*, 397-406.
22. Turkson, J.; Yue, P.; Tius, M; Brotherton-Pleiss, C.; Lopez-Tapia, F. J. Preparation of 2-arylsulfonamido-N-arylacetamide derivatives, including amino acid sulfonamides, as STAT3 inhibitors for the treatment of cancer. US Patent WO 2018136935, Jan 23, 2018.
23. Barluenga, J.; Alvarez-Guiterrez, J. M.; Ballesteros, A.; Gonzalez, J. M. Direct *ortho* Iodination of β - and γ -Aryl Alkylamine Derivatives. *Angew. Chem. Int. Ed.* **2007**, *46*, 1281-1283.
24. Chaturvedi, P. R.; Decker C. J.; Odinecs, A. Prediction of pharmacokinetic properties using experimental approaches during early drug discovery. *Curr. Opin. Chem. Biol.* **2001**, *5*, 452-463.
25. Kley, J.; Hamilton, B. S.; Mack, J.; Redemann, N.; Schoelch, C. Preparation of cyclopentanecarboxamide derivatives as fatty acid synthase inhibitors. Patent WO 2011048018, Apr 28, 2011.
26. Buchwald, S. L.; Yin, J. Pd-Catalyzed Intermolecular Amidation of Aryl Halides: The Discovery that Xantphos Can Be Trans-Chelating in a Palladium Complex. *J. Am. Chem. Soc.* **2002**, *124*, 6043-6048.
27. Youn S. W; Kim, Y. H. Pd(II)/Ag(I)-Promoted One-Pot Synthesis of Cyclic Ureas from (Hetero)Aromatic Amines and Isocyanates. *Org. Lett.* **2016**, *18*, 6140-6143.
28. Hong, W. D.; Gibbons, P. D.; Leung, S. C.; Amewu, R.; Stocks, P. A.; Stachulski, A.; Horta, P.; Cristiano, M. L. S.; Shone, A. E.; Moss, D.; Ardrey, A.; Sharma, R.; Warman, A. J.; Bedingfield, P. T. P.; Fischer, N. E.; Aljayyousi, G.; Mead, S.; Caws, M.; Berry, N. G.; Ward, S. A.; Biagini, G. A.; O'Neill, P. M.; Nixon, G. L. Rational Design, Synthesis, and Biological Evaluation of Heterocyclic Quinolones Targeting the Respiratory Chain of Mycobacterium tuberculosis. *J. Med. Chem.* **2017**, *60*, 3703-3726.
29. Van Breeman, R. B.; Li, Y. Caco-2-cell permeability assays to measure drug absorption. *Expert Opin. Drug. Metab. Toxicol.* **2005**, *1*, 175-185.
30. Prasanth, C. P.; Joseph, E.; Abhijith, A.; Nair, D. S.; Ibnusaud, I.; Raskatov, J.; Singaram, B. Stabilization of NaBH₄ in Methanol Using a Catalytic Amount of NaOMe. Reduction of Esters and Lactones at Room Temperature without Solvent-Induced Loss of Hydride *J. Org. Chem.* **2018**, *83*, 1431-1440.

31. Krishnamurthy, R.; Natarajan, S. Iron-Ammonium Chloride – A Convenient and Inexpensive Reductant. *Synth. Commun.* **1992**, *22*, 3189-3195.
32. MacMillan, D. S.; Murray, J.; Sneddon, H. F.; Jamieson, C.; Watson, A. J. B. Evaluation of alternative solvents in common amide coupling reactions: replacement of dichloromethane and *N,N*-dimethylformamide. *Green Chem.*, **2013**, *15*, 596-600.
33. Huestis, M. P. Rhodium(III)-Catalyzed C-H Functionalization of 1-(2H)-Phthalazinones at C8. *J. Org. Chem.* **2016**, *81*, 12545-12552.
34. Khurana, J. M.; Ray, A. Chemoselective Reductive Coupling of Nitroarenes with Magnesium in Methanol via Single Electron Transfer. *Bull. Chem. Soc. Jpn.* **1996**, *69*, 407-410.